Modelling Environment Dependent Growth of Juvenile Atlantic salmon, *Salmo salar, L.*

Raymond Gani B.Sc. (Hons.) M.Sc.

Submitted for

Degree of Doctor of Philosophy,

Department of Statistics and Modelling Science
University of Strathclyde

February 2000

Acknowledgements

I sincerely wish to thank my supervisors Bill Gurney and Philip Bacon for their guidance and support, as well as substantial help, in the preparation of this thesis. I am also grateful to Alan Youngson, from the Marine Laboratory of Aberdeen, for advice on the biological aspects of this thesis and encouragement throughout.

I would also like to thank David Hay, Mike Donaghy, Ian McLaren and Ross Gardiner, from the Freshwater Fisheries Laboratory, for providing a substantial amount of the data for this thesis as well as useful comments on fish behaviour. In addition I would like to thank Rick Cunjak from University of New Brunswick, Chris Soulsby from University of Aberdeen, and Anne McLay from the Marine Laboratory of Aberdeen. Many thanks also to the computer manager Ian Thurlbeck for all his help and assistance and Wayne Jones at Strathclyde University.

This research was funded by the Natural Environment Research Council and the Department of Statistics and Modelling Science, Strathclyde University. Additional support was provided by the Institute of Terrestrial Ecology, Banchory and the Fisheries Research Services, Aberdeen.

On a personal note, I would like to thank all my friends without whom the last four years would have been impossible, in particular, Cos, Russel, Damian, Isla, Marianne, Anna, Arjun, Adam, Tim and Ewa.

Finally I would like to thank my parents, Zena and Esau and my sisters Salina and Lisa for giving me continued encouragement and support throughout my university education. I dedicate this thesis to them.

Abstract

Catches of Atlantic salmon returning to Scottish rivers have declined steadily since the 1960's and it is highly likely that spawning stocks in some locations are now marginal in their capacity to replenish juvenile numbers. One method of enhancing salmon production is to stock rivers with ova or fry in order to increase the number of juveniles emigrating. The timing, location and scale of stocking is likely to affect the size and age of the emigrants, so it is necessary to be able to predict growth rates in order to develop an efficient stocking strategy.

A functional growth model for Atlantic salmon parr is developed and fitted to electro-fishing data from the Girnock Burn, Scotland. A fitting function, $\phi(t)$, is used to estimate the quality of the local environment between years. Further adaptations enable the model to predict the mean weights, and their variation, for the different age-classes of the resident population. It also predicts the mean lengths, and their variation, for the migrants from different age-classes, and the proportion of each cohort that migrates each year.

$\phi(t)$ is derived for different parts of the Girnock Burn and indicates that, after the effects of temperature on growth have been removed, the quality of habitat available for juvenile salmon growth increases with altitude. A model to estimate consumption rates is also developed and integrated into the growth model, allowing the seasonal maximum and minimum feeding periods of the parr to be determined.

The model can be used as a tool for habitat assessment and to develop optimal stocking strategies, and is part of a larger project to enhance salmon production in Scotland. The applications of this study to the conservation and management of wild Atlantic salmon stocks is discussed.

List of symbols contained within this thesis

Symbol	Meaning	Dimension
a	Condition Factor	g.cm^{-x}
A	Assimilation rate	mgC.day^{-1}
a_1	Coefficient for $D(\gamma)$	dimensionless
a_2	Coefficient for $D(\gamma)$	dimensionless
a_3	Coefficient for $D(\gamma)$	dimensionless
a_h	Coefficient for two-parameter $P(r, p, L)$	dimensionless
a_l	Coefficient for two-parameter $P(r, p, L)$	dimensionless
a_n	Normalised effective search area	cm^{-1}
a_s	Condition Factor for S W-L relationship	mgC.cm^{-b_s}
A_s	Effective search area	cm^2
a_{s_1}	Rescaled condition factor	$\text{mgC}^{c_1}\text{.cm}^{-3}$
A_T	Total effective search area	cm^3
b	Weight exponent	dimensionless
$B(p_1, p_2)$	Biomass between p_1 and p_2	mgC.cm^{-3}
b_s	Allometric Factor for S W-L relationship	dimensionless
c	Coefficient of variation	dimensionless
C_0	Ideal value of $C(\rho)$	dimensionless
c_1	Rescaled W-L allometric coefficient	dimensionless
C_b	Rate of energy gain through consumption	cal.day^{-1}
c_c	Maximum growth rate for 1mg fish	$\text{day}^{-1}\text{.mgC}^{1-\kappa}$
c_g	Maximum growth rate for 1mg fish	$\text{day}^{-1}\text{.g}^{1-\kappa}$
$C(\rho)$	Fraction of net assimilate allocated to S	dimensionless
D	Maximum attack distance of a fish of size L	dimensionless
$D(\gamma)$	Maximum attack distance for γ	dimensionless
$D_{i,j}$	Observed weight for j and i	g
$e_{i,j}$	Error for j and i used in W_1 and W_2	dimensionless
F_b	Rate of energy loss through faeces	cal.day^{-1}
$f(W)$	Weight function in E&H growth model	dimensionless
G	Specific growth rate	days^{-1}
G_c	Specific carbon growth rate	day^{-1}
G_e	Specific growth rate for E&H growth model	day^{-1}
$g(W)$	Temperature function in E&H growth model	dimensionless
h_1	Coefficient of catabolism	dimensionless
h_2	Coefficient of anabolism	dimensionless
i	Age-class	dimensionless
j	Cohort	dimensionless
k	Single constant value of $\phi(t)$	dimensionless
k_1	Arbitrary constants	dimensionless
k_2	Arbitrary constants	dimensionless
L	Fish Fork Length	cm

M	Maintenance rate	mgC.day^{-1}
m_1	Date of first migration	day
m_2	Date of second migration	day
M_H	Uptake rate for a healthy fish	mgC.day^{-1}
M_{HO}	Maintenance cost rate scale	mgC$^{(1-\nu)}$.day^{-1}
n	Sample size	dimensionless
n_1	Allometric factor for catabolism	dimensionless
n_2	Allometric factor for anabolism	dimensionless
p	Food particle length	cm
P	Probability	dimensionless
p_1	Minimum food particle size	cm
p_2	Maximum food particle size	cm
P_b	Rate of energy loss through gamete production and somatic growth	cal.day^{-1}
$P_{i,j}$	Predicted weight for j and i	g
$P(r,p,L)$	Probability of food item of size p being caught at r from a fish of size L	dimensionless
$Q1_{i,j}$	Upper quartile value of j and i	g
$Q3_{i,j}$	Lower quartile value of j and i	g
r	Minimum Distance of approach of food perpendicular to fish in bodylengths	dimensionless
R	Reserve carbon weight	mgC
r_1	Ratio of $W_r(m_1)$ to $W_p(m_1)$	g
r_2	Ratio of $W_r(m_2)$ to $W_p(m_2)$	g
R_b	Rate of energy loss through respiration	cal.day^{-1}
S	Structural carbon weight	mgC
t	Time	days
T	Water temperature	^{o}C
t_0	Starting time for simulations	day
T_0	Temperature at which zero growth occurs	^{o}C
T_A	Uptake characteristic temperature	^{o}C
T_L	Low temperature limit for growth	^{o}C
T_{lag}	Temperature from the previous week	^{o}C
T_m	Mean annual temperature	^{o}C
T_M	Optimum temperature for growth	^{o}C
T_R	Maintenance cost characteristic temperature	^{o}C
T_{RN}	Reformulated SMR characteristic temperature	^{o}C
T_U	High temperature limit for growth	^{o}C
U	Uptake rate	mgC.day^{-1}
U_b	Rate of energy loss through excretion	cal.day^{-1}
U_H	Uptake rate for a healthy fish	mgC.day^{-1}
U_{HO}	Uptake scale	mgC$^{(1-\kappa)}$.day^{-1}
U_{max}	Maximum uptake rate	mgC.day^{-1}
v	Water velocity	cm.days^{-1}

W	Live weight of the fish	g
$W_{0,97}$	Initial mean weight of the 1997 cohort	g
$W_{0,96}$	Initial mean weight of the 1996 cohort	g
W_1	First weighting function	dimensionless
W_2	Second weighting function	dimensionless
W_c	Total carbon weight	mgC
W_{c_1}	Weight of first smolting threshold	g
W_{c_2}	Weight of second smolting threshold	g
$W_{eff}(L)$	Effective biomass available to fish	mgC.cm^{-4}
$W_h(v, L, T)$	Effective half saturation food density	mgC.cm^{-4}
W_∞	Asymptotic Weight	g
$w(p)$	W-L relationship for food particles	mgC
$W_p(t)$	Mean weight of total population at t	g
$W_r(t)$	Mean weight of resident population at t	g
W_T	Final predicted weight of individuals	g
x	Allometric Factor	dimensionless
α	Scaling coefficient of A_T	dimensionless
α_1	Consumption coefficient	$\text{mgC.cm}^{-3}\text{.days}^{-1}$
α_{CGM}	CGM biomass distribution	day^{-1}
α_S	Scaling constant for food step function	$\text{mgC}^{1-c_1}\text{.day}^{-1}$
$\alpha_S(t)$	Scaling coefficient for $\Phi_1(t, S)$	$\text{mgC}^{1-c}\text{.day}$
α_{UFR}	UFR scaling constant for consumption	$\text{mgC}^{1-c_1}\text{.day}^{-1}$
γ	Size of food particle relative to fish size	dimensionless
Γ_0	Constant biomass distribution	mgC.cm^{-4}
γ_{opt}	Optimum food particle relative to fish size	dimensionless
γ_{min}	Minimum food particle relative to fish size	dimensionless
γ_{max}	Maximum food particle relative to fish size	dimensionless
$\gamma(\rho)$	starvation response function for uptake	dimensionless
Δ	Size of hungry to torpid hysteresis	dimensionless
ϵ	RMS error	dimensionless
ε	Assimilation efficiency	dimensionless
$\zeta(p)$	Size frequency distribution of food	cm^{-4}
θ	Reserve control sensitivity	dimensionless
κ	Uptake rate allometric index	dimensionless
$\lambda(\rho)$	starvation response function for maintenance	dimensionless
ν	Maintenance cost rate allometric index	dimensionless
$\xi(T)$	See page 44-45	$\text{mgC}^{(1-\kappa)}\text{.day}^{-1}$
$\xi_{\gamma L}$	Torpid SMR/Normal SMR	dimensionless
$\xi_{\lambda L}$	Torpid uptake/Normal uptake	dimensionless
ρ	Reserve to structural weight ratio	dimensionless
ρ_0	Ideal reserve ratio	dimensionless
τ_2	Threshold ρ/ρ_0 for torpidity	dimensionless
$\tau_h(L, T)$	Handling time per unit biomass	days.mgC^{-1}
$\tau(L, T)$	Handling time per item of food	days

Φ	Food supply	mgC.day^{-1}
$\Phi_1(t, S)$	Food available in step function	mgC.day^{-1}
ϕ_i	Average value of $\phi(t)$ for an individual	dimensionless
ϕ_m	Average value of $\phi(t)$ for population	dimensionless
$\Phi(R, S, T)$	Seasonal dependent food supply	mgC.day^{-1}
$\phi(t)$	Function or index to estimate the quality of environment for parr growth	dimensionless
ϕ_y	Annual values of $\phi(t)$	dimensionless
Ψ_M	See page 44	mgC$^{(1-\kappa)}$.day^{-1}
Ψ_A	See page 44	mgC$^{(1-\kappa)}$.day^{-1}
$\psi(T)$	Temperature dependent changes in food supply	dimensionless

List of acronyms contained within this thesis

Acronym	Meaning
bl	Body lengths
c.v.	Coefficient of variation
CGM	Compensatory Growth Model by Broekhuizen et al. (1994), see section 3.2.
CGM_e	*CGM*/*E&H* Hybrid Growth Model, see section 3.4.
CI	Confidence Intervals
DeeCAMP	Dee CAtchment Management Planning
DSO	Downhill Simplex Optimisation
EF	Electro-Fishing
E&H	Functional parr growth model by Elliott & Hurley (1997), see section 3.3.
EOD	Estimated Ova Deposition
GG73-74	1973-1974 EF data set from Gardiner & Geddes (1980)
GG74-75	1974-1975 EF data set from Gardiner & Geddes (1980)
GIS	Geographical Information System
MD	Mean Deviance
MWE	Mean Weighted Error
MWS	Multi-Sea Winter
NPP	Non-Precocious Parr
PP	Precocious Parr
RMS	Root Mean Square error
RPL1	Data set from Randall & Paim (1982) from site L1
RPC2	Data set from Randall & Paim (1982) from site C2
SGR	Specific Growth Rate
SMR	Standard Metabolic Rate
SE, s.e.	Standard Error
SSVG1	CGM_e fitted to EF data adjusting ϕ_y and the two threshold lengths for smolting whilst assuming data has a gamma distribution
SSVN1	CGM_e fitted to EF data adjusting ϕ_y, the threshold lengths for smolting and with constant c.v.
SSVN2	CGM_e fitted to EF data adjusting ϕ_y and the two threshold lengths for smolting whilst assuming data is normally distributed
SSVN2M	The SSVN2 model fitted to the data from the middle section using estimated temperatures from the middle section
SSVN2L	The SSVN2 model fitted to the data from the lower section using estimated temperatures from the lower section
SSVN2U	The SSVN2 model fitted to the data from the upper section using estimated temperatures from the upper section
SSVN3	The SSVN2 model fitted to the entire data set
SSVN4	The SSVN3 model fitted to the entire data set with variable threshold lengths for smolting

T_1	Habitat type: Rather deep and rapid flow, boulders and rough stones
T_{1A}	Habitat type: Shallow and fast flow, small boulders and rough stones
T_2	Habitat type: Rather deep with slow flow, boulders, coarse gravel and silt
T_3	Habitat type: Median to fast flow water, gravely spawning area
T_P	Habitat type: Deep and generally slow flowing
UFR	Uptake functional response Model, see chapter 8
W-L	Weight-Length
WFD	Weight-Frequency Distribution
WSD	Weighted Sum of Deviance

Contents

Chapter 1

General Introduction

> "For many years I have scarcely done anything else either officially or privately, except to attend to and carefully watch the interests of the King of Fish, the great *Salmo salar*."

So wrote Buckfield (1880), a sentiment echoed by Jones (1959) many years later. Their fascination with the Atlantic salmon is one shared with many, as the salmon is a species that has managed to capture the public imagination. This is partly because of the great variety they exhibit during their life, occupying several ecosystems and embarking on migrations which may be thousands of kilometres long, before returning to their natal rivers to spawn. They have also been hunted for sport for centuries, and as the number of salmon fishing rivers decreases, has led to the sport becoming more exclusive and of great economic value to the regions which they still inhabit (Anon. 1997).

Salmon have always been an important source of food, and the last 30 years has seen the growth of large scale salmon aquaculture, which has coincided with a reduction in the commercial fishing of wild salmon, in particular the off-shore fisheries in the North Atlantic near Greenland and the Faeroe Island (Parrish et al. 1998). Wild Atlantic salmon are still considered a delicacy, but there have been further and more recent reductions in exploitation rates by coastal and freshwater fisheries. This has been in response to global declines in the wild Atlantic salmon population (Gross 1998).

1.1 Life History of the Atlantic Salmon

Atlantic salmon originally occurred in all the countries whose rivers flowed into the North Atlantic Ocean and the Baltic Sea (Mills 1989). Now, however, the populations in some of Europe's major rivers, such as those along the northern coast of continental Europe from Poland to France, and in southern England, have disappeared (Parrish et al. 1998). They are still to be found in Europe from as far north as Norway, Finland and Russia to as far south as Portugal and Spain, and in North America from Greenland and Arctic Canada to New England in the U.S.A. (Folt et al. 1998).

The Atlantic salmon is an anadromous species, which means it breeds and spends the juvenile stages of its life in freshwater but migrates to the sea for part its adult life. There are exceptions to this general rule, and several nonanadromous land-locked subspecies of salmon are known to exist (e.g. *S. salar sebago*). For those that do migrate to sea, salmon from both sides of the Atlantic converge to similar feeding grounds in the North Atlantic, except for those from the Baltic rivers, which tend to feed in the Baltic Sea and East Atlantic (Carlin 1969). Salmon generally spend one or two (rarely three or four) years at sea before returning to freshwater to spawn (Hutchings and Jones 1998). Those that return after one full year at sea are called grilse, those that return after more than one year are called multi-sea-winter (MSW) salmon.

Atlantic salmon possess a well developed homing ability enabling many of surviving adults to return to their natal rivers to spawn (Mills 1989), which will usually occur during autumn, the timing likely to be temperature dependent (Webb and Mclay (1996), Heggberget (1988)). During spawning, the adult females will construct a nest into which she will lay her eggs, called a redd. Adult males compete for the best position along side the females in order to fertilise the eggs (Jones 1959). Also, sexually mature male parr compete amongst themselves, and occasionally with the adult males, to fertilise ova (Fleming 1996). Once fertilisation has taken place, the female covers the redd with gravel, and may go on to construct another redd (Fleming et al. 1997). Most adults die shortly after spawning, (on average 89% of the total, and 78% of the females and 96% of the males (Fleming 1998)), but the survivors, known as kelts, return to the sea, and may spawn again.

The following spring, the eggs hatch and the young salmon, called the alevins, are born with a yolk sac which they live off whilst in the redd (Gorodilov 1996). Once this is depleted they leave to redd as fry. The rates of developments of the eggs and the time of hatching and emergence from the redd are thought to be dependent on temperature (Egglishaw and Shackley (1977), Brannas (1986), Jensen et al. (1989), Crisp (1981)).

The fry disperse from the redd and seek to establish territories, which they will defend against intruders. During this time, competition is severe, and the mortality rates at their highest (Egglishaw and Shackley 1977), where death may occur through predation or starvation (Gardiner and Geddes 1980). When the fry are about 6.5-7.0 cm in length, they start to develop dark blotches along their sides, known as parr marks, and are now defined as parr (Mills 1989).

It is within the defended territories that parr and fry capture and consume their food (Kalleberg (1958), Keenleyside and Yamamoto (1962)). The majority of their diet consists of invertebrates captured from the water column (Allen (1941a), Egglishaw (1967)). They are also able to capture invertebrates of terrestrial origin which fall onto the water surface, as well as being able to forage in the substrate for food, (Stradmeyer and Thorpe (1987a), Wankowski and Thorpe (1979a)) and the larger parr have been known to take fry and ova (Egglishaw 1967). Rapid growth occurs during this period, typically when temperatures exceed 6-7°C (Allen (1940), Allen (1941b), Allen (1969), Gardiner and Geddes (1980), Cunjak (1988), Elliott (1991)). This period of growth, which may last from spring to autumn depending on altitude and latitude, is called the growing season.

Egglishaw and Shackley (1977) found an inverse relationship between salmon fry density and their lengths at the end of the growing season, whilst Prouzet (1978) found that the growth of fry was density dependent for one stream with a steep gradient, but in another stream with a lower gradient, the biomass was regulated by emigration. However, in the Miramichi River, New Brunswick, growth of salmon fry was inversely related to population density, but growth of the parr was not (Randall (1982), Randall and Paim (1982))

The juvenile salmon live along side other fish species in most rivers, such brown trout (*Salmo trutta*) and brook trout (*Savelinus fontinalis* Mitchill). Studies look-

ing at the level of competition between juvenile wild salmon and brook trout observed depression in the growth rates of the salmon (MacCrimmon et al. (1983), Gibson and Dickson (1984)). These studies were conducted in habitats which are preferential to brook trout, and the authors concluded that in the preferred salmon habit, intraspecific competition within year classes of salmon is more severe than the interspecfic competition from the brook trout. Competition between salmon and brown trout was looked at by Gibson and Cunjak (1986) who found that the two species were spatially segregated, and they concluded that the two species were ecologically compatible and competition appeared to be minimised by habitat segregation.

As winter approaches, the juveniles appear to undergo a decrease in feeding motivation, and feeding activity is reduced or stops (Metcalfe et al. (1986), Metcalfe et al. (1988)). During this time their physiological state changes (Berg and Bremset (1998), Shackley et al. (1994)) which coincides with the young salmon changing their habitat. They leave the relatively shallow fast flowing riffles preferring to spend long periods beneath the substrate (Rimmer et al. (1983), Gibson (1978)), which lasts until the water becomes warmer the following spring and they emerge to begin feeding again.

It is possible for both male and female anadromous salmon to become sexually mature whilst they are still parr. This is rare for females, (Gibson (1983), Youngson and Hay (1996)) and may be due to the benefits (e.g. pre-reproductive survival) not being great enough to outweigh the costs (e.g. reduced fecundity and competitive ability) (Fleming 1998). However, early maturation of males is common, and in some populations, up to 100% of males have been estimated to have matured early as parr during their life history (Fleming 1998). There are cost involved to the mature male parr (often called precocious parr) in terms of growth retardation (Myers et al. 1986) and survival (Myers (1984), Berglund et al. (1992)) but a large proportion of the eggs may get fertilised by male parr, estimated at about 11% by Jordan and Youngson (1992) for the Girnock Burn in Scotland.

During the autumn there are large movements of parr (Calderwood 1906), many of which may be precocious males (Pyefinch and Mills 1963), which are in search of adult females (Buck and Youngson 1982). It has also been suggested that the autumn migrants may be the forerunners of the following spring migration (Mills

1989). At this time, they have yet to undergo the physiological adaptation to seawater, called smolting, and maintain their parr-like appearance.

Smolting occurs during the spring, after the parr have spent a numbers of years in freshwater, the time to smolting generally varies with the latitude from as little as 1 year for males in France (Bagliniere and Maisse 1985) to up to 10 years for some anadromous salmon in the Ungava river of Northern Quebec (Powers (1969), Robitaille et al. (1986)). In Scotland, parr tend to smolt after between two and four years in freshwater (Buck and Youngson 1982). Symons (1979) points out that, with the exception of the Ungava rivers, average smolt age of any particular river can be estimated from the number of days each year on which water temperature reaches or exceeds 7°C. Once they have left the rivers, they migrate to their feeding grounds as post-smolts, and begin the marine phase of the life.

1.2 The Status of Wild Salmon in Scotland

The wild Atlantic salmon of Scotland are an important natural resource, both economically and environmentally. Although salmon are now extensively farmed for food on the West Coast of Scotland (more than 94% of worldwide Atlantic salmon population has been estimated to be in aquaculture (Gross 1998)), there are still commercial fisheries for wild salmon. However, the main source of revenue for wild salmon is through sport. In 1995, it was estimated that salmon angling on the River Dee in Scotland contributed between £5 million and £6 million a year to the local economy of the Grampian region (Anon. 1997).

The salmon also form an important part of the ecosystem of Scotland as they are preyed upon by a number of animals during all stages of their lives. During the juvenile phase, older parr and brown trout will eat the fry, and the salmon parr and smolts may be eaten by burbot (*Lota lota*) and the pike (*Esox lucius*) (Mills (1964), Mills (1989)). As parr and smolts, they are prey to fish eating birds, such as sawbill ducks (*Mergus merganser* and *M. serrator*) and the cormorant (*Phalacrocorax carbo*) (Mills (1962), Mills (1965), Blackwell et al. (1997), Feltham and MacLean (1996), Kennedy and Greer (1988)). They have been found in the stomachs of many marine fish whilst at sea, (See Wheeler and Gardner (1974)),

and as adults, they are eaten by the grey seal (*Halichoerus grypus*) and the common seal (*Phoca vitulina*) near estuaries (Rea (1960), Rea and Shearer (1965)). Further up stream, otters (*Lutra lutra*) are known to feed on the adult salmon (Carss et al. (1990), Hewson (1995)).

Part of the MSW adult salmon population are called springers. The springers are salmon that have been at sea for at least two winters, but return to freshwater in the spring, as opposed to autumn for the other MSW salmon. The springers have greater commercial value, as they extend the fishing season, and is the group presently showing the greatest decline in Scotland (Youngson 1994). The number of females counted in the Girnock Burn, a tributary of the River Dee is shown in Fig. 1.1, where the adult population is dominated by springers. There is at present much work being conducted to identify the reasons for the decline and develop management techniques to enhance to current salmon stocks.

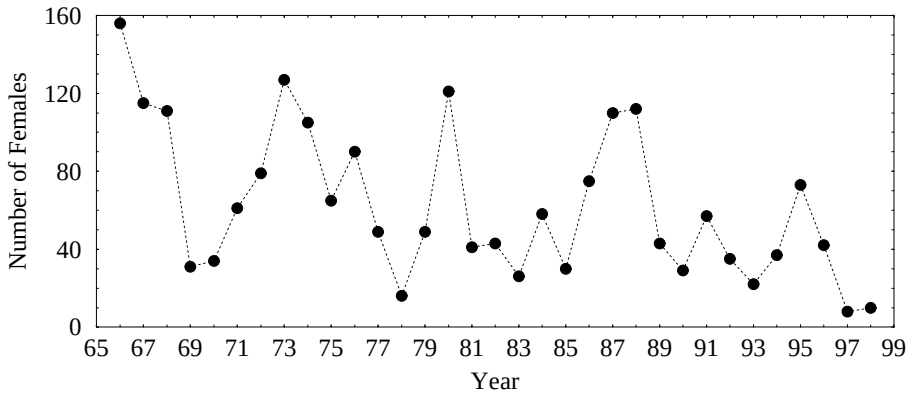

Figure 1.1: *Number of adult females caught at the Girnock burn from 1966 to 1998. Data supplied by FFL.*

Scotland has a long history of salmon conservation, with legislation concerning salmon in Scotland dating back to the 14th and 15th centuries, which involved protecting smolts. Other early legislation was intended to allow salmon access to spawning ground and prohibited to killing of fish during the spawning season (Anon. 1997).

The majority of management techniques are applied at the freshwater stages of the salmon life cycle. This is due to the marine phase being hard to manipulate, though exploitation at sea has been reduced with the closure of many deep sea fisheries in the North Atlantic, angling organisation buying up deep sea fishing

permits to protect wild stocks and international treaties aimed at reducing marine exploitation rates (Vigfusson and Ingolfsson 1993).

The fate of the returning adults has been improved through attempts to increase the proportion of the population likely to spawn. This may be through the control of the numbers of predators, such as mergansers (Elson 1962), (but there is debate as to the effectiveness and ethics of these measures (Davidson and Bielak 1993)), and by restricting activities of coastal and fresh water fisheries through the introduction of quotas (May 1993). The removal of fish through angling has attempted to be minimised by capture-release programs, whereby the angler releases some or all the salmon which are caught (Walker and Walker (1991), Webb (1998)) and also the fishing season in some rivers have been reduced (Mills 1993).

Measures have also been taken to improve the habitat quality of spawning and nursery streams in the hope to improve survival rates and increase the carrying capacity (Shearer 1993). The range of rivers available to salmon has been increased by the construction of fish ladders that allow the adults to migrate to otherwise inaccessible parts of the stream. They have been constructed where dams or other water works have impeded to upstream migration of the salmon (Skalski et al. (1996), Gowans et al. (1999)). Attempts to reintroduce salmon have been made in rivers where they were once abundant, but have since disappeared (Mckeon and Stolte 1993). These disappearances may have been due to pollution and the activities of man, so the water quality has been improved to levels suitable for salmon (Parrish et al. 1998). These methods are aimed at increasing the smolt output in the hope of increasing the numbers of returning adults.

Many enhancement strategies involve stocking rivers where populations have declined below the estimated carrying capacities of the rivers. This may include planting out ova or hatchery reared fry into the rivers (Harris (1978), Kennedy (1988)). Studies have revealed that genetic differences exist between the populations of different rivers, and among fish living in different parts of the same river system (Jordan et al. 1997). This may due to adaptation to a particular environment and introduction of the progeny from different rivers may lower the overall fitness of the fish in that part of the river, with lower returned rates for the stocked fish than the native fish (Garcia de Leaniz et al. 1989).

Efficient stocking strategies maximise the smolt output from the numbers of eggs or fry planted into the river. This requires an understanding of the stock-recruitment relationship. There is at present debate over the shape of the stock-recruitment curve with some studies suggesting that it is domed shaped (Crozier and Kennedy (1995), Gee et al. (1978)) as proposed by Ricker (1954), and others that it is asymptotic (Buck and Hay (1984), Jonsson et al. (1998)). Either way, both relationships imply that there is an optimal stocking density given that there are limited resources. However, these relationships are of limited use as they do not take into account changing environmental conditions, which will influence growth rate and when the parr will smolt.

A successful stocking strategy will then require knowledge of when members of the population will smolt. This will be determined by how the social and physical environment of a river effects the growth rate of the parr. In order to predict the growth rates of the members of the population, a model for individual growth of juvenile parr is required.

1.3 Aims and Objectives

The life of the Atlantic salmon is very complicated, with each parr facing different choices at different stages of its life. These may be when to migrate, to become precocious or where to choose a territory. These choices, which effect the dynamics of the population, invariably depend on the growth rate of the parr (Metcalfe et al. 1990). If we are to understand the dynamics of the population, then we must first be able to understand the growth of the individuals in the population.

Growth of the parr will depend on the abiotic as well as the biotic environment. It is also likely to depend on its interactions with conspecifics within and between cohorts (its social environment). Thus, density may affect growth through competition for limited resources such as territory space. In the wild, such effects are hard to isolate due to the number of other effects on growth, such as temperature and prey abundance. In order to examine growth in the social environment, we must first remove to the effects of the physical environment.

An individual based growth model will be used to model the growth rate of the

juvenile salmon. Whereas a stochastic model would have the advantage of allowing us to model the variability in the growth rate of the whole population, the most probable growth trajectory is likely to follow that predicted by a deterministic model. This trajectory would be the one of primary interest to us, as we would be initially looking at the performance of an average individual in the cohort. It will also be best suited to the type of data that is available, which is examined in Chapter 2.

The model will be designed to predict growth rates in the wild of the resident population using factors in the physical environment as driving variables. It is also intended to predict the dynamics of the smolts from each cohort. This will allow scope for the examination of the social environment on the growth rate, which can then be used as a management tool for stocking rivers.

1.4 Structure of the Thesis

The Girnock Burn, a tributary of the River Dee in Scotland, has been a monitoring site for salmon since 1966. Historical data sets collected there will form the basis of the data that will be used in this thesis. Chapter 2 provides a description of the site and methodology, and some exploratory data analysis that will enable us to adopt the most appropriate strategy.

A number of growth models exist in the literature and Chapter 3 contains a review of these models. A hybrid model is developed from two of these and is parameterised for Atlantic salmon reared at satiation in a tank environment.

This model is adapted to predict the growth rates of wild salmon parr and a method of fitting the model to the data is developed in Chapter 4. The sensitivity of the input variables on the fit of the model to the data is also examined.

Additional data was collected at the Girnock Burn for individuals that were marked from June 1998 until March 1999. In Chapter 5, the model was fitted to this data to test two things. The first was whether the model could actually reproduce the observed growth trajectories of individual wild parr throughout the year. The second was whether fitting to the model to the weights of individuals was substantially different to fitting to the mean weights of the population.

Aspects of smolting are included into the growth model in Chapter 6, which enables to model to predict the weights of the resident parr and lengths of the smolts. Other aspects of the population are estimated, such as the variation of the parr weights and smolt lengths, and the proportions of smolts leaving each cohort at different age-classes.

The model was then fitted to additional data sets from the Girnock Burn, in Chapter 7. Derived estimates of the growth rates in different parts of the Burn were then compared.

A foraging model to estimate consumption rates is derived in Chapter 8 and is fitted to data collected from parr in different streams. The model is fitted to the data by assuming different characteristics of the prey populations available to the salmon, such as a temperature and seasonally dependent size-frequency distribution of the prey.

Chapter 9 contains a summary of the work with a description of what this analysis can tell us about the salmon population. Improvements to the model are suggested and future work proposed which would improve the model to make it a more effective tool for management.

Chapter 2

Data Analysis

2.1 Introduction

Atlantic salmon are widely distributed across Scotland, among some 400 salmon rivers. Among salmon sport fishermen, these salmon rivers are amongst the most highly regarded in the world. Due to the physical landscape of Scotland, the longer and more productive rivers tend to be on the East Coast (Anon. 1997). The River Dee is one such river, which is about 126km long, flowing from the Cairngorm Mountains to the North Sea at Aberdeen. It has 17 major tributaries and a catchment area of approximately 2,100 km^2 which rises to an altitude of approximately 1200m (Maizels 1985). It has been described as perhaps having the greatest length of first-class salmon fishing in Britain (Ashley-Cooper 1987), and between 1952 and 1992 has yielded on average 39% of the total reported Scottish rod catch of MSW salmon landed before April (DSFIA 1994).

Production on the River Dee is extensively monitored (Shearer 1985), particularly at the Girnock Burn, a tributary of the River Dee. This tributary has been kept free from fishing and has been a monitoring site since 1966, and is where many studies have been conducted (Buck and Youngson (1982), Youngson et al. (1983), Buck and Hay (1984), Hay (1987), Armstrong and West (1994), Youngson et al. (1994), Moir et al. (1998)). The majority of the data that will be used in this thesis are from the Girnock Burn and were collected by FRS[1], and covers the period from 1966 to 1999.

[1]The Fisheries Research Services, The Freshwater Fisheries Laboratory, Faskally, Pitlochry, Perthshire, PH16 5LB

2.1.1 The Girnock Burn

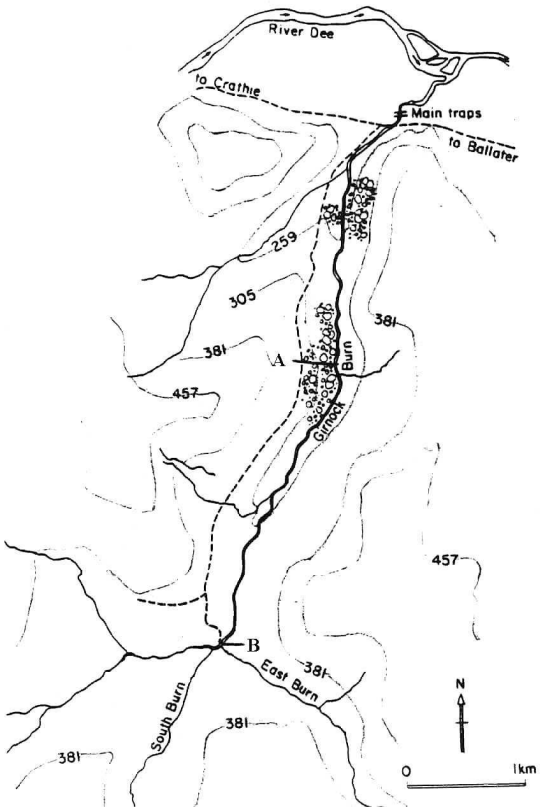

Figure 2.1: *Map of the Girnock Burn* (Buck and Hay, 1984). *The part of the stream between the fish traps and* A *is the lower section, between* A *and* B *is the middle section, and above* B *is the upper section.*

The Girnock Burn flows from a catchment of area 29.77km^2 and joins the River Dee at an altitude of 230m, and about 80km from the sea. The catchment, which rises to an altitude of 570m, contains 32.68 km of streams, with an estimated 11.05km to 13.32km being available to wild salmon (Webb and Bacon 1999). Granite rock dominates the geology of the catchment, particularly in the upper part of the catchment, with schist's and other metamorphic rock being more extensive in the lower reaches (Moir et al. 1998). A map of the burn is shown in Fig. 2.1.

Heather and 'peatlands' (grouse moor) comprises 89% of the vegetation, with 6% rough grass, 3% conifer, 1% broadleaf and mixed woodlands, the remaining 1% being of other types. Deer stalking and grouse shooting takes place during autumn and winter in the upper reaches of the catchment, where heather

dominates. Other fish, as well as salmon, inhabit the Girnock Burn, and include brown trout and sea trout, (*Salmo trutta*), eels (*Anguilla anguilla*), brook lampreys (*Petromyzon planeri*) and minnows (*Phoxinus phoxinus*) but compose less than 3% of the fish population. There is little vegetation within the stream but filamentous algae are widespread in the spring and decaying leaves settle in the lower reaches. The most common invertebrates are the larvae of Chironomidae and Simulidae, Ephemeroptera (mainly *Baetis* spp.) and Plecoptera (mainly *Leuctra* spp.) (Buck and Hay 1984)

The climate and flow rates in the catchment are highly variable and exhibit strong seasonality. The catchment receives an average of 1100mm of precipitation annually, up to 25% of which falls as snow, with the driest months being from May to August (Warren 1985). The river has a mean annual discharge of $0.5 m^3 s^{-1}$ although flow between June and August rarely exceeds $0.1 m^3 s^{-1}$ (Moir et al. 1998). The peak flow rates occur during the spawning season (October and November) and the spring, due to snow melt, when the smolts are migrating downstream.

2.1.2 Data Collection at the Girnock Burn

The Girnock Burn was chosen as a study site for the Dee as it represented what was viewed as a typical salmon spawning stream of the Dee. Adult salmon found in the Girnock are both grilse and MSW salmon, typically 85% of which are 2-sea winter fish (Moir et al. 1998). The juveniles in the stream emigrate both in autumn, as precocious males and sexually immature parr, and during the spring as smolts, the majority of which leave two or three years after hatching (Buck and Youngson 1982).

The salmon population was monitored using three methods. The first was by conducting fishing surveys in different parts of the burn to assess the resident parr population, which is described in Section 2.3. The other two were by collecting data from an adult fish trap at the lower end of the burn, which would be able to capture all the adults ascending the burn in order to spawn, and from a smolt trap, near the adult trap, which attempted to capture all the migrating fish as they descended the burn (Section 2.4). In addition, water temperatures at the burn were monitored and are described in Section 2.2.

2.1.3 The 1978 Experimental Manipulation of the Girnock Burn

In the autumn of 1978, a relatively low number of adult females were caught in the adult trap as they ascended the burn to spawn. It was decided that these adults should be prevented from spawning above the trap, in order that there be no cohort born in 1979. The effect of this 'missing cohort' on the survival and growth rates of previous and future cohorts could then be monitored, and would be an indication of how the resident fish would be affected by a large change in their social environment.

2.2 Temperature Measurements at the Girnock Burn

Records of water temperatures recorded at the Girnock burn fish trap are available from May 1968 until December 1996. The first part of this data set from May 1968 until May 1986 was collected using a continuous water temperature recorder which traced out temperature measurements on rotating paper discs that were changed weekly. These recordings were summarised by averaging daily maximum and minimum temperatures over the whole month. In 1986, the continuos recorder was replaced by a digital recorder, which took temperature measurements every 15 minutes and these temperatures were also summarised into monthly averages. However, gaps remained in the data set due to mechanical failure of the continuous recorder. Temperatures for these missing months were estimated using polynomial interpolation across months. Thus a data set was compiled for the mean monthly temperatures from May 1968 until December 1996, and the mean annual temperatures are plotted in Fig. 2.2.

There is no significant trend in these estimated annual temperatures, and the only significant monthly temperature change with time in years was for April, which increased with year ($F_{1,25} = 3.71,\ P < 0.01$). However the general monthly trends indicated that the summer temperatures (March to August) are increasing whilst the winter temperatures are decreasing (September to February). This is shown in Fig. 2.3, where the coefficient for the slope of the regressions between mean monthly temperature and year are shown with the 95% confidence intervals.

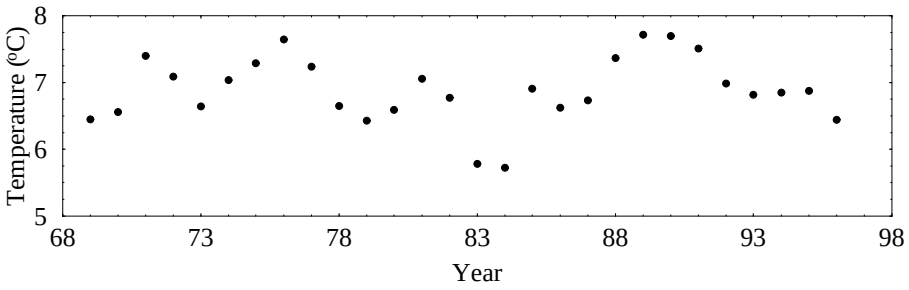

Figure 2.2: *Estimated mean annual temperatures at the fish trap on the Girnock Burn from 1969-1996.*

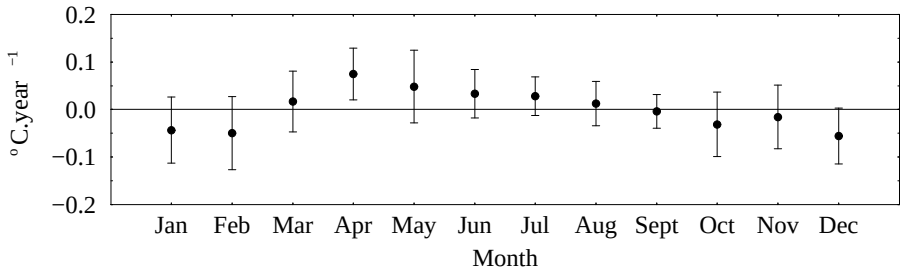

Figure 2.3: *The values of the slope coefficient with its 95% confidence intervals from regressions with mean monthly temperature as the predicted variable and the year as a covariate.*

2.3 Electro-Fishing Data from the Girnock Burn

Samples of the resident parr population were collected by electro-fishing. This involves using an electric device to stun fish so that they can be caught with ease and without causing permanent injury (Jones 1959). The reliability of these surveys may be highly variable and depends on the efficiency of the equipment and the characteristics of the environment in which it is used, such as the conductivity, turbidity, water velocity and water depth (Mills 1989). The electro-fishing methodology of the surveys on the Girnock were shown to be reliable through experiments involving fishing to extinction by R. Chalmers of FRS (unpublished data) but there may still be uncertainty associated with density estimates. However, there is very little reason to believe that even inefficient electro-fishing would bias the sample collected with regard to estimates of the parr sizes.

The electro-fishing data was collected during July and August each year from 1969 to 1986 (except 1980), from the Girnock Burn, in order to monitor population

levels. The burn was divided into five different habitat types, defined according to substrate type and current, which are listed in Table 2.1. In 1969 all five habitat types were fished after which fishing in T_P was abandoned due to the low numbers caught. After 1977, only T_1 and T_{1A} were fished.

Table 2.1: *Definition of the five habitat types in the Girnock Burn.*

Name	Current	Substrate
T_1	Rather deep and rapid flowing	Boulders and rough stones
T_{1A}	Shallow and fast flowing	Small boulders and rough stones
T_2	Slow flowing and rather deep	Boulders, coarse gravel and silt
T_3	Median to fast flow	Gravely spawning area
T_P	Deep and generally slow flowing	

The burn was also divided into four sections based on altitude, called the upper, middle and lower section for the main stem of the Girnock (see Fig. 2.1), and in addition, a small tributary, the South Burn was fished from 1969-71. The areas for each section and each habitat type within them are given in Table 2.2. From 1977 to 1986, fishing was restricted exclusively to the middle section.

Table 2.2: *Area of different habitat types within different stream sections, in* m^2*, estimated by FRS.*

	T_1	T_{1A}	T_2	T_3	T_P	*Total*
Lower Section	13329	4728	2786	297	208	21348
Middle Section	7510	12077	813	4274	686	25360
Upper Section	4203	5037	1379	959	474	12052
South Burn	3481	4416	1898	258	748	10801
Total	28523	26259	6877	5788	2117	69565

The age of the salmon can be determined by examining scale samples from the fish, and thus its year of birth. As the salmon grow, a ringed pattern is produced on the scales. The distance between the rings depends on the rate of growth of the salmon. Periods where the spaces between the rings are relatively large indicate summer growth, and the converse for winter growth. Scale samples can accurately determine which cohort a fish is from. The age of a parr is defined by the number of periods when the rings are close together (i.e. the number of winters), so a fish which was born in April and sampled the next February will

be defined as a one year old fish. If there is some summer growth on the youngest part of the scale (indicating the fish was caught when it was growing well) then a '+' is added to the age. Therefore a fish born in April and sampled the following September will be defined as a '0+' fish. This notation will be used throughout this thesis.

The method of electro-fishing has remained the same for each site during every year. An area of between $100m^2$ and $150m^2$ was fished three times with stop nets. The age of all fish caught was determined either by inspection or by taking scale samples. This was straightforward for the 0+ fry as there was a distinct difference in lengths between the largest 0+ and the smallest 1+ parr. The ages of the larger 1+ and all the 2+ and 3+ parr had to be determined by taking scale samples. Due to the large numbers of 0+ fish caught, only a small subsample had their lengths measured, and these were chosen randomly from those caught. All the other parr caught had their lengths measured.

There are gaps in the data set. For 1975 and 1976 there are no lengths available for the 0+ and only partial data for the 1+ fish (only the proportion scaled). No survey was conducted in 1980 due to high currents in the burn (this decreased the water conductivity and reduced the effectiveness of electro-fishing). The missing cohort from 1979 caused another gap in the data set.

2.3.1 Weight-Length Relationships

A useful functional growth model would need to predict changes in weight before it could predict changes in length, as the consumption rate would be required to have the same units as the fish weight. No weight measurements were taken during the electro-fishing surveys in the Girnock from 1969-1986, so a weight-length relationship was required to provide the link between the data and model predictions. This relationship is unlikely to be the same for parr throughout the year due to variations in their biological condition, e.g. over winter weight loss, but it only needs to be correct when the data measurements are taken (i.e. during the periods of the surveys).

The form of the weight-length relationship that we shall use will be the allometric

relationship of

$$ln(W) = ln(a) + x.ln(L), \tag{2.1}$$

which has been frequently used for fish (Manooch and Potts (1997), Dulcic and Kraljevic (1996), Petrakis and Stergiou (1995), Potts et al. (1998), Planes et al. (1997)). W is the wet weight (g) and L is the fork length (cm) of the fish[2], with a being a scaling constant (also known as the condition factor) and x the exponent (the allometric factor).

There are two sets of weight-length data available from the tributaries of the River Dee. The first is from two electro-fishing surveys carried out in the middle section of the Girnock burn on 27th July 1998 and 26th August 1998. During each of these surveys, two sites were fished once (both of habitat type T_{1A}), and the weights and fork lengths of all the parr caught were measured.

In addition to this, data was available from the River Ey, a tributary of the Dee at the top end of the catchment. It is in a U-shaped valley, where heather moorland dominates, and the main land use is grouse shooting. An electro-fishing survey was carried out at two different habitat types in the River Ey on 7th August 1996. The first site was habitat type T_1, and the second site was of type T_{1A}. At both sites, there was little vegetation in the river and no overhanging vegetation. Each site was fished three times and had an area of about 100m^2. A subsample of the 0+ fish and all of the older fish caught were weighed and measured for fork length.

Values of $ln(a)$ and x were derived by fitting equation (2.1) to the data the River Ey, and the two surveys from the Girnock Burn. The values found and their standard errors are shown in Table 2.3.

Table 2.3: *Parameters for equation.(2.1) to derive a weight-length relationship for juvenile salmon. The coefficients are shown with their standard errors brackets.*

River	*Date*	*ln(a)*	x	Sample Size
Ey	7/8/96	-4.608 (0.072)	3.046 (0.036)	98
Girnock	27/7/98	-4.734 (0.169)	3.115 (0.078)	72
Girnock	26/8/98	-4.708 (0.155)	3.099 (0.071)	92

[2]The fork length is defined as the length of the fish from its snout to the middle (the 'fork') of its tail. Other measurements that may be used are total length, e.g. Potts et al. (1998).

When the site was placed as a factor in the regression model for the Ey data, it was found not to be significant ($F_{1,95} = 0.0013,\ P = 0.972$). The derived parameters shown in Table 2.3 and are the same irrespective of habitat type or tributary. Their condition would be expected to change during different times of the year (e.g. over winter) or during periods of physiological changes (e.g. smolting or early sexual maturation).

It was therefore decided to convert the length measurements from the Girnock electro-fishing surveys into weights using equation 2.1 with the coefficients from the Ey in Table 2.3 for all the parr caught in each of the habitat types.

2.3.2 Size Differences of Parr Between Habitat Types

All parts of the Girnock Burn that were available to salmon could be classified into one of the habitat types defined in Table 2.1. Each of them contained parr aged 0+ to 3+, apart from type T_P. However, the density estimates varied between habitat types, to the extent that fishing was abandoned in type T_P after the first year, and the data collected from type T_P will be omitted from this analysis. From 1978 to 1986, only the two most productive habitat types, T_1 and T_{1A} (in terms of numbers caught), were fished. The differences in the habitat types may be enough to alter the growth rates of the parr significantly. It is therefore important to know if this is likely to happen, and if so, to what extent.

Box plots have been produced in Fig. 2.4 for each age-class in each habitat type for the years 1969-1977. In these plots, the centre line represents the median of the data with the box as the interquartile distance (IQD). The error bars extend to the extreme values of the data or a distance 1.5×IQD from the centre, whichever is less. For data having a Guassian distribution, approximately 99.3% of the data would fall within the error bars. The horizontal lines outside of the error bars are outlying values. These graphs also indicate whether the data may be skewed.

A one-way ANOVA was used to test if the variation within habitat types was greater than the variation between habitat types. This was shown to be true for the 0+ ($F_{3,858} = 18.73,\ P < 0.001$), 1+ ($F_{3,4235} = 89.19,\ P < 0.001$) and 2+ ($F_{3,2455} = 30.24,\ P < 0.001$) age-classes, but not for the 3+ age-class ($F_{3,136} =$

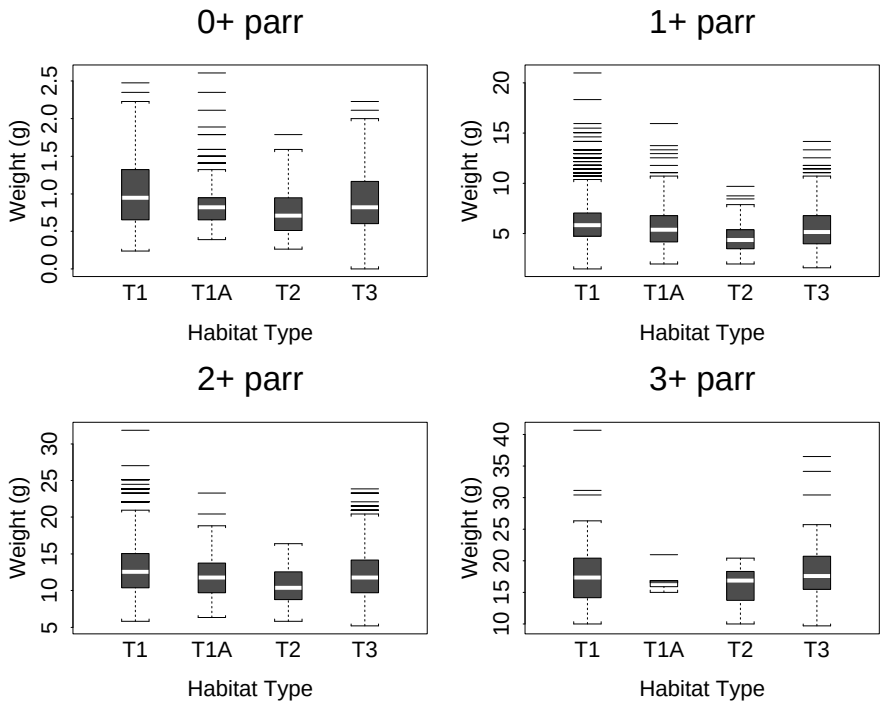

Figure 2.4: *Box-plot of the weights of the parr from different age-classes divided into different habitat types, from 1969-1976. For normally distributed data, approximately 99.3% of the data would fall within the error bars, and the horizontal lines outside of the error bars are outlying values.*

$0.78,\ P = 0.507$).

The mean weights from the different habitat are similar but there are systematic differences across the age-classes between the habitat types. These differences are emphasised in Table 2.4, which shows the mean weights predicted by the ANOVA with their standard errors. With the exception of the 3+ age-class, the mean weight of the fish caught in T_1 is always the largest, and the smallest fish are always caught in T_2. The fish caught in T_{1A} and T_3 tend to be similar in weight for the 0+, 1+ and 3+ age-classes and 2+ at T_{1A} being larger than those at T_3.

2.3.3 Size Differences of Parr Between Stream Sections

The Burn was divided into different sections based on altitude, which are given in Table 2.5. Shackley and Donaghy (1992) found a significant relationship between

Table 2.4: *Mean weights for different age-class predicted using a one-way ANOVA for the different habitat types fished from 1969-1976, with standard errors in brackets.*

Age-Class	T_1	T_{1A}	T_2	T_3
0+	1.034(0.023)	0.916(0.038)	0.743(0.031)	0.917(0.025)
1+	6.184(0.044)	5.547(0.126)	4.502(0.107)	5.500(0.046)
2+	12.80(0.088)	11.52(0.278)	10.66(0.269)	11.91(0.103)
3+	17.84(0.526)	16.86(2.026)	15.89(2.220)	18.80(0.785)

the length of 1+ parr and altitude in the Dee catchment, so it was important to know if there were systematic differences between in the weights of parr caught in different sections.

Table 2.5: *The maximum and minimum altitudes of the different stream section of the Girnock Burn.*

Stream Section	Min. Alt. (m)	Max. Alt. (m)
Lower	240	285
Middle	285	320
Upper	320	370

The data was divided into different age-classes and sections and has been summarised in the box-plots in Fig. 2.5. The data from the South Burn is not a reliable indicator of section effects as it was only fished in three years and subject to strong year effects. There are consistent differences between the median weights of parr from different sections across the three age-classes. The largest fish are found in the lowest section of the burn, followed by the middle section and then the upper section.

A one-way ANOVA was used to test if the variation within stream sections was greater than the variation between stream sections. This was shown to be true for the 0+ ($F_{2,859} = 161.26,\ P < 0.001$), 1+ ($F_{2,4236} = 351.16,\ P < 0.001$), 2+ ($F_{2,2456} = 215.65,\ P < 0.001$) and 3+ ($F_{2,137} = 15.79,\ P < 0.001$) age-classes. The mean weight predicted using the ANOVA are shown in Table 2.6, and for each age-class, the mean weight of the parr decreases with altitude.

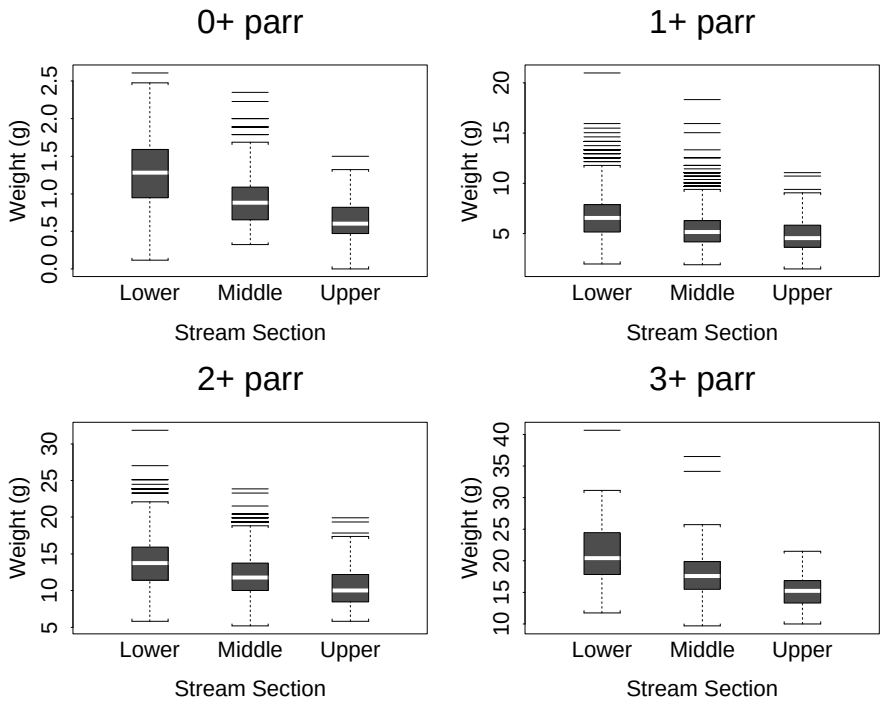

Figure 2.5: *Box-plot of the weights of the parr from different age-classes divided into the different stream section, from 1969-1976. For normally distributed data, approximately 99.3% of the data would fall within the error bars, and the horizontal lines outside of the error bars are outlying values.*

2.3.4 The Test Electro-Fishing Data Set

The data collection can be divided into two parts: that collected from 1969-77 and from 1978-86. The mean weights of the parr from each age-class during each year will depend on which habitat type and stream section the data is from. Therefore taking the average weight for all the parr of a particular age-class each year is inappropriate if we wish to examine changes in weight across years. Correction factors could be incorporated into any analysis, but this would increase its complexity by the addition of many more parameters.

A simpler way to remove the bias would be to remove the data that is causing the bias. The sites that were consistently fished from 1969-1986 were habitat types T_1 and T_{1A} in the middle section. These are the two most populated habitat types and the middle section is the most representative of the burn, and each year was fished to same number of times. The dates for each of the mean weights will be taken as the average date for that sample.

Table 2.6: *The means weights predicted by the one-way ANOVA between the different sections of the stream with standard errors in brackets for the data from 1969-1976.*

Age-class	Lower Section	Middle Section	Upper Section
0+	1.262(0.025)	0.911(0.018)	0.657(0.023)
1+	4.796(0.063)	5.354(0.044)	4.796(0.063)
2+	13.89(0.105)	11.93(0.087)	10.49(0.134)
3+	21.55(0.821)	17.83(0.516)	15.25(0.771)

The main cost in the reduction of the data set will be the loss in degrees of freedom and a consequent increase in the standard errors of the mean weights. This will be most evident for the 3+ age-class where the sample sizes are already small. However, the samples will be of a comparable size to those in the later years and the overall data set will be standardised.

The test data set that will be used is shown in Fig. 2.6. It can be seen that there is missing data for the 0+ and 1+ age-classes in 1975 and 1976, and for all age-classes for 1980. There is also a gap where the missing cohort from 1979 should be.

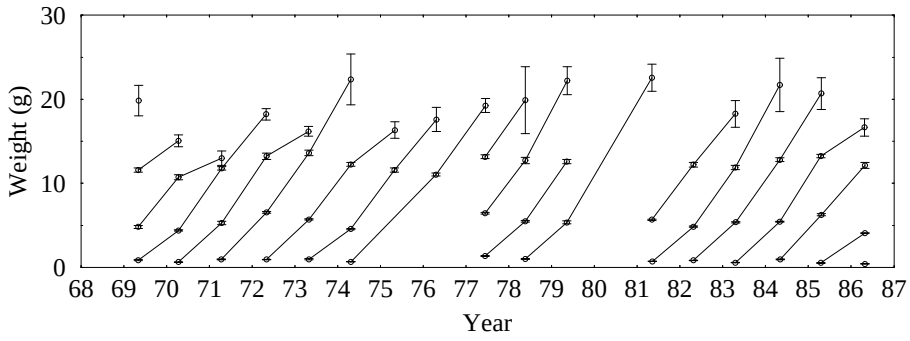

Figure 2.6: *Mean weights, with standard errors, of parr from cohorts, indicated by solid lines, divided into different age-classes.*

2.4 Data from the Fish Traps at the Girnock Burn

2.4.1 The Girnock Burn Fish Traps

The adult fish trap was situated 520m upstream from confluence of the River Dee and the Girnock Burn. The trap consisted of a deflecting fence and a holding box that allowed all the ascending salmon to be caught. Once caught, they were weighed, their fork lengths were measured and scale samples taken to determine age. Sex was determined from external secondary sexual characteristics. The fish were then released above the fish traps and allowed to spawn naturally (except in 1978).

Fish descending the burn were caught in a modified Wolf trap (Wolf 1950) located 80m upstream from the adult trap. The fish were sieved out of the stream into a holding tank, and their fork lengths were measured. Scale samples were taken from every fifth fish to determine age and fish $>$ 9cm were tagged. Descending kelts were also caught in the trap. A fuller description of the fish traps is given by Buck and Hay (1984). Occasionally during the autumn spates, the trap became clogged with leaves, with meant that water, and possibly parr did not go through the trap as they were able to swim over it. Therefore, for these years, the number of parr caught in the trap provided a lower bound of the total number of migrants that autumn.

2.4.2 Data from the Adult Trap

Ultimately, from a management perspective, the most important stage of the salmon life cycle is the adult's freshwater stage. This is when they have their highest economic value and these fish will sustain the population.

A minimum ova deposition is required to maintain the river at its carrying capacity, and for the Girnock, it is estimated that levels of more than approximately 200,000 eggs would not result in an increased migrant parr population under average (environmental) conditions (Buck and Hay 1984). Estimates of ova deposition (EOD) were calculated for the Girnock Burn from a relationship derived from salmon in the Dee by Pope et al. (1961), and are shown in Fig. 2.7. There

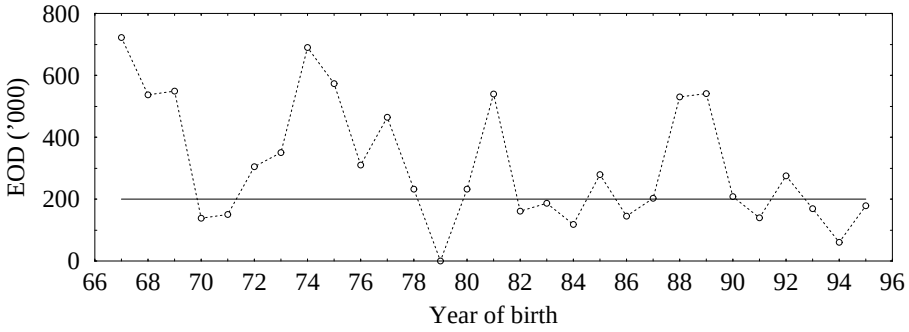

Figure 2.7: *Estimated ova deposition (EOD) above the fish trap at the Girnock Burn, with the solid line representing the estimated deposition required to maintain the Burn at carrying capacity.*

has been gradual decline in the EOD over the period when the trap has been in operation, and in recent years has fallen below the estimated carrying capacity. Considering how the population responded to previous periods of low spawning may enable us to determine how the present population is being affected.

2.4.3 Data from the Spring Smolts

The main migration period is from February to May, when the migrants become smolts and migrate downstream to the sea. The majority of smolts are three years

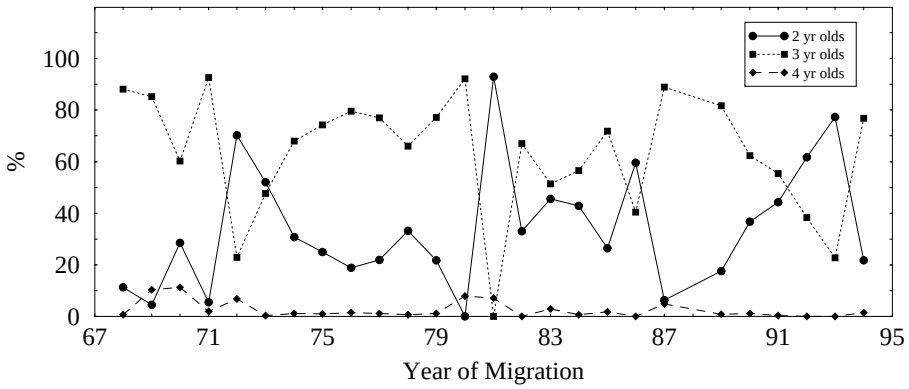

Figure 2.8: *The percentage of the age-classes which make up the spring migration from 1968-1994.*

old, followed by two then four, the percentages being shown in Fig. 2.8. Exceptions to this occur two years after low egg depositions, as in 1970, 1979, 1984 and the early 1990's, as can be seen in Fig. 2.7. In each migration season, the mean

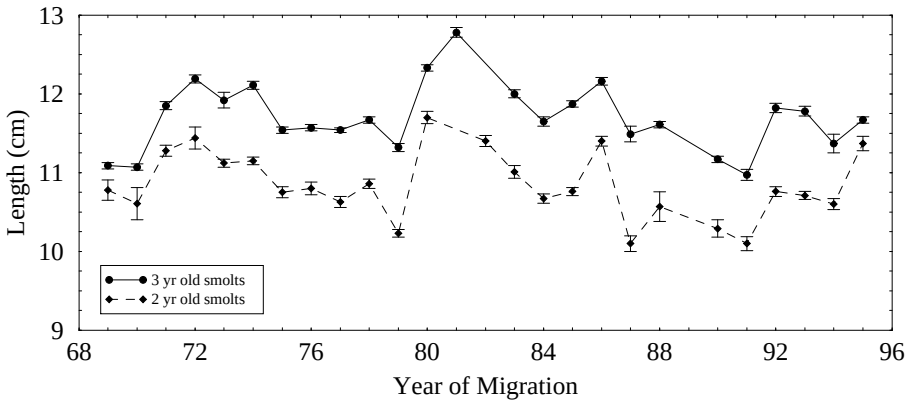

Figure 2.9: *Mean lengths of two and three year old spring smolts from 1968-1995 with standard errors.*

lengths of the older smolts are larger, as can be seen in Fig. 2.9, with the lengths of the two and three year olds being highly correlated ($r = 0.801,\ P < 0.001$). Typically, two years low EOD, the mean lengths of both two and three year old spring smolts are larger than expected, and the EOD is negatively correlated to with lag 2 to the lengths of the two ($r = -0.352,\ P < 0.05$) and the three ($r = -0.643,\ P < 0.001$) year olds. However, three years after low EOD, there are no significant correlations with smolt length.

2.4.4 Data from the Autumn Parr

During the autumn of each year, large numbers of parr are caught in the smolt trap as they are moving down stream, which has been called the autumn migration. The autumn migrants will not have developed into smolts, though tagging has shown that some will migrate to sea the following spring. Estimates of the numbers of autumn migrants are not as accurate as for the spring smolts as the trap can become clogged with leaves. This means that the accuracy of the estimates varies from year to year. However, the sample sizes are large enough to estimate the mean lengths and the proportion from each age-class, which are shown in Figs. 2.10 and 2.11.

As with the smolts, the older migrants are the generally larger and comprises the largest proportion of the autumn migration, except following periods following low spawning, when the 1+ dominate. The lengths of the 1+ and 2+ parr are correlated with each other ($r = 0.397,\ P < 0.05$) and the lengths of the 2+ are

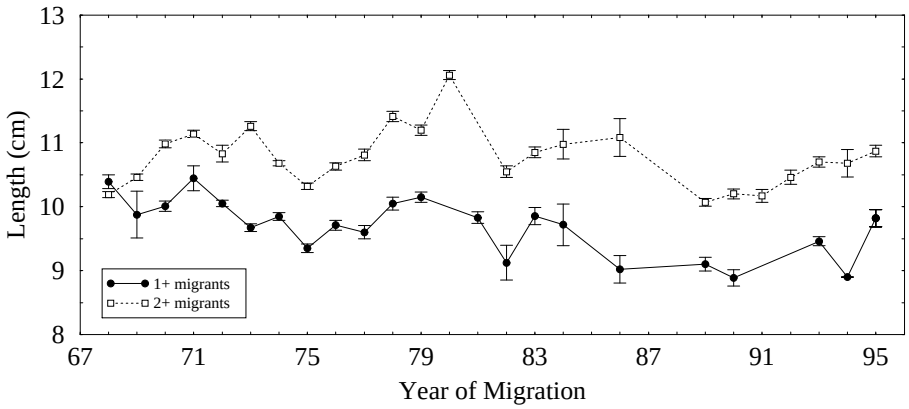

Figure 2.10: *Mean lengths of 1+ and 2+ autumn migrants which were caught in the smolt trap from 1968-1995 with standard errors.*

negatively correlated to the EOD in the previous year ($r = -0.536,\ P < 0.01$).

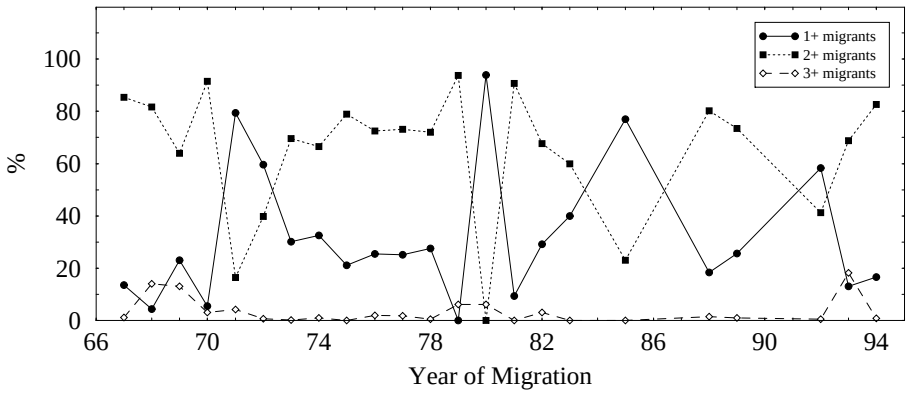

Figure 2.11: *Percentage of different age-classes which make up the autumn migration.*

Both precocious parr (PP) and non-precocious parr (NPP) were caught in the fish trap during the autumn migration from the Girnock Burn. For the years 1968-1976, an average of 6.3% (s.e=0.022) of the 1+ and 18.6% (s.e=0.027) of 2+ autumn migrants each year were identified as PP. This had risen considerably to 26.4% (s.e=0.105) for the 1+ and 47.0% (s.e=0.109) for the 2+ for the years 1989-1995, which may be due to the PP migrating in search of females as fewer ascend the burn to spawn in later years. Data regarding the precocity of the autumn migrants was not available from 1977-1988.

The lengths of a sample of PP and NPP caught in the trap during autumn from 1989-1995 were measured. Comparisons within age-classes within years revealed

that the PP were not significantly different in length to the NPP except in 1989 when the 2+ PP were greater ($F_{1,103} = 11.545,\ P < 0.001$).

2.4.5 Comparing Data from Spring and Autumn Migrants

Approximately $\frac{2}{3}$ of juveniles that leave the burn during any migration season (defined as from September until May), do so during the spring migration, as shown in Fig. 2.12.

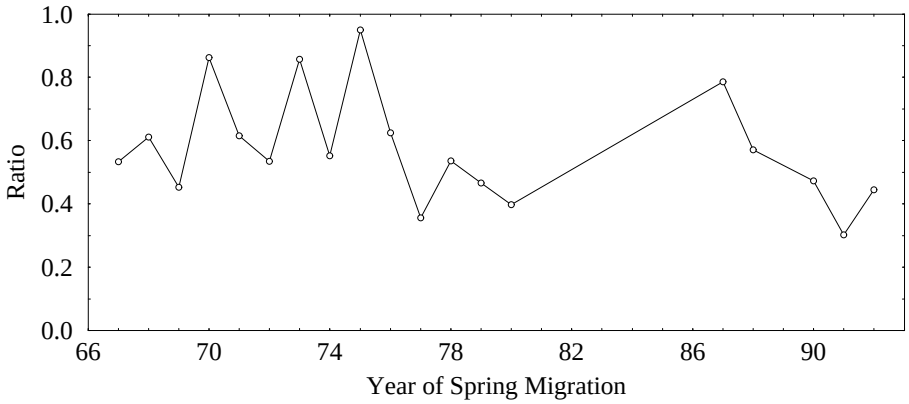

Figure 2.12: *Ratio of the numbers of autumn to spring migrants leaving the Girnock Burn. Ratios are only given for the years where the numbers of autumn migrants leaving are thought to be reliable, the mean being 0.575.*

The differences in the lengths of the autumn and spring migrants from the same cohorts are shown in Fig. 2.13. The difference between the 1+ and 2 yr. olds, and between the 2+ and 3 yr. olds is fairly similar and constant, with the spring migrants generally being larger. The only exception being 1979 during the time of the manipulation of the spawning activities of the salmon. With no females above the trap, large numbers of PP may have migrated in search of females (Buck and Youngson 1982). Some of these migrants may have been fish which would have otherwise chosen to migrate the following spring, as the mean weight of the migrants during autumn 1978 are relatively large, and those during spring 1979 relatively small.

Over the life of each cohort, a number of the members leave at different times. Fig. 2.14 shows what percentage of the migrants from cohorts born from 1968-1977 leave during different migration seasons. Data were not available for later

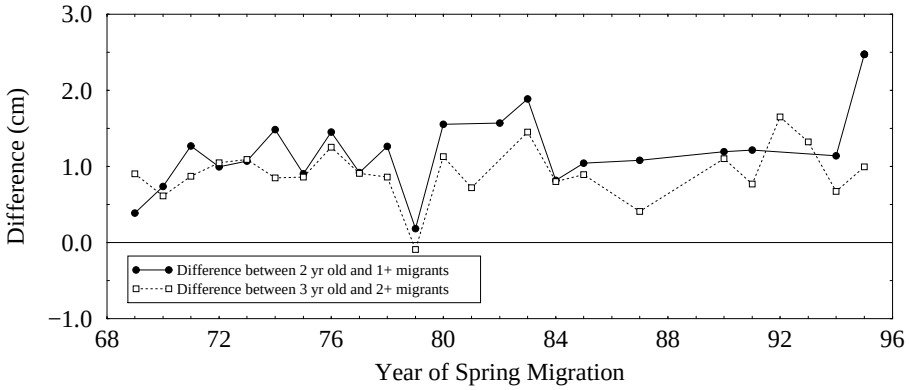

Figure 2.13: *Difference in the lengths of the autumn and spring migrants from the same cohorts.*

years due to unreliable estimates for the numbers of autumn migrants. On average, 28.3% leave when they are either 1+ or 2 yr. olds, 70.0% leave at either 2+ or 3 yr. olds, and 1.7% leave at either 3+ or 4 yr. olds.

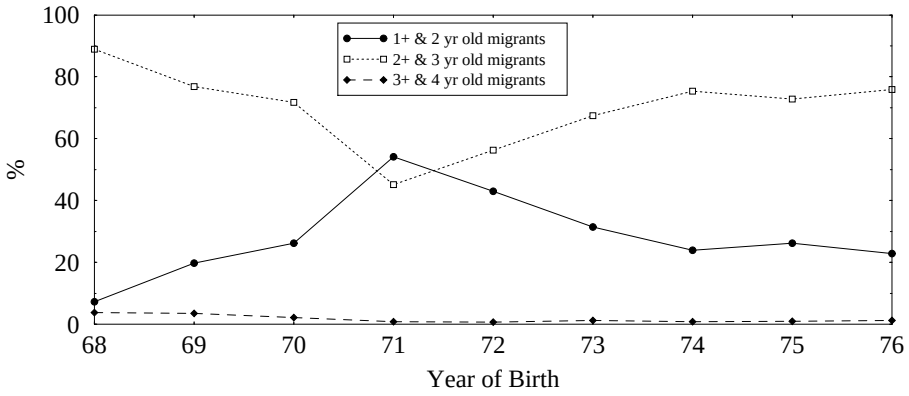

Figure 2.14: *Percentages of migrants from the cohorts from 1968-1976 to have emigrated during different seasons.*

2.5 Summary and Conclusions

Juvenile salmon exhibit a great deal of flexibility in terms of the decisions they may take and their response to changes in their environment. Temperature is an important factor in the physiological processes of growth, and as the climate changes, the growth rate will be affected (Power and Power (1994), Mangel (1994)). Although the increases in summer temperatures at the Girnock (Fig.

2.3) have been offset by decreases in the winter, the net effect on the growth rate of parr in the wild is not known.

Salmon are known to have preferred habitat types (Bult et al. (1999), Heggenes et al. (1999)), with the largest Girnock parr being found in the faster flowing waters with gravely substrates. These types are more suited to the salmons' foraging habits of taking food from the water column or foraging in the substrate.

Altitude may be a surrogate for temperature, as larger parr are found in the lower parts of the burn. However, these differences may in part be due to other factors in the local environment. The lower section has more overhanging vegetation so more invertebrates of terrestrial origin are available as food for the salmon if they fall onto the water surface. There are also higher levels of detritus, which provide food for the invertebrates on which the salmon feed.

Ova deposition is negatively correlated with the lengths of the emigrant parr during autumn and spring, which suggests that increased density depresses growth. The scale of these social effects cannot be assessed without taking into account other environmental effects such as temperature. Also, Ova deposition may be related to temperature (Webb and Mclay 1996). A method of accounting for growth due to temperature is to develop a growth model dependent on temperature and consumption as driving variables.

Unfortunately, measurements of parr food are unavailable for the Girnock, so will need to be inferred from the data via a model. Surrogates for consumption may be in the form of limiting quantities such as space (territory size), and these estimates of consumption are likely to change for parr from the different habitat types and stream sections. This would give an indication of the differences in the quality of habitat between different parts of the Burn and allow us to assess differences in suitability of different parts of the stream for salmon growth.

A growth model will have to consider the effects of migration on the resident population. Migration from the burn occurs during autumn and spring when a large proportion of the population leaves the stream. As these fish leave, there will be an effect on the mean weight of the population within the stream if the decision to migrate is based on the size attained by the parr.

The PP are also moving around the burn during autumn. The PP that were

caught at the trap were similar in length to the NPP migrating at the same time. The condition, and the weight-length relationship, for the PP is likely to be different from the NPP, as they are allocating resources toward reproduction rather than somatic growth, but this cannot be confirmed for the Girnock as these parr were not weighed. However, given that the lengths of the PP are not noticeably different from the NPP, and that a growth model would be fitted to population mean weights, derived from the parr lengths, there is no need to treat the PP differently from the other members of the population during the initial stages of the growth model.

An energy balance model will be developed to determine the environmental effects on the growth of the juvenile parr. It will first be tested on parr fed to satiation, then adapted to wild parr where smolting is occurring in the population. It will then be used to predict the overall dynamics of the population.

Chapter 3

Growth Models

3.1 Modelling the Growth of Fish

An important tool in fisheries management is use of growth models to predict the weight and length of both for farmed and wild fish. On fish farms, models allow managers to make informed decisions regarding production (Seiwarth and Summerfelt (1993), Soderburg (1992)). In the wild, growth models are more frequently becoming part of overall management strategies, which aim to improve fish production whilst maintaining a balanced ecosystem. They have been used to assess the impact of changes to the environment on the growth rate of the fish (Limburg (1996), Trebitz and Nibbelink (1996)), determine optimum stocking densities fish (Deangelis et al. (1993), Breck (1993)), and suitable feeding regimes (Yang 1998).

A model is required for the Girnock burn, which is able to predict the weight and length of parr given temperature and estimates of initial weight. Juvenile parr lose weight during the winter (Metcalfe and Thorpe 1992) so the model must be able to predict weight loss as well as gain. In the wild, the biomass of the invertebrate drift available as food to the parr may change, so the consumption rate must be able to vary. Rates of consumption and maintenance are affected by both temperature and fish size, so must be included in the model. Finally, the model must be parameterised and be applicable throughout the juvenile phase of the Atlantic salmon lifecycle.

3.1.1 Weight Based Empirical Growth Models

These models assume that the specific growth rate, G, is a dependent on weight, W, as in equation (3.1), and a selection of these types of models are shown in Table 3.1.

$$G = \frac{dW}{Wdt} \tag{3.1}$$

Table 3.1: *Growth models based on achieved size, where specific growth rate, $G = dW/Wdt$, is a function of weight, W.*

Model	$G^{\dagger}$
Logistic	$k_1(1 - W/W_\infty)$
Gompertz	$k_1(log_e W_\infty - log_e W)$
Monomolecular	$k_1((W_\infty/W) - 1)$
Richards	$[1 - (W/W_\infty)^{k_2}]k_1/k_2$

**Source:* Causton *et al.* (1978).
$^{\dagger}W_\infty$ asymptotic weight; k_1 and k_2 are constants.

They are fitted to data in order to determine the parameters, then used to predict the growth of fish raised in similar conditions (Baker et al. 1991), (Schnute 1981). However, these models give no insight into the causes of growth, or how growth varies with changes to the environment of the fish. This problem began to be addressed by Bertalanffy (1957), whose model took into account different aspects of growth.

3.1.2 The Bertalanffy Growth Model

Bertalanffy (1957) developed a physiologically dependent growth model that was used to predict weight and length. It was based on the principle that the rate of change of weight equals the rate of anabolism less the rate of catabolism, such that

$$\frac{dW}{dt} = h_1 W^{n_1} - h_2 W^{n_2} \tag{3.2}$$

where h_1 and h_2 are the coefficients for anabolism and catabolism, and n_1 and n_2 are how these quantities scale with weight.

This model still lacked any environmental input or dependence on rates of food consumption and is used more as a descriptive rather than a predictive model,

e.g. Ismen (1995), Xiao (1994), Chen et al. (1992), Crisp and Beaumont (1995). Changes have been made to the Bertalanffy format, such as making the anabolic and catabolic rates on dependent uptake and temperature, as well as body weight (From and Rasmussen 1984). Other adaptations have been used to predict density dependent (Lorenzen 1996) and seasonal (Fontoura and Agostinho 1996) effects on growth. The principles of growth proposed by Bertalanffy have been extended to bioenergetic models that take into account more aspects of fish growth.

3.1.3 Bioenergetic Growth Models

Bioenergetic models for growth take the energy budget of the fish and divide it up into its component parts, such as

$$C_b = F_b + U_b + R_b + P_b \tag{3.3}$$

where C_b is the energy of the food consumed, F_b and U_b are the energy lost in faeces and excretion, R_b is the standard, digestive and activity metabolism and P_b is somatic growth and gamete production (Wootton 1990). Typically, these components are further subdivided in order to predict P (see *Trans. Am. Fish. Soc. 122*(5) (1993), Kitchell et al. (1977), Stewart et al. (1983)). This type of model has also been used to estimate consumption rates (Brodeur et al. 1992), (Stockwell and Johnson 1997) and foraging behaviour (Brandt and Kirsch 1993), (Goyke and Brandt 1993).

Due to the number of factors affecting growth that are included in bioenergetic models, they can become very complex. Functions are required for each factor, which in turn may require many parameters. Feedback into the system is hard to implement as the models generally express the whole fish as composed of material that can be metabolised, so any weight loss will affect the whole energy equation causing a reduction in the proposed consumption rate, due to its dependence on total weight. Weight loss is unlikely to reduce the capacity for consumption, as the parts involved cannot be metabolised, e.g. mouth parts and bones. Therefore, when sufficient food becomes available to enable growth, the model is unable to simulate consumption at its previous maximum rate.

3.1.4 A Carbon-Based Functional Growth Model

A model that can be used for salmonids is a compensatory growth model by Broekhuizen et al. (1994), with growth measured in units of carbon, rather than energy. Using units of energy ignores the fact that different parts of the fish have different energy content. Energy is assimilated and converted into weight, and as the fish is not homogeneous, different parts of the fish will require different conversion rates. The same problem occurs when the energy is remobilized. Using carbon bypasses these problems, as it is not converted into other forms. This model is able to demonstrate weight loss and can easily be adapted for seasonal variations in temperature and food supply. More importantly, it is able to simulate changes in the behaviour of the fish as it loses weight so that there is an element of control, which is reflected by the health and condition of the fish. Such controls can mimic the changes in uptake and metabolic rates that may occur at low temperatures or food supply.

3.2 The Compensatory Growth Model

3.2.1 Introduction

Compensatory growth occurs when an animal undergoes an accelerated growth rate after the period of starvation, which results in a higher body mass than would have occurred had the starvation not taken place. This has been observed for different salmonid species (Dobson and Holmes 1984), (Miglavs and Johnson, 1989a, b), and the compensatory growth model (CGM) by Broekhuizen et al. (1994) has been used to successfully predict weight changes in tank reared salmonids caused by cyclic feeding patterns. It was originally tested on rainbow trout (*Oncorhynchus mykiss*) and Arctic charr (*Salvelinus alpinus L.*) with parameters derived from the literature. This type of model will be suitable for parr, as they lose weight during the winter (Cunjak 1988), (Metcalfe and Thorpe 1992), (Berg and Bremset 1998). Salmon parr have been observed to experience compensatory growth after periods of restricted temperature and photoperiod by Mortense and Damsgard (1993) and restricted temperature and food by Nicieza and Metcalfe (1997).

The model is based on two central principles, the first is that the total fish weight, W, can be divided into to two component materials in terms of carbon: those of structural tissue, S, and reserve tissue, R. Structural tissue can not be remobilized once it has been laid down so will never decrease, and includes bones, nerves and mouth parts. Reserve tissue can be remobilized once laid down, and is converted into energy to meet the needs of the fish and includes lipids and parts of the musculature, so R is able to decrease.

The second is that the fish will seek to maintain a constant ideal ratio between R and S. Any effects from starvation will lead to a decrease in R but not S, so $\rho = R/S$ can be taken as a measure of health. A healthy fish will have an ideal ratio of ρ_0 and will allocate material to R and S in such a way as to keep ρ as close to ρ_0 as possible. Sufficiently large decreases in ρ from ρ_0 will lead to behavioural changes in the fish which are its response to starvation. ρ_0 is assumed to be constant, although it may change if parr become sexually mature and allocate resources to reproduction.

3.2.2 Derivation of the CGM

The model assumes that the fish assimilates material at a rate A and loses material due to maintenance costs at a rate of M. The difference between A and M is then divided between R and S depending on a function of ρ, $C(\rho)$. The rates of change of R and S are given in equations (3.4).

$$\frac{dR}{dt} = A - M - \frac{dS}{dt} \qquad\qquad \frac{dS}{dt} = C(\rho)\left[A - M\right]^{+}, \tag{3.4}$$

(where $[x]^{+}$ denotes $max\{x, 0\}$). $C(\rho)$ must decrease when $\rho < \rho_0$ and increase when $\rho > \rho_0$. When $\rho = \rho_0$, $C(\rho)$ must remain constant at the value in equation (3.5),

$$C(\rho) = C_0 = \frac{1}{1 + \rho_0}. \tag{3.5}$$

Moreover, $C(\rho)$ must have an upper limit so that when ρ is relatively high, all assimilated material will be allocated to S. Conversely, there must be a lower limit where all assimilated material must be allocated to R. Thus $C(\rho)$ has been defined as a function which varies between 0 and 1 and is given a gradient of $C_0\theta$ (θ being the reserve control sensitivity), which determines how quickly the limits

are reached. $C(\rho)$ is defined as

$$C(\rho) = min\{1,\ C_0\ [1 + \theta(\rho - \rho_0)]^+\}. \tag{3.6}$$

The assimilation rate is assumed to be dependent on the assimilation efficiency, ε, food supply, Φ and the maximum uptake rate, U_{max}. Assimilation efficiency is the proportion of food consumed that ends up as body tissue. It takes into account the costs of digestion, incomplete absorption, and specific dynamic action. As tank reared fish are likely to feed at their maximum uptake rate if there is sufficient food available, the total assimilation rate can be defined by equation (3.7).

$$A = \varepsilon\ min\{\Phi, U_{max}\} \tag{3.7}$$

An important part of the model is to show how a fish responds to being healthy, hungry or torpid. It assumes that the behaviour of the fish changes as it loses weight, which affects both U_{max} and M. These changes are shown in the model by the starvation response functions, $\gamma(\rho)$ and $\lambda(\rho)$. U_H and M_H are defined as the uptake and maintenance rates for a healthy fish, and so U_{max} and M can be written as

$$U_{max} = \gamma(\rho)U_H \qquad\qquad M = \lambda(\rho)M_H. \tag{3.8}$$

$\gamma(\rho)$ and $\lambda(\rho)$ are step functions which change in value when ρ passes through certain threshold values. When ρ decreases below the healthy/hungry threshold, the uptake rate increases and M remains the same. Below the hungry/torpid threshold, both costs and uptake rates decrease. This is to simulate a strategy that the fish may adopt until food becomes more abundant. An additional feature of the starvation response functions is when ρ increases from below to above the hungry/torpid threshold, the behaviour remains the same for a small increment (Δ) of ρ above the threshold. This is intended to simulate observations where the fish does not immediately resume the costs of a hungry fish. These observations may be due to the fish being unable to change its physiological or behavioural state instantaneously, or it might be a cautious type of behaviour. These two functions are defined in Broekhuizen et al. (1994) Table 1.

The model states that U_H and M_H vary as geometric functions of body weight and exponential functions of temperature. U_H will be dependent on gut and

mouth parts so will scale allometrically (with constant κ) with S. With the scaling constant U_{HO} and the characteristic temperature for uptake T_A, U_H is thus derived as equation (3.9).

$$U_H = U_{HO} S^{\kappa} exp\left(\frac{T}{T_A}\right) \tag{3.9}$$

All body tissue will require maintenance so M_H will scale allometrically with total weight (with allometric constant ν). The scaling constant is denoted as M_{HO} and the characteristic temperature for maintenance T_R. This yields the equation (3.10), which completes the model.

$$M_H = M_{HO}(R+S)^{\nu} exp\left(\frac{T}{T_R}\right) \tag{3.10}$$

3.2.3 Parameterizing the CGM for Salmon Parr

The CGM was developed to predict growth rates for tank reared salmonids, and changes need to be made in order to apply it to the wild. The definition of A given by equation (3.7) states that the fish will eat all food presented to it if $\Phi < U_{max}$, otherwise it will feed at U_{max}. This is a reasonable assumption in a tank environment as the parr have no problem finding food, but in the wild, they are unlikely to be able to feed at U_{max}. Ideally, equation (3.7) would be redefined to include the type II functional response, derived by Holling (1959) which has been used to estimates consumption rates in wild freshwater fish (Madenjian and Carpenter 1991), (Stockwell and Johnson 1997), (Eby et al. 1995). Unfortunately, there is insufficient data regarding prey density in the Girnock Burn for this to be done.

An empirical growth model, developed by Elliott and Hurley (1997), has been used to predict growth rates of wild salmon parr. It uses weight and temperature to determine the specific growth rate and was parameterised using data from Atlantic salmon parr. In the next section, this model will be applied to data from the Girnock Burn to assess its effectiveness. Elements of the Elliott and Hurley (1997) model will then be combined with the CGM to create a new growth model for Atlantic salmon parr.

3.3 Elliott and Hurley Growth Model for Juvenile Atlantic Salmon

3.3.1 Introduction

An empirical growth model derived by Elliott (1975a, b) to predict the growth of brown trout, (*Salmo trutta* L.), has recently been modified (Elliott and Hurley (1995), Elliott et al. (1995)). It has also been reparameterized for immature stone-loach, (*Barbatula barbatula* L.) (Elliott et al. 1996) and juvenile Atlantic salmon, (Elliott and Hurley 1997). The model assumes that the fish are feeding to satiation and growing at their maximum rate for a given temperature. Predictions from the model appear to be very good for well-fed tank reared salmon parr grown at constant temperatures.

The Elliott and Hurley (1997) (E&H) model can be used to simulate growth trajectories for different cohorts in the Girnock Burn. Predicted weights can then be compared to the estimated mean weights of the resident parr, which have been derived from electro-fishing data. The quality of the E&H model can then be determined by examining the residuals between the model and the data.

The E&H model describes the proportional growth rate, G_e, as in equation (3.11), at a water temperature of T^oC and at an instant in time when the live mass of the fish is W grams.

$$G_e \equiv \frac{1}{W}\frac{dW}{dt} = c_g W^{-b}\left[\frac{T - T_0}{T_M - T_0}\right], \tag{3.11}$$

where

$$T_0 = \begin{cases} T_L & T \leq T_M \\ T_U & \text{otherwise} \end{cases} \tag{3.12}$$

There are five parameters in the model; three associated with water temperature and two with fish size. The temperature for optimum growth is set at T_M with the upper and lower temperatures when zero growth occurs being T_U and T_L. The mass exponent b is the power transformation of mass that produces linear growth with time and c_g is the growth rate of a $1g$ fish at the optimum temperature. Thus in order to predict the weight of a fish at time t using this model, we require its initial weight at t_0 and the water temperatures between t_0 and t.

Table 3.2: *Parameters for the E&H juvenile salmon growth model*

Parameter	*Symbol*	*Value*	*Units*
Weight exponent	b	0.31	dimensionless
Maximum growth rate for 1gm fish	c_g	0.035	$\mathrm{d}^{-1}\mathrm{gm}^b$
Optimum temperature	T_M	15.9	^oC
Low temperature limit	T_L	6.0	^oC
High temperature limit	T_U	22.5	^oC

3.3.2 Simulations using the Girnock data

Electro-fishing surveys were conducted during the summer from 1968 to 1986, with the exception of 1981. From these records, we have length measurements of the resident parr at ages 0+, 1+, 2+ and 3+. Older fish were too rare to be included in the analysis. There are no lengths for the 0+ and 1+ age-classes for the years 1975 and 1976 due to lost data. The weight-length relationship derived in Chapter 2 was used to convert the lengths into weights, which were then summarised into mean weights for each age-class in each cohort. The temperature data has been summarised into monthly mean temperatures, as described previously.

Simulated growth trajectories were produced using the E&H model with the temperatures from the Girnock Burn, the parameters in Table 3.2, and initial fish weights of $0.15g$ on the 1^{st} April. The initial weight and starting data are the nominal birth weights and dates for salmon in the Girnock Burn (D. W. Hay, *pers. comm.*). Simulations were carried out for each cohort born from 1968-1986 except for 1979 when adult fish were prevented from spawning the previous year, which resulted in no cohort born that year. Fig. 3.1 shows the simulations with the estimates of fish weights from the electro-fishing data, with standard errors.

3.3.3 Analysis of the E&H Model

Fig. 3.1 shows that there are large discrepancies between the model predictions and the weight estimates from the electro-fishing data. The parameters were derived from well-fed fish reared in a controlled environment so the model should at least over-predict the parr weights and ideally be an upper bound for growth at the given temperature. Nearly all of the predicted weights are less than the

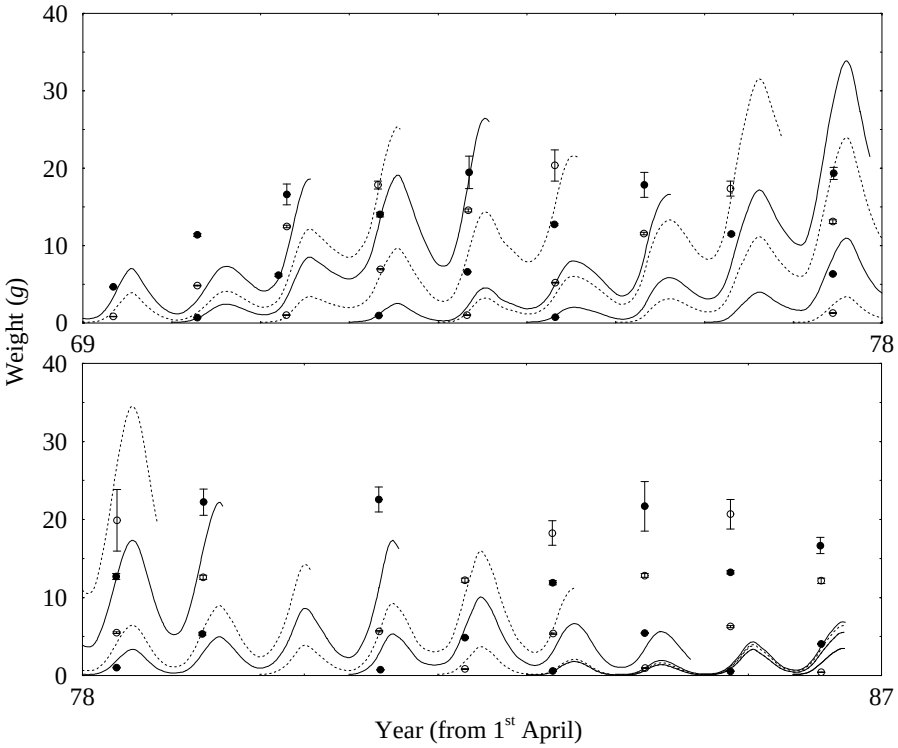

Figure 3.1: *Growth trajectories for cohorts of salmon parr in the Girnock Burn derived using the E&H model. Data points are the mean weights of each age-class from each cohort, where the filled circles are associated with the solid lines and the open circles with the dotted lines.*

observed weights, and many substantially so. Also, the over winter weight loss predicted by the model is very large and in some cases is roughly equivalent to the weight gain during the summer. From the data, it can be seen that the predictions for the Girnock are clearly not realistic.

Elliott & Hurley, (1997) used this model to simulate growth trajectories of wild parr in the R. Eden, a stream in Northwest England. These simulations did not produce the large winter weight loses seen when using the Girnock temperature data and there was a tendency for the weights of the 1+ age-class to be under-predicted, although the weights of the 2+ age-class were over-predicted. However, in general, the fit was realistic, so the model appears to be appropriate for the R. Eden but not the Girnock Burn. Possible reasons for this are that either the parameters are incorrect, the model is structurally wrong, or both.

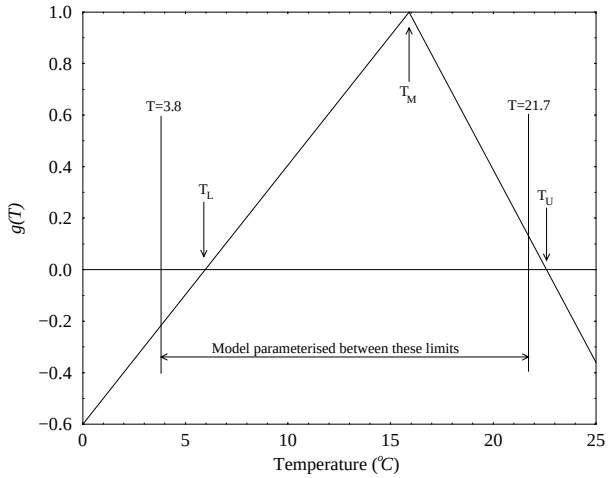

Figure 3.2: *The function $g(T)$ as defined in equation(3.14).*

The specific growth rate can be split into two parts, $G_e = f(W)g(T)$, where

$$f(W) = c_g W^{-b} \tag{3.13}$$

and

$$g(T) = \frac{T - T_0}{T_M - T_0} \tag{3.14}$$

with the parameters defined as above. The function $g(T)$ is plotted out in Fig. 3.2 and illustrates how G_e is affected by temperature. When $T = T_U$ and $T = T_L$, G_e is zero, and the maximum growth rate will occur when the temperature is at T_M. At temperatures below T_L or above T_U, weight loss will occur. In Fig. 3.3, we compare the Girnock temperatures and the Eden temperatures and we can see that more weight loss is predicted by the model when temperatures from the Girnock are used. In the Girnock, large parts of the year are spent at temperatures that are below that required for growth and, according the E&H model, the fish is predicted to lose weight.

Different parameter values would reduce the weight loss predictions and increase overall growth. Reducing T_U, T_M or T_L increases weight gain and reduces weight loss at low temperatures. However, there is lots of evidence to suggest the estimates are reasonable (T_M: Wankowski and Thorpe (1979a), Dwyer and Piper (1987), Peterson and Martin-Robichaud (1989), and T_L: Evans et al. (1985), Lee and Power (1976), Jensen et al. (1989)). The mean monthly temperatures in the Girnock are rarely greater than T_M, so the value of T_U will have a very small

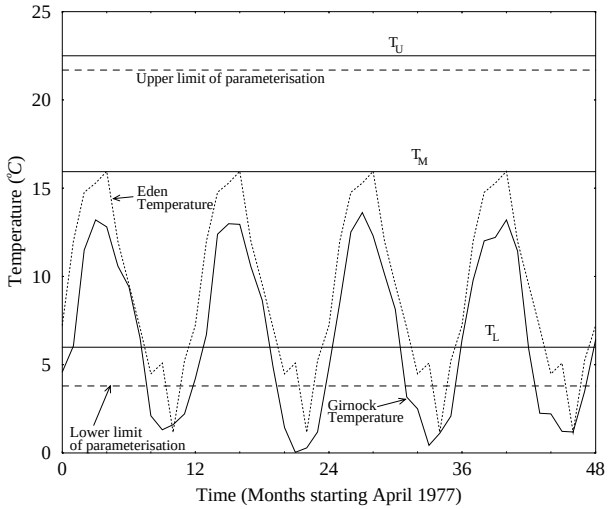

Figure 3.3: *Comparisons of the temperatures used by Elliott Hurley from the R. Eden and those found in the Girnock over same period (April 1977 to April 1981).*

effect on weight predictions in the Girnock. The remaining two parameters b and c_g are independent of the temperature so if these were changed, G_e would still be negative for temperatures below T_L. The weight loss can be reduced by altering b and c, but this will also cause the growth rate at temperatures above T_L to be reduced.

The real problem lies within the structure of the model. As the temperature decreases from T_M, the growth rate will decrease linearly for a fish of constant size. G_e becomes negative when $T = T_L$ and continues to decrease until T reaches its minimum at 0^oC. During periods of cold temperatures ($< \ 6^oC$), parr will become less active and reduce their metabolic costs (Metcalfe and Thorpe (1992), Cunjak (1988), Gardiner and Geddes (1980)), but there is no such mechanism included in this model, which predicts continued weight loss. Changes need to be made to the model so that it will no longer produce growth trajectories with large weight losses during the winter but still be able to fit the experimental data used by Elliott & Hurley to parameterise their model. The CGM does take into account these aspects of fish growth and a new model is constructed in the final section of this chapter, which will combine components of the E&H and the CGM. This will enable us to create a realistic upper bound for the growth of parr in the Girnock.

3.4 Combining Aspects of the E&H model with the CGM

3.4.1 Restructuring the CGM

The E&H model is not suitable in its present form, but any credible model must be able to fit the data from Elliott and Hurley (1997) as well as the E&H model is able to. Due to the structural inadequacies of the E&H model, the CGM model will form the basis of a new model.

A well-fed fish can be assumed to have ρ maintained at its optimum value ρ_0, so that $S = W_c/(1+\rho_0)$, where W_c is the fish weight in carbon. Rearranging the left-hand member of (3.4) gives

$$G_c \equiv \frac{1}{W_c}\frac{dW_c}{dt} = \frac{1}{W_c}(A - M) = W_c^{\kappa-1}\left[\Psi_A - \Psi_M\right] \tag{3.15}$$

where

$$\Psi_A \equiv \frac{\varepsilon U_{H0}}{(1+\rho_0)^\kappa}\exp\left(\frac{T}{T_A}\right) \qquad \Psi_M \equiv W^{\nu-\kappa}M_{H0}\exp\left(\frac{T}{T_R}\right). \tag{3.16}$$

To harmonise the CGM and the E&H model requires two things. First $\nu = \kappa = 1-b$ is set so that Ψ_A and Ψ_M depend only on temperature and $G_c \propto G_e \propto W^{-b}$. This harmonises the weight scaling of the two models. Second, two functions, $\Psi_A(T)$ and $\Psi_M(T)$, are chosen such that so that

$$\Psi_A(T) - \Psi_M(T) = c_g\left[\frac{T - T_0}{T_M - T_0}\right]. \tag{3.17}$$

Equation (3.17) is clearly incompatible with *both* Ψ_A and Ψ_M having the forms given in equation (3.16). The standard metabolic rate (SMR) is often described as being exponentially dependent on temperature, (Wootton 1990), but this is not always the case with U_{max}. Van Winkle et al. (1998), Stockwell and Johnson (1997), Lantry and Stewart (1993) and Rand et al. (1993) all use the function Ψ_M for the SMR, but use a function developed by Thornton and Lessem (1978) to describe how U_{max} is dependent on temperature. Since the evidence for the SMR being exponentially dependent on temperature is stronger than that for uptake, Ψ_M will remain as defined in equation (3.16), and have

$$\Psi_A = \frac{1}{(1+\rho)^\kappa}\xi(T) \tag{3.18}$$

where

$$\xi(T) = (1+\rho_0)^{\kappa}\left[M_{H0}\exp\left(\frac{T}{T_R}\right) + c_g\left(\frac{T-T_0}{T_M-T_0}\right)\right]^{+}. \qquad (3.19)$$

The '+' in this equation is there to avoid negative uptake. This leads to a final model in which

$$\frac{dR}{dt} = A - M - \frac{dS}{dt} \qquad \frac{dS}{dt} = C(\rho)\left[A-M\right]^{+}, \qquad (3.20)$$

where $C(\rho)$ is defined by equations (3.5) and (3.6), and

$$A = \lambda(\rho)S^{\kappa}\xi(T) \qquad M = \gamma(\rho)M_{H0}(R+S)^{\kappa}\exp\left(T/T_R\right) \qquad (3.21)$$

with $\xi(T)$ defined by equation (3.19), T_0 as defined in equation (3.12), and λ and γ are defined in Broekhuizen et al. (1994) (Table 1).

Table 3.3: *Main Parameters for the Modified CGM salmon growth model*

Parameter	*Symbol*	*Value*	*Units*
Weight exponent	κ	0.69	dimensionless
Maximum growth rate for 1mg fish	c_c	0.155	$\mathrm{d}^{-1}\mathrm{mgC}^{1-\kappa}$
Optimum temperature	T_M	15.9	^oC
Low temperature limit	T_L	6.0	^oC
High temperature limit	T_U	22.5	^oC
SMR characteristic temperature	T_R	12.5	^oC
SMR at 0^oC	M_{H0}	0.04	$\mathrm{d}^{-1}\mathrm{mgC}^{1-\kappa}$
Ideal Reserve ratio	ρ_0	1.5	dimensionless
Reserve control sensitivity	θ	3	dimensionless

The main parameter values for this model can be adopted from Elliott and Hurley (1997) and Broekhuizen et al. (1994). Since the CGM is formulated in terms of carbon weight (mgC) and E&H in wet weight (g), the units of c_g must be changed from $\mathrm{d}^{-1}\mathrm{gm}^b$ to $\mathrm{d}^{-1}\mathrm{mgC}^b$, and will be redefined as c_c. Using the CGM parameters for the SMR, we arrive at the parameter set shown in Table 3.3. The other model parameters, which govern the behaviour of the starvation/recovery part of the model, can be taken from CGM.

Finally, in Fig. 3.4 the weight-scaled assimilation and basal metabolic rates against temperature are plotted. The 'clipping' of the assimilation function does not act until $T < 2.5^oC$, which indicates that the model reproduces all of the region of E&H's model which is supported their data.

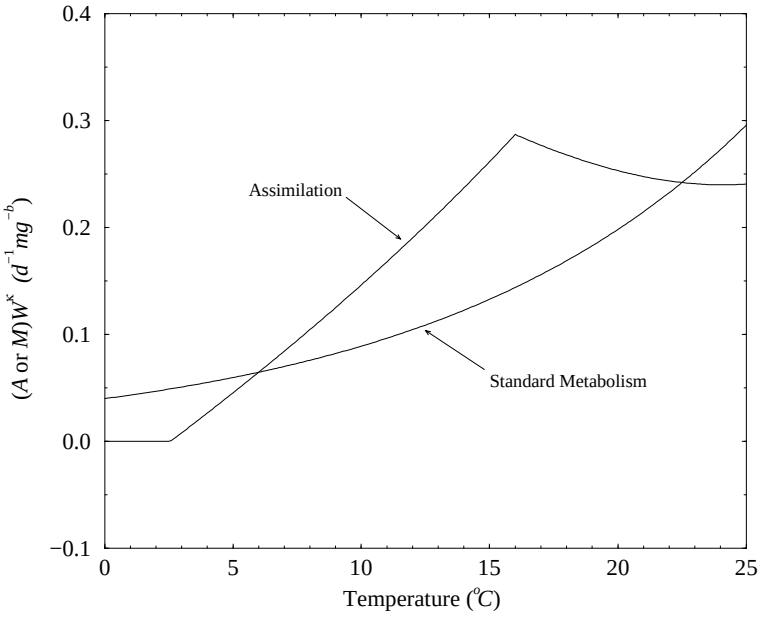

Figure 3.4: *Weight-scaled assimilation (A/W^{κ}) and weight scaled SMR (M/W^{κ}) for the CGM modified so as to force compliance with the E&H picture of the temperature dependence of growth rate. Parameters taken from Table 3.3 .*

3.4.2 Parameterizing the CGM/Elliott model

Combining the E&H model with the CGM has guaranteed that, over the temperature range of Elliott and Hurley (1997) data, the CGM/Elliott model (CGM_e) will reproduce their observed growth rates for satiated fish. This is independent of our choices of SMR and the starvation/recovery responses. However, for the model to predict an upper bound to growth in conditions where long-term weight loss occurs, appropriate values for the SMR and starvation/recovery parameters must be obtained.

The CGM_e requires new parameters for Atlantic salmon parr, and the first change is the carbon content of the Atlantic salmon which ranges from 11.4-12.5%, with a mean of 11.93% (Carter et al. 1992), from the value of 15% for rainbow trout used by Broekhuizen et al. (1994). The hysteresis in the starvation response functions will also be dropped from the model. The effect of this on the growth trajectories will small as they will only be affected once a year, during the spring as they gain weight after the winter. The hysteresis can also cause numerical problems to occur at certain levels of assimilation.

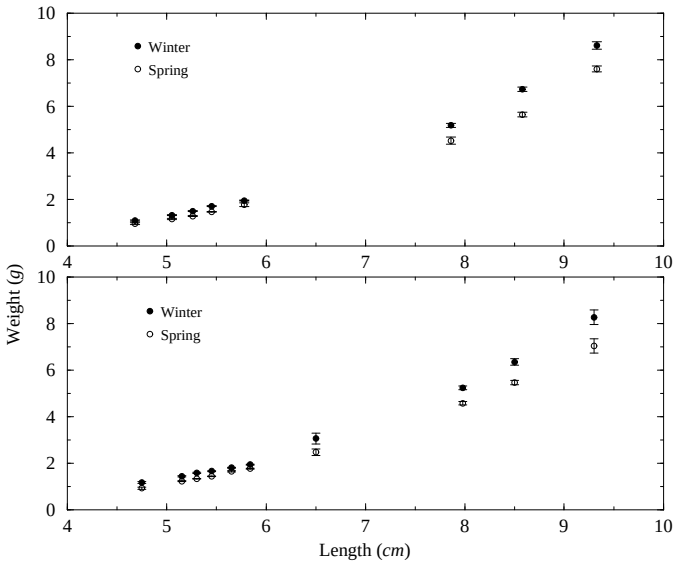

Figure 3.5: *Mean weights by length class (± s.e.) for fish caught in Catamaran brook in the autumn and spring of 1992-93 (upper) and 1993-94 (lower).*

Winter weight loss in Catamaran Brook

Electro-fishing surveys were conducted at a single site in the Catamaran Brook, New Brunswick in autumn and spring of the years 1992/93 and 1993/94 (R.A. Cunjak, unpublished data).In each survey, weights and fork lengths were measured for the Atlantic salmon parr that were caught. In Fig. 3.5 the mean weight of autumn and spring fish classified by length are shown. The spring fish of a given length class are noticeably lighter than autumn fish of the same length. To confirm this result, a weight length curve was fitted to each data-set (Table 3.4), such that $W = aL^b$ where W is weight, L is fork length and a and b are constants. Temperatures in the brook between the autumn and spring surveys are continuously below the $T_L = 6^oC$ limit for growth, so this difference will be assumed to be due to over-winter weight loss.

Table 3.4: *Weight-length coefficients for the Catamaran brook data*

Season	a	b
Autumn 1992	0.0090	3.081
Spring 1993	0.0092	2.990
Autumn 1993	0.0108	2.972
Spring 1994	0.0095	2.964

Short term starvation experiments

Two data sets in which weight loss was measured over short periods of starvation by Carter et al. (1992) and Wainwood et al. (1992) were found in the literature. In the Wainwood et al. (1992) experiment, juvenile Canadian salmon were starved for 43 days at a constant temperature of $13°C \pm 1^oC$. Scottish juvenile salmon were used by Carter et al. (1992), and were starved for 30 days with varying temperatures of $5 - 8°C$. Details of the results are given in Table 3.5.

A starvation-recovery experiment

Another data set that involved starvation was by Metcalfe and Thorpe (1992). Over a 29 day period, fish were starved for the first 21 days, then fed to satiation for four days, then starved for a further two days before undergoing a two day appetite trial. During the trial, the fish were offered food and their growth response was noted. By the end of the trial, the fish were refusing food, which indicates that they were fed to satiation. Over the experimental period the temperature changed from $10.2 - 10.5°C$ at the beginning in 26-27 October to $8.3 - 8.6°C$ by the end in 23-24 November. Estimates of the mean specific growth rate per day over this period are given, as well fork lengths of the fish.

Parameterizing weight loss

To form a data set in order to parameterise the starvation response part of the CGM_e, weight loss for three representative starting weights (5, 10 and 15 g) was calculated from the Catamaran brook data for 1992/3 and 1993/4 using the derived weight-length relationships in Table 3.4. The two short-term experiments were added to this, resulting in the complete data set shown in Table 3.5. The Metcalfe and Thorpe (1992) experiment was omitted from consideration at this time, since its results are dominated by the recovery process and only tell us about weight loss indirectly.

In the CGM_e, the SMR is related to weight and temperature by

$$M = \gamma(\rho) M_{HO} W^{\kappa} exp\left(\frac{T}{T_R}\right) \tag{3.22}$$

Table 3.5: *The parameterisation data set for SMR and starvation parameters*

Experiment	Start Date	Finish Date	Initial Weight (g)	Final Weight (g)	Temp °C
Carter	3 Feb	5 Mar	12.30 (2.03)	11.12 (2.12)	6.2(1.0)
Wainwood	5 Mar	17 Apr	20.2 (0.7)	16.9 (1.0)	13(1)
1992/93	13 Nov	3 May	15	12.47	0
	13 Nov	3 May	10	7.11	0
	13 Nov	3 May	5	3.60	0
1993/94	4 Nov	28 Apr	15	13.00	0
	4 Nov	28 Apr	10	8.68	0
	4 Nov	28 Apr	5	4.34	0

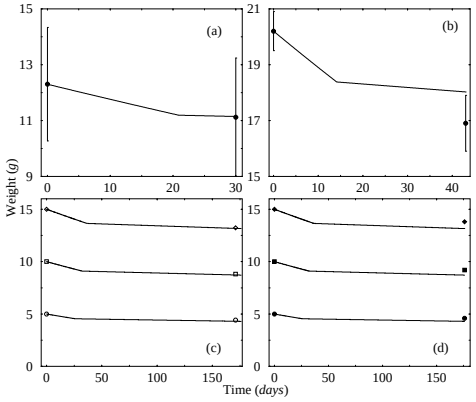

Figure 3.6: *Fits to the test dates using best fit parameters in Table 3.6 a)Carter b) Wainwood c)Catamaran brook 1992/3 d) Catamaran brook 1993/4.*

where

$$\gamma(\rho) = \begin{cases} 1 & \rho/\rho_0 > \tau_2 \\ \xi_{\gamma L} & \tau_2 \geq \rho/\rho_0 \end{cases} \tag{3.23}$$

This attempt at parameterisation assumes that the weight and temperature scaling are correct, and treats M_{H0}, τ_2 and $\xi_{\gamma L}$ as fitting parameters. Since an analytic solution for the weight trajectory under starvation conditions can be obtained, an automatic optimisation by the downhill simplex method (Press et al. 1989) was used and the parameters constrained. Constraints of $0.026 \leq M_{H0}$ and $0.4 \leq \tau_2 \leq 1$ needed to be placed on these parameters to ensure the model still fitted the Elliott and Hurley (1997) data. The constraint on $0.1 \leq \xi_{\gamma L} \leq 1$ was set to prevent it from becoming negative. The best fit values are given in Table 3.6 and the quality of fit is shown in Fig. 3.6.

Table 3.6: *Best fit parameters - attempt 1*

Error Measure	M_{HO}	τ_2	$\xi_{\gamma L}$	Error (g)
Mean Absolute Error	0.0260	0.8580	0.1000	0.3400
Root Mean Square Error	0.0260	0.8440	0.1000	0.5001

Table 3.6 suggests that the quality of the optimal fit is not very good. Examination of Fig. 3.6 shows that all the experiments are well fitted *except* the Wainwood et al. (1992) experiment, which is the only one not carried out at low temperature. This suggests that the temperature scaling of SMR needs to be adjusted. This is not just a question of adjusting T_R, since this changes both the slope of the curve and its absolute position on the axis. The present SMR will be assumed to be correct at the lower zero-growth temperature, T_L, so

$$M = \gamma(\rho) W^{\kappa} \left[M_{H0} \frac{\exp\left(T_L/T_R\right)}{\exp\left(T_L/T_{RN}\right)} \right] \exp\left(\frac{T}{T_{RN}}\right). \tag{3.24}$$

T_{RN}, τ_2, and $\xi_{\gamma L}$ are now the fitting parameters, with constraints $3.8 \leq T_{RN}$, $0.4 \leq \tau_2 \leq 1$ and $0.1 \leq \xi_{\gamma L} \leq 1$. Downhill simplex fitting gives the results shown in Table 3.7. The resulting quality of fit is illustrated in Fig. 3.7 and is much better than the previous attempt, so these new parameters will be used to describe SMR for Atlantic salmon parr.

Table 3.7: *Best fit parameters - attempt 2*

Error Measure	T_{RN}	τ_2	$\xi_{\gamma L}$	Error (g)
Mean Absolute Error	5.2465	0.8601	0.1008	0.1497
Root Mean Square Error	4.8720	0.8744	0.1000	0.2685

Parameterizing recovery from starvation

When the fish begin feeding after a period of starvation during which they have lost sufficient weight to become torpid, they recover to a healthy state, given enough food and time. The function $\lambda(\rho)$ shows how uptake changes with the condition of the fish. The form that $\lambda(\rho)$ takes is

$$\lambda(\rho) = \begin{cases} 1 & \rho/\rho_0 > \tau_2 \\ \xi_{\lambda L} < 1.0 & \tau_2 \geq \rho/\rho_0 \end{cases} \tag{3.25}$$

The model will be fitted to data from Metcalfe and Thorpe (1992) by varying the parameters that are associated with recovery from starvation. These are

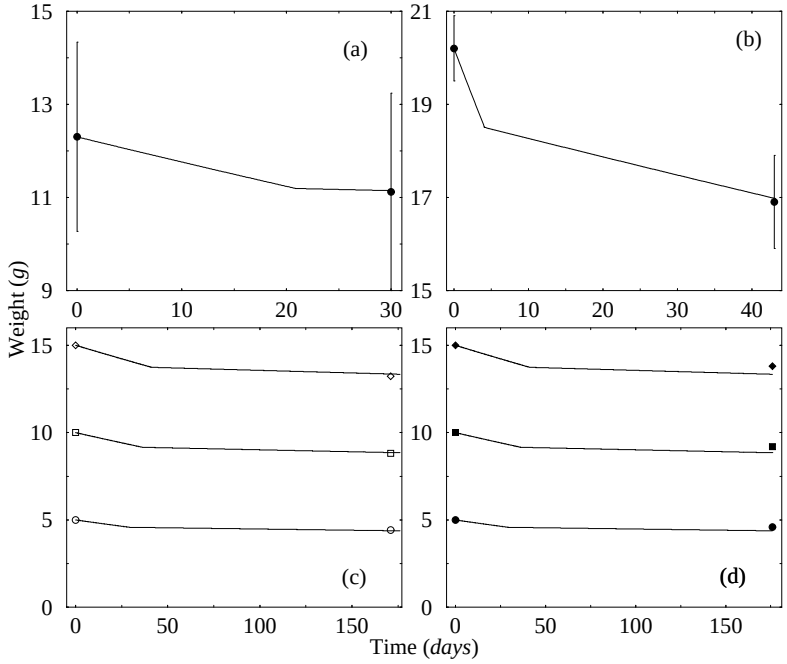

Figure 3.7: *Fits to the test data set using best fit parameters in Table 3.7 a)Carter b) Wainwood c)Catamaran brook 1992/3 d) Catamaran brook 1993/4.*

θ, the reserve control sensitivity and $\xi_{\lambda L}$, the torpid/hungry uptake ratio. These parameters were varied individually with the other parameters in the model being held constant at their previous values. The errors between the model prediction and the data point as the parameters are varied are shown in Table 3.8.

Changing the value of θ will alter the allocation of assimilated material between R and S and hence affect the rate of recovery of the fish. Lower values of θ mean more material is allocated to S and recovery is slower. At a value of $\theta = 1$, the fish remains in a torpid state throughout the period of feeding. Therefore it is useful to derive the error at this value as any lower values of θ would produce the same trajectory. As θ is increased, the fish recovers from starvation quicker, which decreases the error in the Metcalfe and Thorpe (1992) data. However large increases in θ produce increasingly smaller decreases in the error, so only at unreasonably high values of θ is the error at an acceptable level.

Varying the $\xi_{\lambda L}$ will produce an excellent fit to the data when $\xi_{\lambda L}$ is changed from its original value of 0.8 to 0.42. This implies that when salmon parr are fed to satiation after a period of starvation, their growth rate would be lower than expected for rainbow trout, from which the original parameter was derived. The

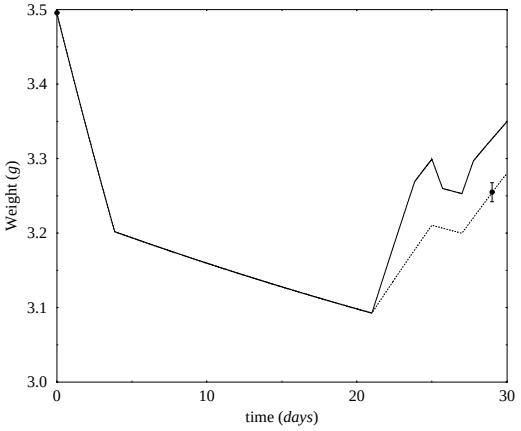

Figure 3.8: *Simulation on the data from Metcalfe and Thorpe (1992). The original value of $\xi_{\lambda L}$ has been used in one simulation (solid line) and a value of $\xi_{\lambda L} = 0.42$ for the other simulation. The error bar has been derived from errors in the estimate of the daily specific growth rate.*

simulations shown in Fig. 3.8 are for original set of parameters and with the new value of $\xi_{\lambda L} = 0.42$ that will be used in the model.

Table 3.8: *Errors associated with different parameters when fitting the model to the data from Metcalfe and Thorpe (1992) starvation-recovery experiment. Parameters in the model were varied one at a time whilst the others were kept at their value in the CGM. Errors associated with varying that particular parameter are given below.*

Parameter Value	Error (grams)
Original Parameters	0.071
$\theta = 100$	0.005
$\theta = 5$	0.01
$\theta = 1$	0.193
$\xi_{\lambda L} = 0.42$	0.001

3.4.3 Fully Parameterised CGM_e Model

Finally, reverting to the parameterisations of SMR and the uptake response function given in equations (3.23) and (3.25), our current view of the best model parameters is summarised in Table 3.9. Simulations using these parameters are

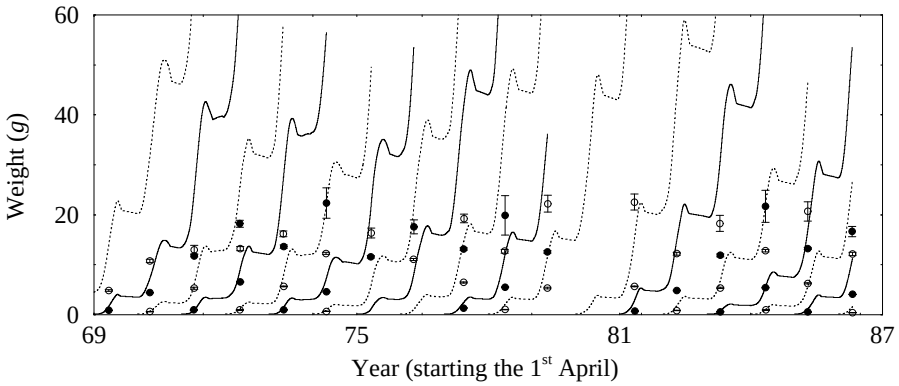

Figure 3.9: *Simulations from the CGM_e with data from the Girnock Burn. The solid lines correspond to the data points with the filled circles, and the dotted lines are the growth trajectories of the cohorts with the open circles.*

shown in Fig. 3.9 for cohorts born in 1968 to 1986 with the exception of 1979, when no cohort was born, and the data from the electro-fishing surveys conducted on the Girnock Burn. As expected, the model over-predicts the weights of the wild salmon parr and more importantly, over winter weight loss is reasonable. Thus, the current parameters can be viewed as providing a reasonable upper limit to the growth of juvenile salmon in the Girnock Burn.

Table 3.9: *Parameters for the CGM_e salmon growth model*

Parameter	*Symbol*	*Value*	*Units*
Weight exponent	κ	0.69	dimensionless
Maximum growth rate for 1mg fish	c_c	0.155	$\mathrm{d}^{-1}\mathrm{mgC}^{1-\kappa}$
Optimum temperature	T_M	15.9	^oC
Low temperature limit	T_L	6.0	^oC
High temperature limit	T_U	22.5	^oC
SMR characteristic temperature	T_RN	5.3	^oC
SMR at 0^oC for a healthy 1mgC fish	M_{H0}	0.021	$\mathrm{d}^{-1}\mathrm{mgC}^{1-\kappa}$
Ideal Reserve ratio	ρ_0	1.5	dimensionless
Reserve control sensitivity	θ	3	dimensionless
Threshold ρ/ρ_0 for torpidity	τ_2	0.86	dimensionless
Torpid SMR/Normal SMR	$\xi_{\gamma L}$	0.1	dimensionless
Torpid uptake/Normal uptake	$\xi_{\lambda L}$	0.42	dimensionless

Chapter 4

Protocols for Fitting the Growth Model to Freshwater Data

4.1 Introduction

The model derived in Chapter 3 is able to simulate long term growth rates for well-fed salmon parr given initial weight and water temperatures, and so estimate an upper bound for growth. In the wild, the fish are unlikely to be feeding to satiation so the effects on the growth rate of a limited food supply must be included in the model. These effects will be represented by a single function $\phi(t)$, where t is time. As each cohort grows throughout its juvenile phase, $\phi(t)$ will account for some of the differences between the growth rates of well-fed and wild parr. In this chapter, a method will be developed for deducing $\phi(t)$ using electro-fishing data from the Girnock Burn.

4.1.1 Individual Observations and Averages

Ideally, measurements of individuals should be used to derive $\phi(t)$. This is not possible, as individuals were not identified from one survey to the next for the historical data set. The weights of the fish sampled from each cohort needed to be summarised in a way that take into account variation in the weights of the population. This was done by deriving the mean with the standard error (s.e.) and the median with the quartile values for each age-class in each cohort. Fitting the model to this data assumes that an individual will grow at the same rate as

the average of each age-class. There is evidence to suggest that the growth rate of wild parr is different for different members of the same cohort. Nicieza and Brana (1993) observed that the smaller members of a cohort increased their growth rate during the spring and the larger members decreased theirs, which resulted in each group having similar sizes by the summer. The Girnock Burn data were collected during the summer and it will be assumed that the growth rates of the individual resident parr are not different from the growth rate associated with the mean lengths from the samples of the cohort.

The data were collected from six electro-fishing surveys spread across the summer. As the mean weight of the fish caught from each age-class during the surveys each year was being used as a summary of an individuals weight, a single date was required to be associated with each mean weight. As different numbers of fish were measured at each survey, the mean capture date was used.

4.1.2 Population Structure vs. Average Individual

As the cohorts age, the numbers caught from each age-class in each sample decreases. This is not all due to mortality, as large numbers of parr leave the burn during autumn and spring. The autumn migrants leave as either normal or precocious parr whilst the spring migrants leave as smolts. Therefore, by the time a cohort is two years old, there has been some emigration from the population and when it is three years old most of the fish from that cohort will have died or migrated. This means that the electro-fishing samples are not a true subsample of the survivors of that particular cohort at ages 2+ and 3+, but only of the resident parr in the stream.

Fitting the model through the mean or median weights assumes that the average weights of all the fish caught are typical of the individuals in that cohort. In particular, it does not take into account any size selective effects on removal from the population. Measurements of the lengths of the migratory juveniles are available, but for now, we shall concern ourselves solely with fitting the model to the electro-fishing data.

4.1.3 Incorporating $\phi(t)$ into the Growth Model

The function $\phi(t)$ is intended to indicate the difference between the growth of parr in the wild and those fed to satiation and will be a fraction (between 0 and 1) of the assimilation rate. $\phi(t) = 1$ indicates that a parr is assimilating material at its maximum rate and $\phi(t) = 0$ means that the fish is not assimilating anything, at time t. The change to the CGM_e model, defined in Section 3.4, is by changing equation (3.20) to

$$\frac{dR}{dt} = \phi(t)A - M - \frac{dS}{dt} \qquad \frac{dS}{dt} = C(\rho)\left[\phi(t)A - M\right]^{+}. \tag{4.1}$$

This change will only affect the growth rate when the parr are assimilating material: the rate of weight loss due to metabolic costs remains unaffected.

4.1.4 The Data Set

Different data sets will produce different values for $\phi(t)$, as it is an indication of the environmental state within which the parr has grown. The best fitting procedure and form of $\phi(t)$ will be determined using the data from the Girnock Burn. The subset of the Girnock data selected in Chapter 2 will be used with standard errors for the means and quartile values for the medians. Temperature data and the weight-length relationship required for the model have been described in Chapter 2 and the birth weights and dates will be those previously used in Chapter 3.

4.2 Fitting the Model to Average Individuals with Time Dependent Temperature

4.2.1 Fitting and the use of $\phi(t)$

The model will initially be fitted to the means and medians of the data set with $\phi(t) = k$, where k will have a constant value for all t. In order to find the best fit to the data, k will be varied between 0 and 1. The series of criteria described in Section 4.2.3 are used to determine the best fit of the model to the data.

4.2.2 Method of Deriving a Single Optimal k

Estimates of k are most likely to be $0 < k \leq 1$. Values of $k < 0$ are not applicable as they lead to a negative assimilation rate. $k > 1$ will indicate that the fish grows better in the wild than in tanks where they are fed to satiation. As this is improbable, it might indicate that there is a flaw in the model. The best fit to the data will be the value of k between 0 and 1 which minimise an error term. In order to find the optimum value of k (the value of k at which the error term is minimised), the error was evaluated from $k = 0$ to $k = 1$ at increments of 0.01. This is a robust method and will enable us to see how the error varies with k. The model will initially be fitted to both the mean and the median weights of the different age-classes from the different cohorts, in case there is a skewed distribution of the weights which is able to bias k.

4.2.3 Determining the Goodness of Fit of the Model to the Data

Running the model produces a growth trajectory for each cohort. Each cohort has at most four data points, one for each age-class from 0+ to 3+, where data is available. In order to examine to goodness of fit of the model to each age-class, a table of results has been complied. The descriptions of what each of these statistics indicate in Tables 4.2-4.5 is as follows.

The first column is the age-class for which the rows of statistics apply. The second column is the average of the mean weights for that age-class, which can be compared with the average of the predicted mean weights in column three. The range of the predictions is in column four. The absolute mean error is in the next column and the percentage error in sixth, which is the absolute mean error divided by the observed mean weight multiplied by 100.

The column *Sign. same* is derived using two-tailed paired $t-$test between the predicted weights and the observed mean weights. The observed mean weights from each age-class approximate a normal distribution so the predictions should also form a normal distribution indistinguishable from the observations. A $t-$test will be used to test this. The term 'Y' indicates that the two means cannot be distinguished, which is what is required, whereas 'N' indicates that the means

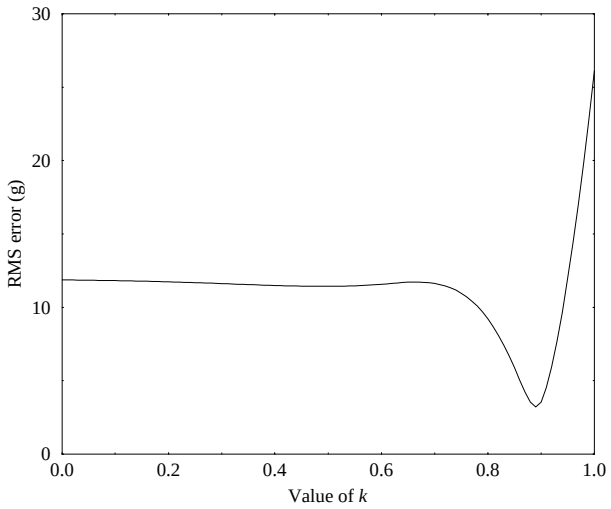

Figure 4.1: *Graph showing the RMS error, for different values of k, between the model prediction and the mean weights of the different age-classes from the different cohorts. There is a global minimum at* $k = 0.89 \pm 0.005$.

are significantly different.

The final column, labelled *Sign. correl.*, which determines whether the predictions are correlated with the observations, as desired. In this column, *NS* means the correlation is not significant, * means it is at $P < 0.05$, ** means it is at $P < 0.01$ and *** means it is at $P < 0.001$.

4.2.4 Estimating k by Fitting the Model to the Means and the Median Weights

The minimum root mean square (RMS) error was calculated for all likely possible values of k with both the mean and the median data sets. Fig. 4.1 shows how the RMS error between the model and the data varies with k. A global minimum can be seen at $k = 0.89 \pm 0.005$ and there is unlikely to be a minimum at $k > 1$. A similar picture is produced when the model is fitted to the median weights. Optimum k and the RMS error for the mean and median weights are shown in Table 4.1, and a description of the fit to the two data sets are given in Table 4.2.

There is a strong tendency for the 1+ and 2+ age-classes to be under predicted whilst 3+ age-class weights are predicted relatively well. Small changes in k produce increasingly large changes in the growth trajectories as time increases.

Table 4.1: *The optimum values of k which minimise the RMS error between the model predictions and the observed mean and median weights.*

	k	RMS error (g)
mean	0.89	3.24
median	0.89	3.15

Table 4.2: *The fit of the model to the observed mean and median weights when the optimal value of k is found by minimising the RMS error.*

Age-class	*Average Weight (g)*	*Predicted Weight (g)*	*Range of Predictions (g)*	*Mean Abs. Error (g)*	*% Error*	*Sign. same*	*Sign. correl.*
Fitted to the mean when k=0.89							
0+	0.82	0.75	0.42-1.38	0.24	29	Y	NS
1+	5.35	3.63	2.21-5.30	1.81	34	N	NS
2+	12.34	9.26	5.70-13.78	3.28	26	N	NS
3+	18.92	20.07	14.41-27.67	3.49	18	Y	NS
Fitted to the median when k=0.89							
0+	0.79	0.75	0.42-1.38	0.24	30	Y	NS
1+	5.17	3.63	2.21-5.30	1.70	33	N	NS
2+	12.12	9.26	5.70-13.78	3.13	26	N	NS
3+	18.21	20.07	14.41-27.67	3.37	18	N	NS

This results in a large change in the error at the 3+ stage and smaller changes in the error for the 0+, 1+ and the 2+ parr. Therefore, the best fit will be heavily influenced by the weights of the 3+ age-class.

In order to force the model to fit the younger age-classes better, whose sample sizes and abundance are much larger, the fitting procedure can be altered so that it would take into account the sample sizes and the spread of the data.

4.2.5 Estimating k by Fitting the Model to the Data by Minimising a Weighted Function

Two weighting functions that take into account the spread of the data and the sample sizes are W_1 and W_2 in equations (4.2) and (4.3). The RMS error is replaced by the weighting function, which will be calculated as k varies. The

best fit will be the value of k which minimises W_1 or W_2.

$$W_1 = \sum_j \sum_i \left(\frac{P_{i,j} - D_{i,j}}{e_{i,j}} \right)^2, \tag{4.2}$$

$$W_2 = \sum_j \sum_i \frac{|P_{i,j} - D_{i,j}|}{e_{i,j}}. \tag{4.3}$$

The subscript j refers to the cohort and i to the age-class. When used with the means, $P_{i,j}$ represents the predicted weight which corresponds with $D_{i,j}$, the observed mean weight, which has a standard error of $e_{i,j}$. These functions can also be used with the median weights, where $e_{i,j}$ is derived from the quartile values, as in equation (4.4)

$$e_{i,j} = \frac{Q1_{i,j} - Q3_{i,j}}{2}. \tag{4.4}$$

where $Q1_{i,j}$ and $Q3_{i,j}$ are the upper and lower quartile values respectively and $D_{i,j}$ is the observed median weight.

The two functions W_1 and W_2 were evaluated for values of $0 < k \leq 1$ at increments of 0.01. The values of k which minimise W_1 and W_2 for both the means and median weights are shown in Table 4.3, with descriptions of the fit given in Table 4.4. Use of the weighting functions changes the emphasis of the fitting

Table 4.3: *Values of k which minimise the weighting functions when applied to the means and the medians weights.*

	W_1	W_2
mean	0.89	0.90
median	0.87	0.89

procedure. In the case of the means, it has caused an increase in the value of k when W_2 is used. This is due to an optimum value of k being found that fits better to the age-classes with more accurate means (which have a smaller s.e.), which tend to be the 1+ and 2+ age-classes. This effect appears to be offset when W_1 is used as the squared term creates a bias towards reducing the errors associated with the data points with the larger standard errors, which tend to be the 3+ age-class.

The optimal values of k derived when the model is fitted to the medians are lower than for the means. This is due to the differences in the quartile values being

Table 4.4: *The fit of the model to the observed mean and median weights the optimal value of k is found using the weighting functions W_1 and W_2.*

Age-class	*Average Weight (g)*	*Predicted Weight (g)*	*Range of Predictions (g)*	*Mean Abs. Error (g)*	*% Error*	*Sign. same*	*Sign. correl.*
Fitted to the mean when k=0.89 using W_1							
0+	0.82	0.75	0.42-1.38	0.24	29	Y	NS
1+	5.35	3.63	2.21-5.30	1.81	34	N	NS
2+	12.34	9.26	5.70-13.78	3.28	26	N	NS
3+	18.92	20.07	14.41-27.67	3.49	18	Y	NS
Fitted to the mean when k=0.90 using W_2							
0+	0.82	0.80	0.43-1.51	0.23	28	Y	NS
1+	5.35	4.03	2.43-5.92	1.66	31	N	NS
2+	12.34	10.44	6.38-15.62	2.88	23	N	NS
3+	18.92	22.83	16.33-31.54	4.96	26	N	NS
Fitted to the median when k=0.87 using W_1							
0+	0.79	0.65	0.38-1.16	0.26	33	N	NS
1+	5.17	2.91	1.81-4.20	2.25	43	N	NS
2+	12.12	7.19	4.50-10.57	4.93	41	N	NS
3+	18.21	15.26	11.04-20.96	3.45	19	N	NS
Fitted to the median when k=0.89 using W_2							
0+	0.79	0.75	0.42-1.38	0.24	30	Y	NS
1+	5.17	3.63	2.21-5.30	1.70	33	N	NS
2+	12.12	9.26	5.70-13.78	3.13	26	N	NS
3+	18.21	20.07	14.41-27.67	3.37	18	N	NS

relatively similar in size compared to those of the standard errors. The weighting functions are defined as residual divided by e_{ij} so is relatively large when the quartiles are used, especially for the larger fish. Thus the weighting functions are minimised with low values of k which fit the 3+ parr better. As with the means, the squared term in W_1 places greater weight on the larger errors which tend to be the larger fish, which further reduces the value of optimal k.

The sample size of the 3+ fish form a small part of the whole data set, yet have so far had a very influential role in finding optimal k. The next step will be to exclude the 3+ data from the fitting procedure to assess its influence and determine whether a more satisfactory value of k can be derived.

4.2.6 Estimating k by Fitting the Model to only the 0+, 1+ and 2+ Age-Class Data

All the data for parr older than 2+ were excluded from the data set and the fitting procedure was applied to the mean and the median weights as in Section 4.2.4. and Section 4.2.5. The different error functions were minimised in order to derive the optimum values of k shown in Table 4.5, with descriptions of the fits in Table 4.6.

Table 4.5: *Values of k which minimise the weighting functions and the RMS error between the model and the observed mean and median weights when the 3+ data have been excluded.*

	RMS	W_1	W_2
mean	0.91	0.91	0.91
median	0.91	0.90	0.90

Table 4.6: *Fit of the model to the observed weights when the 3+ data has been excluded from the fitting procedure.*

Age-class	*Average Weight (g)*	*Predicted Weight (g)*	*Range of Predictions (g)*	*Mean Abs. Error (g)*	*% Error*	*Sign. same*	*Sign. correl.*
Fitted to the mean when k=0.91							
0+	0.82	0.85	0.45-1.63	0.24	29	Y	NS
1+	5.35	4.46	2.66-6.59	1.55	35	N	NS
2+	12.34	11.73	7.11-17.62	2.83	23	Y	NS
3+	18.92	25.86	18.43-35.78	7.33	39	N	NS
Fitted to the median when k=0.91							
0+	0.79	0.85	0.45-1.63	0.24	30	Y	NS
1+	5.17	4.46	2.66-6.59	1.54	30	Y	NS
2+	12.12	11.73	7.11-17.62	2.80	23	Y	NS
3+	18.21	25.86	18.43-35.78	7.68	42	N	NS
Fitted to the median when k=0.90							
0+	0.79	0.80	0.43-1.51	0.23	29	Y	NS
1+	5.17	4.03	2.43-5.92	1.59	31	N	NS
2+	12.12	10.44	6.38-15.62	2.83	33	N	NS
3+	18.21	22.83	16.33-31.54	5.04	28	N	NS

The optimum values of k found have all increased in value as a result of the exclusion of the 3+ data. This is to be expected, as lower values of k are more

suited to this age-class. These rises do indicate that the 3+ have an effect on the values of k, even when functions which discriminate against them due to their small sample sizes are used. However, those effects are quite small: the means change from 0.89 and 0.90 to 0.91; medians change from 0.87 to 0.89 and become 0.90 to 0.91. These small changes probably do not justify omitting the information from the 3+ data, as the bias is very small.

4.2.7 Determining the Most Appropriate Fitting Procedure for Estimating k

The fitting procedures for k produce a narrow range of values, which vary from 0.87 to 0.91, none of which provide an adequate fit of the model to the data. They all produce systematic errors in predicting the weights of different age-classes, with a tendency for the 1+ and 2+ to be under predicted or the 3+ to be over predicted. The next stage will be to fit a different value of $\phi(t)$ for each year in order to indicate variation in the assimilation rate between years, by redefining $\phi(t) = \phi_y$, where y represents the year. This can be done only after the choices of whether to fit means or the medians and which fitting procedure to use has been made.

ANOVA tables can be produced to test if there are significant improvements in the fit of the model to the data for the different methods of deriving optimal k. These would compare the predictions when optimal k is derived from the data and the predictions when the default value of $k = 1$ is used. For each method an $F-$statistic can be calculated, and it was found that the use of k provided a highly significant improvement to the fit between the model and the data, with $P < 0.001$ in all cases. However, it would be inappropriate to compare the different $F-$statistics due to their derivation. When the RMS error is minimised, the $F-$statistic is calculated from the sum of the squares, and when the weighted functions are used, the $F-$statistics is calculated from the sum of the weighted residuals. Each of these methods places a different emphases on different aspects of the fit and so produce different $F-$statistics. Therefore, other criteria will be used to decide on the best method.

When k is derived by fitting the model to the means and medians of all the data (Subsection 4.2.4), there is a tendency for the RMS optimisation procedure

to fit the weights of the 3+ better than the 1+ and 2+ parr. This would be inappropriate as the 3+ form a very small part of the sample size, so simply fitting the data to all the medians or means by minimising the RMS error will be discarded. The method of fitting k to only the 0+, 1+ and 2+ data will also be discarded, as it ignores an important point on the growth trajectory. One of the weighting functions will be used, as they take into account the accuracy of the estimates of the mean weights.

The weighting function W_1 will be biased towards the points with the largest errors, which are from the 3+ age-class. As the sample sizes for these fish are relatively small, it would be better to use a fit that was more associated with the bulk of the data, which are the 1+ and 2+ age-classes. Therefore, the W_2 weighting function will be used to minimise the error between the model and the data.

Fitting to the mean and the median weights gives different values of k, which are a consequence of the spread of the data and the sample sizes. The means do not reflect the spread of the data as well as the median, but the medians are less influenced by the sample size. However, as the accuracy of the means can be estimated well, due to the large sample sizes, the W_2 weighted function fitted to the means will be used as the preferred fitting procedure. Thus, the final choice is weighting function W_2 fitted to the mean weights of all the age-classes.

The simulated growth trajectories estimated with the value of $k = 0.90$ are shown in Fig. 4.2 (with a description to the fit in Table 4.4). There are still systematic differences between the residuals and the data, where the 3+ are under predicted and the 1+ and 2+ are generally over predicted. The model as it stands does not provide a good estimate of the growth rates for wild parr. Using a single constant value of $\phi(t) = k$ assumes that the difference between the growth rate of wild parr and parr reared when fed to satiation is a constant fraction of the maximum assimilation rate. The next step will be to investigate what happens if this fraction varies annually.

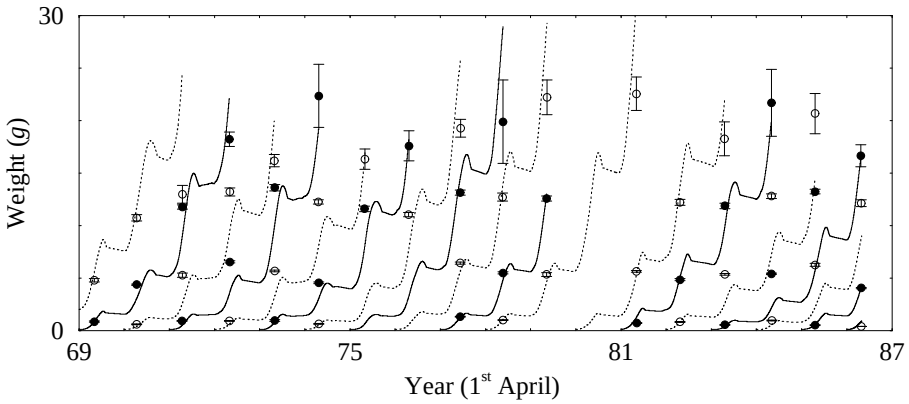

Figure 4.2: *Simulations produced when $\phi(t)$=0.90 in the CGM_e with the electrofishing data summarised into the means with the standard errors for each age-class from the cohorts born from 1968-1986.*

4.3 Inferring Year Quality from the Model

4.3.1 Estimating Annual Values of ϕ_y

Deriving a constant value of $\phi(t)$ does not provide a good fit to the observed weights, but an optimal method has been developed to fit the model to the data. This method will be extended and use $\phi(t) = \phi_y$, which will be a set of discrete values. Each value will be constant within each year but will vary between years so that the value of ϕ_y will affect the predicted growth rate of all cohorts present in year y.

The values for ϕ_y will be derived by minimising W_2 between the model and the observed mean weights, using the downhill simplex method of optimisation, as described in Appendix A, with the initial conditions described in Subsection 4.3.2.

The growth model has so far been fitted to the weights of the fish. As it is actually estimating growth rates, it will also be fitted to the observed specific growth rate (SGR) of parr. This is useful as many growth models, such as the E&H model, are designed to predict SGR. In addition, we are at the looking directly at the growth rates in the population, so fitting to growth rate may provide a better fit to the observed mean weights.

The descriptions of the fits between the model and the mean weights in Tables 4.7-4.10 are the same as previously described in Subsection 4.2.3. The fits of the

model to the SGR described in Tables 4.7 and 4.8 are similar to those described in Subsection 4.2.3. except they do not apply to weight but to growth in units of % day^{-1}.

4.3.2 The Fitting Procedure

The Downhill Simplex Method of Optimisation (DSO)

There will be at least 18 values of ϕ_y that need to be found for the data from the Girnock Burn. The values are not independent, as fish weight during one year will affect their weight the next year, so the method previously described to find k is inappropriate. The DSO will be used as it can find this number of unknown parameter values more efficiently.

The DSO requires a set of initial values of ϕ_y and a step size to begin the fitting procedure. The value of $k = 0.90$ was used as the initial value of ϕ_y, for all y, with a step size was 0.01. The value of $k = 0.90$ was chosen as it provided the best fit of the model to the data in Section 4.2. With these initial conditions, the DSO was able to minimise the error between the model predictions and the data to produce different values for ϕ_y for each year.

Other initial conditions were used in order to see if the DSO would converge to the same values of ϕ_y. It was found that they did not, which meant that the minimum found by the DSO was dependent on the initial conditions. The values of the error function, W_2, found from each set of initial conditions were compared and varied little between them ($< 2\%$ from the average value). This indicated that the solutions produced from the different initial conditions might have been tending towards the global minimum but that the error surface was either too flat or too rough for it to be reached.

Five different sets of initial conditions were used (with k=0.88, 0.89, 0.9, 0.91 and 0.92 each being the initial conditions for all years) to produce five sets of ϕ_y. As the fitting procedure did not converge to the same minimum for different initial conditions, then the values of ϕ_y associated with the lowest error value may not represent the global minimum but it indicated the best fit to the data that could be found. The growth simulations were then produced using these values of ϕ_y. An error term was derived for each value of ϕ_y based on the standard error of the

values derived from the different initial conditions. This would give an indication of how accurately each value of ϕ_y was known.

4.3.3 Fitting the Model to the Mean Weights by Adjusting ϕ_y

Now that the values of ϕ_y are being derived for each year, the data that the model is being fitted to needs to be defined more rigorously. For the simulations in this subsection, the first growth trajectories will start at the time of hatching of the cohort that is born in 1968, whose first data point is in 1969, at the 1+ age-class. The trajectory for the second cohort will begin at hatching in 1969. The value of ϕ_{69} will therefore be derived primarily from the 0+ and 1+ age-class of 1969, but this value will also account for most of the growth in 1968. This means $\phi_{68} = \phi_{69}$ and that they are not estimated separately.

In Table 4.7, the fit to the mean weights is shown. In addition to this is the fit between the observed and the predicted SGR between consecutive age-classes are shown. The values of ϕ_y have been derived by minimising the error function between the predicted and the observed mean weights.

Table 4.7: *Fit of the model to the observed mean weights and SGR when ϕ_y is derived by minimising the weighted error between the observed and predicted weights.*

Fit of the model to the mean weights							
Age-class	*Average Weight (g)*	*Predicted Weight (g)*	*Range of Predictions (g)*	*Mean Abs. Error (g)*	*% Error*	*Sign. same*	*Sign. correl.*
0+	0.82	0.84	0.48-1.40	0.12	14	Y	***
1+	5.35	4.38	2.94-5.67	1.00	19	N	*
2+	12.34	11.83	7.73-14.23	0.96	8	Y	***
3+	18.92	25.73	21.20-28.73	6.81	36	N	NS
Fit of the model to the SGR							
Age-classes	*Average SGR % day^{-1}*	*Predicted SGR % day^{-1}*	*Range of Predictions % day^{-1}*	*Mean Abs. Error % day^{-1}*	*% Error*	*Sign. same*	*Sign. correl.*
0+-1+	0.40	0.36	0.31-0.41	0.05	11	N	NS
1+-2+	0.22	0.25	0.21-0.31	0.04	21	N	NS
2+-3+	0.11	0.20	0.16-0.26	0.09	87	N	NS

The fit of the model to the data has improved considerably by the change from $\phi(t) = k$ to $\phi(t) = \phi_y$, with significant positive correlations between the observed and predicted 0+, 1+ and 2+ weights and the absolute mean error lower by a large amount, as shown by comparing Tables 4.7 and 4.4. for each age-class. There are differences between the predicted and observed weights of the 1+ age-class.

The fit of the model to the SGR has also been calculated and it can be seen that the 0+ to 1+ growth rates have generally been under predicted, whilst the 1+ to 2+ growth rates are over predicted. The 2+ to 3+ growth rates are over predicted, as would be expected due to the weighting function. The model will next be fitted to the SGR and the fit compared to the table above.

4.3.4 Fitting to the SGR by Adjusting ϕ_y

The model will be fitted to the SGR by minimising the weighting function W_2 in equation (4.3), with $P_{i,j}$ as the predicted SGR and $D_{i,j}$ as the observed SGR. The SGR will have a different error in the weighting function and fewer data points than the mean weights so will produce different values for ϕ_y. SGR will be defined as

$$SGR_{i,j} = \left(\frac{W_{i+1,j} - W_{i,j}}{t_{i+1,j} - t_{i,j}}\right) / \left(\frac{W_{i+1,j} + W_{i,j}}{2}\right), \tag{4.5}$$

where j is the cohort, i is an age-class and $W_{i,j}$ is the weight of the fish. t has units of days and is the mean date of the survey for age-class i in cohort j. Therefore, $SGR_{i,j}$ is the SGR between age-classes i and $i+1$ of cohort j.

The fitting procedure has to be weighted down so an error term for the SGR is required. This will not be straightforward as measurements for individual fish do not exist. Also the sample sizes vary greatly between age-classes so we are unable to use regression to determine the SGR because there will be a bias towards the age-classes with larger sample sizes.

An error for the SGR between two mean weights was derived from the standard errors of the mean weights. An upper limit for the error term was calculated as the SGR between the point one s.e. below the mean weight of the younger age-class and one s.e. above the mean of the older age-class. The lower limit was the SGR between the point one s.e. above the mean weight of the younger

age-class and one s.e. below the mean of the older age-class. This will not be the true s.e. of the observed SGR but will be adequate as a weighting function. It is determine by the spread of the data and the size of the sample, is similar to the weighting function used previously and provides an error that can be applied consistently and quickly across the data set. The upper and lower limits that have been derived for the SGR are different sizes, so the average of the two was used as the weight.

A new set of ϕ_y was derived by minimising the error function between the predicted and observed SGR using the same initial values for ϕ_y and step sizes as for the means weights. The quality the fit between the predictions and the observations shown in Table 4.8.

Table 4.8: *Fit of the model to the observed mean weights and observed SGR when ϕ_y is derived by minimising the weighted error between the observed and predicted SGR.*

Fit of the model to the mean weights							
Age-class	*Average Weight (g)*	*Predicted Weight (g)*	*Range of Predictions (g)*	*Mean Abs. Error (g)*	*% Error*	*Sign. same*	*Sign. correl.*
0+	0.82	0.87	0.19-2.86	0.48	59	NA	NS
1+	5.35	6.10	0.80-27.73	3.99	74	NA	NS
2+	12.34	15.43	1.88-61.99	10.04	81	NA	NS
3+	18.92	30.85	7.08-116.37	20.13	106	NA	NS
Fit of the model to the SGR							
Age-classes	*Average SGR % day^{-1}*	*Predicted SGR % day^{-1}*	*Range of Predictions % day^{-1}*	*Mean Abs. Error % day^{-1}*	*% Error*	*Sign. same*	*Sign. correl.*
0+-1+	0.40	0.35	0.24-0.42	0.05	11	N	*
1+-2+	0.22	0.24	0.21-0.30	0.02	11	Y	NS
2+-3+	0.11	0.18	0.14-0.26	0.07	62	N	NS

Table 4.8 shows an improvement in the fit of the model to the data when the SGR is fitted when compared to the fit to the SGR in Table 4.7, as would be expected, but the fit to the means is substantially worse. The paired $t-$test between the observations and predictions is no longer applicable due to the unequal variance between these two quantities, as can be shown using an $F-$test. This case is denoted as NA in column seven of Table 4.8.

When the model is fitted to the mean weights, the residuals between both the

observed and predicted SGR's and mean weights appear reasonable. This is not the case when the SGR is used to derive ϕ_y, where although the fit to the SGR has improved, the fit to the mean weights has deteriorated considerably. This deterioration may be due in part to the loss of a degree in freedom experienced when deriving the SGR but is probably mainly due to the fact that the SGR is a relative measure of growth rather than an absolute measure.

In view of these results, the model will no longer be fitted to the SGR, but instead to the mean weights. The next subsection will look at how the fit is affected deriving separate values of ϕ_{68} and ϕ_{69}.

4.3.5 Fitting the Model to the Mean Weights with ϕ_{68} and ϕ_{69} Derived Separately

This method of fitting the model to the data is very similar to the previous method except that values for ϕ_{68} and ϕ_{69} are derived separately. Therefore ϕ_{69} is primarily dependent on the growth that is produced in 1969. As there is no data for 1968, ϕ_{68} is largely determined by the subsequent data for that cohort. Note that no value of ϕ_y is determined by the data from any single year as the values are not independent. This new method has been used to derive the results in Table 4.9, by minimising the error function between the predicted and observed weights.

Table 4.9: *Fit of the model to the observed mean weights when ϕ_y is derived by minimising the weighted error between observed and predicted mean weights when ϕ_{68} and ϕ_{69} are derived separately.*

Age-class	*Average Weight (g)*	*Predicted Weight (g)*	*Range of Predictions (g)*	*Mean Abs. Error (g)*	*% Error*	*Sign. same*	*Sign. correl.*
Fit of the model to the mean weights							
0+	0.82	0.86	0.49-1.42	0.13	16	Y	**
1+	5.35	4.46	3.18-5.98	0.89	17	N	*
2+	12.34	11.99	7.31-14.11	0.80	6	Y	***
3+	18.92	26.23	19.94-29.81	7.31	39	N	NS

There is a slight improvement to the fit of the 1+ and 2+ age-classes when compared to Table 4.7, but there is also a decrease in the quality of fit to the 0+ and 3+. This has to be considered with the fact that there is an extra value of

ϕ_y used in this method.

Other data does exist from the electro-fishing surveys from 1969 and 1970, which has yet to be used, may produce a better predictions and will be used in the next subsection.

4.3.6 Deriving ϕ_y with an Extended Data Set

Data exists for the four age-classes caught in 1969 and 1970 but not all of which has been used previously in predicting ϕ_y. This has been because the temperature data does not extend back beyond 1968, so no complete growth trajectories (from birth) for cohorts born before 1968 can be produced and extended forward to the data for 1969. The following method requires data from the 0+, 1+ and 2+ age-classes from 1969 and all four age-classes in 1970 to be included in the analysis.

The starting weights for simulated growth trajectories for the cohorts born from 1967-1969 will be the mean weights of the 0+, 1+ and 2+ age-classes from the 1969 electro-fishing survey. The 3+ mean weight cannot be used as it is the only data point for that cohort. As the data is collected during the summer, ϕ_{69} will be calculated for the period from the electro-fishing survey to the end of the year, rather than for the whole year as with the subsequent values of ϕ_y. This method requires that the reserve to structural tissue ratio be known. During the summer, the fish are growing at a rate where $\rho = \rho_0$, as shown by the model. When the trajectories for the cohorts born from 1967-1969 are started, it will be assumed that this is the case.

This method fits to fewer data points as the data from the first year (1969) is used as starting points for the trajectories and so the model is no longer being fitted to this data. The fit of the model to this new data set is shown in Table 4.10.

Table 4.10 does not produce a clear difference from the previous two methods of fitting to the mean, both in terms of the residuals between the predicted and observed means or correlations.

Table 4.10: *Fit of the model to the observed mean weights when ϕ_y is derived by minimising the weighted error between the observed and predicted weights when the extended data set is used.*

Age-class	*Average Weight (g)*	*Predicted Weight (g)*	*Range of Predictions (g)*	*Mean Abs. Error (g)*	*% Error*	*Sign. same*	*Sign. correl.*
Fit of the model to the mean weights							
0+	0.81	0.87	0.42-1.35	0.15	19	Y	**
1+	5.39	4.40	4.07-6.56	0.99	18	N	*
2+	12.34	11.97	10.75-13.62	0.85	7	Y	***
3+	18.67	25.71	13.00-22.56	7.04	38	N	*

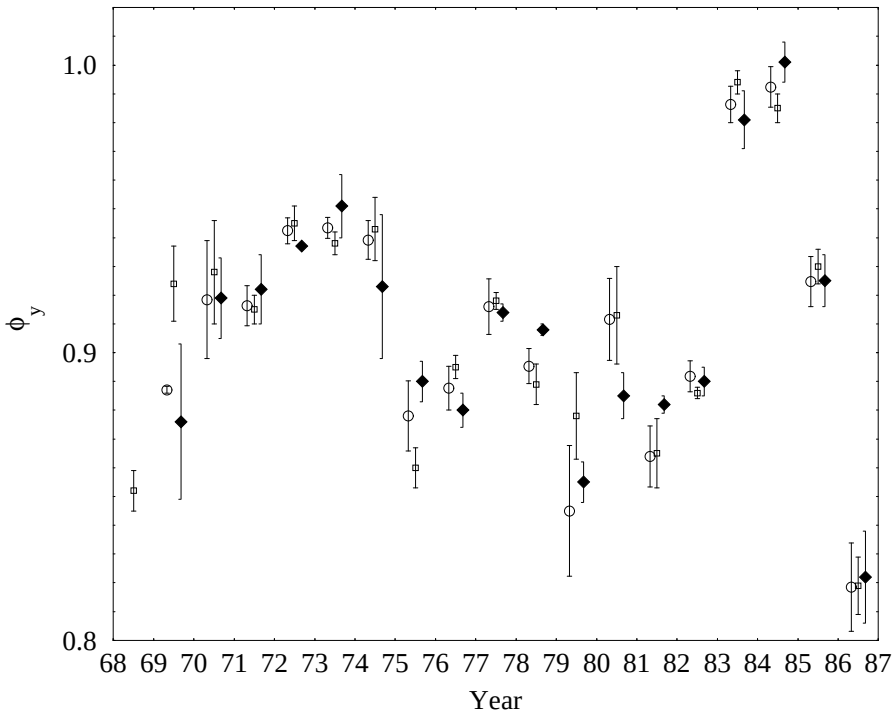

Figure 4.3: *Values of ϕ_y derived when minimising the error function between the observed and predicted weights: the open circles are from the first method outlined in this section, the filled diamonds are from the second method and the open squares are from the third method.*

4.3.7 Comparison of Fits

The most suitable method of minimising the error between the observed mean weights and the model in order to derive ϕ_y needs to be chosen. The values of ϕ_y from the first two methods vary little, as shown in Fig. 4.3. Tables 4.7 and 4.8

show that there is little difference in the quality of fit. When the third method is used, more of the values for ϕ_y are different, but the quality of fit is very similar, so it is hard to determine which is the best method on this basis.

Tables 4.11 to 4.13 are the ANOVA tables which describe the significance of the parameters which have been used to fit the model to the data. They show that the improvement by ϕ_y has significance around the 5% level. The $F-$values have been calculated from the total weighted deviance, which is a more robust method than using the total sum of the square. However, as the significance levels are all similar, we require other criteria to determine which is the best method.

Table 4.11: *ANOVA table calculated from the weighted sum of deviancies (WSD) using the fitting procedure outlined in Subsection 4.3.3.*

	d.f.	WSD	MD	F	P
k	1	1318.0	1318.0	156.4	< 0.001
ϕ_y	17	259.4	15.3	1.811	0.0616
Residual	40	337.0	8.4		
Total	58	1914.4			

Table 4.12: *ANOVA table calculated from the weighted sum of deviancies (WSD) using the fitting procedure outlined in Subsection 4.3.5.*

	d.f.	WSD	MD	F	P
k	1	1318.0	1318.0	161.5	< 0.001
ϕ_y	18	278.2	15.5	1.894	0.0474
Residual	39	318.2	8.2		
Total	58	1914.4			

The third method described in Subsection 4.3.6. has a number of advantages over the others. The first is that the values of ϕ_y are derived with as much of the data as possible so the derivation of values with age-classes missing is minimised. The second advantage is that the temperature record required is only from the date of the first mean weight measurement. This will be useful when fitting to other data sets where temperature data may not exist before the electro-fishing surveys were conducted.

Therefore, the method of deriving ϕ_y that will become the default procedure for fitting the model to the mean weights will use the method defined in Subsection

Table 4.13: *ANOVA table calculated from the weighted sum of deviancies (WSD) using the fitting procedure outlined in Subsection 4.3.6. Note that the d.f. change which is due to using different starting conditions that reduce the data points used.*

	d.f.	WSD	MD	F	P
k	1	1268.1	1268.1	149.2	< 0.001
ϕ_y	17	270.1	15.9	1.876	0.0520
Residual	39	330.6	8.476		
Total	57	1858.4			

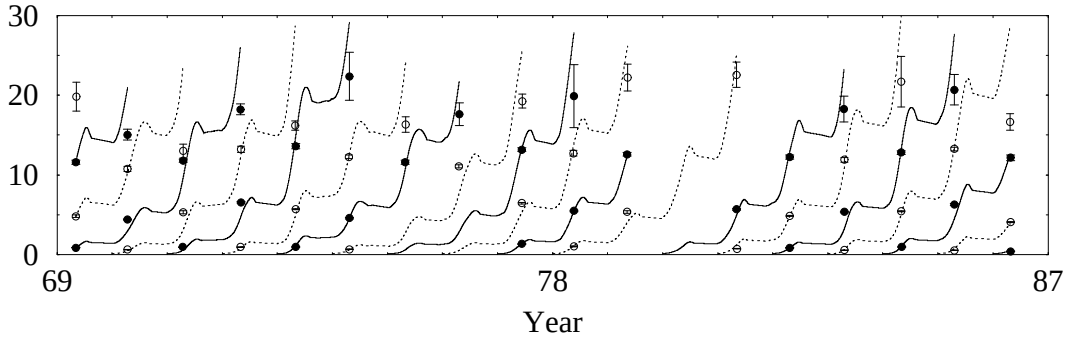

Figure 4.4: *Simulations produced with the values of ϕ_y derived by fitting the model to the mean weights with the extended data set (as in Subsection 4.3.6). Trajectories with broken lines refer to the cohorts with open circles.*

4.3.6. Fig. 4.4 shows the simulations produced using this method with the data. The overall fit is now clearly better, as, for the first time, it is obvious which curve fits which data points and to which trajectories the few discrepant points should fit. Table 4.14 shows how the fit of the model has improved as the fitting procedure has developed from the E&H model to the CGM_e when ϕ_y is used in Subsection 4.3.6.

4.4 Sensitivity Analysis

Variation of the input variables will affect the values of ϕ_y and the extent to which this happens needs to be known. The input variables are approximations, and in order to predict ϕ_y with sufficient accuracy, their effect on ϕ_y needs to be known and understood in order to prevent misleading results. In this section, the four input variables will be varied, and their effect on ϕ_y examined. These are

Table 4.14: *R^2 values derived from the fit of the model to the data for the various models used. n represents the numbers of data points to which the R^2 value applies. These values were derived by correlating observations with the predictions.*

$Age-Class$	$E\&H$		CGM_e		$\phi(t)=k$		$\phi(t)=\phi_y$	
	R^2	n	R^2	n	R^2	n	R^2	n
0+	0.126	14	0.166	14	0.154	14	0.512	13
1+	0.104	15	0.001	15	0.001	15	0.242	14
2+	0.114	15	0.005	15	0.006	15	0.735	15
3+	0.006	14	0.125	14	0.124	14	0.235	15
All	0.418	58	0.834	58	0.854	58	0.915	57

the temperature, time of hatching, the weight-length relationship and the weight at first feeding.

In order to test the sensitivity of the model to these quantities, how well each of these quantities has been approximated needs to be known. Then the factors outlined in the previous paragraph will be varied and different values of ϕ_y derived. These will then be compared to each other in order to see if the magnitude and the relative values of ϕ_y are preserved.

4.4.1 Sensitivity of the ϕ_y to Temperature

The model uses average mean monthly temperatures, derived from the maximum and minimum daily temperatures throughout the month. The resolution of monthly temperature was taken as the actual daily temperatures did not exist for all months. For these months, summaries were available as monthly means which had previously been calculated by D.W. Hay using the method above. In order to have a uniform data set, all monthly temperatures were used and calculated using this method.

Subsequent data from the Girnock (from May 1986 to December 1996) has been taken by an electronic measuring device that takes the temperature every 45 minutes, which can be regarded as a continuous record. From this, more accurate estimates of monthly mean temperature were calculated, and these were compared to estimates made using the previous method. From this, an idea of the error associated with the original method could be deduced.

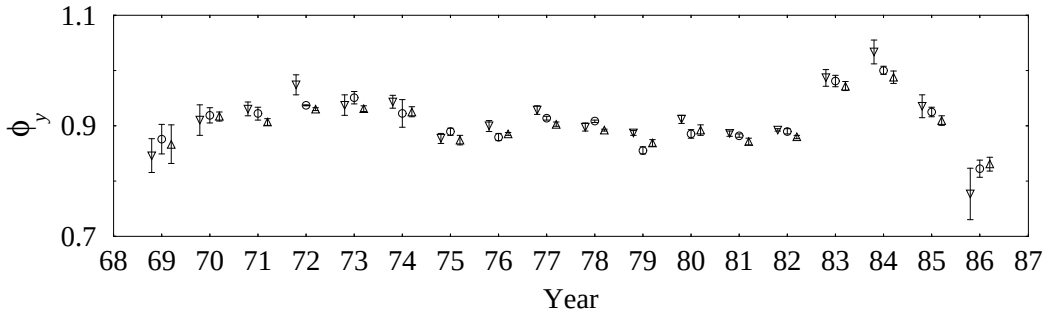

Figure 4.5: *Values of ϕ_y with their standard errors when the temperature is lowered (∇) and raised ($\triangle$) by 0.2°C compared to the original values ($\circ$).*

Results from Different Temperature Regimes

The error between approximating the monthly mean by averaging the daily minimum and maximum temperatures and by taking the average of the temperatures in a month when they are measured every 45 minutes was always less than 0.2°C for each month. Therefore, ϕ_y was derived with temperatures raised and lowered by 0.2°C.

When the temperatures are varied by ± 0.2°C, the sets of ϕ_y , which are shown in Fig. 4.5, were highly correlated ($P < 0.001$, $R^2 > 0.9$). This implies that the error associated with the method of estimating the temperature from the data is not large enough to perturb the relative values of ϕ_y sufficiently to change their pattern. The absolute values of ϕ_y do change because lower temperatures decrease growth rates which is compensated by an increase in ϕ_y. A two-way ANOVA with year and temperature regime as factors shows that temperature is a significant factor. However, the differences in the average values of ϕ_y are less than 0.016, which is unlikely to perturb the growth trajectory by a large amount.

4.4.2 Sensitivity of ϕ_y to the Weight-Length Relationship

The weight-length relationship that has been used was derived using data from the River Eye is in the form of equation (4.6),

$$W = \alpha L^{\beta} \tag{4.6}$$

where α and β are constants. Altering the weight-length relationship would produce new data sets to which the model can be fitted, by adjusting ϕ_y.

Deriving ϕ_y with Different Weight-Length Relationships

Four sets of ϕ_y were derived with different coefficients for the weight-length relationship. ϕ_y was derived with β lowered by one s.e. and increased by one s.e., then with α was lowered by one s.e. and increased by one s.e.

An additional two sets of ϕ_y were calculated. The first used weights calculated at the upper 95% confidence interval of the weight-length relationship, so that they all weights increased. The second used weights calculated at the lower 95% confidence interval so they all decreased.

Results Using Different Weight-Length Relationships

The six new sets of ϕ_y could be compared to the values derived in Section 4.3. and are shown in Fig. 4.6. It was found that all the sets of ϕ_y were highly correlated ($P < 0.001$, $R^2 > 0.8$ in all cases) with each other. A two-way ANOVA showed that there were significant differences between ϕ_y derived with the different weight-length relationships. This is because the data to which the model is being fitted has changed in a systematic way. However, the mean absolute difference is very small, being less than 2% of ϕ_y derived from the original weight-length relationship. This indicates that the error associated with the weight-length relation is small enough not to distort the general pattern of the values of ϕ_y.

4.4.3 Deriving ϕ_y Using the Variable Hatching Weights

The initial weight of an emerged hatched fish is currently assumed to be 0.15 g. This is the assumed hatch weight of the live alevins. The initial weight may affect ϕ_y, so this will be tested by varying the initial weights and comparing the resulting values of ϕ_y.

Estimates of the emergence weights of alevins exist in the literature for Atlantic salmon. Gunnes (1979) reared Norwegian salmon eggs from fertilisation to emergence at different temperature regimes and found their weight at hatching to vary between 0.062 and 0.16. Peterson and Martin-Robichaud (1989) used Canadian Atlantic salmon fry that had been raised at various temperatures with initial

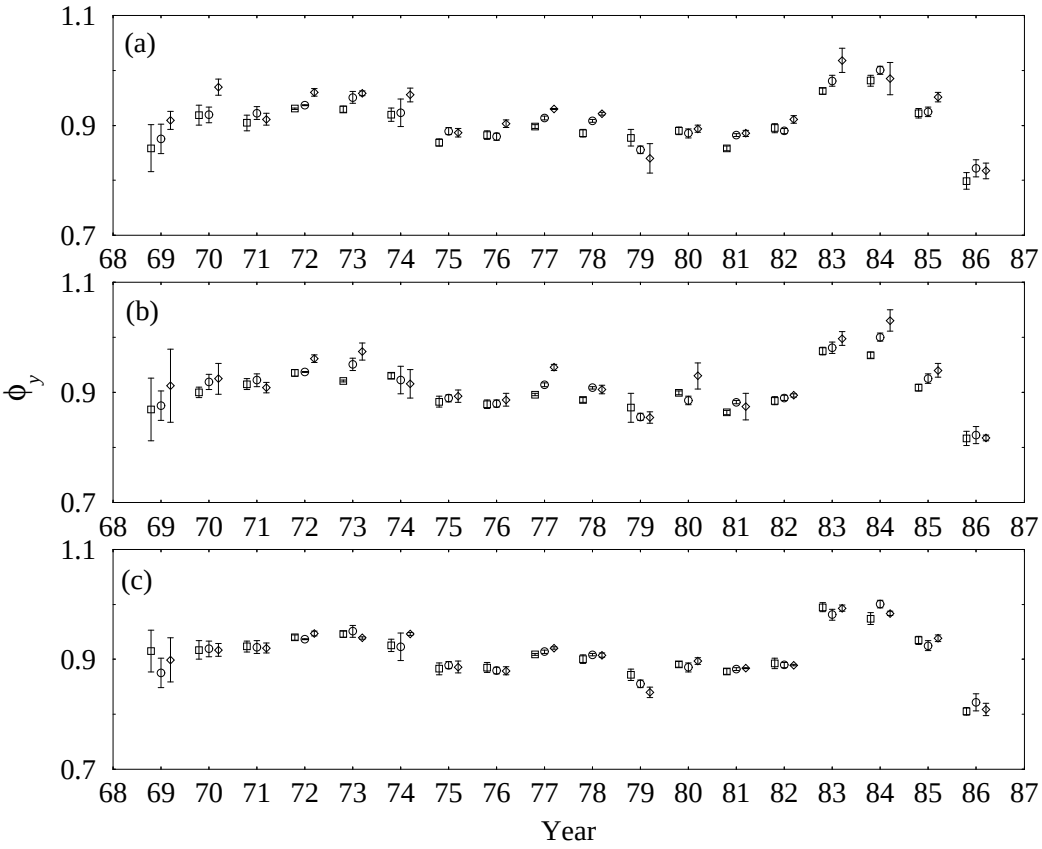

Figure 4.6: *Values of ϕ_y with their standard errors when the when different weight-length relationships are used. (a) has the scaling constant α lowered (□) and raised (◇) by one s.e. In (b) the exponent β is lowered (□) and raised (◇) by one s.e. For (c) weights were derived using the upper (□) and lower (◇) 95% confidence intervals. These were all compared to the original values (○).*

weights of between 0.171 and 0.181 g.

The sensitivity analysis requires two extreme sizes of Atlantic salmon for the derivation of ϕ_y. Based on the sizes above, they will be a lower limit of 0.05 g and an upper limit of 0.2g.

Results Using Different Hatching Weight

The values of ϕ_y derived by using different hatching weights are highly correlated with ($P < 0.001$, $R^2 > 0.895$), and a two-way ANOVA, with year and hatch weight as factors, does not show hatch weight to be a significant factor. This size of variation in the starting weights does not have a significant effect on the

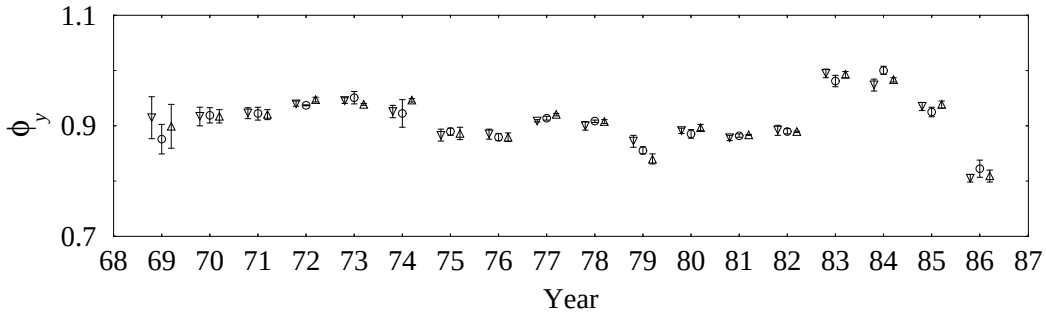

Figure 4.7: *Values of ϕ_y with their standard errors when the when different birth weights are used. The ∇ represents ϕ_y derived from a low birth weight and $\triangle$ are the ϕ_y derived from a high birth weight. ϕ_y derived when birth weight is 0.15g are shown by $\circ$.*

derived values of ϕ_y.

4.4.4 Sensitivity of ϕ_y to a Temperature Dependent Emergence Date

A nominal hatching date has been used as the starting date for cohorts whose growth is being predicted from birth. A more appropriate starting time may be the date of emergence. After the eggs have hatched, the alevins stay in the gravel for a period, after which they emerge to disperse and feed (Crisp 1981). During the period when they are in the gravel, they are able to survive from nutriments from a yolk sac with which they are born (Brannas 1988). The length of the growing season is defined from the date of emergence and it is possible that it will have a large influence on the weight of the fish at the end of the growing season (Shackley and Donaghy 1992).

ϕ_y is a measure of year quality, so emergence date could one of its components. Introducing emergence date into the model will allow us to see if this is true by judging the changes of ϕ_y, as the variation of ϕ_y should decrease. Therefore, a variable growing season will be introduced into the model.

A variety of methods can be applied to estimate the time of emergence. Egglishaw and Shackley (1977) calculated the degree-days from 1stDecember to emergence for a population of salmon in Shelligan Burn in southern Perthshire, Scotland. This was calculated as 622 degree-days from eggs fertilised in 1972 to emergence

as fry the following year. This estimate has since been used to estimate emergence times in the River Dee (Shackley and Donaghy 1992).

Other methods exist to calculate the time from fertilisation to hatching (Crisp 1981), hatch date to emergence (Brannas (1988), Jensen et al. (1989)), and fertilisation date to emergence (Crisp 1988). These were derived from experiments where temperature was regulated.

A more complicated model exists to predict emergence period for sea trout, *Salmo trutta* L. by Elliott and Hurley (1998), but there is insufficient field data from the Girnock to reparameterize and use this model for Atlantic salmon.

Deriving ϕ_y Using Temperature Dependent Emergence Dates

Spawning usually takes place in the Girnock during November and coincides with the autumn spates. Buck and Youngson (1981) and Webb and Mclay (1996) observed that spawning occurred between 28$^{\text{th}}$ October and 20$^{\text{th}}$ November.

Temperature and estimates of the spawning time are available for the Girnock so the equation by Crisp (1981) can be used to predict time from fertilisation to hatching, defined as D in days, from temperature, T ($^{\text{o}}$C). It is given below as (4.7),

$$log\ D = -2.6562\ log(T + 11) + 5.1908. \tag{4.7}$$

Then equation (4.8), which is taken from Jensen et al. (1989), can be used to estimate the time from hatching to emergence, E,

$$E = 472T^{-1.27}. \tag{4.8}$$

This method has previously been used by Jensen et al. (1991) to estimate time between fertilisation and hatching, given temperature records, for Atlantic salmon. Equations(4.7) and (4.8) were calculated for fish reared at constant temperatures, and in the wild over this period, there are large changes in temperature.

D was calculated first by taking a range of dates between fertilisation and an assumed maximum hatching date, D'. The average temperature between fertilisation and each date up to D' was calculated and was then used in equation (3.7.) to produce a series of values of D. The hatching date was taken when $D' = D$.

A similar process was used to calculate E. This was repeated for all the years from 1970-1986 for three different fertilisation dates.

Three sets of ϕ_y were produced using this method. They corresponded to an early, middle and late fertilisation date (1^{st} , 10^{th} and 21^{st} November respectively) which produced emergence dates that ranged from 16^{th} April to 23^{rd} June. A fourth set of ϕ_y was produced using the method described by Egglishaw and Shackley (1977) which was based on degree-days, which gave emergence dates between 2^{nd} March and 1^{st} April.

Results Using Different Emergence Dates

These simulations represented a large range of starting dates yet produced very similar and highly correlated values of ϕ_y, which are shown in Fig. 4.8. When correlated with each other and the values of ϕ_y derived in Subsection 4.3.6, $P < 0.001$ and $R^2 > 0.73$. A two-way ANOVA with year and emergence date as factors showed that emergence date was not a significant factor for the values of ϕ_y.

4.4.5 Overall Robustness of the model

The pattern of ϕ_y produced by the original data set has been preserved well for all the simulations in this section. This indicates that the model's predictions of ϕ_y are robust for the magnitude of measurement error of the input variables. The values of ϕ_y from the simulations are shown in Fig. 4.9 and have also been summarised into mean values with 95% confidence limits.

The model now needs to be tested on data that has more than one data point for each cohort per year so that we can see if the growth trajectories within years represent the growth of the population within years. The assumption that the mean growth rate of the population can represent the growth rate of an individual needs to be tested. These will be done using data for individual fish in the Chapter 5.

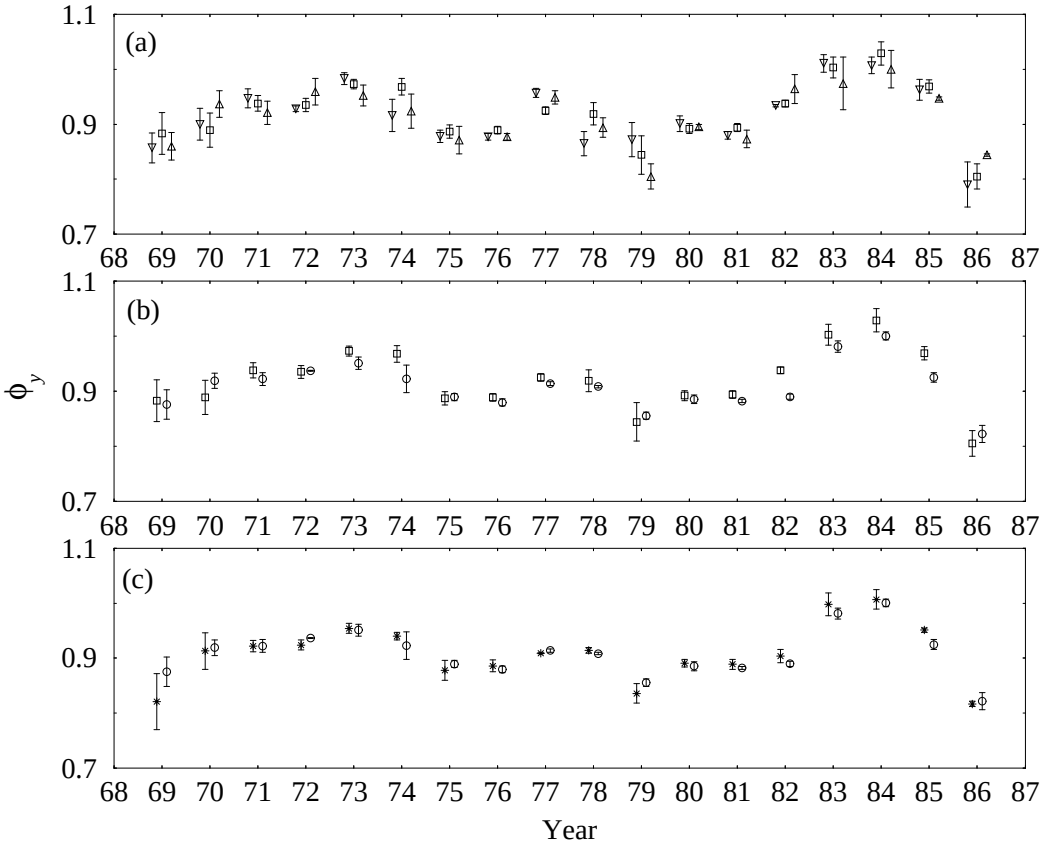

Figure 4.8: *ϕ_y derived from different emergence dates. (a) are ϕ_y derived from emergence dates based on fertilisation dates and over winter temperatures. ϕ_y derived from three fertilisation dates are shown, where ∇ is early, $\square$ is mid and $\triangle$ is late. The middle birth date is compared to the original ϕ_y ($\circ$) in (b). (c) compares the ϕ_y when it is derived from the E&S formula ($*$) and the original values.*

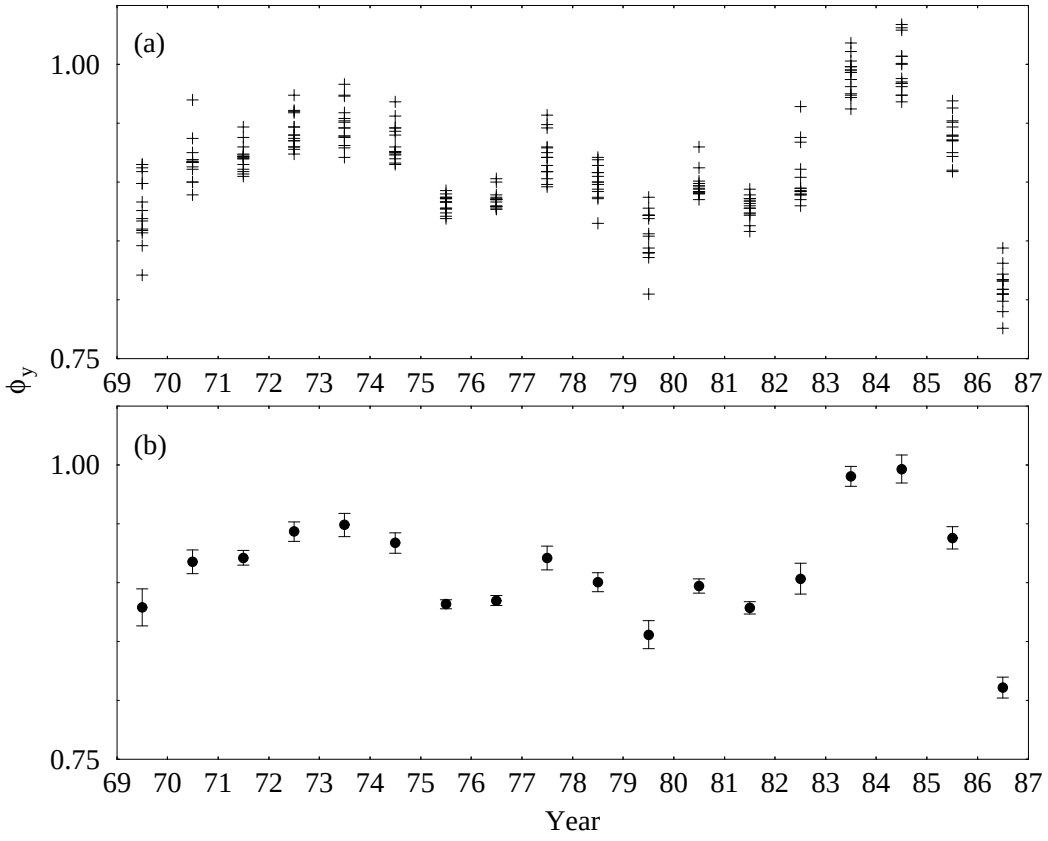

Figure 4.9: *Values of ϕ_y derived from the sensitivity analysis and the values derived in Subsection 4.3.6. (a) Scatterplot of ϕ_y, (b) the 95% CI are shown from all the ϕ_y derived in this section and the original values.*

Chapter 5

Fitting the Growth Model to Data from Individual Parr

5.1 Introduction

The model developed in Chapters 3 and 4 has been used to predict the mean weights of different age-classes for different cohorts. The mean weight of the parr from each age-class in each year has been used to represent the weights of the individuals of the population. Also, the growth trajectories have only been fitted to the mean weights for parr sampled during the summer. These trajectories have been assumed to be applicable to an individual in that population all year round.

In this chapter, we aim to test two aspects of the model. The first will be: How well can the model predict the mean weights of the population during months between summer surveys? The second will be: Is the model able to predict the growth trajectories of individual parr?

These aspects will be tested using a set of data that was collected at approximately monthly intervals from summer 1998 until spring 1999. It consists of electro-fishing samples taken in the middle section of the Girnock Burn. A selection of parr at each survey were individually marked, so if they were subsequently recaptured at a later survey, they could be identified. This would then give an indication of the growth rates of individual parr over this period.

Previously, the model has been fitted to the data by adjusting the function $\phi(t) =$

ϕ_y, an annual step function which changes at the start of each year. The model will now be fitted to the data by adjusting a single constant value of $\phi(t) = \phi_m$ applied from June 1998 until March 1999. This single annual value will make comparisons between different parr straight forward, particularly for parr only captured before or after 1st January 1999 which would have had only one value whereas the other parr would have had two. Once the model has been fitted to the mean weights and to the individual parr weights, the predicted growth rates can be compared by seeing if $\phi(t)$ differs for individuals and the population.

5.2 Data from the Girnock Burn from 1998-99

5.2.1 Data from Individual Salmon Parr

Ten electro-fishing surveys were conducted from June 1998 to March 1999 at two sites in the middle section of the Girnock Burn. During each survey, salmon parr had their length and weight measured. Unmarked parr longer than 80mm were marked using a long lasting panjet marking code that was individually unique. They were often re-caught at subsequent surveys. Scale samples were taken to determine the parr's age, and most of the parr caught were from the 1996 or 1997 cohorts. Parr from other cohorts comprised too small a sample to use. Marked parr captured at the fish trap during the autumn and spring migrations also had measurements were taken in the same way.

5.2.2 Temperature Data

The water temperature over the period of the surveys was measured using a digital recorder every 45 minutes, which was located downstream at the fish trap. The recordings for each month were summarised into monthly temperatures by taking their average. These average monthly temperatures were then used in the model.

5.3 Fitting the Model to the Population Mean Weights

5.3.1 Fitting the Model to the Data

A method was required to test whether the growth trajectories produced by the model were similar to those that are observed in the wild population. The model had previously been fitted to the mean weights during the summer, represented by just one measurement each year. It could now be fitted to mean weights from the population sampled on a monthly basis from June 1998 until March 1999.

Three fitting parameters were used. The first was the annual year quality estimator, $\phi(t) = \phi_m$, which would be kept constant across all age-classes. The other two were the starting weights for the growth trajectories of the age-classes, denoted $W_{0,97}$ and $W_{0,96}$, for the 1997 and 1996 cohorts respectively. The trajectories would start at the time of the measurement of the first mean weight for each age class, which was on 8th June. The starting weights were fitted parameters rather than fixed points from which the trajectory could start as there is some uncertainty associated with each data point. The reserve to structural weight ratio was assumed to be at its ideal value during the summer when the growth simulations were started.

The parameters were found using the DSO procedure and minimising the weighted error function, W_2 described in equation (4.3). The initial conditions for the DSO procedure were varied and always converged to the same minimum, and the fitted parameters are shown in Table 5.1.

Table 5.1: *Parameters derived from fitting the model to the mean weights of the population by minimising the W_2 weighting function.*

$W_{0,97}$ (g)	$W_{0,96}$ (g)	ϕ_m	Mean weighted error
4.852	10.016	0.76656	1.2629

5.3.2 The Predicted Mean Weights

The model has been fitted to mean weights of the population sampled at various times from June until March, a period that covers the autumn migration and

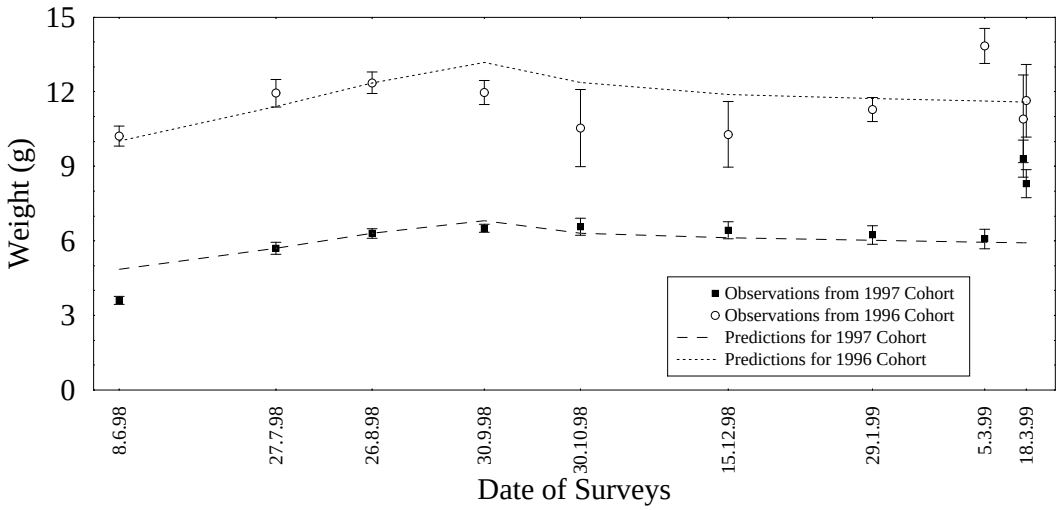

Figure 5.1: *Fit of the model to the mean weights for the 1996 and 1997 cohort from the electro-fishing surveys. The observations are shown with their standard errors and the parameters used in the model are those in Table 5.1.*

the start of the spring migration. Individuals from the marked population were found to have migrated during this time as they were recaptured downstream at the smolt trap. As the older parr form the majority of the migrants, the 1996 cohort will be the one which is most affected.

The data to which the model was fitted, with the standard error of the means, and the predictions from the model using the parameters in Table 5.1, are shown in Fig. 5.1. There are two aspects of the cohort's mean weights that the model is unable to reproduce. The first is the decrease in the mean weights from September until December for the 1996 cohort: the model over predicts observed weights. This is not apparent for the 1997 cohort, where the changes in the mean weights are predicted well. As the spring migration is beginning, the model is able to predict the mean weights of the resident parr from the 1996 cohort on the final two surveys during the 17th and 18th March but not for the weights for the previous survey, on the 5th March. The observed weights of the 1996 cohort fall between 5th March and 18th March 1999 may be due to the larger members of the population smolting, and the decrease in the mean weights of the cohort during autumn may be due to the autumn migration.

There are no mechanisms in place in the model to cope with the effects of migration on mean weights of the resident population. If the decision to migration

is based on the growth rate, which it is generally thought to be (Elson (1957), Metcalfe et al. (1990), Økland et al. (1993), Osterdalh (1969)), then this will lower the weight of the resident population, and the model will over predict their weight, which appears to be the case.

The second aspect that the model fails to predict is a large increase in the mean weight during the spring. This occurs between the January and the first March survey for the 1996 cohort, and between the first and the final two March surveys for the 1997 cohort. Over this period the model predicts weight loss due to the water temperature being less than 6^oC. The reasons why these data are fitted badly are discussed in Section 5.5.

Another large error occurs between the prediction and observation of the mean weights of the 1997 cohort on 8th June 1998. The model over predicts by a large amount, and the errors of the subsequent predictions over the summer for the cohort are relatively small. As the spring weights are under predicted, the period of rapid growth may last from March until June. This would indicate that the predicted growth rate was too low and that, over this period, ϕ_m is too low.

5.4 Fitting the Model to Individuals' Weights

The aim of the model is to predict the growth rates of individual parr, and we have so far assumed that fitting the model to the mean weights of the population is representative of fitting to the weights of individuals. We will be able to test this assumption by fitting the model to data from individual parr. During the electro-fishing surveys on the Girnock from 8th June 1998 to 18th March 1999, 124 marked parr were caught more than once. This meant that we were able to fit the model to each individual by adjusting $\phi(t) = \phi_i$. From these parr, we would be able to compare ϕ_m to the values of ϕ_i and also examine the distribution of the residuals to assess the goodness of fit.

5.4.1 Derivation of ϕ_i

Applying the DSO procedure

A growth trajectory was fitted to each individual parr which was caught at least twice using the weight at first capture as a starting point for the trajectory and adjusting ϕ_i to fit the observations. Four different initial values of ϕ_i were used in the fitting procedure (ϕ_i=0.65, 0.75, 0.85 and 0.95) in order to see if they would converge to the same solution. The starting value of ρ needed to be adjusted for those parr first caught late in the season, as the parr could no longer be assumed to be healthy (i.e. $\rho = \rho_0$). They were assumed healthy in June, and from the parr caught in June, ρ was estimated at the dates of the following surveys. Therefore, as the season progressed, these values of ρ were used at the start of the simulations for newly caught parr. The weighting function could not be used as there was no standard error associated with each data point, so the RMS error was minimised. Using this procedure, a value of ϕ_i was derived which could be used to produce a growth trajectory for each parr.

Using the four different initial conditions of ϕ_i mentioned above, it was found that the DSO did not always converge to a unique solutions. Moreover, the value of ϕ_i for all the parr first caught after the August survey was highly sensitive to the initial conditions. No parr were first caught during the September survey, but those from the October survey required simulations to begin on the 30th October 1998, which is six days before the predicted assimilation rate becomes and stays at zero until 12th March 1999. This means that ϕ_i will have little or no effect on the growth trajectory over this period, so all parr which were first caught after the August survey were excluded from further analysis.

Summary of Individual Data

We shall be using the trajectories fitted to the final data set of 71 individual parr. Table 5.2 shows when the parr were first caught, and the numbers recaptured at subsequent surveys, with the dates of all the surveys. Of the 71 parr, 45 were caught more than twice, 26 more than three times, 14 more than four times and seven more than five times. The parr which were caught the most often tended to be those which were caught the earliest.

Table 5.2: *Summary of the capture dates for the parr to which the model was fitted.*

Date of Survey	Number first caught	Number of marked parr caught	Mean number of recaptures
8-Jun-98	23	-	2.435
27-Jul-98	37	11	2.324
26-Aug-98	11	43	2.273
30-Sep-98	0	38	-
30-Oct-98	0	16	-
15-Dec-98	0	15	-
29-Jan-99	0	11	-
5-Mar-99	0	10	-
17-Mar-99	0	11	-
18-Mar-99	0	12	-

5.4.2 Analysis of ϕ_i

The values of ϕ_i derived from the individuals ranged from 0.592 to 0.905 and are displayed in Fig. 5.2. Each of these histograms represents a different subsample of parr, which are defined by the minimum number of times each parr was caught. The values of ϕ_i are approximately normally distributed, and as the parr which are caught least are removed, the standard deviation of the distribution tends to decrease, as shown in Fig. 5.3.

As the resolution of the data increases, the less variation there is in the derived values of ϕ_i, and indicates that there may be a single 'site' value of ϕ_i, and the observed variation is this site value perturbed by experimental error. This can be tested by looking at the size of perturbations required to produce the observed distribution of ϕ_i for the individual parr which were caught most often.

Error Associated with Recorded Weights

Deducing the size of the perturbation to the data that would produce the spread ϕ_i which is seen in Fig. 5.2.e. would allow us determine if the spread of ϕ_i was the result of measurement error or due to another process. In order to do this, the size of the experimental error needed to be determined.

Parr caught during the surveys were placed in a holding tank for between half an

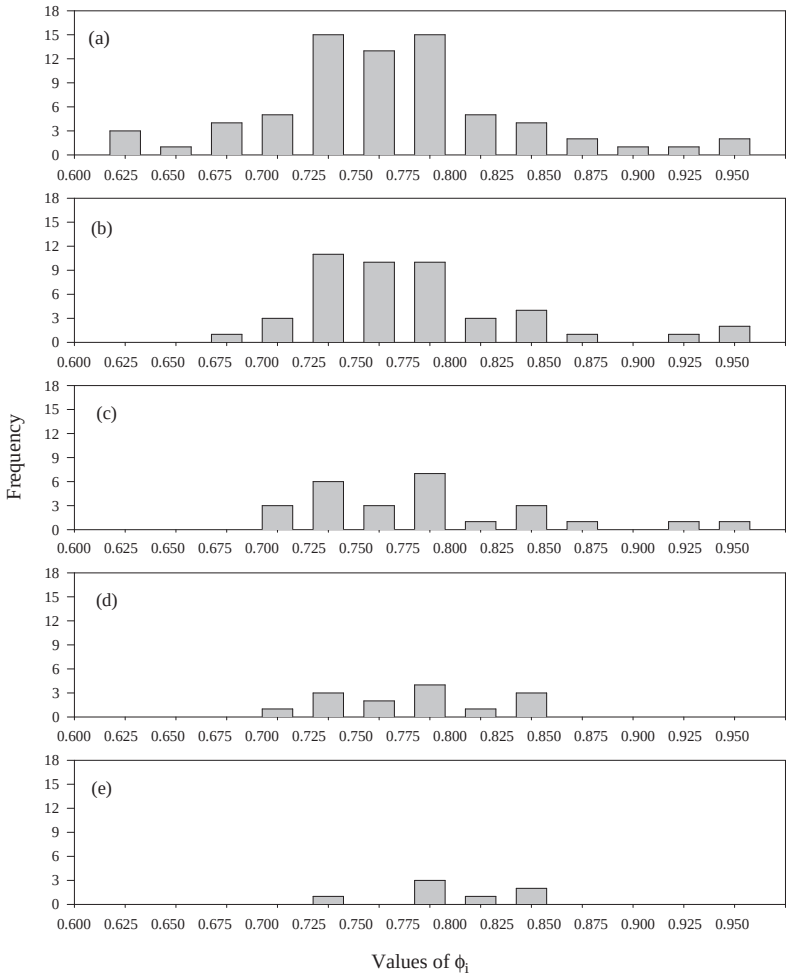

Figure 5.2: *Histograms of ϕ_i derived from individual parr. The top histogram (a) is for all 71 individuals, (b) is from parr which were caught more than twice, (c) from parr which were caught more than three times, (d) for parr which were caught more than four times and (e) is from parr which were caught greater than five times.*

hour and three hours before being weighed. During this time, it was possible that the parr may have become lighter through evacuation of the gut. If the parr was recaptured on a subsequent survey, and weighed after a different amount of time in the tank, then the level of evacuation would be different. These differences would them produce random errors in the data set, so it was important to know what the scale of this error was likely to be.

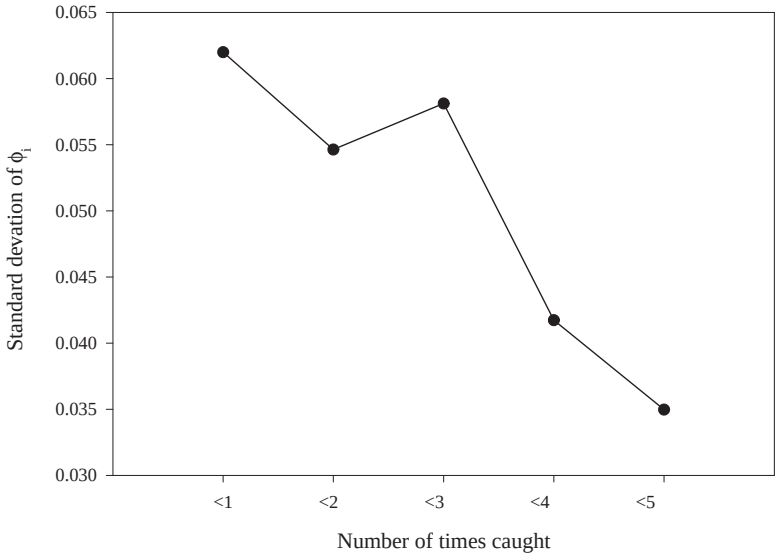

Figure 5.3: *The standard deviation of different subsamples of ϕ_i from the individual parr. The subsamples are defined by the minimum number of times a parr is caught.*

There is little literature on the gastric evacuation rates of juvenile Atlantic salmon. Rates for brown trout and rainbow trout reared at 11°C are $0.437\text{mg.g}^{-1}.\text{hr}^{-1}$ and $0.786\text{mg.g}^{-1}.\text{hr}^{-1}$ respectively, are given by Kristiansen (1998) for fish which were fed and then starved. The weight range of individual marked parr used in the random simulation tests above was 6.5-16.2g, which over a period of three hours, equates to 0.0382g and 0.0213g for a 16.2g fish at 11°C.

In addition, some of the marked parr were caught and measured at the fish trap and were remeasured three days later, when, on average, they were 0.483g (SD=0.1169g) lighter. Talbot et al. (1984) observed that it took Atlantic salmon (approx. 8g live weight) kept at 9-13°C approximately 60 hrs to evacuate a meal during a period of starvation. If we assume the weight loss was due to constant evacuation over this period and the parr were not feeding in the fish trap, then we derive a figure for evacuation of $0.022 - 0.036$g for a 16.2g parr kept at approximately 3.7°C over three hours. This provides an upper limit for weight loss due to gut evacuation in the holding tank.

We shall further assume that the weight loss due to metabolic cost in the tank is negligible. The parr were weighed on a balance with an accuracy of 0.1g, which gives an error of ± 0.05g. This gives a combined estimate of the experimental error of approximately $< \pm 0.09$g for a large parr.

The Effect of the Perturbations to the Data on ϕ_i

Using the data from the seven parr for which were caught more than five times, the weight at each capture was perturbed by a random amount taken from a uniform distribution between ± 0.2g. The model was refitted to this new data set, and this process repeated 50 times for each parr. From the 50 values of ϕ_i from each of the seven parr, the variance was calculated and compared to the variance of the distribution in Fig. 5.2.e. using an F-test to compare sample variances.

It was found that assuming a random error of ± 0.2g, the variance of the simulated distributions were significantly less than for the distribution in Fig. 5.2.e, and for each parr $P < 0.001$. Further to this, simulations were carried out with a random error of ± 1.0g, and the variance was significantly less for four of the seven parr ($P < 0.01$). This indicates that the variation in the distribution of ϕ_i cannot be accounted for by random variations of $< \pm 0.2$, and so cannot be explained through experimental error alone.

Correlating ϕ_i with Final Predicted Weight

The model may be used to predict the weight of the parr at any time, and predicted weights can be used as a comparison between fish. The final predicted weight, W_T, will be used as an estimate of the size of a fish relative to others. Other factors that can be associated with each parr are its age-class and if and when it was caught in the fish trap, implying that it was emigrating. These factors may be used to explain some of the variation in ϕ_i.

A one-way ANOVA was used to look for differences between the values of ϕ_i between the age-classes, and was found not to be significant ($F_{1,69} = 0.53,\ P = 0.469$).

The values of ϕ_i can be correlated with the final predicted weights of the parr. As

ϕ_i is a measure of the quality with which the parr grows, it may indicate if parr of different sizes grew at different rates. Table 5.3 is the accumulated ANOVA table from a regression model which fits ϕ_i with the final predicted weights of the parr as a covariate and age-class as a factor. Although the fit is significant, it only explained 20.7% of the variance. Whether or not the parr migrated, and the

Table 5.3: *Accumulated analysis of variance table for the fit between ϕ_i and the predicted weight from the CGM_e model, W_T. Age-class is a factor and W_T is a covariate.*

	d.f.	SS	MSS	F-value	P	% Var.
W_T	1	0.0266	0.02662	8.51	0.005	9.90
Age-Class	1	0.0292	0.02922	9.34	0.003	10.87
Residual	68	0.2128	0.00313			
Total	70	0.2687	0.00384			

season in which they migrated were other factors used in the regression model, neither of which was significant.

Comparing $\phi(t)$ from the Mean and Individuals

The value of ϕ_m derived from the mean weights of the population, in Table 5.1 was compared to the mean ϕ_i from the individuals using a t-test for the different subgroups of parr. The results are in Table 5.4, and show that ϕ_m is not different when compared to the mean of different subsets based on the least number of times the parr were caught.

Table 5.4: *Results from using a two tailed t-test to look at the differences between $\phi_m = 0.767$ and ϕ_i.*

Times Caught	n	Mean of ϕ_i	P
> 2	46	0.755	0.14
> 3	26	0.759	0.51
> 4	14	0.754	0.30
> 5	7	0.772	0.68

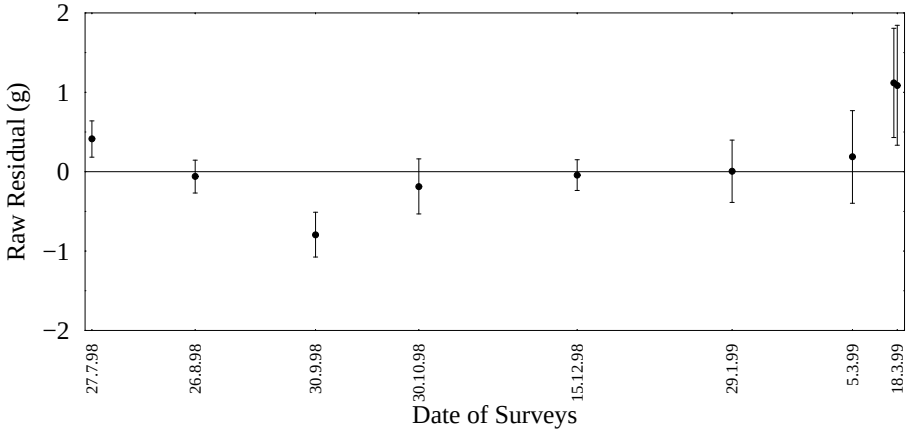

Figure 5.4: *Residuals from fitting the model to the individual data summarised into means with their 95% CI for parr caught more than twice (residuals shown are observations-predictions).*

5.4.3 Analysis of the Residuals

The residuals from all of the parr that were caught more than twice were calculated and indicate how well the model fits to the individual data. Fig. 5.4 shows the mean raw residuals, calculated as the prediction subtracted from the observation, with 95% CI. The tests in Table 5.5 are based on the normalised residuals, which were calculated from the raw residuals divided by observed weight. This was done so that the predictions would not be biased by fish size, as they contain two different age-classes. The t-tests in Table 5.5 indicate whether the means of the normalised residuals are different from zero.

Table 5.5: *Results from t-tests for the normalised residuals from the model for parr caught more than twice.*

No.	Date	n	Mean normalised residual	P
2	27-Jul-98	8	0.0343	< 0.01
3	26-Aug-98	31	-0.0075	0.41
4	30-Sep-98	31	-0.0726	< 0.001
5	30-Oct-98	15	-0.0320	0.23
6	15-Dec-98	15	-0.0066	0.51
7	29-Jan-99	11	0.0166	0.60
8	05-Mar-99	10	0.0048	0.90
9	17-Mar-99	11	0.0858	< 0.01
10	18-Mar-99	10	0.0806	0.055

The residuals from survey 2 are all positive and 14/15 from survey 4 are negative. Trajectories with large residuals cannot be accounted for by individuals with few data points, and correlations between normalised residuals and number of times caught indicate that for survey 4, the larger normalised residuals are associated with parr which were caught the most often ($R^2 = 0.67,\ P = 0.011$). The pattern of these residuals suggest that for the period between survey 1 until survey 3, the value of ϕ_i is too low, and between survey 3 to 5, it is too high.

The predicted weights of the parr during the late autumn and winter fit the observed weights well. Over this period, the assimilation rate is close to or at zero. This indicates that the function for the maintenance rate of individuals and the parameters derived for it are able to predict over winter weight loss in the wild.

The residuals for the final two surveys in March are both greater than zero, and the reasons why this might be are discussed in Section 5.5.

5.5 Summary and Conclusions

5.5.1 Differences between the Predictions and the Observations

When the model is fitted to both the mean weights of the population and the weights for the individuals, it under predicts the weights in spring. This is the period when the water begins to warm and the parr are able to resume feeding. If the parr were not eating during the winter, then it is likely that they have an empty gut. The model only predicts somatic growth, so the under prediction by the model may in part be a result of the gut contents of the parr. A rough estimate of gut content can be derived from six parr, which were caught and held in the fish trap at the Girnock for a period of three days. They were weighed on 19th March and reweighed on 22nd March, and the mean weight difference and standard error was 0.48g$\pm$0.048 lower after three days, which is enough to account for the significance of the residuals of surveys 9 and 10 from zero.

If the gut contents are having a large effect on the overall weight in spring, then there must be a corresponding weight loss when the parr cease feeding during

autumn and over winter. This may be seen as the model over predicting the parr weight at survey 4 (30/9/98).

However, during March, the model predicts that the parr are still in a torpid state, where the predicted assimilation rate is at a very low level, lower than its predicted metabolic rate. Under these conditions, the parr are still in the behavioural state that they adopt to survive over winter and the model predicts that they are losing weight.

When the E&H model was fitted to the data for the River Eden by Elliott and Hurley (1997) they found that they under predicted the weight during spring and over predicted during late autumn. This was explained by seasonal changes in appetite (Metcalfe and Thorpe 1992). As the CGM_e uses the same function for the assimilation rate as the E&H model, the same problem may be occurring. The CGM_e is unable to distinguish changes in appetite, food availability or food assimilation within years, which have been generalised into the function $\phi(t)$.

5.5.2 Variation in ϕ_i

The variation of ϕ_i cannot be explained by random measurement errors of the appropriate magnitude, which indicates that not all the observed variation in ϕ_i can be explained by measurement error around a site value, which is a constant and the average for all individuals. However, a significant part of the variation can be explained by the final predicted weight of the individual parr (Table 5.3), and the fish that manage to achieve higher values of ϕ_i are heavier than otherwise expected at the end of the surveys.

During the surveys, no parr less than 80mm in length were marked. This meant that as the surveys progressed, a greater proportion of the parr caught could be marked and the marked individuals became more representative of the entire population. The marked parr that were most frequently recaptured were those which were marked earliest in the season, and the lengths of these parr were biased high with respect to the whole population.

The mean value of ϕ_i tends to increase with frequency of capture. As both the residuals and the fit to the mean weights indicate, higher values of ϕ_i are required to fit the period of summer growth. If a fish was just sampled during

this period, its value of ϕ_i would be high compared to a fish which was more frequently sampled after late autumn. This was be tested by correlating the average survey date (ASD) with ϕ_i, as the ASD can be used as a relative measure of when the parr were sampled. The relationship was found to be significant ($r_{70} = 0.222,\ P < 0.05$) which indicates that the variation in ϕ_i may be a result of the size selective marking procedure.

We are therefore unable to determine if the variation in ϕ_i is due to the size selective marking procedure or the variation in the sizes of the individual parr. In order to determine this would require all of the individual parr to be marked at a similar time.

5.5.3 Differences in $\phi(t)$ Between Data Sets

When the values of ϕ_i are compared to ϕ_m, the significance of the difference depends on the number of times the parr are caught. It is more appropriate to compare ϕ_m to the ϕ_i for the parr most frequently sampled as these parr cover a longer time span and are better able to approximate the growth trajectory over a similar time span. This would imply that $\phi(t)$ is similar when fitting to mean weights and individual weights. The values of ϕ_i vary greatly from those derived from fitting the model to the historic electro-fishing data from 1969-86, where the average annual value of ϕ_y was 0.9127. Three possible reasons why this might be are listed below.

The first is that the conditions for growth within the stream have decreased over this period. We are unable to tell if there has been a change in the stream conditions, as sufficient data do not exist. However, we are aware that the temperature profile is changing, as shown in Chapter 2, which would alter the conditions for growth in the Burn. These temperature changes are the largest in the spring, which is the period for which individual data is unavailable. As the model attempts to predict growth having accounted for temperature, there may be other environmental changes (such as food or density) which have caused a reduction in $\phi(t)$

In 1998/99, ϕ_i has only fitted across two age-classes and in Chapter 4 it is fitted across four, where the weights of the 1+ age-class during the summer were gen-

erally under predicted, whilst the 2+ age-class were fitted well. In order for the model to fit both these age-classes equally well for the 1969-86 data would require ϕ_y to *increase* in value. It is by fitting to the 3+ age-class which prevents this increase, so the relatively low values of ϕ_i and ϕ_m in 1998/99 cannot be explained by fitting to just the 1+ and 2+ age-classes.

The most likely explanation is that the differences occur because ϕ_i is fitted only to the part of the year that misses the growth spurt during spring. This appears reasonable as ϕ_i is a measure of the average growth potential over a period of time, and if this time period excludes a short but vital part of the growing season, then it would be expected to be lower than a value which includes the entire growing season.

5.5.4 Improvements to the Model

The model fails to predict the increase in weight during the spring and the predicted growth trajectories over this period are too low. This would require structural changes to the model, but individual data do not exist for a sufficiently long period of time to parameterise such a new model, and the electro-fishing data from 1969-86 does not cover this part of the season.

When fitting the model for data within years, a variable function for $\phi(t)$, allowing it to change on a monthly basis, would seen more appropriate. This would allow for the changes in consumption throughout the year. However, with the 1969-1986 Girnock data, there is only one data point per age-class per year, so fitting a variable ϕ_m would not be feasible. The values of ϕ_i derived for the different age-classes do not differ significantly, so the same value can probably be used across all age-classes.

There are drawbacks in fitting to the mean weights of age-classes rather than to individual weights, particularly in a population with size selective migration. The model needs to be adapted to account for the effects of migration on the mean weights of the resident parr. This means that a mechanism needs to be introduced into the model that will alter the prediction of the mean weights of the 2+ and 3+ resident parr. This amended model will more accurately predict the growth of the smaller parr that do not migrate and we shall develop such a

model in Chapter 6.

Chapter 6

Adapting the Model to Include Size Selective Migration

6.1 Introduction

The CGM_e model has not been able to fit all the age-classes equally well, in particular the 3+ fish which are always over predicted. The 1+ age-class is also badly fitted, in general being under predicted.

A major feature of the juvenile life history has yet to be included in the model, which is emigration from the population. Migration from a cohort begins during the autumn when the parr are approximately 18 months old. There is a lull over winter and few are caught in the fish trap between December and February. There in an increase in the number of migrants the following spring, when the parr become smolts, at around 24 months old. The same migration pattern occurs in the cohort the following year.

It is unclear what proportion of the cohort migrates during the autumn because not all of them are caught at the fish trap, but for the years for which good data does exist approximately a third leave in autumn and the rest in spring. The average annual percentage of autumn migrants that are 1+ is 32%, and 65% are 2+ parr, the rest (3%) being mostly 3+. Of the spring smolts, an average of 34% leave annually when they are two year olds and 64% when they are three year olds, the remaining 2% being four and five year old fish.

Different factors will affect the season the parr in the Girnock migrate, such as

the numbers of adult females above the fish trap, which affects the numbers of precocious parr migrating, or the flow rates within the burn (Buck and Youngson (1982), Youngson et al. (1983)). The critical factor which determines the season in which the parr migrate appears to be growth rate, and if the parr are too small, they can postpone migration until the following year (Metcalfe et al. (1990), Økland et al. (1993)). The result of this behaviour is that the timing of the parr's migration is not dependent on the age of the fish, but on its size, and that migration from the cohort is size selective.

Therefore, as the cohort ages, the mean weights of the resident parr become less representative of the mean weight of the entire cohort. The growth model was parameterised with juvenile salmon data that excluded the effects of migration on the population. When the model was fitted to data from wild parr, it was fitted to the mean weights of the resident parr, which may change due to effects of migration. At present, there is no mechanism within that model to account for this.

In order to include size selective migration from the population in the model, we must be able to model the variation in the weights within the age-classes in each cohort. Previously, the model has predicted changes in the mean weight of age-classes from each cohort, and now it will be adapted to predict the growth of the weight-frequency distribution (WFD) of the cohort.

The first step to modelling the variation in the WFD of the cohort will be to fit the model to the data from the 0+ and 1+ summer electro-fishing surveys. There will have been no seaward migration from these age-classes as they are too small to undergo smolting. Parr from these age-classes have been observed in the fish trap at the Girnock over the period from 1969-86, which may have been due them dispersing in search of territories. Fitting to these age-classes will indicate how the population grows before parr begin to migrate.

6.2 Modelling the Variation in the Weight of the Population

6.2.1 Fitting the model to the Quartile Values of the 0+ and 1+ Data

The data for each age-class within each cohort shows that each has a different range of weights. If we are to assume that the proportion of the 2+ and 3+ age-classes that migrate is based on WFD of the population, then we must be able to model the actual changes in the WFD of the cohort, rather than just predicting the mean weight of the resident parr population.

We have so far assumed that the initial weight for all the members of a cohort has been constant at 0.15g and that the growth rate of all the members of the population has been the same. We shall now look at the growth rates of the distribution of the 0+ weights by fitting the quartile values of this age-class to the quartile values of the 1+ age-class of the same cohort by adjusting ϕ_y. This will indicate differences in the growth rate of different parts of the 0+ distribution.

Growth simulations were produced with starting weights from the 0+ data. These were the median, upper and lower quartile values of the 0+ WFD. The DSO procedure was used to find the values of ϕ_y, and the initial conditions were the values of ϕ_y found previously in Chapter 4, which were varied between $\phi_y \pm 0.02$ at increments of 0.01. The fitting procedure minimised the RMS error as each trajectory was only being fitted to a single point.

The model could only be fitted to 12 cohorts as this was the number for which data for the 0+ and 1+ were available, and the values of ϕ_y with their standard errors are shown in Fig. 6.1. Each of the sets of ϕ_y from the fits to the different quartiles are highly correlated, with $r > 0.7$ and $P < 0.01$ in each case.

6.2.2 Analysis of ϕ_y from the Quartile Values

When fitting to the quartile values of the mean weights of 0+ and 1+ parr sampled in the electro-fishing surveys from 1969-1986, the values of ϕ_y are not different for the different quartile values. A two-way ANOVA can be used to show that,

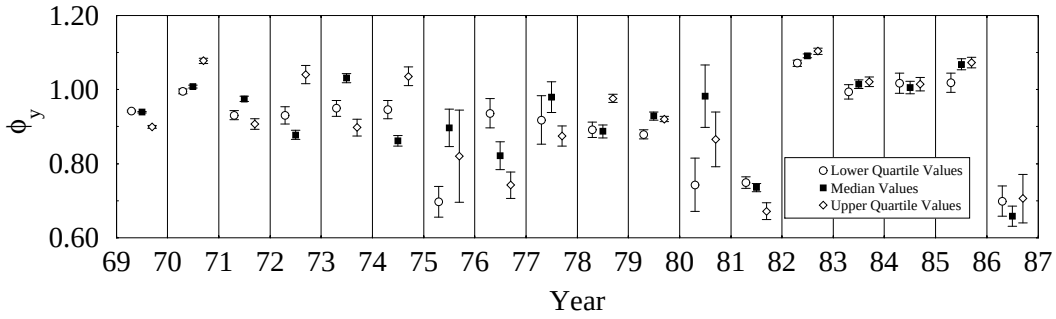

Figure 6.1: *The optimal values of ϕ_y derived from fitting the model to different quartile values of the 1+ WFD, with their standard errors.*

although the between year differences in ϕ_y are significant ($F_{17,34} = 9.303,\ P < 0.001$), the differences between the values derived for the different quartile values are not ($F_{2,34} = 0.839,\ P = 0.441$). This can be seen from Fig. 6.1, where the values are similar for most years and they are not systematically different based on the quartiles to which the model was fitted. The mean values of ϕ_y with their standard deviation are given in Table 6.1 along with the RMS error from the fit between the model and the data.

Table 6.1: *Mean values of ϕ_y when the model is fitted to the different quartile values of the 1+ WFD, with their standard deviations, in brackets, and the RMS error.*

	Lower Quartile	Median Quartile	Upper Quartile
Mean (S.D.)	0.906 (0.112)	0.931 (0.112)	0.925 (0.130)
RMS Error	1.34E-03	5.22E-06	5.87E-04

The fit to the data is very good as can be seen by the RMS errors and for each set of quartile values, 18 parameters are being fitted to 24 data points. The values of ϕ_y are not independent and fitting to the mean weights of the 0+ and 1+ age-classes for each cohort will involve two values of ϕ_y (i.e. one for the first year and another for the second year). There are also gaps in the data, and some of the values of ϕ_y are determined by the data in the proceeding or subsequent years.

For the years 1970-4, 1978 and 1982-5, ϕ_y is derived when both 0+ and 1+ age-classes are present, and when the 0+ and 1+ data are available for these two cohorts. For these years, there are still not systematic differences between the

values of ϕ_y for the different quartiles. If the values of ϕ_y for the different quartiles were found to be systematically different, then this would indicate that the WFD of the parr was changing. These results imply that the WFD is not changing for the cohorts between the 0+ and 1+ age-classes.

6.2.3 The WFD of the 0+ and 1+ Parr

In Chapter 5 we observed that the values of ϕ_i were positively correlated with the final predicted weights of the parr when derived over the period from June 1998 until March 1999. This variation in ϕ_i may be too subtle to be detected when fitting to mean weights and when ϕ_y is derived over a different period of time. The variation in the shape of the WFD can be examined by comparing the coefficient of variation (c.v.) of the 0+ and 1+ parr. These have been plotted in Fig. 6.2 for the cohorts from which the data is available.

A two-tailed paired t-test can be used to show that the c.v. from 0+ and the 1+ do not vary significantly, ($t_{11} = 2.201,\ P = 0.184$) and so are not systematically different. Although this supports the findings that ϕ_y should be the same across the 0+ and 1+ age-classes, it does not negate the finding that ϕ_i is correlated with size if there is size selective mortality occurring in the population.

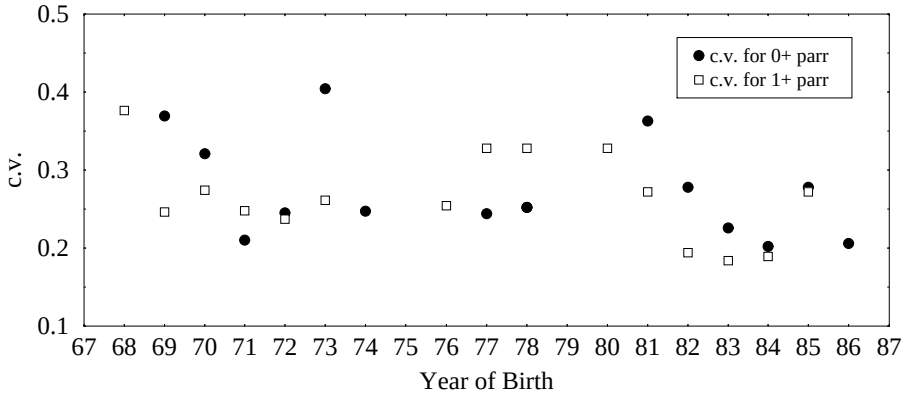

Figure 6.2: *The coefficient of variations for the 0+ and 1+ age-classes for which data is available.*

Some values of ϕ_y derived and displayed in Fig. 6.1 have values of greater than 1.0, and for the years 1970 and 1984, the mean values of ϕ_y for each quartile are significantly greater than 1.0. This would indicate that the parr are growing better than the optimal conditions of the tank reared parr on which the model

was parameterised. Each value of ϕ_y represents an annual growth index and, as we have seen in Chapter 5, the model under predicts spring growth. In order to compensate for this, the value of ϕ_y increases during the summer. They may also be greater than 1 because of size selective mortality. If the smaller members of 0+ age-class died before the population was resampled at 1+, then the median weights would change towards that for the larger members of the population.

However, the values of ϕ_y are a measure of the relative growth of the population. We are unable to determine if size selective mortality is occurring in the population, as the appropriate data do not exist. Given that ϕ_y appears to be constant over age-classes when fitted to the data that is available and that the variation in the population does not change significantly from the 0+ to 1+ age-classes, we shall assume that the different variations in the sizes of the parr within age-classes are not due to differing growth rates but from the initial WFD of the population.

6.3 Fitting the Model to the Data with Threshold Weights for Smolting

The two main periods of migration for any cohort will be between the summer measurements of the 1+ and 2+, and the 2+ and 3+ age-classes. If the fish are too small to migrate during the first period, they may wait until the following year. This will give the majority of them sufficient time to attain a suitable weight. In this section, the model will be adapted to take into account the fact that a large proportion of the population will leave during migration, and that proportion will be dependent on the distribution of weights of the parr population.

6.3.1 Changes to the Model to Allow Size Dependent Migration

Changes to the Model

We shall use the following assumptions to adapt the model to take into account the effects of migration on the mean weight of the resident parr in the stream. We shall define residents as those fish that are in the stream when the electro-fishing data is collected. The mean weights to which the model is fitted are those of the

resident parr, and will be denoted by $W_r(t)$ at time t. The present model predicts the growth trajectories of all individuals. We shall assume that this trajectory, denoted $W_p(t)$ at time t, is the mean weight of the whole population, regardless of whether members have smolted. Thus we would expect $W_p(t)$ to fit to the 0+ and 1+ data well, but over predict the 2+ and 3+ age-classes.

We shall assume that migration will take place on a fixed date between consecutive summers. This date is fairly arbitrary, as we are interested in the effect of the migrants on the mean weight of the resident population, which is measured during the summer. The date of migration will be set at the 1st April each year as it is about the peak time of migration.

The distribution of the weights of the population about $W_p(t)$ will be assumed to be Gaussian and its coefficient of variation, c, is constant for the population at all times.

We shall assume that there are two constant threshold weights above which parr will migrate. These will be denoted by W_{c_1} for the first set of migrants from a cohort and W_{c_2} for the second set. Therefore, at the migration date, all fish above the threshold weights will leave the population. The two migration dates are denoted m_1 and m_2 for the first and second migration respectively. We can therefore deduce the mean weight of the resident population at migration, denoted $W_r(m_1)$ and $W_r(m_2)$, given that we know the weight of the whole population at the migration dates, where $W_p(m_1)$ is the mean population weight at the first migration and $W_p(m_2)$ is the population weight at the second migration date.

Given that we have a constant c, if we define

$$r_1 = \frac{W_r(m_1)}{W_p(m_1)} \qquad\qquad r_2 = \frac{W_r(m_2)}{W_p(m_2)} \tag{6.1}$$

then we can say that

$$W_r(t) = \begin{cases} W_p(t) & t < m_1 \\ r_1 W_p(t) & m_1 \leq t < m_2 \\ r_2 W_p(t) & t \geq m_2 \end{cases} \tag{6.2}$$

Note that $r_1 \geq r_2$ to ensure that the parr which migrate at m_1 are not 'reintroduced' at m_2. Fig. 6.3 give a schematic view of the changes which the cohort undergoes.

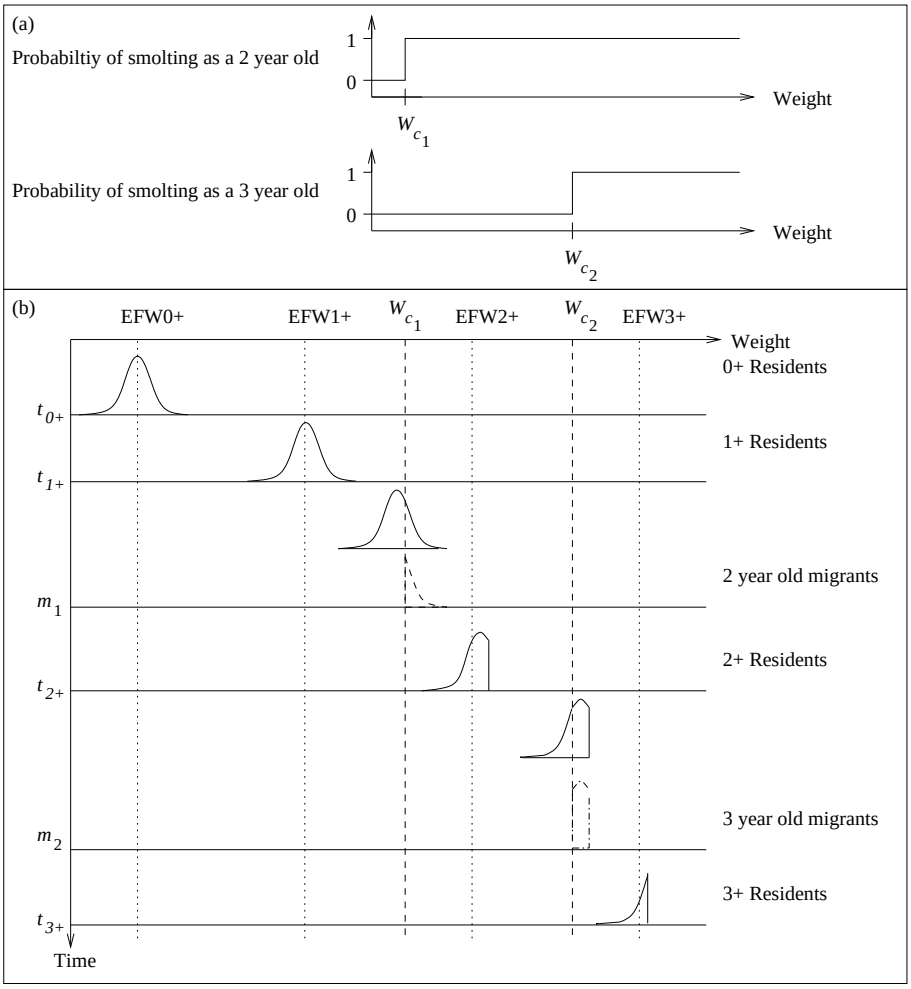

Figure 6.3: *These two diagrams show how the model is fitted to the data when a proportion of the cohort migrates at m_1 and m_2. (a) These functions describe the probability of smolting for the different age-classes. (b) The initial WFD of the cohort will have a coefficient of variation, c, and mean weight of 0.15g. As time increases and the weight of the cohort increases, the mean weight of the distribution will be fitted to the observed 0+ and 1+ mean weights of* EFW0+ *and* EFW1+ *at times t_{0+} and t_{1+}. At time m_1, the proportion of the cohort of length $> W_{c_1}$ are removed from the resident population, and are assumed to have migrated. The remaining part of the distribution continues to grow, and the mean weight of the distribution at t_{2+} is fitted to the observed mean weight of* EFW2+. *The distribution remains unchanged until the second migration period at m_2, where all parr of length greater than W_{c_2} are removed from the resident population and are assumed to have migrated. The remaining part of the distribution continues to grow up to t_{3+} where its mean weight is fitted to* EFW3+, *the observed mean weight of the 3+ parr.*

Fitting with Constant $\phi(t) = k$

The model was first fitted to the electro-fishing data from 1969-1986 by adjusting c, W_{c_1}, W_{c_2}, and $\phi(t) = k$ representing a constant value of $\phi(t)$ across all years. The DSO was used with a variety of initial conditions, and the parameter values which minimised the mean weighted error (MWE) shown in Table 6.2. The trajectories are plotted out in Fig. 6.4 and the fit of the model to the different age-classes is shown in Table 6.3.

Table 6.2: *Parameters found from fitting the model to the data by adjusting c, W_{c_1}, W_{c_2} and k. Also shown is the MWE.*

k	$W_{c_1}(g)$	$W_{c_2}(g)$	c	MWE
0.933	12.1	19.3	0.568	9.04

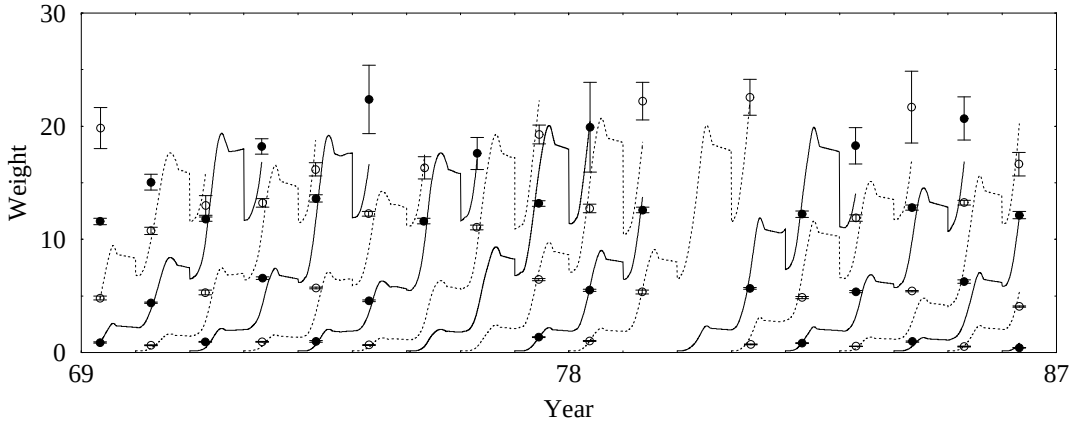

Figure 6.4: *Simulations of parr weights produced with the parameters in Table 6.2. Trajectories with broken lines refer to the cohorts with open circles.*

In Fig. 6.4, the cut-off point for the three year old migrants can clearly be seen, but is less obvious for the two year olds (these are not actual growth trajectories for individuals, but rather the mean weights of the resident population assuming that migrations occurs at a specific date). The fit to the age-classes has not improved over the model with ϕ_y except for the fit to the 3+ age-class, where the percentage error has decreased from 38% to 14% (see Tables 4.10 and 6.3).

From Table 6.4, we can see that the scale of the reduction in the MWE from fitting with the single parameter and compare it to fitting with ϕ_y. Looking at

Table 6.3: *The fit of the 4 parameter model to the mean weights of the different age-classes of the electro-fished parr.*

Age-class	*Average Weight (g)*	*Predicted Weight (g)*	*Range of Predictions (g)*	*Mean Abs. Error (g)*	*% Error*	*Sign. same*	*Sign. correl.*
0+	0.81	0.73	0.35-1.43	0.26	32	Y	NS
1+	5.39	4.57	2.68-7.20	1.61	30	N	NS
2+	12.24	11.12	7.50-15.92	2.19	18	N	NS
3+	18.92	18.12	14.02-22.25	2.70	14	Y	NS

the accumulated ANOVA table, in Table 6.5, we see that there is not a significant improvement to the model.

Table 6.4: *Comparison of the MWE for the different models.*

Fitted Parameters	MWE
1 parameter of $\phi(t) = k$	10.357
Current 4 parameter model	9.035
18 parameters when $\phi(t) = \phi_y$	5.832

Table 6.5: *ANOVA table calculated from the total weighted deviance from the four parameter model.* $R^2 = 0.723$.

	d.f.	WSD	MD	F	P
$\phi(t)$=k	1	1268	1268	128	< 0.001
W_{c_1}, W_{c_2}, c	3	75	25	2.35	> 0.05
Residual	52	515	9.9		
Total	56	1858			

Using the cut-off points for the migration of individuals does have the desired effect of reducing the error associated with the least well fitted age-class, the annual mean weights of the 3+ parr. We shall now combine these parameters into a model where we fit $\phi(t) = \phi_y$ instead of $\phi_y = k$.

Fitting with Annual $\phi(t) = \phi_y$

The next stage was to fit the model to the data by adjusting the values of ϕ_y as well as c, W_{c_1}, W_{c_2}. This would involve fitting 21 parameters and was done using the DSO. Again, a variety of initial conditions were used, and the parameters

that gave the best fit are in Table 6.6 with the trajectories shown in Fig. 6.5. This version of the model will be defined as SSVN1.

Table 6.6: *Parameters derived from fitting the model with the new parameters c, W_{c_1}, W_{c_2} and ϕ_y to the data.*

c	$W_{c_1}(g)$	$W_{c_2}(g)$	Range of ϕ_y	MWE
0.428	13.761	16.948	0.809-1.042	4.9

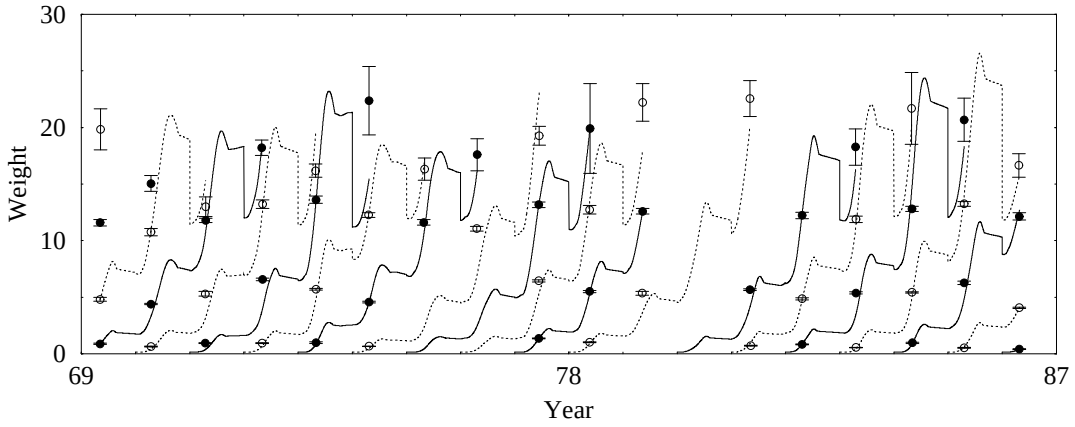

Figure 6.5: *Simulations of parr weights produced with the parameters in Table 6.6. Trajectories with broken lines refer to the cohorts with open circles.*

The fit of the model to the separate age-classes is shown in Table 6.7 and the fit for the 0+, 1+ and 2+ is as good as formerly, though not better. However, the fit to the 3+ is considerably improved, as expected.

Table 6.7: *The fit of the model with the new parameters c, W_{c_1}, W_{c_2} and ϕ_y to the mean weights of the different age-classes.*

Age-class	*Average Weight (g)*	*Predicted Weight (g)*	*Range of Predictions (g)*	*Mean Abs. Error (g)*	*% Error*	*Sign. same*	*Sign. correl.*
0+	0.81	0.92	0.57-1.55	0.17	21	Y	**
1+	5.39	4.54	3.35-5.59	0.95	18	N	NS
2+	12.34	12.35	7.14-14.93	0.84	7	Y	***
3+	18.92	18.32	15.52-23.31	2.46	13	Y	NS

Table 6.8 shows that there is not significant improvement to the fit when ϕ_y is used with the new parameters. Also, the predictions for the 1+ mean weights are still too low and the predictions of the 3+ are not correlated with the observations.

Table 6.8: *ANOVA table calculated from the total weighted deviance from the model with the new parameters c, W_{c_1}, W_{c_2} and ϕ_y. $R^2 = 0.853$ and MWE=4.88.*

	d.f.	WSD	MD	F	P
k	1	1268	1268	161.3	< 0.001
ϕ_y	17	258	15.2	1.95	< 0.05
W_{c_1}, W_{c_2}, c	3	59	19.7	2.53	> 0.05
Residual	35	273	7.8		
Total	56	1858			

The model has fitted a common value for the coefficient of variation (c.v.) for all of the cohorts. This value of 0.428 higher than the observed values of the c.v. for the 0+ and 1+ age-classes in Fig. 6.2, which range from 0.210-0.404 for the 0+ parr and 0.189-0.376 for the 1+ parr. Therefore, the variation in the WFD of the cohort is being over predicted. The assumption of a constant c.v. appears to be too ridged a constraint given the variation in the observed c.v. In the following subsection, we shall look more closely at the shape of the WFD to find a more appropriate method of predicting its change.

6.3.2 Assuming Different WFD's for Population

Fitting the Data with Different WFD's

The WFD has so far been assumed to be Gaussian for the 0+ and 1+ age-classes. The growth of a cohort was defined by the growth of the mean of a Gaussian distribution, which became truncated at the migration dates defined as times m_1 and m_2. We shall consider using different distributions as the starting points for the cohorts.

The WFD's of the 1+ age-class for which data was available was fitted with three different probability density functions (PDFs). The PDFs, which were fitted to the data by minimising the log likelihood function, were the Gaussian, Gamma and Weibull, each of which are defined by two parameters. The Gamma and Weibull PDFs were chosen as they were skewed to the right, which would be the case for a population with differential growth rates and similar initial weights. For each cohort, the 1+ data was normalised before the fitting procedure began.

For all of the cohorts fitted, the Gaussian provided the best fit to the data, followed by the Gamma then the Weibull. Using the Weibull distribution to describe the spread of the 1+ data was discarded as it fitted the data least well. The Gamma and Gaussian distributions would be used to define the WFD of the 1+ parr from each cohort. For the Gaussian, the spread of the data would be based on the c.v. For the Gamma, the spread of the data would be determined by the shape parameter of the distribution. Due to the missing data for the 1974 and 1975 cohorts, the spread of these 1+ distributions were approximated by taking the average value from the other cohorts.

Fitting the Data with a Gaussian Distribution with Variable C.V.

The model was refitted to the electro-fishing data as before but with the following changes. Instead of fitting the parameter c, each cohort will have a value of the c.v. determined from the observations. This version of the model will be defined as SSVN2.

Table 6.9: *Parameters derived from fitting the model SSVN2 with the parameters* W_{c_1}, W_{c_2} *and* ϕ_y *to the data.*

$W_{c_1}(g)$	$W_{c_2}(g)$	Range of ϕ_y	MWE
8.81	13.79	0.821-1.080	2.56

The parameters which provided the best fit to the data are shown in Table 6.9. Both of the threshold values for smolting have decreased substantially and the values for the MWE has decreased by 48% in spite of the model being fitted to the data with one less parameter. The accumulated ANOVA table in Table 6.10 shows that the parameters now account for a significant amount of the variation between the mean weights.

The fit of the model to the different age-classes are shown in Table 6.11. The predicted weights of all of the age-classes are correlated with the observations and there are no longer systematic differences between the data and the predictions.

Table 6.10: *ANOVA table calculated from the total weighted deviance from the model SSVN2 with the parameters W_{c_1}, W_{c_2} and ϕ_y. $R^2 = 0.923$ and MWE=2.55.*

	d.f.	WSD	MD	F	P
k	1	1268	1268	317	< 0.001
ϕ_y	17	258	15	3.75	< 0.001
W_{c_1}, W_{c_2}	2	189	95	23.75	< 0.001
Residual	36	143	4		
Total	56	1858			

Table 6.11: *The fit of the model SSVN2 with the new parameters W_{c_1}, W_{c_2} and ϕ_y to the mean weights of the different age-classes.*

Age-class	*Average Weight (g)*	*Predicted Weight (g)*	*Range of Predictions (g)*	*Mean Abs. Error (g)*	*% Error*	*Sign. same*	*Sign. correl.*
0+	0.81	0.76	0.41-1.23	0.12	15	Y	**
1+	5.39	5.15	3.44-6.58	0.26	5	Y	***
2+	12.34	12.39	9.13-15.16	0.77	6	Y	***
3+	18.92	18.27	14.26-23.35	2.05	11	Y	*

Fitting the Data with Gamma Distribution with Variable Shape Parameter

We have thus far assumed that the WFD of the population is Gaussian. The distributions of the cohorts will now be assumed to be Gamma, with the average growth trajectory up to the 1+ data being that of the mean of the Gamma distribution. As smolting occurs, the distribution will be truncated as previously, with the mean of the remaining part of the distribution being fitted to the data. As the cohort grows in size, the shape parameter of the distribution will remain constant. The fitting procedure will otherwise remain the same as for SSVN2. This version of the model will be defined as SSVG1.

Table 6.12: *Parameters derived from fitting the model SSVG1 with the parameters W_{c_1}, W_{c_2} and ϕ_y to the data.*

$W_{c_1}(g)$	$W_{c_2}(g)$	Range of ϕ_y	MWE
8.22	12.68	0.745-1.102	2.98

The parameters which provide the best fit to the data are shown in Table 6.12

and shows a large improvement over SSVN1 and similar to SSVN2. The variation in the data accounted for by the two smolting thresholds is significant, as can be seen from Table 6.13.

Table 6.13: *ANOVA table calculated from the total weighted deviance from the model SSVG1 with the parameters W_{c_1}, W_{c_2} and ϕ_y. $R^2 = 0.910$ and MWE=2.98.*

	d.f.	WSD	MD	F	P
k	1	1268	1268	273	< 0.001
ϕ_y	17	258	15	3.23	< 0.01
W_{c_1}, W_{c_2}	2	165	82.5	17.78	< 0.001
Residual	36	167	4.64		
Total	56	1858			

The predictions from the model and the observations from the different age-classes are now correlated, and also the predictions and the observations are not systematically different for any of the age-classes.

Table 6.14: *The fit of the model SSVG1 with the parameters W_{c_1}, W_{c_2} and ϕ_y to the mean weights of the different age-classes.*

Age-class	*Average Weight (g)*	*Predicted Weight (g)*	*Range of Predictions (g)*	*Mean Abs. Error (g)*	*% Error*	*Sign. same*	*Sign. correl.*
0+	0.81	0.76	0.24-1.25	0.14	4	Y	***
1+	5.39	5.29	4.07-6.56	0.21	4	Y	***
2+	12.34	12.75	9.64-15.68	1.07	9	Y	**
3+	18.92	18.19	14.41-22.09	2.33	12	Y	*

Determining the Best Model

Of the three models tested in this section, SSVN1 is clearly the worst as the MWE is the highest and the fit to the age-classes the worst in spite of using an extra parameter. The models SSVN2 and SSVG1 both have similar MWE are significant improvements over fitting with only ϕ_y. In addition, they are able to predict the weight well across all age-classes.

As the model is able to predict the WFD of the 2+ and 3+ age-classes, we are able to derive an estimate of its variation that can be compared to the observed

variation in the data from the 2+ and 3+ age-classes. The c.v. was chosen as a measure of variation, and derived for the 2+ and 3+ observations and the predictions from the two models. The observed and predicted c.v. from the models for the 2+ and 3+ age-classes are plotted in Fig. 6.6.

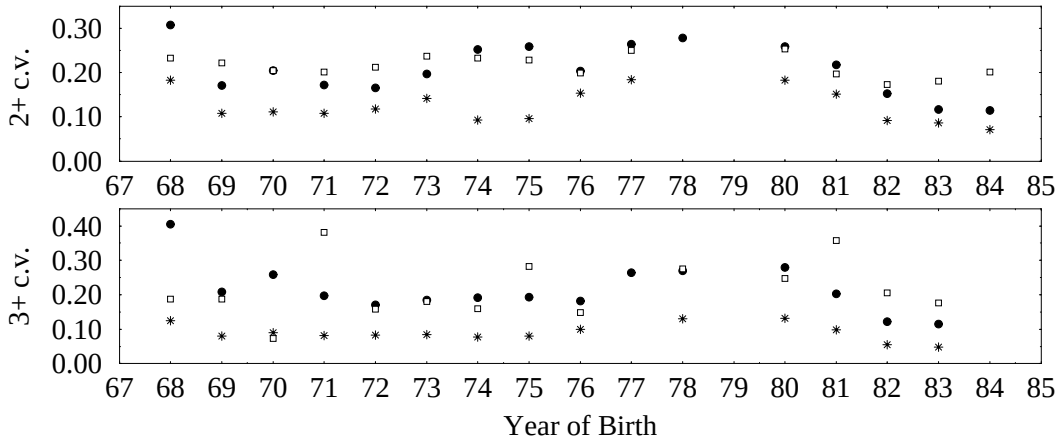

Figure 6.6: *Predicted and observed c.v. of the 2+ and 3+ age-classes. The observations are the open squares, the predictions from SSVN2 are the closed circles, and the predictions from SSVG1 are the stars.*

The predictions of the c.v. for the 2+ are correlated with the observation for both SSVN2 ($r = 0.736,\ P < 0.05$) and SSVG1 ($r = 0.588,\ P < 0.05$), but not for the 3+. The predictions from the model SSVG1 are clearly systematically lower for both age-classes, which is not the case with SSVN2. This indicates that using a Gamma distribution would not be appropriate as it underestimates the variation in the weights of the resident 2+ and 3+ parr. Also, the 1+ data are better approximated by a Gaussian distribution than by a Gamma, as was seen earlier. As this is the case, we shall model the population using a Gaussian distribution and the model SSVN2 will be used to predict other aspects of the population.

6.4 Comparing Predictions to the Smolt Data

One of the benefits of having the threshold weight for smolting is that as well as enabling predictions to be made regarding the resident population, predictions can also be made about the migrants. The proportion of the cohort that leaves the resident population each year can be used to predict the mean weight or lengths of the migrants as well as the variation of the sizes of the migrating population.

The model can also be used to predict what proportion of the cohort will migrate each year.

Data from the smolt trap exists which will allow comparison between predictions and observations. Unlike the electro-fishing data, which is site specific, the data from the smolt trap is collected from the whole of the burn. Also, the estimates of the proportion of fish leaving from each cohort for the years 1977-1986 are incomplete. This is due the trap becoming clogged with leaves during the autumn, which allows an unknown number of fish to avoid being caught in the trap. However, this data does give us an indication of the population dynamics and will enable us to see how well the SSVN2 model is able to predict these characteristics of the population.

6.4.1 Structural Weight-Length Relationship

The weight-length relationship has so far been used to convert the lengths of the parr into weights. The model predicts weight, and if we are to compare the predictions to the smolts then we require a relationship between the two. Simply comparing the predicted weights to the observed weights of the smolts is insufficient for a number of reasons.

The predicted weights are for parr, and so comparing the two will involve comparing fish in different physiological states. This will not take into account the physiological cost of smolting, when the parr are under going the changes, including shape, or weight to length changes, which adapt them to living in seawater.

We can, however, compare the lengths of the smolts with those predicted by the model. This is due to the model calculating the fish weight as the sum of the reserve and structural weights. The structural weight (SW) does not decrease as the fish loses weight. Using a SW-length relationship will allow a direct comparison between the observed lengths of the smolts and the predicted lengths of the migrants from the parr population. The relationship will be of the form in equation (6.3).

$$ln(L) = ln(a_s) + b_s ln\left(\frac{W}{1+\rho}\right) \tag{6.3}$$

where W is the predicted weight by the model and ρ is the reserve to structural weight ratio. The coefficients a_s and b_s are derived from the data used for the

original weight-length relationship in Chapter 2, which was collected during August when the fish are assumed to be healthy with their reserve to structural weight ratio being at its ideal value of $\rho = 1.5$. The coefficients used are those in Table 6.15.

Table 6.15: *Parameters for the regression used to derive a length from structural weight. The coefficients are shown, with their standard errors in brackets.*

$\ln(a_s)$	b_s
1.815 (0.0052)	0.324 (0.0038)

With this relationship, the predicted weights can be converted into predicted lengths at any time of the year and vice versa. Although at smolting the parr may be losing weight, its structural weight will not decrease and this can be used to estimate its length.

6.4.2 The Observed and Predicted Smolt Lengths

Using the data from the smolt trap, the mean lengths of the two year old and the three year old spring smolts were derived. These have been compared to the smolt lengths predicted for 1 April each year. The observations with their standard errors are plotted in Fig. 6.7 with the predictions from the SSVN2 model.

As can be seen in Fig. 6.7, the model under predicts the data for the two year old smolts in all years, and over predicts in all but two years for the three year olds. The predictions are positively correlated with the observations, but not significantly. For the two year olds, $r = 0.460$ with $P = 0.073$ and for the three year olds, $r = 0.239$ with $P = 0.39$.

6.4.3 The c.v. of the Smolt Lengths

The predicted smolt lengths are derived from the part of the distribution that emigrates from the cohort each year. This part of the distribution has been used to estimate the c.v. of the emigrant population, and has been compared to the observed c.v. of the smolt lengths in Fig. 6.8.

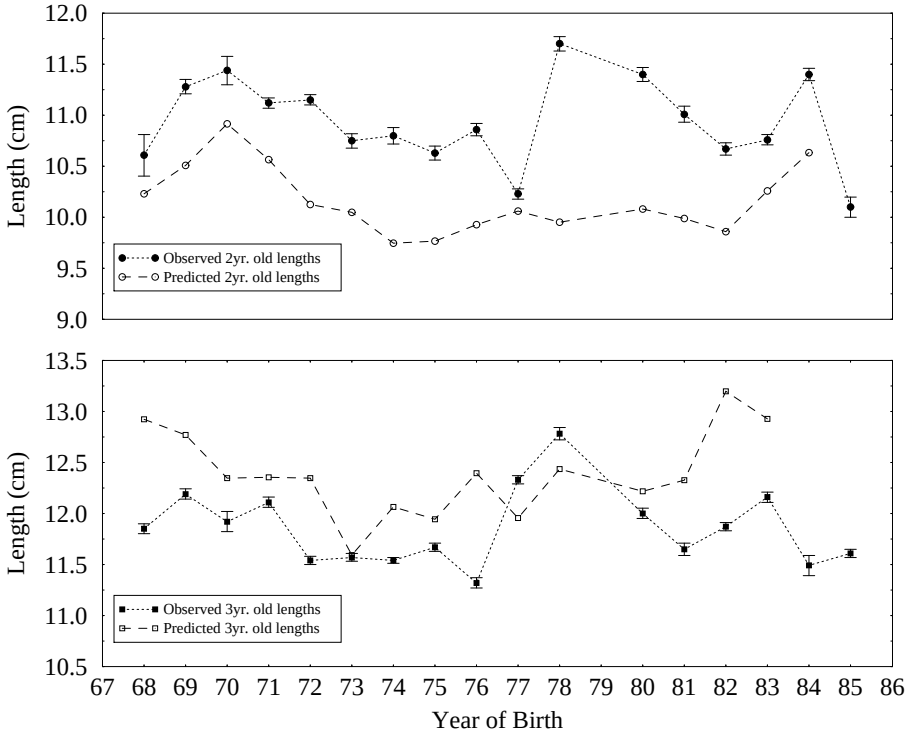

Figure 6.7: *Predicted and observed mean lengths of the smolts migrating in the spring.*

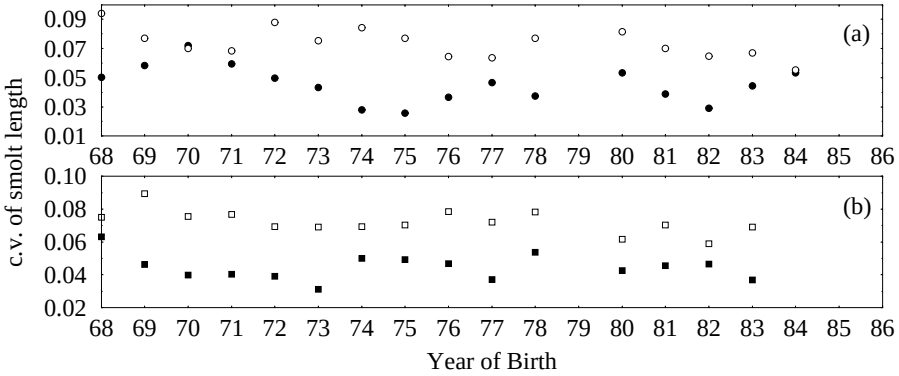

Figure 6.8: *Predicted and observed c.v. of the lengths of the smolts migrating in the spring. The filled symbols are the predictions and the empty ones are the observations, and the two year old smolts are in Fig. a, the three year old smolts in Fig. b.*

The model tends to under predict the c.v. for both age-classes. Also the predictions are not correlated with the observations, for the two year olds ($r = 0.055,\ P = 0.838$) or the three year olds ($r = 0.161,\ P = 0.566$).

6.4.4 Smolt Proportions

Estimates of the proportion of smolts that migrate each year from each cohort can be made from the data from the Girnock fish traps. These estimates vary in their accuracy due to the changes in the collection procedure. For the cohorts born from 1969-1976, the estimates are reliable due to the amount of effort put into counting the numbers of emigrants in the trap. After 1976, estimates of the number of autumn migrants are inaccurate with the degree of uncertainty being unknown. Therefore, for the cohorts born after 1976, the proportion migrating from each age-class during each year has been estimated from the spring migrants and the estimates of the average proportions emigrating in autumn for the years 1969-1976.

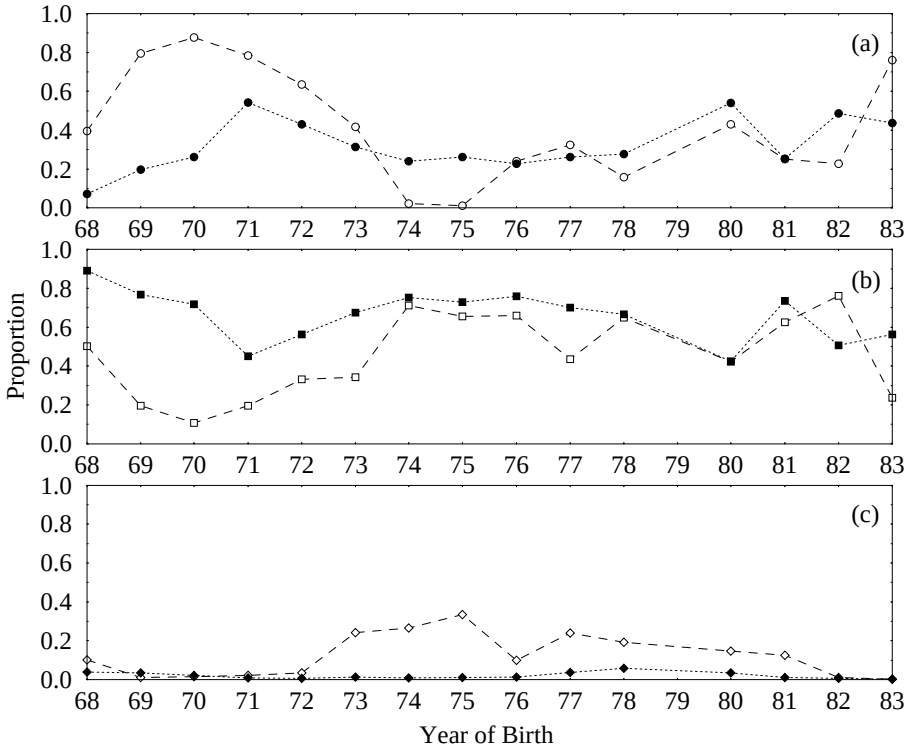

Figure 6.9: *Proportion of each cohort predicted to leave at each age-class for the 1+/2yr. old in (a), the 2+/3yr. old in (b) and the 3+/4yr. old in (c). The filled symbols are the observations and the empty ones are the predictions.*

6.4.5 Summary of Fit to the Data

The predictions by the model fit the electro-fishing data well for both the weight to which it is fitted, and the c.v. of the 2+ and 3+ data which it predicts. The predicted weights are both correlated with the observations and do not systematically over or under predict the observed weights. The same applies to the observed and predicted c.v. of the 2+ weights, although the predictions and observations of the c.v. for the 3+ weights are not correlated.

The predicted smolt lengths at two year olds are smaller than the observations and the predicted lengths of the three year old smolts are greater than their observation. The predictions are correlated with the two year old observations which implies the under prediction is of a constant amount. The c.v. of the smolt lengths is under predicted for the two and three year old smolts.

The predicted proportions of the cohort smolting show the greatest deviation from the predictions. Attempting to predict characteristics of the smolt population by fitting to the electro-fishing weight alone has failed to produce the observed data. The next step will be to fit the model to the entire data set, which will allow us to consider what changes may be necessary to complete the model.

6.5 Fitting the Model to the Entire Data set

6.5.1 Adapting the Model to Fit the Entire Data set

In Section 6.3, the model was fitted to the electro-fishing weights and then used to predict other characteristics of the juvenile population. The use of a threshold weight for smolting has considerably improved the fit of the model to the electro-fishing weights as well as giving a good indication of the c.v. of the age-classes. The model has failed to predict the lengths of the spring migrants or the c.v. of their lengths and has failed to give realistic predictions for the proportion of the population smolting. The next step will therefore be to fit the model to the whole data set in order to see the extent to which the predictions of the smolt data can be improved.

The model SSVN2 was fitted to data with a new error function calculated as the

total error from each of the different variables. These were the four age-classes from the electro-fishing data, the c.v. of the 2+ and 3+ parr, the lengths and the c.v. of the two year and three year old smolts and the proportion of migrants from each of the age-classes in each cohort. The mean absolute error from each variable was normalised by dividing by the mean observation for that variable, and these were summed to produce an overall estimate of the fit of the model to the data. The change to the model will be defined as SSVN3.

The errors from SSVN2 and SSVN3 are given in Table 6.16, and are further broken down into the error associated with each of the different data sets. The % change in the error measurement is also given.

Table 6.16: *Mean proportional error associated with different characteristics of the juvenile population when the model is fitted to the data by two different methods.*

variable	Age-class	SSVN2	SSVN3	% change
Total		2.9412	2.2540	-23.4
EF Weight	0+	0.1474	0.1899	+28.8
	1+	0.0493	0.1437	+191.5
	2+	0.0627	0.0855	+36.4
	3+	0.1004	0.1075	+7.1
Smolt Length	2	0.0753	0.0865	+14.9
	3	0.0486	0.0476	-2.1
C.V. of Weights	2+	0.1557	0.1349	-13.4
from EF Data	3+	0.3692	0.3471	-6.0
C.V. of Lengths	2	0.4633	0.5267	+13.7
from Smolt Data	3	0.3928	0.3564	-9.3
Proportion	2	0.7083	0.0915	-87.1
migrating	3	0.3683	0.1331	-63.9

Overall, the fit to the entire data set has improved by 23.4%. As the model is no longer being fitted to only the weights of the resident parr, the error being attributed to these groups has increased. This has ensured that the error has, in general, decreased for other groups, the largest decrease for the proportion migrating and the predictions and observations are displayed in Fig. 6.10. The largest errors are now associated with the c.v. of the smolt lengths which are still under predicted as can be seen from Fig. 6.11.

We attempted to improve the fit to the data further through the introduction

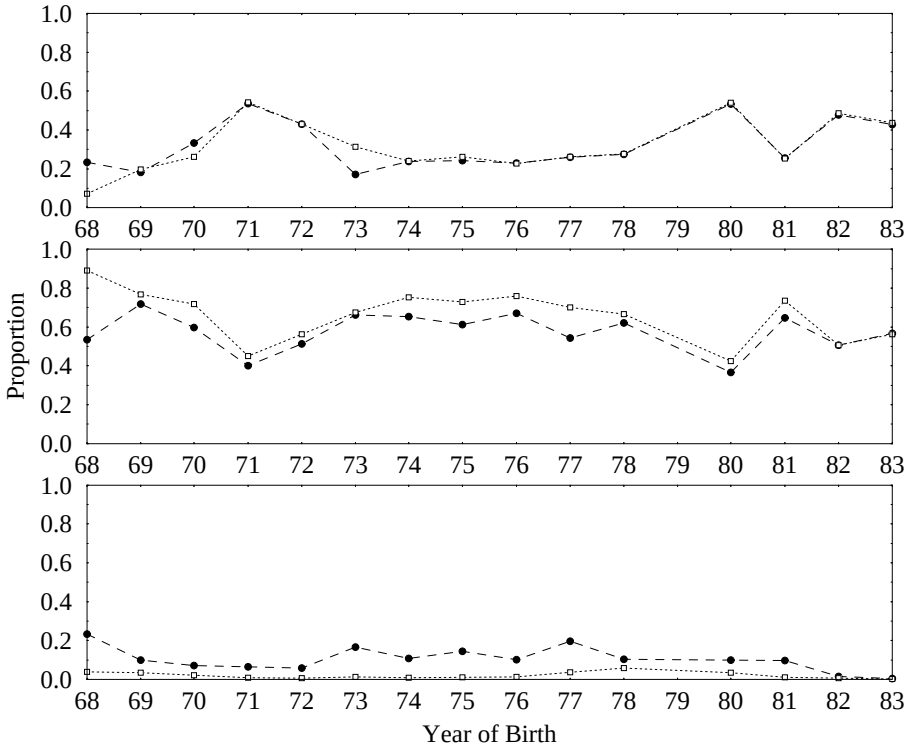

Figure 6.10: *Proportion of each cohort predicted by SSVN3 to leave at each age-class for the 1+/2yr. old in the upper graph, the 2+/3yr. old in middle and the 3+/4yr. old in lower. The filled circles are the predictions and the empty squares are the observations.*

a different smolting threshold each year. This required fitting W_{c_1} and W_{c_2} on an annual basis, and would increase the number of fitted parameters from 20 to 49. Using the DSO procedure to find these parameters proved unsuccessful as it either failed to reach the convergence criteria or when convergence did occur, many of the parameters were unchanged from their initial values. This suggested that the error surface was unsuitable for using the DSO procedure. Rather than develop a new fitting procedure, an alternative strategy of changing the smolting thresholds was sought.

The largest errors are now associated with the c.v. of the smolt lengths indicating that the spread of the migrants WFD is greater than predicted. The variation in the predictions can be changed using a variable smolting threshold, where the parr have different probabilities of smolting.

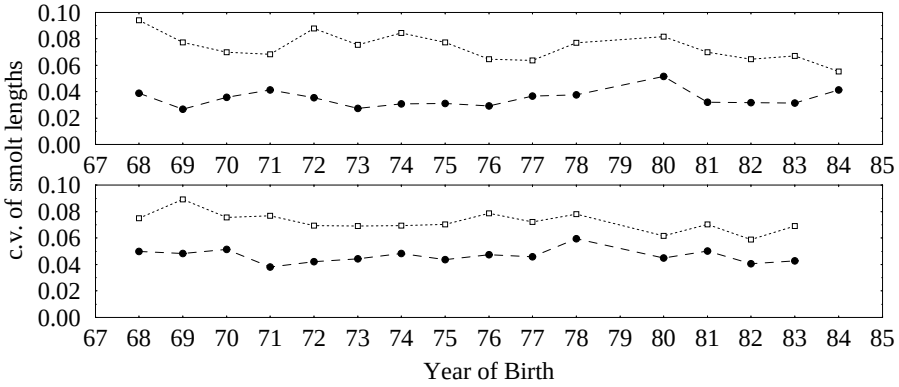

Figure 6.11: *Predicted and observed c.v. of the lengths of the smolts migrating in the spring using the SSVN3 model. The filled symbols are the predictions and the empty ones are the observations, and the 2yr. old smolts are the top graph and the 3yr. old smolts in lower graph.*

6.5.2 Introducing a Variable Smolting Weight to the Model

Fitting the Model to the Data

Observations of the lengths of the smolts indicate that there is not an exact smolting length, but a range of lengths at which the parr may choose to migrate. This aspect of smolting behaviour can be introduced into the model using a variable probability of smolting. We shall assume that for the two periods of migration, there is a maximum and a minimum smolting threshold. These will be defined as α_2 and β_2 for the two year old smolts and α_3 and β_3 for the three year old smolts. The α's will denote the minimum and the β's will be the maximum. During any single migration season, on the 1st April, all parr with length $> \beta_i$ migrate and all those with length $< \alpha_i$ will stay, where i denotes the age of the smolts. The probability of smolting will increase linearly between α_i and β_i. This means that the distribution of each cohort will be divided into parts as indicated in Fig. 6.12.

Fig. 6.12 shows how the cohort would be divided up, given that the c.v. of the entire cohort will remain constant throughout its lifetime. The whole distribution will grow as dictated by the model, and proportions of the distribution will leave based on the values of α_i and β_i. The model was fitted to the entire data set with the error function defined for SSVN3. This version of the model will be called SSVN4.

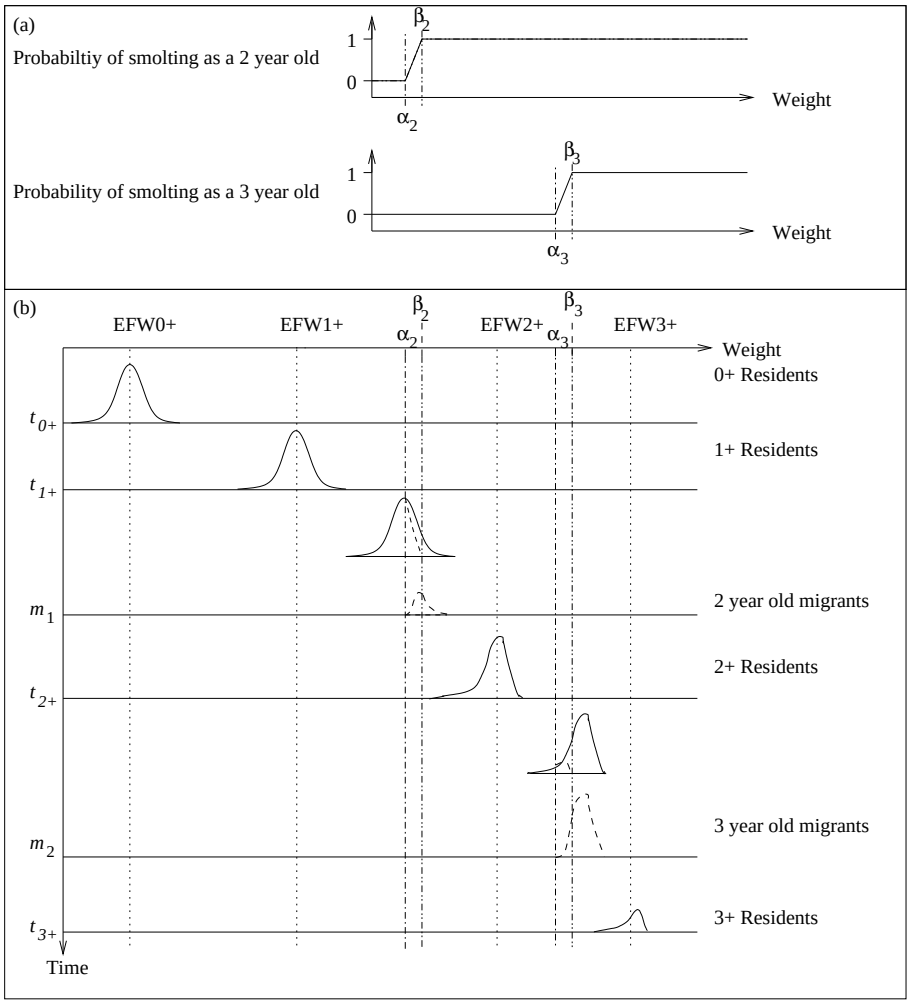

Figure 6.12: *These diagrams demonstrate how the cohorts are divided up given that there is a variable smolting threshold. (a) The probability of smolting will vary between α_2 and β_2 for the two year olds, and α_3 and β_3 for the three year olds. (b) The model will fit the mean of the distribution to the 0+ and 1+ mean weights as before. At m_1, a proportion of the cohort migrates, from which the mean length its c.v. are calculated and fitted to the observations of the smolts. The size of this proportion of the cohort is used to predict how many leave during this migration season. At t_{2+}, the mean weight and c.v. of this distribution is fitted to the observed mean weight and c.v. of the 2+. At m_2, another proportion of the population leaves, from which the lengths and their c.v. and the proportion smolting are fitted to the observations of the three year old smolts, and finally at t_{3+}, the mean and c.v. of this distribution are fitted to the observations from the data from the 3+ resident parr.*

The Fit of SSVN4 to the Data

This change to the model reduces the overall error by 39.7%. The errors associated with the electro-fishing data have in general increased and the largest

Table 6.17: *Comparisons between the errors of the models SSVN3 and SSVN4 with the % change in the error.*

variable	Age-class	SSVN3	SSVN4	% change
Total		2.2540	1.8573	-39.7
EF Weight	0+	0.1899	0.1952	+2.79
	1+	0.1437	0.1597	+11.1
	2+	0.0855	0.0736	-13.9
	3+	0.1075	0.1358	+23.3
Smolt Length	2	0.0865	0.1043	+20.6
	3	0.0476	0.0417	-12.4
C.V. of Weights	2+	0.1349	0.1458	+8.08
from EF Data	3+	0.3471	0.3535	+1.84
C.V. of Lengths	2	0.5267	0.3223	-38.8
from Smolt Data	3	0.3564	0.1336	-62.5
Proportion	2	0.0915	0.0826	-9.73
migrating	3	0.1331	0.1092	-18.0

reductions are through predicting the c.v. of the smolt lengths. The predicted and observed c.v. of the lengths of the smolts are plotted in Fig. 6.13. In spite of the large improvements, the c.v. for both age-classes are still under predicted. However, now the c.v. of the smolt lengths are correlated for the two year olds ($r = 0.524,\ P < 0.05$) but not for the three year olds ($r = 0.407,\ P > 0.05$).

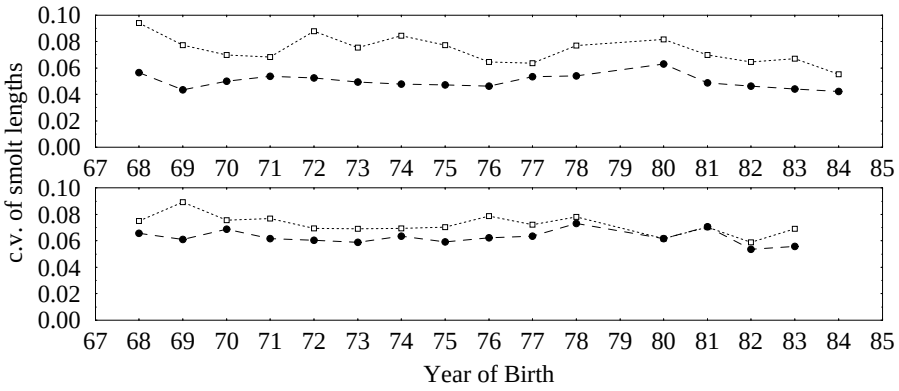

Figure 6.13: *Predicted and observed c.v. of the lengths of the smolts migrating in the spring using the SSVN4 model. The filled symbols are the predictions, the empty ones are the observations, and the two year old smolts are the top graph and the three year old smolts in lower graph.*

The quality of fit to the mean weights for the different age-classes of the electro-

fishing data has decreased through the successive fits from SSVN2 to SSVN4, at the cost of fitting to other parts of the data. Table 6.18 shows the fit of the SSVN4 model to the data for the different age-classes, and shows that although the predictions and the observations remain correlated, both the 1+ and 3+ age-classes are generally under predicted.

Table 6.18: *The fit of the model SSVN4 to the mean weights of the electro-fishing data*

Age-class	*Average Weight (g)*	*Predicted Weight (g)*	*Range of Predictions (g)*	*Mean Abs. Error (g)*	*% Error*	*Sign. same*	*Sign. correl.*
0+	0.81	0.72	0.4-1.15	0.16	20	Y	**
1+	5.39	4.67	3.1-6.4	0.86	16	N	*
2+	12.34	12.40	9.3-15.0	0.91	7	Y	***
3+	18.92	16.45	12.9-19.9	2.57	14	N	*

The c.v. for the electro-fishing data for the 2+ parr has been fitted well, with the observations being correlated with the prediction ($r = 0.763,\ P < 0.001$). However, this is not the case with the 3+ parr ($r = 0.151,\ P > 0.05$), and both the predictions and the observations for the c.v. are shown in Fig. 6.14.

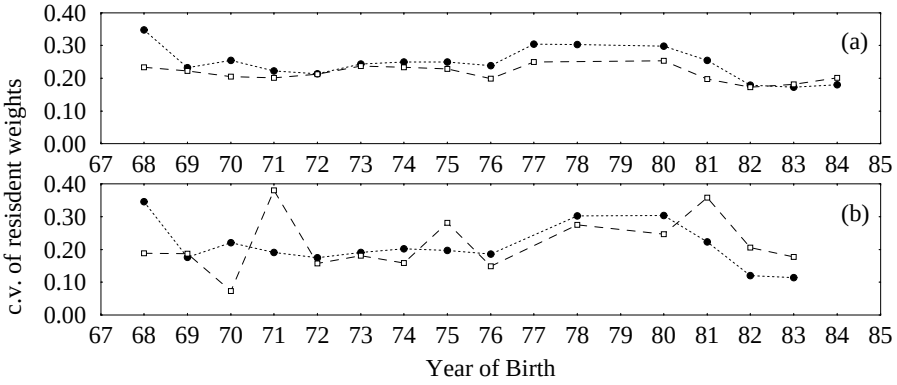

Figure 6.14: *Predicted c.v. of the 2+ and 3+ weights using the SSVN4 model with the observations. (a) is for the 2+ and (b) is the 3+. The open squares are the observations and the closed circles the prediction.*

Although the error associated with the lengths of the smolts are relatively small, the prediction for both age-classes are not correlated with the observations and are still systematically low for the two year old migrants and generally too high for the three year olds, as can be seen in Fig. 6.15.

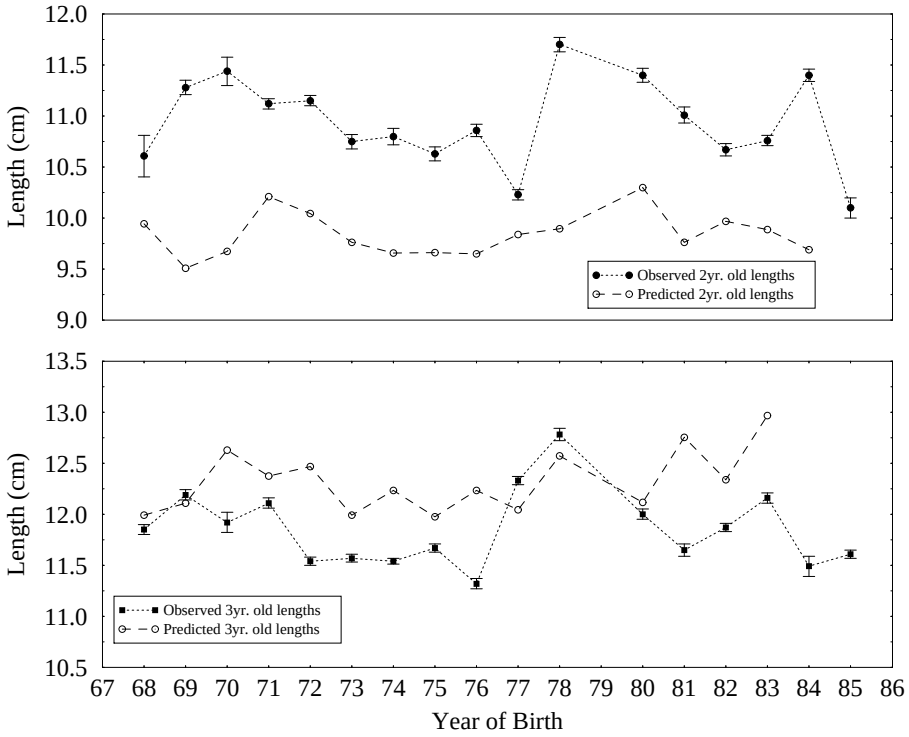

Figure 6.15: *The observed and predicted mean lengths of the smolts using the model SSVN4.*

The largest single improvements between SSVN2 and SSVN4 has been in fitting the model to the proportion smolting from each age-class, and the fit is shown in Fig. 6.16. The proportions leaving during the first migration season have been predicted well, whereas those leaving the next season have been slightly under predicted, with the proportion leaving later being over predicted.

The model has attempted to predict many aspects of the population. In some of the cases, the predictions have described the observations well, whilst for others the there are systematic differences or the observations are not correlated with the predictions. The reasons why the model may be badly predicting different aspects of the population is discussed in the final section of this chapter.

6.6 Summary and Conclusions

The SSVN4 variant of the model will be the final version that is developed in this thesis. There are a number of reasons why further developments are unlikely

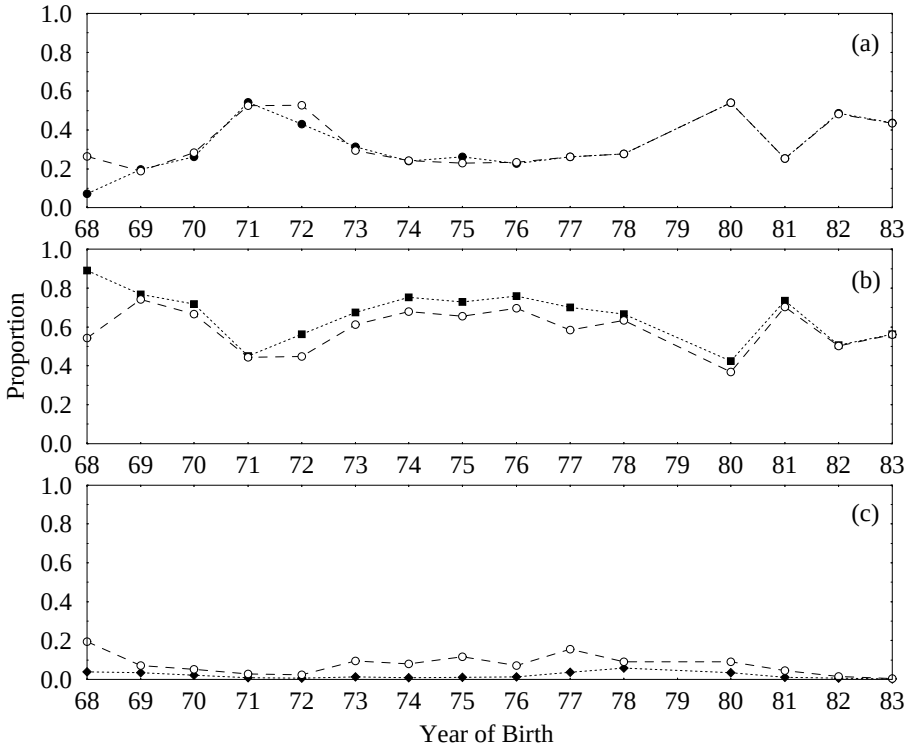

Figure 6.16: *Proportion of each cohort predicted by SSVN4 to leave at each age-class for the 1+/2yr. old in the upper graph, the 2+/3yr. old in middle and the 3+/4yr. old in lower. The filled circles are the predictions and the empty squares are the predictions.*

lead to a significantly greater understanding of the dynamics of the population.

6.6.1 Limitations of the Data

The data to which the model was fitted was collected from two sources. These were from the electro-fishing surveys and from the smolt trap. The electro-fishing data has been modelled well with the exception of the c.v. of the 3+ weights. These observations are highly variable when compared to the observed c.v. of the 2+ and the predictions for both the 2+ and 3+ parr, as can be seen in Fig. 6.14. This variation may be due to the relatively small sample sizes for this age-class that has a large variation in individual weights. This leads to the mean weights and the standard deviation being variable and the model is unable to predict them.

The data that are collected from the smolt trap is from across the whole of the burn. As was shown in Chapter 2, there are differences in the weights of the resident fish based on the altitude in which they were measured. This could imply a similar relationship for the migrating fish. If this was so, then the model would under predict the observed variation in the lengths of the smolts.

The lengths of the smolts are likely to be affected by the stream section in which they lived before migration, and the size of the effect on the mean length would be dependent on the numbers emigrating from the different section. If the lower part of the stream was more productive in terms of the number of smolts produced than the upper section, the model would be expected to under predict the lengths. If it were the other way around, then the model would over predict.

The lengths of the migrants are over predicted for the two year olds and under predicted for the three year olds, which suggests there are other factors involved other than a bias due to the productivity of the different stream sections. A major part of the migration season occurs in autumn when many migrants leave as parr. The model assumes that the growth rates of the autumn emigrants would be similar to those that did stay and migrated in the spring, if they had of stayed. The mean lengths of the autumn emigrants are considerably lower than for the spring smolts, and it is not clear how their lengths differ from those that choose to migrate the following spring.

Larger proportions of the 2+ migrants are precocious parr than for the 1+ parr and they are not significantly larger than the other members of the autumn migration are. However, if large numbers of precocious parr leave the population during the autumn, the mean weights of the three year old smolts next spring may be lower. Therefore, the effect of precocious parr on the mean spring lengths will be to lower them, and the effect will be stronger for the three year old parr. This will lower the observed mean lengths to which the model has been fitted, and may be a reason why the model over predicts the three year old lengths but not the two year olds.

The predictions for the age-class at which different proportions of the cohort migrate are predicted well. However, these observations have been derived with an unknown bias from 1977-1986. When predicting the proportion leaving at different age-classes, estimates of the mortality rates have not been included.

We would therefore expect to over predict the 3+/four year old proportions and under predict the 1+/two year old proportions.

The temperatures that have been used in the model were collected at the smolt trap at the lower end of the Burn. These temperatures are likely to be higher than those in the middle section of the burn are. The effect of this on the predictions is that the values of ϕ_y may have been under estimated. Data exists for different sections of the stream, and estimates of the differences in temperature for the different parts of the stream can be made. In Chapter 7, the SSVN2 model will be used to predict the weights of parr in different parts of the stream assuming that there are differences in the water temperatures.

6.6.2 Under Predicting Spring Growth

The model has been shown to under predict the growth rates of the parr in spring. This is due to the predicted growth rate being less than zero for temperatures $\leq$ approximately 6^oC, whereas for these temperatures, growth has been seen to occur. This would lead to the model under predicting spring lengths and the c.v. of the predicted lengths as has occurred.

These under predictions in the weights result in the model under predicting the reserve to structural weight ratio, ρ, so that it is too low. In order to make the model be able to predict these large changes in weight would require structural changes to the model. This would require a more detailed understanding of individual growth rates of the juveniles in the wild.

Many of the values of ϕ_y are greater than 1 which indicates that either the model is under predicting growth at some point during the year or the data with which the model was parameterised with was not predicting maximum growth. It appears that assuming that ϕ_y is a constant throughout the year may be too simple, but again, this would require long term individual data too correct.

6.6.3 The Fitting Procedure

The DSO is unable to find the global minimum for the error function based on the residuals from the model. As the model increases with complexity, this is likely

to result in the error surface becoming less appropriate for the fitting procedure. Therefore, although a minimum is found, and we can estimate its accuracy by the variation in the parameters derived from different initial condition, how close we are to the true minimum is still unknown.

A more sophisticated method of fitting is required if a more complex model is to be used. Only by finding the true global minimum will we be able to accurately assess how well the model fits the data.

6.6.4 Characteristics of the Social Environment

The factors temperature, weight and $\phi(t)$ have been used to predict growth but are unlikely to be the only factors that affect growth rates. These three factors have been used to describe the effects of the physical environment on the juvenile parr.

As was seen in Chapter 2, the lengths of the predicted autumn and spring migrants are closely related to the estimated ova deposition. Further changes to the model need to involve factors associated with the social environment of the parr. This must include density dependent effects on the growth rates of individuals and size selective mortality in the population. A mechanism for competition is suggested in Chapter 8.

However, the model as it is can be used to assess the quality of habitat within the burn through the derivation of $\phi(t)$. This index can be compared between different parts of the burn to determine their suitability for salmon growth. The model will be applied to the data from different parts of the burn, which will be the subject of Chapter 7.

Chapter 7

Fitting Model to Different Parts of the Stream

7.1 Introduction

The SSVN2 model (Gaussian WFD, variable c.v., fitted to the parr data only) is able to predict the growth rates of the resident parr by estimating the year quality given that there is size selective migration within each cohort. It has been parameterised with data from both tank reared and wild juveniles, and has previously been fitted to data from the middle section of the burn using the temperatures from the fish trap. The data from the middle section was collected at an altitude of approximately 65m higher than the fish trap. The model will now be fitted to the mean weights of parr from different altitudes in the burn, but with the same habitat types, with estimates water temperatures at different altitudes.

When compared to the fish in the middle section of the stream, those in the lower section are generally larger, and those in the upper are generally smaller (see Chapter 2). If water temperature can be estimated using a temperature-altitude relationship, we could attempt to predict the differences between the lengths of the fish from different stream sections. If ϕ_y is constant across the burn and the residuals are similar across sections, then this indicates that to predict the growth rate in any part of the stream only requires a temperature-altitude relationship.

A further step that can be taken is to actually fit the model to the electro-fishing

data from the different sections with the temperatures adjusted appropriately. This would result in different sets of ϕ_y for the three sections. If they are dissimilar, then this may indicate that the across year annual effects on growth are different between stream sections, and the differences in growth between sections cannot be solely attributed to differences in temperature. This analysis will use a shorter data set from 1969-1976, as this is the only period for which data exist for all three sections.

7.2 Data outline

7.2.1 Summarising the Electro-Fishing Data

Lengths of parr measured during the summer electro-fishing survey in habitat types T_1 and T_{1A} are available for the years 1969-1976 for the upper and lower sections of the burn, after which only the middle section was fished. These lengths were converted into weights using the same weight-length relationship used on the parr from the middle section, then summarised into means for the parr from each age-class in each cohort, and their standard errors derived.

These new data sets from the upper and lower sections were not as complete as the one from the middle section. No measurements from 3+ parr were recorded in the upper section during 1970 or in the lower section during 1971 as none were caught. Otherwise, the data sets are comparable, and form the data to which the model would be fitted.

7.2.2 Deriving a Temperature-Altitude Relationship

The maximum and minimum altitudes of the three sections are given in Table 7.1, and the sections are shown on the map in Fig. 2.1. Surveys were carried out within each section and the estimated altitude for each section used was the average between the minimum and maximum altitudes. This provided a good approximation of the mean as each section has a fairly constant gradient.

A formula from C. Soulsby (*pers. comm.*) states that water temperature decreases at a rate 6°C for every 1000m increase in altitude. This has been applied

Table 7.1: *The altitude of the different stream section of the Girnock Burn.*

Stream Section	Minimum Altitude (m)	Maximum Altitude (m)
Lower	240	285
Middle	285	320
Upper	320	370

to the sections in the Girnock and the estimated differences between the temperatures at the fish trap and the different stream sections are given in Table 7.2.

Table 7.2: *The difference in temperatures between the position of the temperature recorder and the average altitude of each stream section calculated using the formula from C. Soulsby.*

Stream Section	Difference in temperature from the fish trap (°C)
Lower	-0.135
Middle	-0.375
Upper	-0.57

An additional data set of temperatures were recorded at a point at the upper end of the middle section from 26/3/81 until 4/12/81. From these records, the maximum and minimum daily temperatures were used to estimate daily temperatures. This is the same method as was used for the fish trap data. It was found that the temperatures from the two recorders were highly correlated and the mean difference between the two recorders was 1.2°C. The mean monthly temperatures with their s.e. are shown in Fig. 7.1.

There are significant variations between months and there may well be a seasonal effect, but given the limited data, we are unable to show this is true so we will assume that there is a constant difference between the two recorders all year round and that temperature changes linearly with altitude over the Girnock.

This relationship states that there will be a decrease of $14.1^{\circ}\mathrm{Ckm}^{-1}$ with increasing altitude. The differences in temperature between sections calculated with this formula are shown in Table 7.3.

The estimates in Tables 7.2 and 7.3 differ considerable, with the C. Soulsby

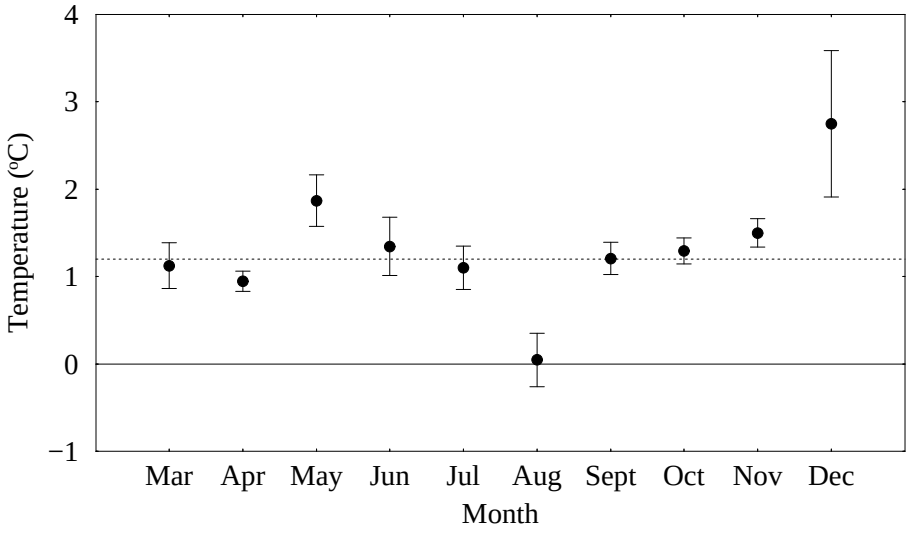

Figure 7.1: *Average monthly differences in temperature between the two temperature recorders on the Girnock, with standard errors. The dotted line represents the mean monthly difference.*

Table 7.3: *The difference in temperatures between the position of the recorder at the fish trap and the average altitude of each stream section calculated using data from an additional recorder.*

Stream Section	Difference in temperature from the fish trap (°C)
Lower	-0.32
Middle	-0.88
Upper	-1.34

formula being approximately half of the relationship derived from the data. As the second relationship has been derived using site specific data, it will be used to estimate the temperature differences between the sections of the burn.

In Chapter 4, the sensitivity of the models predictions to variations in temperature was tested by varying it by $\pm 0.2^o$C. The model was then fitted to the electro-fishing data for each of the different temperatures to derive different sets of ϕ_y. The values of ϕ_y were significantly altered by these temperature variations although they remained correlated (see Fig. 4.5). If $\phi(t)$ is constant throughout the burn, we would expect that the changes in temperature are of a sufficient size to explain the changes in the mean weights of the resident parr between section of the burn.

7.3 Predicting Weights in Different Parts of the Burn

7.3.1 Using Constant Fitted Parameters Across Sections

The SSVN2 model was fitted to the data from the middle section of the burn, and ϕ_y for 1969-1976 and the two cut-off points at W_{c_1} and W_{c_2} were derived. This was done using the DSO procedure as outlined previously and the parameters which produced the best fit are given in Table 7.4. The predictions made with these parameters are shown in Fig. 7.2, and the fit to the age-classes are given in Table 7.5. This version of the model will be defined as SSVN2M.

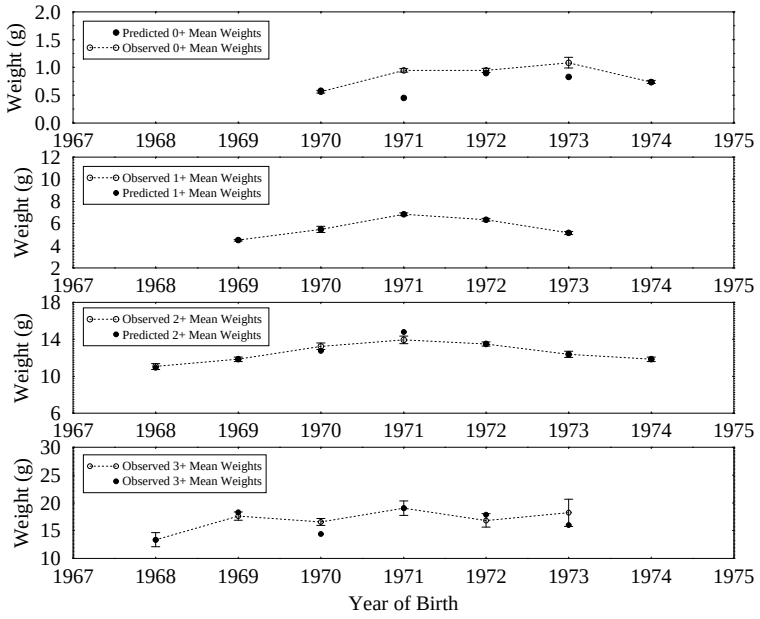

Figure 7.2: *Predicted weights using model SSNV2M and observed mean weights of the different age-classes with their standard errors for the middle section only.*

Table 7.4: *Summary of the parameters derived from fitting the model to the data from the middle section with model SSNV2M.*

$W_{c_1}(g)$	$W_{c_2}(g)$	Range of ϕ_y	MWE
8.97	13.55	0.977-1.149	1.337

In order to test if these parameter values are applicable across the entire burn, they will be used to make predictions of the mean weights for the parr in different

Table 7.5: *Fit of the model to the different age-classes when fitted to the data from the middle section of the burn from 1969-1976 with model SSNV2M.*

Age-class	*Average Weight (g)*	*Predicted Weight (g)*	*Mean Abs. Error (g)*	*% Error*	*Sign. same*	*Sign. correl.*
0+	0.854	0.697	0.164	19.2	Y	NS
1+	5.673	5.674	0.002	0.0	Y	***
2+	12.53	12.57	0.222	1.8	Y	**
3+	16.95	16.51	1.023	6.0	Y	*

parts of the stream. Differences in the predictions will be due to the adjusted temperatures being put into the model, which will be those shown in Table 7.3.

Fig. 7.3 shows the observed mean weights of the parr from the upper section of the stream with the predictions from the SSNV2M model with the estimated temperature from the upper section of the stream. Although some of the mean weights of some of the cohorts have been estimated well, such as the 1968 and 1970 cohorts, there are systematic differences in the residuals. The predictions for the 0+ and 1+ are either below or within the s.e. of the observations, and the predictions for the 3+ are either above or within the s.e. of the observations.

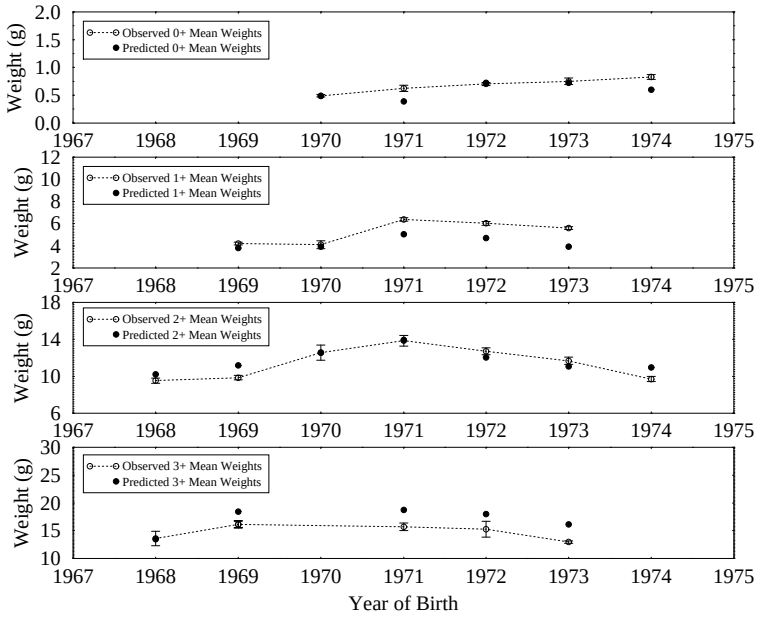

Figure 7.3: *The predicted mean weights of parr from the upper section using model SSNV2M and the estimated temperatures in the upper section, with the observed mean weights of the different age-classes with their standard errors.*

The predictions of the mean weights of the parr from the lower section are shown in Fig. 7.4, which are predicted from the SSNV2M model with the estimated temperature from the lower section of the stream. Here, the residuals are in general larger, and all predictions of the 0+, 2+ and 3+ being lower or within the s.e. of the observations.

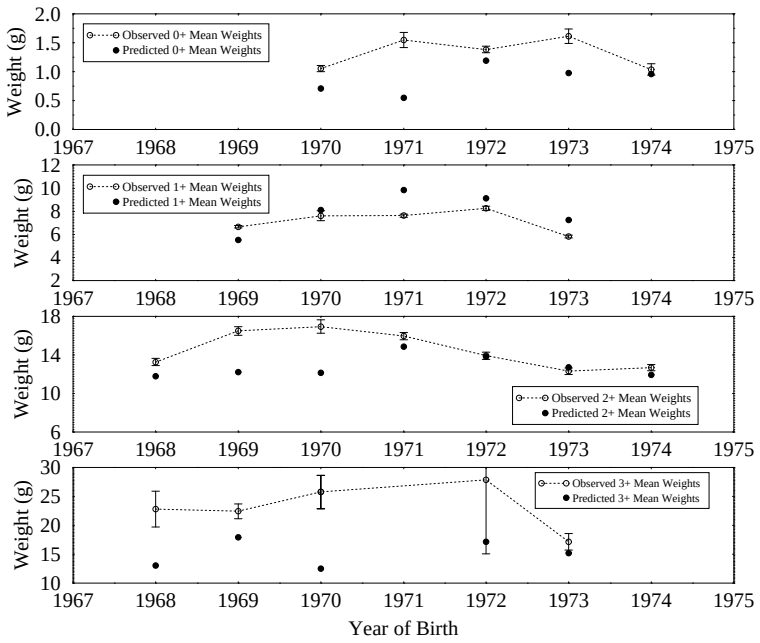

Figure 7.4: *The predicted mean weights of parr from the lower section using model SSNV2M and the estimated temperatures in the lower section, with the observed mean weights of the different age-classes with their standard errors.*

The above predictions of the weights from the different sections have been made using the same values of ϕ_y and the same threshold smolting weights, and then applied to each section using the appropriate temperatures. As the temperature is increased, the predicted weights of the 0+ and 1+ will also increase. This will not necessarily be the case for the 2+ and 3+ parr due to the threshold weight for smolting. When the weight-frequency distribution is truncated, the mean of the remaining part of the distribution will be different at different temperatures, and for sufficiently large temperature differences and low cut-off points, the mean of the distribution at the higher temperature will be lower than the mean of the distribution at the lower temperature.

When the model is fitted to the different stream sections with the different temperatures, the fits for the different sections vary, and the MWE between the

different sections are shown in Table 7.6. This means that the parameters that have been derived for the middle section are not appropriate for the other sections.

Table 7.6: *The mean weighted error from the fit of the model SSNV2M to the data from the different sections with the different temperatures but same values of ϕ_y and threshold weights for migration.*

UPPER	MIDDLE	LOWER
3.986	1.337	4.885

As using the same fitted parameters does not provide an adequate fit to all the data, an alternative approach will be used. The model will be fitted to the data from the upper and lower sections with the different temperatures by adjusting the fitted parameters of the smolting threshold weights and ϕ_y. The values of the fitted parameters between sections can then be compared.

7.3.2 Using Different Fitted Parameters Between Sections

The model was fitted to the data from the upper and lower section as was done for the middle section in Section 7.3.1. From the fitting procedure, a set of fitted parameters was derived, so that each section had its own unique set of ϕ_y values and smolt threshold weights.

The fit of the model to the data from the upper section of the burn, which will be defined as SSNV2U, is shown in Fig. 7.5, and the fit to the data has improved. The fit of the model to the data from the lower section, which is shown in Fig. 7.6 and will be defined as SSNV2L, is able to provide good fits to the 1+ and 2+ age-classes, but tends to under predict the mean weights of 0+ and 3+ age-classes. The changes in the % error for each age-class for the two new models are shown in Table 7.7, where, in each case, the least well fitted age-class is the 0+ and best fitted is the 1+.

The fits to the upper and lower sections are appreciable improvements. The MWE when the model is fitted to the three stream sections are shown in Table 7.8, which shows a decrease in the goodness of fit as the altitude decreases.

The largest problem with the fit of the data to the lower section is the under

Table 7.7: *Mean % errors for each age-class derived from fitting the different models to the mean weights from the different sections of the burn.*

SECTION	MIDDLE	UPPER		LOWER	
MODEL	SSNV2M	SSNV2M	SSNV2U	SSNV2M	SSNV2L
Age-Class					
0+	0.192	0.151	0.119	0.339	0.394
1+	0.000	0.185	0.016	0.169	0.001
2+	0.018	0.058	0.026	0.127	0.067
3+	0.060	0.155	0.051	0.347	0.181

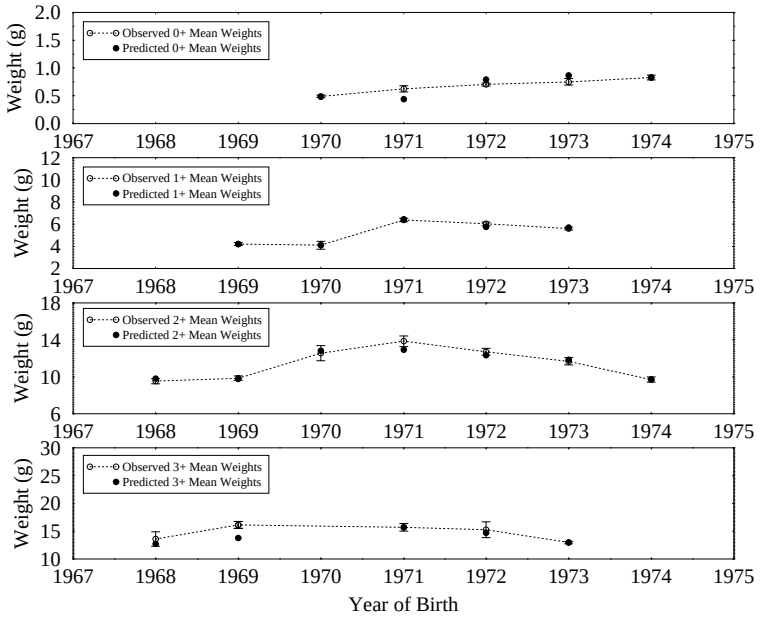

Figure 7.5: *The observed mean weights with s.e. and the predictions from the model SSNV2U when fitted to the data from the upper section of the burn with the estimates of the upper section temperatures.*

prediction of the 0+ parr. The growth trajectories are able to fit the 1+ age-class very well, which indicates that the growth rate between birth and 1+ is too low. It is interesting to note that for the cohorts born in 1970 and 1971, apart from for the 1+ age-class, all of the predictions are too low. By looking at Fig. 1.1, we see that in the years 1969 and 1970, the number of females caught in the trap were the lowest from 1966-1977, and these were the females that would give birth to the 1970 and 1971 cohorts.

This, however, cannot explain why all of the 0+ are under predicted. One possible

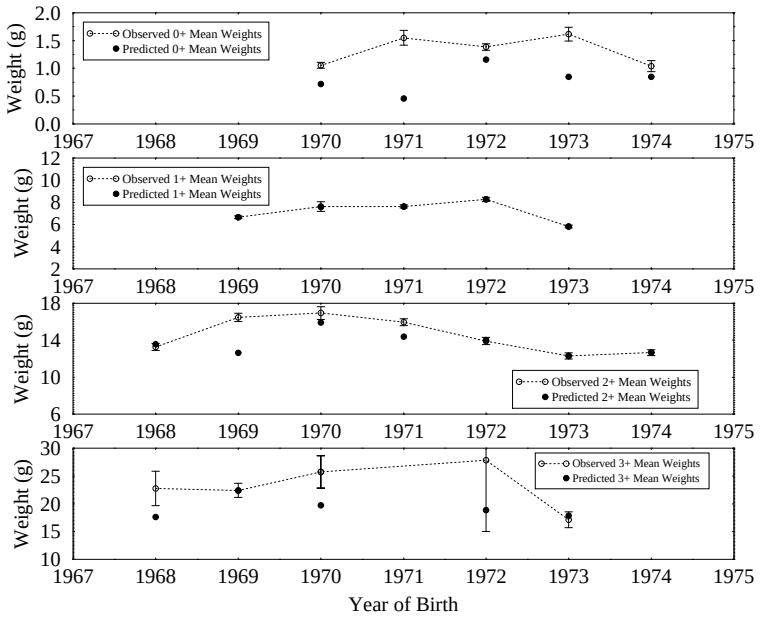

Figure 7.6: *The observed mean weights with s.e. and the predictions from the model SSNV2L when fitted to the data from the lower section of the burn with the estimates of the lower section temperatures.*

explanation may be that the intensity of competition is greatest in the lower section of the stream, and by the time of the 0+ census, a large proportion of the smaller fry have perished, leaving the larger ones in the stream. This bias would cause the 2+ and 3+ to be over predicted.

Table 7.8: *The mean weighted error from the fit of the models SSNV2U, SSNV2M and SSNV2L to the data from the upper, middle and lower sections of the burn respectively. The improvements of the fits can be seen by comparing this table with Table 7.6.*

UPPER	MIDDLE	LOWER
0.9687	1.337	2.1459

7.3.3 Variation of Fitted Parameters between Sections

Variation in ϕ_y between Sections

For the different stream sections, a set of the values of ϕ_y were derived, and the set which provided the best fit of the models to the data were used to produce

Figs. 7.2, 7.5 and 7.6. The error associated with these sets of ϕ_y were derived from using different initial conditions of the fitting procedure. The values of ϕ_y for the different sections with their errors are plotted in Fig. 7.7.

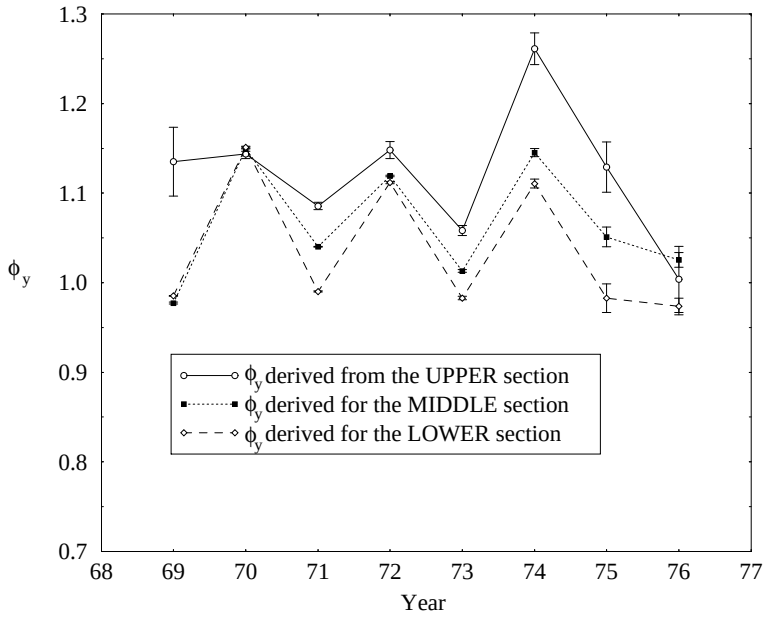

Figure 7.7: *Values of ϕ_y from the different sections of the stream.*

A two-way ANOVA with year and stream section as factors can be used to show that a significant amount of the variation values of the ϕ_y's is due to year ($F_{7,14} = 9.39,\ P < 0.001$) and the stream section ($F_{2,14} = 10.9,\ P < 0.0014$). Year as a factor accounts for 64.7% of the variation and provides an indication of the years when conditions for parr growth were best. The stream section accounts for 21.5% of the variation, with the lower section of the stream providing the lowest vales of ϕ_y, whilst the upper section provides the higher values.

On the basis of these results, there does not appear to be a single set of values of ϕ_y that can be applied across the burn. Instead, the values of ϕ_y from each of the sections are correlated with each other[1] and ϕ_y appears to increase with altitude.

[1]The correlation coefficient between the upper and lower section is $r_7 = 0.666$, between upper and middle is $r_7 = 0.644$ and between middle and lower is $r_7 = 0.931$. The critical value of r_7 below which $P < 0.05$ is $r_7 = 0.669$.

Variation in the Smolting Threshold between Sections

The values of the two threshold weights for smolting for the three sections were determined by the values that produced the best fit to the data. As with ϕ_y, the errors associated with the threshold weights were calculated from using different initial conditions of the fitting procedure. The values with the errors are displayed in Fig. 7.8.

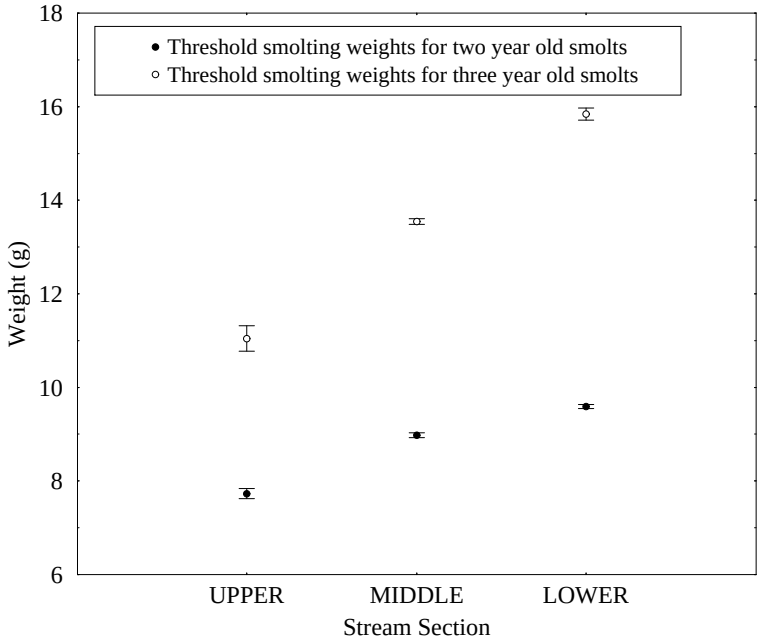

Figure 7.8: *Estimated values of the threshold weights for smolting from the different sections of the steam with their standard errors.*

The threshold weights for smolting are clearly different for the three sections. The lowest weights are associated with the upper section, and the middle weights with the middle section and the highest weights with the lower section.

7.3.4 Relating ϕ_y to Social Environment of the Parr

Density estimates for the juveniles in each age-class at each survey were made during each the electro-fishing surveys, which approximate the overall strength of each age-class in each section of the stream. As sets of values of ϕ_y's for the different sections have been derived, we can use the data regarding the social environment of the parr to attempt to explain some of the variation in ϕ_y.

The estimated densities for each age-class were correlated with the values of ϕ_y which were derived for the three sections of the stream, and were found to be significantly negatively correlated for the 0+ ($r_7 = -0.740,\ P < 0.05$) and the 2+ ($r_7 = -0.667,\ P < 0.05$) age-classes in the upper section of the burn but no significant correlations were found in the middle or lower section.

Further to this, the values of ϕ_y were lagged and then correlated with density. When density was correlated with ϕ_{y-1}, there was a significant correlation for the 1+ age-class in the upper section ($r_7 = -0.769,\ P < 0.05$), and when correlated with ϕ_{y-2}, there was a significant negative correlation for the 0+ age-class in the upper section ($r_6 = -0.748,\ P < 0.05$). The only significant correlations in the other two sections occurred with ϕ_{y-3} for the 1+ age-class (middle section, $r_5 = -0.956,\ P < 0.01$ and lower section, $r_5 = -0.862,\ P < 0.05$).

The correlations were repeated using the biomass of each age-class, which was calculated as the product of the density and the mean weight of the parr in that age-class. ϕ_y and biomass were found to be significantly negatively correlated for the 0+ ($r_5 = -0.928,\ P < 0.05$) and the 2+ ($r_7 = -0.721,\ P < 0.05$) age-classes in the upper section of the burn.

When biomass was correlated with ϕ_{y-1}, there was a significant positive correlation for the 0+ in the upper section ($r_5 = 0.837,\ P < 0.05$). When correlated with ϕ_{y-2}, there were significant negative correlations for the 0+ in the upper section and the 2+ in the lower section, and when correlated with ϕ_{y-3}, there were significant negative correlation for the 1+ in the upper ($r_4 = -0.953,\ P < 0.05$), middle ($r_4 = -0.925,\ P < 0.05$) and lower ($r_4 = -0.954,\ P < 0.05$) sections.

In addition, the estimated total biomass was correlated with the values of ϕ_y and this was repeated when the data was lagged. No significant correlations were found for each stream section and lag. The estimated ova deposition was also correlated with ϕ_y from the different sections with different lags, none of which were found to be significant.

A considerable number of correlations were attempted, in particular for the ϕ_y and lagged correlation tests, four significant results were found from 36 correlations, and with the ϕ_y and lagged biomass tests, six significant results were found from 36 correlations. Given that the significant results were neither consistent across

age-class or section, it is likely that they are due to chance[2]. All other significant positive correlations are found in the upper section of the burn.

There are complications with this analysis as the values of ϕ_y are not independent and it is likely that the densities not either. There are also few data points, with a maximum of 8 values of ϕ_y used for each section, with missing data from different age-classes in different years. Further and more complex linear models will not be used to explain the variation in ϕ_y due to the limitations of the degrees of freedom available in the data.

These correlations show that there may be an inverse relationship between ϕ_y and density or biomass in the upper section, but these effects are undetectable in the middle and the lower section. Otherwise, the correlations of ϕ_y do not appear to be related to biomass and density in any clear and consistent way.

7.4 Conclusions

There are clear and systematic differences between the parameters derived for each section of the stream. They are consistently different, as are the errors, and together form a consistent view of the quality of growth in the different parts of the burn.

As the altitude decreases, the fit of the model to the data deteriorates, which may be an indication of the increasing complexity of the life style of the juveniles whose growth we are attempting to model. This may be a result of increases in the complexity of the ecosystem as the temperature increases. The lower part of the burn is more populated with salmon as well as other species, and the surrounding vegetation is more diverse. There are a greater number plants with vegetation with over hangs the river, which increases the carbon input into the burn.

Higher values of ϕ_y are associated with faster growth after the effects of temperature have been removed. This indicates that the local environment for the growth of parr is better in the higher part of the stream than the lower part. The higher growth rates in the lower part of the burn can be attributed mainly

[2]The chance of getting $\geq$4 correlations with $P < 0.05$ from 36 attempts is 10.4% and $\geq$6 from 36 is 0.8%.

to higher temperature.

Differences in ϕ_y between sections may be due to the lower density and less competition further upstream. The water is likely to be cleaner and the proportion of the stream suitable for parr higher. In general, habitat quality would be expected to be better in the upper reaches of the stream otherwise the adult would not make the extra effort required to get there.

Parr smolt at a smaller size in the upper part of the burn. We must bear in mind that although the cut off point is termed as the threshold weight for smolting, it is a threshold weight for parr leaving the resident population. The smaller emigrants from the upper section could move to the middle section and form part of the population below the threshold weight there.

The differences in the parameter values across the stream indicate that once the effects of temperature have been removed, the growth and behaviour of the parr from the different sections changes. The parr in the upper section are able to grow better than those in the lower section, and are able to migrate at a lower weight, which would be necessary as there is a shorter growing season at higher altitudes.

ϕ_y is a general term that encompasses many aspects of feeding, and its values derived in Section 7.3.3 range from approximately 0.95 to 1.3. These values suggest that the parr are growing at a far higher rate than the theoretical maximum growth rate predicted by the model, and the model does tend to over predict the weights of the 0+ parr whilst being able to predict the 1+ mean weights relatively well. These aspects of the model will be discussed further in Chapter 9. ϕ_y is a term for consumption and in Chapter 8, we offer an alternative theoretical model for ϕ_y based around the Type II functional response (Holling, 1959).

Chapter 8

Functional Response Uptake Model for Atlantic Salmon Parr

The temperature dependent growth models developed in the previous chapters have been fitted to the data by adjusting the function $\phi(t)$. This function has been assumed to be constant within years and across age-classes. In this chapter, we shall further develop $\phi(t)$ so that it is dependent on the size of the parr and able to vary within years. These variations will be determined by the characteristics of the invertebrate populations that form the diet of the parr.

A foraging model, dependent on the size of the individual parr, the size and density of the invertebrate populations and the current, will be developed to estimate the consumption rate of the parr. This model will then be integrated into the CGM model (Broekhuizen et al. 1994) and fitted to electro-fishing data, with different assumptions about the distribution of the stream dwelling invertebrates.

8.1 The Foraging Behaviour of Parr

8.1.1 Behaviour of the Invertebrate Drift

The food on which the salmon feed is comprised of a variety of aquatic insects, such as larvae, pupae, nymphs, and insects of terrestrial origin that have fallen onto the surface of the water (Mundie (1969), Egglishaw (1967), Allen (1940)), and is known as the freshwater invertebrate drift.

The aquatic insects live mainly in the substrate and on underwater plants, from which they enter the water column. This is either through their own need to move in order to settle somewhere else, or through the turbulence of the current (Waters 1969) and it is when they are in the current that they are available as food for the salmon.

Drift occurs with diel periodicity with observed peaks at sunset and sunrise, with high quantities of drift occurring at night (Mundie 1969). The quantity of the drift is dependent on factors such as the amount of detritus (overhead vegetation, stream plants and algae) within the stream (Egglishaw and Morgan (1965), Egglishaw (1964)) and the chemical composition of the stream (Egglishaw and Morgan (1965), Egglishaw (1968)). Size of the individual invertebrates increases throughout the year and seasonal changes in the composition of the bottom fauna has been observed in Scottish streams (Egglishaw and Mackay 1967).

Drift is related to production, with higher drift leading to increases in production and higher growth rates (Waters 1969) although predation by parr does have an impact on the quantity of drift.

8.1.2 Methods of Foraging

Salmon parr must gain a sufficient amount of weight before they are able to migrate to sea, which they do by feeding on invertebrates in the stream (Wankowski 1981). Parr are sit-and-wait predators, who remain stationary at the focal point of a defended territory from which they make rapid forays to capture and consume their prey. The four basic methods by which they feed are described by Stradmeyer and Thorpe (1987a) below.

Surface Feeding
Surface feeding is the consumption of terrestrial food items that have fallen onto the surface of the water. The parr will see a food item floating on the surface which it swims towards and eats.

Midwater Drift Feeding
This is when is food that is taken from the water column, which contains mainly benthic invertebrates. This type of feeding can happen in a variety of ways:
I. Direct feeding The salmon attacks the prey item with a rapid burst of swimming

into the current.

IIa Indirect feeding (active) The salmon will move up into the water column towards the prey item which it will either attack with a rapid movement or ignore and return to station.

IIb Indirect feeding (partly passive). This occurs in two ways. The salmon will drift downstream with the current, facing the prey item, which it either attacks with a rapid snap or returns to its station. The second method is similar to the first except before it attacks the prey, the salmon will turn around and capture the prey item as it moves downstream. This occurs in higher water velocities with faster moving prey.

Head-jerk Feeding

Prey items moving in the drift passing close to the fish are captured with rapid side-to-side snapping movements of the head without body displacement such that the fish does not leave its station.

Bottom Feeding

The fish makes attacks from the feeding station and snaps at the prey as it forages amongst the substrate.

These types of foraging methods have been widely observed (Keely and Grant (1995), Wankowski and Thorpe (1979b), Stradmeyer and Thorpe (1987a)) and this information will be used to derive an estimate of the uptake rate based on the foraging behaviour of the parr. The predominant method of foraging is when the fish takes food from the water column, which includes midwater and head jerk feeding.

Maximum attack distances given by Wankowski and Thorpe (1979b) range from 1 to 5.8 body lengths, those from Stradmeyer and Thorpe (1987a) are approximately 103cm[1]. Keely and Grant (1995) give an average attack distance of about 3 body lengths. Any foraging model that is developed must have similar attack distances and be dependent on the water velocity.

[1]Distances in body lengths are not given by Stradmeyer and Thorpe (1987a), but may be 6.87-10.3 body lengths based on the size of the parr observed in the study.

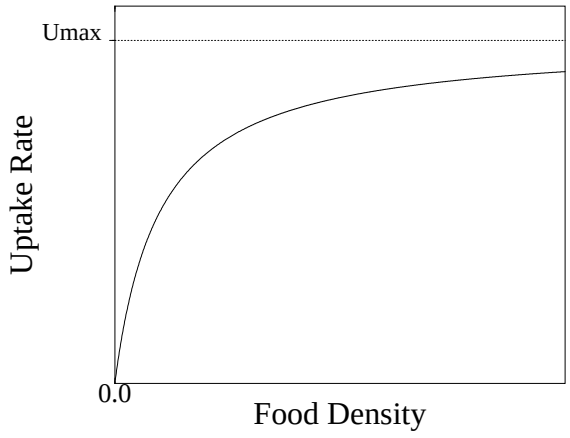

Figure 8.1: *With a Type II functional response, the uptake rate will tend to U_{max} as the food density tends to infinity.*

8.1.3 Modelling Foraging Behaviour in Fish

Hollings Type II Functional Response

Many foraging attempts are unsuccessful, especially for younger inexperienced parr, resulting in food being rejected or the ingestion of low nutritional food such as insect exuviae (Mundie 1969). Visibility may be poor and the water turbulent. Danger exists from predators which deters foraging (Metcalfe et al. 1987) and competition exists from conspecifics (Symons (1971), Gotceitas and Godin (1992)). Therefore the maximum uptake rate, U_{max}, is unlikely to be attained. We shall use the Type II functional response (Holling 1959), whose form is shown in Fig. 8.1 and derivation in Appendix B, to model the uptake rate. This has been widely used for variety of fish species (Madenjian and Carpenter (1991), Peterson and Deangelis (1992), Wright et al. (1993), Eby et al. (1995), Stockwell and Johnson (1997)) in order to determine uptake.

The general form of the Type II function response is given by equation (8.1) where U is the uptake rate and Φ is the rate at which food is found whilst foraging. In order to estimate the uptake rate, we must determine expressions for U_{max} and Φ.

$$U = U_{max}\left(\frac{1}{1+\frac{U_{max}}{\Phi}}\right) \tag{8.1}$$

8.2 A Functional Response Model for Salmon Parr

8.2.1 Probability of Catch

Juvenile salmon show a high degree of prey selection based on size (Allen 1941a) and travel different distances depending on the size of the prey item (Wankowski and Thorpe 1979a). Therefore the probability of capture of a food particle of size p at distance r from a fish of length L will be defined as $P(r, p, L)$. r will be defined as the minimum distances of approach of the food particles perpendicular to the flow of the water and will have units of fish body lengths. Although this is not the actual distance swam by the fish in order to consume an item of prey, it indicates how close to the fish the particle needs to be in order for it to be attacked.

Determining $P(r, p, L)$ requires data that will give the probability of food items of a particular size being caught at a given distance. Data sets from Wankowski (1981) and Metcalfe et al. (1986) relating to the attack distances, which give the probability of catch and the size of food particles, were examined. These studies with hatchery reared salmon parr were conducted from June to September.

Foraging Data Sets

Data from Metcalfe et al. (1986)

A study by Metcalfe et al. (1986) investigated how feeding behaviour was related seasonal changes in consumption and used food particles that were set at a size to optimises growth rate (Wankowski and Thorpe 1979a). The data is reproduced in Table 8.1 and shows that at distances of about one body length distance from station, the fish ignored about 80% of the food that drifted passed, with high probabilities of capture only very close to the fish (< 1 body length). There were no restrictions to foraging such as the tank size being too small and there were no deterrents to foraging such as predators or competition. These experimental fish were mostly head jerk feeding and did not travel far in search of food. We are unable to use this data as it does not accurately portray the foraging behaviour of wild parr.

Table 8.1: *Percentage of particles ingested with the attack distances in terms of minimum distance of approach. These are given in absolute and relative terms.*

% caught				Min. Dist. (bl)		
June	July	August	Min. Dist.(cm)	June	July	August
67.42	0.4	0.08	0.4	0.1	0.084	0.082
20.00	1.3	0.25	1.3	0.31	0.27	0.27
20.76	2.6	0.49	2.6	0.625	0.55	0.53
11.16	4.5	0.85	4.5	1.1	0.95	0.92
11.16	6.5	1.23	6.5	1.56	1.37	1.33
2.87	8.5	1.60	8.5	2.04	1.8	1.73
3.37	11.0	2.08	11.0	2.65	2.3	2.25

Data from Wankowski (1981)

This data set from Wankowski (1981) consisted of four experiments, which attempted to determine the size of food particles that the fish preferred. The experiments were conducted with salmon that had previously been starved for seven days before being presented with different sized food particles, and their response and attack distances were noted. The average attack distance was 3.64 body lengths, which is similar to those found in the wild. These factors enabled us to make use of this data, which is shown in Table 8.2.

Determining the function $P(r, p, L)$

Two functions describing $P(r, p, L)$ were fitted to the data in Table 8.2 in order to determine the most appropriate form $P(r, p, L)$ should take. The first was a one parameter elliptic function and the second a two parameter discontinuos function. The term r represented the attack distance in body lengths and γ represented the size of the food particle relative to the length of the fish, such that $\gamma = p/L$.

One parameter Model

The functional form for $P(r, p, L)$ that was first fitted to the data is shown by equation (8.2). This states that all food is consumed at $r = 0$ and none at distances greater than the maximum attack distance D.

$$P(r, p, L) = \begin{cases} \sqrt{1 - \left(\frac{r^2}{D^2}\right)} & r \leq D \\ 0 & r > D \end{cases} \tag{8.2}$$

Table 8.2: *Number of food particles caught and missed at different distances from the parr and for different sized food particle during the feeding trails by Wankowski (1981). r is the attack distance in terms of fish body lengths. A, B, C and D are the four experiment with increasing size of food particle with whether the food was eaten (E) or missed (M).*

	A		B		C		D	
r	M	E	M	E	M	E	M	E
0 - <1	1	1	0	3	0	0	0	4
1 - <2	0	1	0	7	0	5	0	1
2 - <3	1	0	0	4	0	3	0	1
3 - <4	0	0	0	2	0	2	0	1
4 - <5	2	0	0	3	0	7	0	3
5 - <6	0	0	0	1	0	4	0	2
6 - <7	0	0	2	1	1	1	0	4
7 - <8	0	0	1	0	1	1	1	1
8 - <9	0	0	3	0	2	1	2	1
9 - <10	0	0	2	0	1	1	2	0

Table 8.3: *The values of D derived by fitting equation (8.2) to the data in Table 8.2, for the four food particle sizes, by minimising the RMS error, ϵ, for the one parameter model.*

Experiment	γ	D	ϵ
A	0.013	2.5	0.173
B	0.018	7.5	0.137
C	0.025	10.06	0.145
D	0.051	9.43	0.124

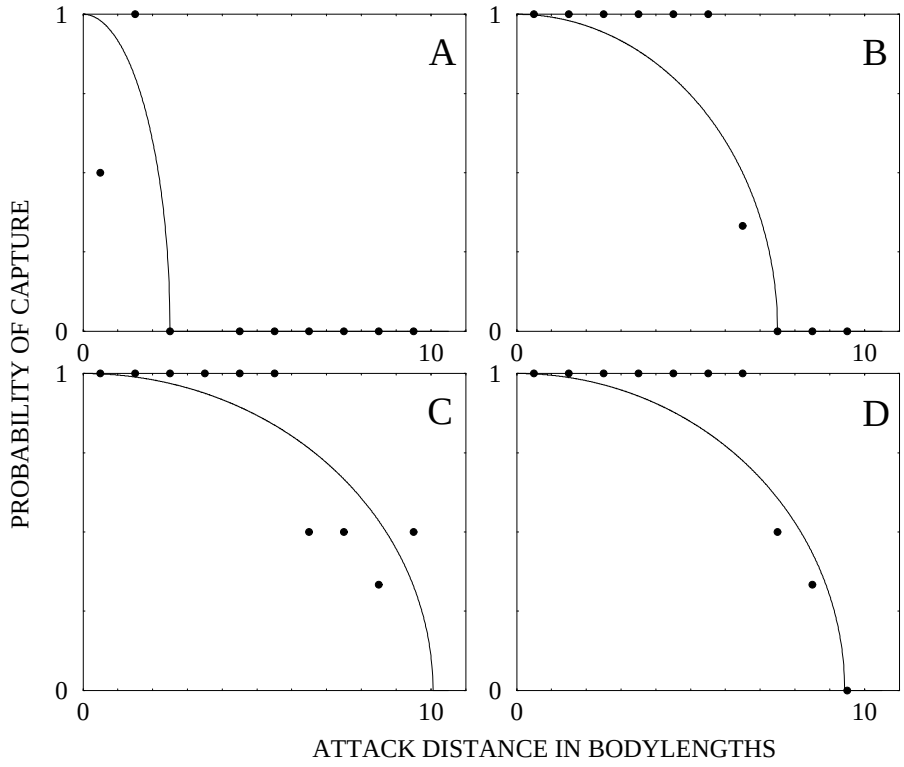

Figure 8.2: *The one parameter model fitted to the data from the four experiments by Wankowski (1981).*

Equation (8.2) was fitted separately to the data from each of the four food sizes by adjusting D through minimising the RMS error, ϵ. The values of D and ϵ for the four food sizes are shown in Table 8.3 and the trajectories from equation (8.2) using these values of D are plotted, along with the data, for the four food sizes in Fig. 8.2.

The values of D in Table 8.3 indicate how the maximum attack distance of the parr varied with the size of the food particle. A relationship between D and γ was derived by fitting equation (8.3) to the values in Table 8.3 by minimising the RMS errors.

$$D(\gamma) = [a_1 + a_2\gamma + a_3\gamma^2]^+ \tag{8.3}$$

Equation (8.3) is plotted, along with the data to which it is fitted, in Fig. 8.3, using the coefficients found are in Table 8.4.

A quadratic was used because it enforces an optimal particle size. Items smaller than the optimum have less energy value and are less appealing due to the cost involved in their capture, which increase as the attack distance increases. Smaller

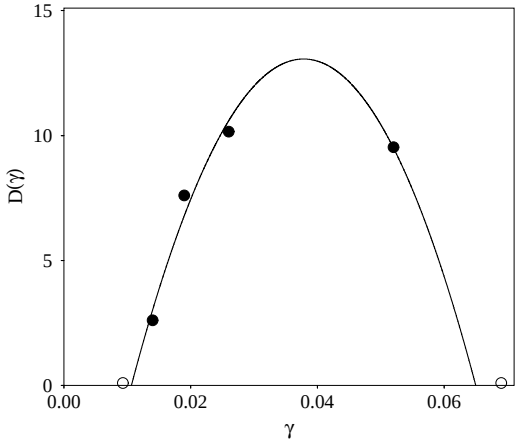

Figure 8.3: *Values of D (denoted by $\bullet$), from Table 8.3, and the fitted curve $D(\gamma)$, which represent maximum attack distances for all γ. $D(\gamma)$ is a quadratic, which is within the morphological limitations of food size for juvenile salmon (denoted by $\circ$).*

Table 8.4: *Values of coefficients derived from fitting equation (8.3) to the data in Table 8.3 by minimising the RMS error, which has a minimum value of 0.505 body lengths.*

Coefficient	Value
a_1	-11.1
a_2	1305
a_3	-17720

particles are also less visible at greater distances. Attempting items larger than the optimum means that more time and energy is required for manipulation prior to ingestion and also have a greater chance of rejection (Wankowski and Thorpe 1979a).

The values of γ at which $D(\gamma) = 0$ are $\gamma_{min} = 0.0098$ and $\gamma_{max} = 0.064$. This is in close agreement with the morphological natural limits derived from Wankowski (1979). Salmon feed by sucking food and water into their mouths and then squeezing the water out through the gills. Food particles too small will be expelled with the water. The gill rakers, which filter the food out, scale linearly with parr length and will retain food of relative size $\gamma > 0.0083$. Upper limits are imposed due to the internal breath of the mouth. This also scales linearly with length and the salmon can consume particles of relative size $\gamma < 0.068$. These values

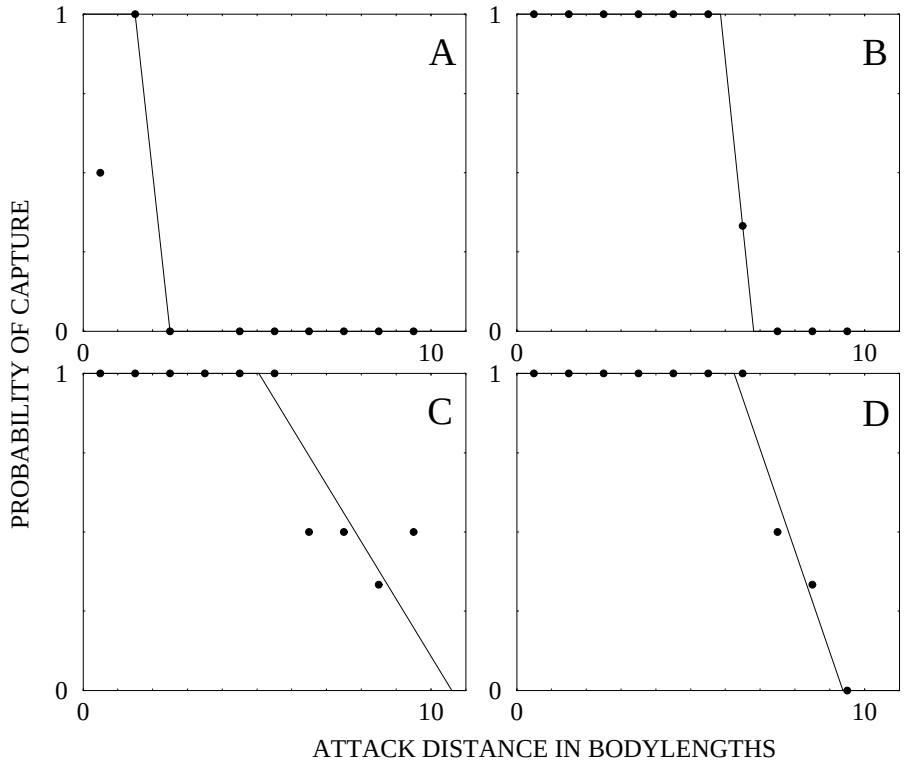

Figure 8.4: *Two parameter model fitted to the data from the four experiments by Wankowski (1981).*

are applicable for parr from approximately 4cm to 20cm in length.

Two parameter Model

The function in equation (8.4) will be used as the second model with r defined previously and a_h and a_l being the fitted parameters.

$$P(r, p, L) = min\{1, [a_h + a_l.r]^+\} \tag{8.4}$$

This model assumes that the parr take all the food within a certain distance and as the distance of the food particle from the fish increases, the probability of capture rapidly decreases. The parameter a_l is the gradient of the slope and a_h is the point where this slope would intercept the vertical axis. The model was fitted to the data in Table 8.2 by minimising ϵ, and the parameters that provided the best fit are given in the Table 8.5 and plotted in Fig. 8.4.

The Upper cut-off point is the attack distance at which the salmon no longer takes all the food presented to it. The Lower cut-off indicates the attack distance at which no food is accepted. These cut-off points, along with the fitted parameters

Table 8.5: *Values of a_h and a_l which minimise the mean square error, ϵ, for each experiment with relative particle size and the values of the upper and lower cut-off points.*

Experiment	a_h	a_l	Upper cut-off	Lower cut-off	ϵ
A	2.50	-1	1.5	2.5	0.167
B	7.097	-1.040	5.857	6.818	0.000
C	2.079	-0.196	5.051	10.606	0.138
D	3	-0.32	6.25	9.375	0.044

and ϵ, are shown in Table 8.5.

Choice of Model

The fit to the data of the two parameter model is better than for the one parameter model. However the parameters for the two parameter model do not change in a consistent way so fitting a function to explain how a_h and a_l are related to γ is likely to be more complex than $D(\gamma)$. The function $D(\gamma)$ fits within the natural constraints that are imposed and is behaviourally consistent. It provides a good relationship between maximum attack distance and food particle size so we shall use the one-parameter model to describe $P(r, p, L)$.

8.2.2 Effective Search Volume

As the salmon is foraging, it makes most of its attacks from the centre of its territory and food that is available to the salmon will pass through the territory. We shall define the area through which food passes as a semicircle perpendicular to the flow of water, shown in Fig. 8.5. The radius of this area is $D(\gamma)$ and dependent on the size of the fish and the food particle. Although the whole of this area is accessible to the salmon, food will not be taken from it uniformly because as r increases, $P(r, p, L)$ decreases.

We shall take the effective search area, $A_s(p, L)$ as the area that will provide food for the salmon. To derive $A_s(p, L)$, we shall first determine the effective search area over a small annulus of width $d(rL)$. The area of this annulus can be approximated by $\pi rLd(rL)$ so the effective search area of the annulus is $P(r, p, L)\pi rLd(rL)$, and the total effective area searched $A_s(p, L)$ is the integral over rL in equation (8.5).

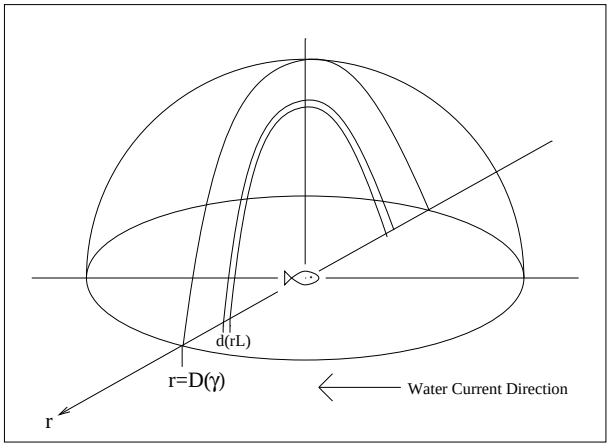

Figure 8.5: *This is the shape in which the salmon will forage. All the food that will be available will pass through the hemisphere perpendicular to the flow of water.*

$$A_s(p, L) = \int_{rL=0}^{\infty} P(r, p, L)\pi rLd(rL), \tag{8.5}$$

$A_s(p, L)$ represents an area from which an amount of food will be gathered of size p. To determine $A_s(p, L)$ over all food particle sizes, we integrate over p to give

$$A_T(L) = \int_{p=\gamma_{min}L}^{\gamma_{max}L} A_s(p, L)dp. \tag{8.6}$$

$A_T(L)$ represents the range over which foraging will occur and is constrained by the food size range and foraging distance and is shown in Fig. 8.6. It has constant value for each size of salmon. We can normalise $A_s(p, L)$ to get $a_n(p, L)$,

$$a_n(p, L) = \frac{A_s(p, L)}{A_T(L)}. \tag{8.7}$$

We can further prove that $A_T(L) = \alpha L^3$ where $\alpha = 5.479$ which is determined from the coefficients of $D(\gamma)$, with the proof of this in Appendix C. By multiplying $A_T(L)$ by the water velocity, we are able to derive the effective search volume of the foraging salmon.

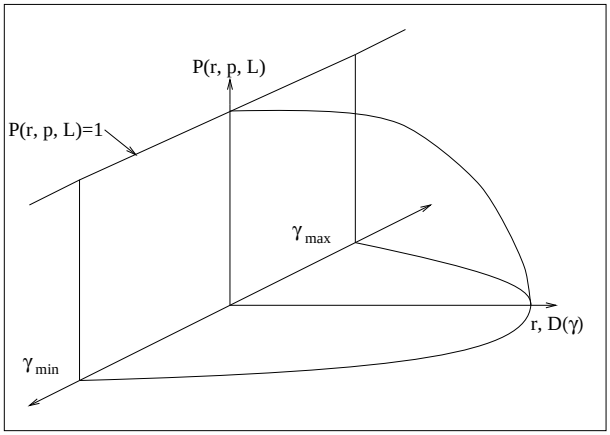

Figure 8.6: *The salmons' effective search area is defined by the food particle size. As L increases the maximum attack distance increases, as well as the absolute particle size range. This will causes the food available to scale with* L^3.

8.2.3 Biomass Available to the Parr

We need to estimate of the size distribution of the invertebrates available to the salmon. We shall use the function $\zeta(p)$ to describe the size-frequency distribution, which will give the number of particles per unit volume over a given diameter range of p_1 to p_2 as $\int_{p=p_1}^{p_2} \zeta(p)dp$. In order to estimate the biomass available between p_1 and p_2 requires the weight-length relationship of the invertebrates, $w(p)$. Therefore the biomass per unit volume, $B(p_1, p_2)$, of food items of size p_1 to p_2 is

$$B(p_1, p_2) = \int_{p=p_1}^{p_2} \zeta(p)w(p)dp. \tag{8.8}$$

8.2.4 Handling Time

The handling time per item for a fish of length L at a temperature T, $\tau(L, T)$, is the time between searching whilst actively foraging. It is assumed to be dependent on temperature, as temperature rises can increase digestion rates as well as foraging activity. Salmonids have been observed to have two bouts of feeding during warm weather because they are able to digest more food. This extra food can then be allocated to growth (Elliott 1973). For salmon, $\tau(L, T)$ will involve orientation towards prey, capture and ingestion, then return to station where it resumes searching. We shall assume that handling time is independent of food

particle size.

The handling time per unit biomass is denoted as $\tau_h(L,T)$. This is a more useful term than $\tau(L,T)$ because we will be working in units of biomass. Given $\tau(L,T)$ and the weight of the food particles that are consumed, we can estimate $\tau_h(L,T)$. We shall assume that a fish of length L will consume particles with an average weight $w(\gamma_{opt}L)$, where

$$\gamma_{opt} = \frac{\gamma_{min} + \gamma_{max}}{2}, \tag{8.9}$$

which enables us to calculate the biomass handling time for when a fish is actively foraging as

$$\tau_h(L,T) = \frac{\tau(L,T)}{w(\gamma_{opt}L)}. \tag{8.10}$$

8.2.5 Full Functional Response

We are now able to construct our functional response. The effective volume searched for food particles of size p is $vA_s(p,L)$ where v is the water velocity. The biomass distribution per unit volume is $w(p)\zeta(p)$, so the total food available to a fish of length L will be the integral from $p = \gamma_{min}L$ to $\gamma_{max}L$. With our term for the handling time we have

$$U = \frac{\int_{p=\gamma_{min}L}^{\gamma_{max}L} vA_s(p,L)w(p)\zeta(p)dp}{1 + \tau_h(L,T)\int_{p=\gamma_{min}L}^{\gamma_{max}L} vA_s(p,L)w(p)\zeta(p)dp} \tag{8.11}$$

It is convenient to take out the factor

$$U_{max}(L,T) \equiv 1/\tau_h(L,T) \tag{8.12}$$

to which the uptake will tend as the food density tends to infinity. We shall further simplify by dividing the top and bottom by $vA_T(L)$. This has the effect of normalising the effective search area and enables us to have one term with v. Thus we can define

$$W_h(v,L,T) \equiv \frac{U_{max}(L,T)}{vA_T(L)} \tag{8.13}$$

and

$$W_{eff}(L) \equiv \int_{p=\gamma_{min}L}^{\gamma_{max}L} a_n(p,L)w(p)\zeta(p)dp. \tag{8.14}$$

$W_{eff}(L)$ is the effective biomass of the food population that is available to a foraging salmon of length L and $W_h(v, L, T)$ is the half saturation food density. Thus we have the form

$$U(v, L, T) = U_{max}(L, T) \left(\frac{W_{eff}(L)}{W_h(v, L, T) + W_{eff}(L)} \right) \tag{8.15}$$

as the full functional response and will be defined as the UFR model.

8.3 Applying the UFR model

We now wish to apply this model to wild Atlantic salmon, which are known to feed less during the winter (Metcalfe and Thorpe 1992). During this period they exhibit low growth rates whilst in the summer growth rates are higher (Skilbrei 1988). In this section, we shall integrate the UFR into the CGM (Broekhuizen et al. 1994) and apply this to electro-fishing data sets from different rivers whilst assuming different distributions for the invertebrate drift.

8.3.1 Electro-Fishing Data Sets

Electro-fishing data sets were found in the literature which were suitable for testing the UFR model. These data sets gives us the opportunity to apply the model over both the periods when the salmon undergo rapid growth prior during the spring and weight loss during the autumn.

Data from Gardiner and Geddes (1980)

Mean weight and length measurements from samples of wild salmon parr were taken in the Shelligan Burn (described in Egglishaw and Shackley (1977)) from April 1973 until April 1975. The data for the 1973 cohort will be denoted as GG73-74 and the data for the 1974 cohort will be denoted GG74-75, and the mean weight measurements will be displayed with their 95% CI. Temperatures for this river over these periods are given by given by Egglishaw and Shackley (1977) and in the form of the mean weekly water temperatures, which would be used in the model.

Data from Randall and Paim (1982)

Two further data sets from populations of wild parr were obtained from two sites in a stream in New Brunswick, denoted RPL1 and RPC2 over the period from summer 1977 until autumn 1978. Randall and Paim (1982) provide maximum and minimum temperature profiles at each of the sites with mean weight and length measurements of salmon from emergence until 16 months later, and the error bars for the mean weights will represent ±1SE. The series of temperature measurements were taken at intermittent times during the year and were converted into weekly average temperatures, using linear interpolation, for the maximum, minimum and median temperatures, which would then be used in the model.

8.3.2 Assumptions about Food Abundance

The feeding regime was hard to estimate due to lack of data. It is known that invertebrate drift varies seasonally. It was therefore assumed that:
i) Biomass particle size distribution function was proportional to temperature with a constant lag of one week. This was to give the biomass time to react to changes in temperature.
ii) The biomass that was available for the fish to consume was dependent on the weight of the salmon. This meant that as the salmon grew in size, the amount of food that was available for them to consume increased. As a fish grows, its range of food particle sizes increase as will its territory size (Grant and Kramer (1990), Keely and Grant (1995)). Therefore, as they grow, more food is accessible to them.

We shall be using a uniform food biomass distribution of value α_{CGM}. The function used to indicate seasonal temperature dependent fluctuation in the food supply will be defined as $\psi(T)$,

$$\psi(T) = \frac{T_{lag}}{T_m} \tag{8.16}$$

where T_{lag} is the temperature from the previous week and T_m is the mean annual temperature.

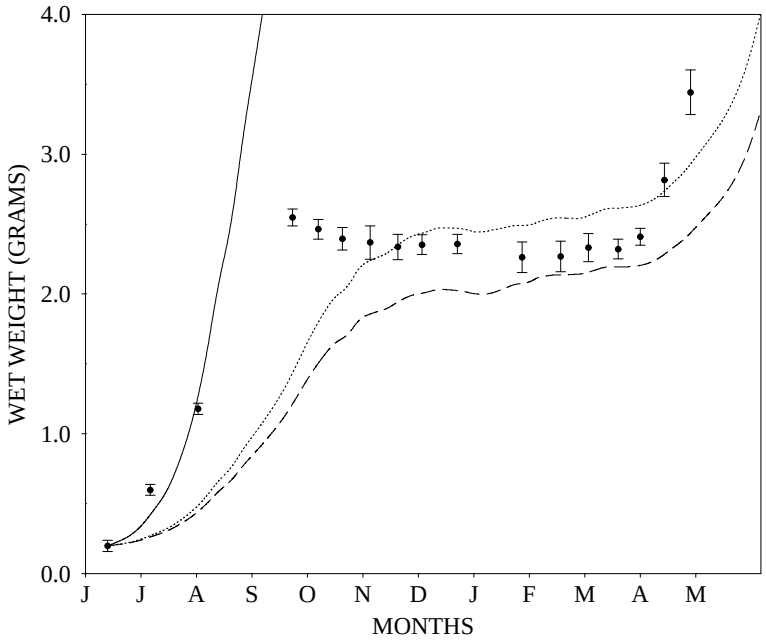

Figure 8.7: *Growth curves at different quantities of food available. The solid line represent U_{max}. The curves are superimposed onto the data set GG73-74.*

This gives our function for the food available as

$$\Phi(R, S, T) = \alpha_{CGM}\psi(T)(R + S). \tag{8.17}$$

As $\Phi(R, S, T)$ has units of $mgC.day^{-1}$, α_{CGM} will have units day^{-1}.

8.3.3 Testing the model

Using these new environmental parameters and the physiological parameters for Atlantic salmon in the CGM, simulated growth trajectories were derived by altering α_{CGM}. In the CGM, the assimilation rate is defined as

$$A = \varepsilon \; min\{\Phi, U_{max}\} \tag{8.18}$$

and will be changed to use the Type II functional response such that $A = \varepsilon \; U$ where U is defined in equation (8.1). We can let U_{max} be the same as the uptake in the CGM so as the food available increases, the uptake will tend to U_{max}.

The data from GG73-74 is shown with the simulated growth curve in Fig. 8.7. The values of α_{CGM} are 0.075 for the dashed line and 0.085 for dotted line. These

values are equivalent to the fish being offered 7.5% and 8.5% carbon body weight of carbon food weight per day although not all is eaten. The value of the solid line is the maximum growth that the model can predict given the current temperature, when the salmon is feeding at U_{max}. The defects with these simulations are that the growth rates are insufficient during the spring and autumn and too high during the winter. These problems will be addressed later but first the full UFR model will be integrated into the CGM model.

8.3.4 Combining the UFR Model with the CGM

We are now in a position to combine our two models by using the ratio of F_H/F, which is the ratio of the food density, F, to the half saturation food density, F_H. It appears in both of the CGM as

$$\frac{F_H}{F} = \frac{U_{max}}{\Phi} \tag{8.19}$$

where

$$\frac{U_{max}}{\Phi} = \frac{U_{max}(T,S)}{\psi(T)(R+S)\alpha_{CGM}} \tag{8.20}$$

and in the UFR as

$$\frac{F_H}{F} = \frac{W_h(v,L,T)}{W_{eff}(L)} \tag{8.21}$$

where

$$\frac{W_h(v,L,T)}{W_{eff}(L)} = \frac{U_{max}(L,T)}{vA_T(L)\int_{p=\gamma_{max}L}^{\gamma_{min}L} a_n(p,L)w(p)\zeta(p)dp} \tag{8.22}$$

We shall assume that the biomass distribution is constant over the range that we will be using which will vary according to the temperature. Therefore we can let $w(p)\zeta(p) = \Gamma_0$, which is constant and can be taken out of the integral of equation (8.22). $a_n(p,L)$ has been normalised so will integrate to unity and $A_T(L) = \alpha L^3$ which can be substituted into equation (8.22). By redefining $\Gamma_0 \alpha v \equiv \alpha_1$ and including the term for the temperature dependence of Γ_0, we can rewrite equation (8.22) as

$$\frac{W_h(v,L,T)}{W_{eff}(L)} = \frac{U_{max}(L,T)}{\psi(T)\alpha_1 L^3}. \tag{8.23}$$

To interchange between equations (8.20) and (8.23) requires a weight-length relationship. The structural carbon weight to length relationship of the form

$$S = a_s L^{b_s}, \tag{8.24}$$

can be converted to

$$L^3 = a_{s_1}^{c_1} S^{c_1}, \tag{8.25}$$

where $c_1 = 3/b_s$ and $a_{s_1} = a_s^c$. This can be substituted into equation (8.23). Thus the food available in the UFR is $\psi(T)\alpha_{UFR}S^{c_1}$, where $\alpha_{UFR} \equiv a_{s_1}\alpha_1$ and is a constant. $\Phi(S,T)$ will replace the term $\Phi(R,S,T)$ in the CGM. The terms for the maximum uptake rates, $U_{max}(L,T)$ and $U_{max}(T,S)$ are interchangeable, therefore the only changes that need to be made to the CGM uptake function are

$$\frac{F_H}{F} = \frac{U_{max}(S,T)}{\psi(T)\alpha_{UFR}S^{c_1}}. \tag{8.26}$$

Estimates of the coefficients for the structural weight-length relationship for the different data sets are given in Appendix D, along with estimates of other factors in the URF model.

This will use the constant biomass spectrum with α_{UFR} having units of mgC^{1-c}. day^{-1}, and varying α_{UFR} changes the quantity of the biomass available passing through the foraging area per unit time. Simulations with this type of uptake are produced in Figs. 8.8 for GG73-74, 8.9 for GG74-75 and 8.10 for RPL1.

The values for U_{max} are the same in both Figs. 8.7 and 8.8. The curves in Fig. 8.8 are generally smoother due to the independence of the uptake on R. Thus uptake will not decrease due to weight loss, only through lack of food, and the two values of α_{UFR} are 0.085 and 0.095. The values of α_{UFR} are much higher for GG74-75 at 0.175 and 0.165 (Fig. 8.9), and for RPL1 in Fig. 8.10, $\alpha_{UFR} = 0.073$. This is for the median weekly average temperature. The maximum and minimum temperature with this value of α_{UFR} are also shown on Fig. 8.10.

From observing the curves, we can see that the uniform food distribution proportional to temperature does not appear to be correct. Although it is likely to be closely correlated to temperature, assuming that it is directly proportional may be to simplistic. We can though see that the data can be fitted by an appropriately varying food availability. This can be applied to all the data points except for those at the very beginning of the data sets. This will be discussed later. We will now attempt to fit the data by using a step function to describe the food distribution.

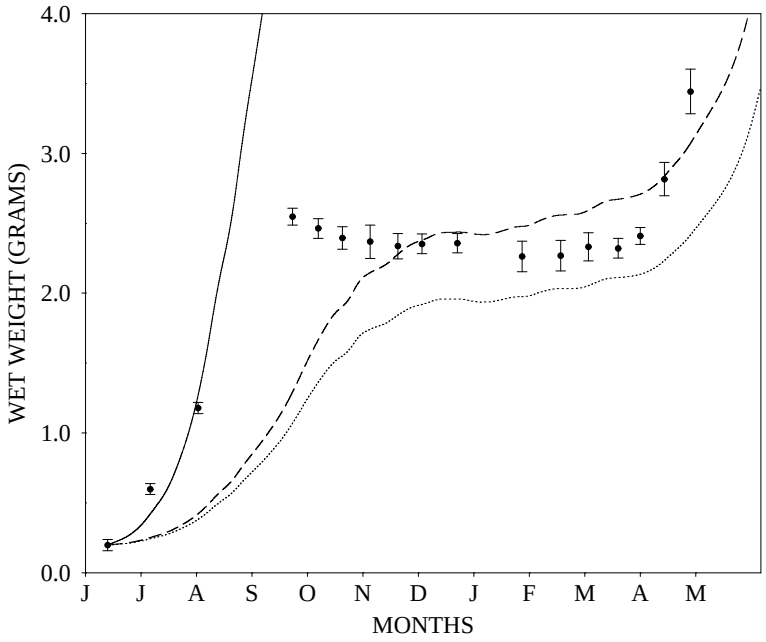

Figure 8.8: *Simulated growth curves using the UFR for different quantities of food available ($\alpha_{UFR} = 0.085$ for the dotted line and $\alpha_{UFR} = 0.095$ for the dashed line). The solid line represent U_{max}. The curves are superimposed onto the data from GG73-74.*

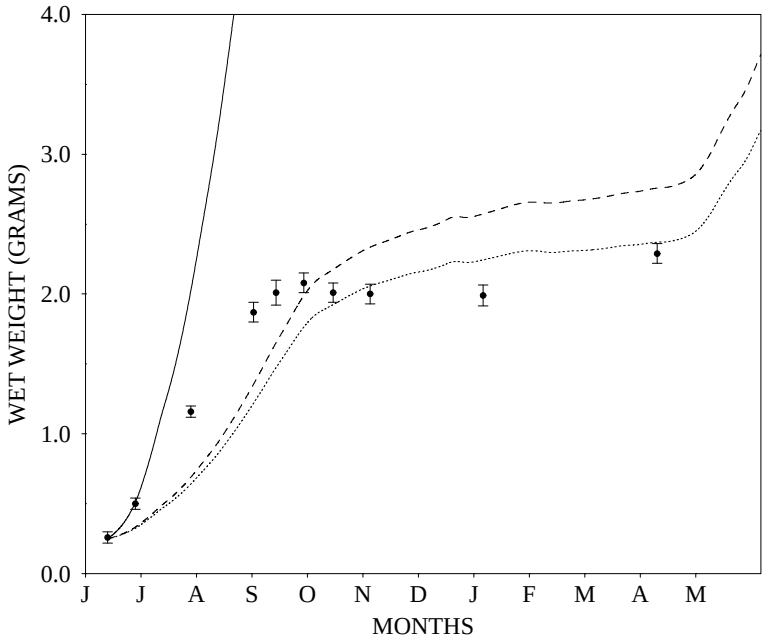

Figure 8.9: *The UFR is fitted to the data from GG74-75 with a different temperatures and value of* α_{UFR}. *The solid line represents* U_{max}, *and the dotted line is the value of* $\alpha_{UFR} = 0.165$ *and the dashed line has the value of* $\alpha_{UFR} = 0.175$.

8.3.5 A Step Function to Describe the Food Available

The biomass spectrum previously used was a uniform distribution proportional to temperature which scaled allometrically with structural weight. This did not produce adequate results so different type of biomass spectrum will be examined. The approach that will be taken in this section is to assume that the biomass distribution of food available to the parr is the step function $\Phi_1(t, S) = \alpha_S(t)S^{c_1}$, which replaces the previous function $\Phi(S, T)$ used in equation (8.26).

The threshold values for the step function changes are dependent on when the rapid bursts of growth begin and end. The values of the step function alternate between a high value close to or at U_{max} and a low value which will maintain the fish at a weight that may decrease, but not allow the fish to starve. The step function was fitted to the data set from GG73-74, RPL1 and RPC2 by hand in Figs. 8.11, 8.12 and 8.13.

Fitting the step function $\alpha_S(t)$ to the data has considerably improved the fit of the model to the data compared to the previous attempts. For GG73-74 (Fig. 8.11),

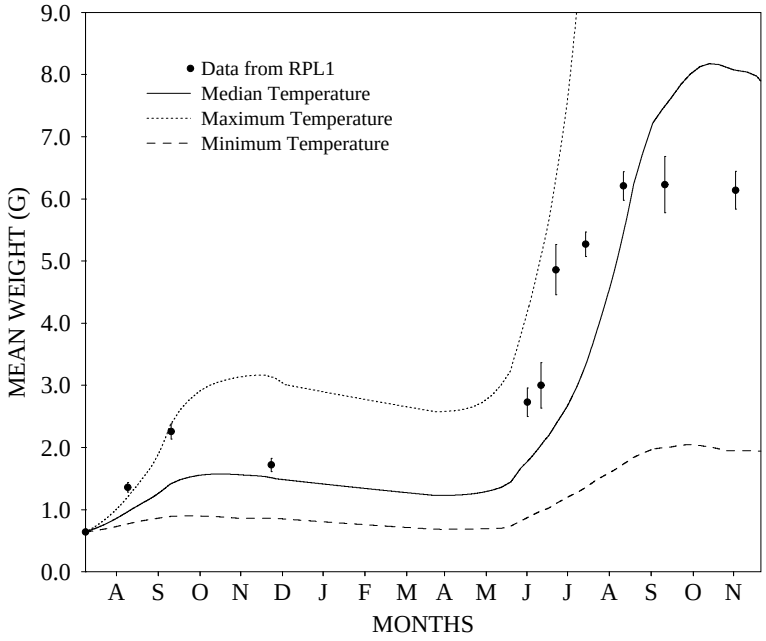

Figure 8.10: *These simulations have the same parameters as the model for GG74-75 except for the temperate and* α_{UFR}. *The three curves are those simulated at the maximum, minimum and medium temperature profiles, with* $\alpha_{UFR} = 0.073$ *used on the data set RPL1.*

the fish are feeding at close to U_{max} ($\alpha_S(t) = 9$) for the first 71 days. After this in mid September $\alpha_S(t) = 0.025$ until the second threshold during the following April when it is increased U_{max}. The temperature at the two thresholds are $13.8°C$ and $2.6°C$.

For RPL1 in Fig. 8.12, $\alpha_S(t) = 0.34$ for the first 60 days until the first threshold occurs during September. During the winter until the end of April $\alpha_S(t) = 0.0005$, after which it increases to 0.4 until during July when $\alpha_S(t)$ is reduced to 0.005. This when the first migrations occurs.

The graph for RPC2 has similar parameters for the threshold of the changes in $\Phi_1(t, S)$. This could be due to the similar average weekly temperature at these times. At the first threshold, the temperature at RPL1 is $15.6°C$ and at RPC2 $14.8°C$. The temperature at the second threshold at RPL1 is $2.4°C$ and at RPC2 $2.0°C$. The third threshold at RPL1 is $17.1°C$ and at RPC2 is $17.3°C$.

The four values of $\alpha_S(t)$ are 0.32, 0.018, 0.48 and 0.005 respectively for RPC2 in Fig. 8.13. The first value is lower than that for RPL1, which is reflected in the lower growth rates and smaller fish. The second value is higher, as the fish actually gain a small increment of weight before the onset of winter. This may be caused by the fish needing to attain a minimum weight in order to survive the winter. The next value of $\alpha_S(t)$ occurs during a rapid period of growth where the relative weight gain for RPC2 is higher than RPL1. The final value of $\alpha_S(t)$ is the same as RPL1. This occurs during the period when the first migrations occur as some of the parr become smolts. This part of the model has not been modified to account for the effects of migration on the mean weights of the resident population. This will cause a reduction in their mean weight of those staying, and a possible growth spurt from those that will attempt to migrate (Metcalfe et al. 1988).

Although the parameters of the step function have been set to give the best fit, it does illustrate that some type of dramatic change is occurring at the threshold points. The temperature at the thresholds after periods of rapid growth during the autumn are very high relative to those before rapid growth in the spring. This may be related to the behaviour of the invertebrate drift at these times of year. After emergence when the fry are small, there will be lots of food items of the appropriate size for them to consume. For those that have survived to the

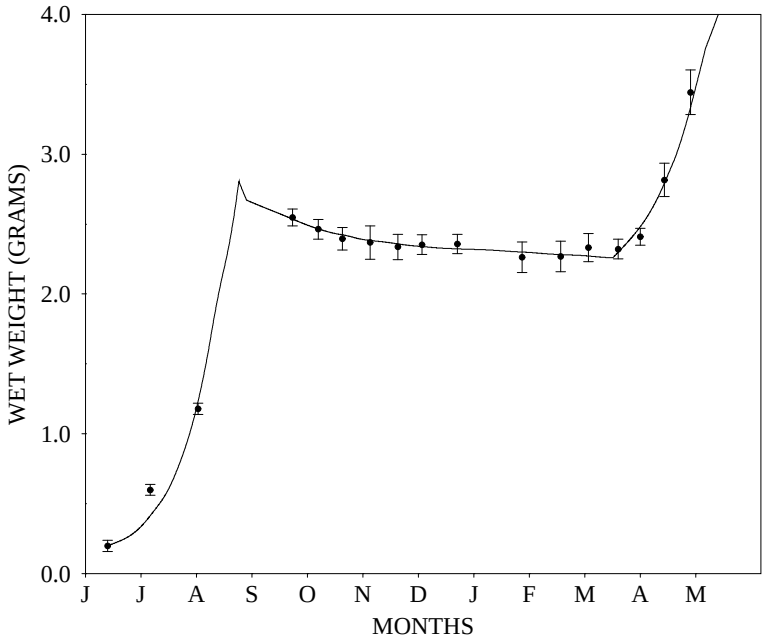

Figure 8.11: *The CGM with a functional response uptake function with the data set GG73-74. A step function is used to describe the biomass available. The solid line is the simulated growth curve.*

first threshold there will be many less of their preferred size. If at this time of year the growing season for the invertebrates is over and they have laid their eggs and are dying out before the winter, then this could be reflected in a change in food abundance for the salmon.

However the biomass spectrum is unlikely to undergo such dramatic changes described by the step function although drift abundance does decrease during the winter. It has been suggested that even if there is sufficient drift abundance for growth during the winter, but the parr will ignore this (Metcalfe et al. 1986). This is due to insufficient temperature occurring to digest the food that is available so rather than risk foraging, the salmon will prefer to become more inactive.

What we are seeing seems more like a behavioural change that the salmon undertake. During the first summer the fry will feed at a very high rate, which has been suggested to happen in order to build up reserves of tissue that will sustain them throughout the winter (Metcalfe et al. (1986), Metcalfe and Thorpe (1992)). The timing of the changes in the step function are likely to be triggered by some environmental cue other than temperature like photo-period or a closer link to

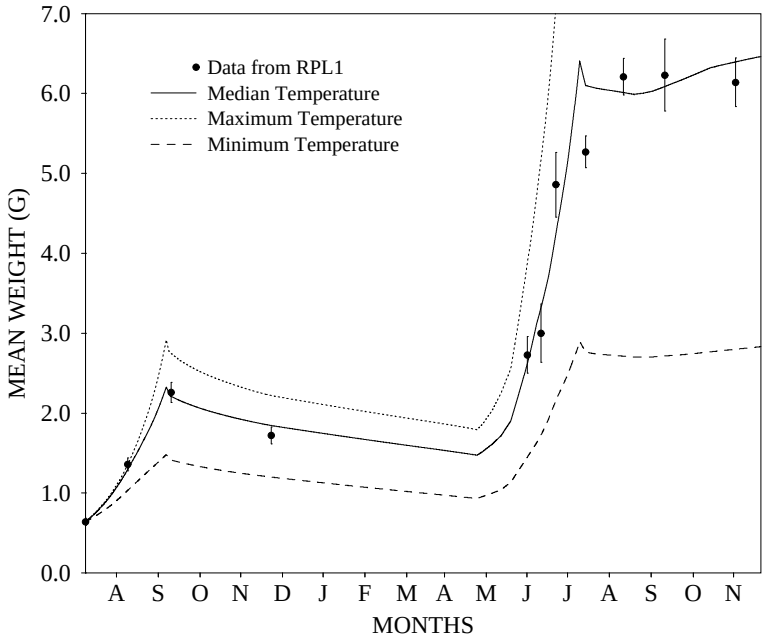

Figure 8.12: *This is the graph with a step function on the data from RPL1. The three curves are for the medium, maximum and minimum average weekly water temperatures.*

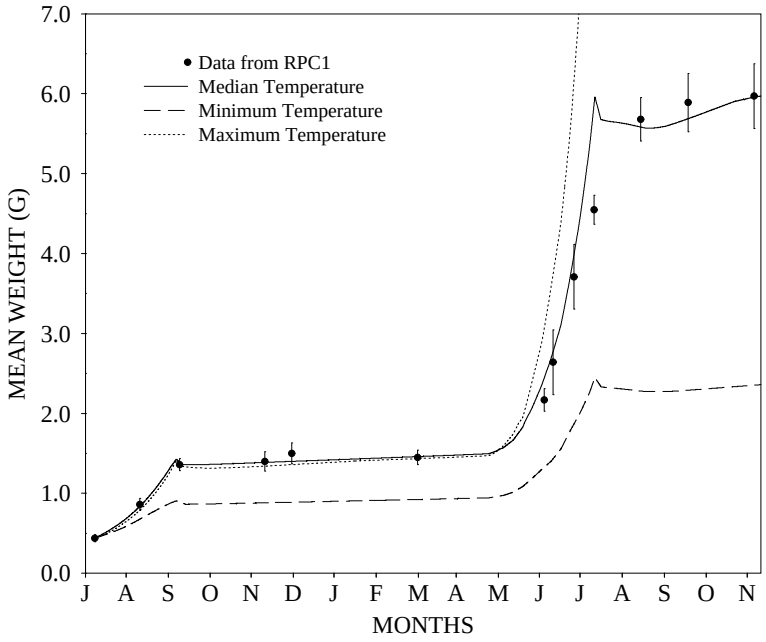

Figure 8.13: *This is the graph with a step function on the data from RPC1. The three curves are for the medium, maximum and minimum average weekly water temperatures.*

food supply. In order to predict such thresholds and biomass density values, we must know their causes.

8.4 Summary and Conclusions

The simulations from the model show that a number of additions and corrections must be made. The first is that even when the salmon is feeding at U_{max}, there are cases where this growth is less than or equal to the observed growth, as in Figs. 8.8 and 8.11. Due to the functional response curve, one would expect the growth at U_{max} to be an overestimate at the very least, which is not the case.

Additional data regarding maximum growth rates of artificially reared parr at different temperatures from Austreng et al. (1987) was examined. These measurements were from fast growing parr from aquaculture and it was found that the growth rates of these fish were less than the apparent growth rates of the salmon parr in the wild.

A possible explanation for this may be that the weight-frequency distribution of the electro-fishing data is positively skewed. If there is size selectivity mortality within the population, such that the survival rates of the smaller par is less than for the larger parr, the larger fish would survive and go on to be measured in the next sample. There is at present no mortality effects in the model.

However, the model may not be appropriate for fish of this size, as at this age the salmon are still fry and the allometric relationships be able to represent the physiological state of the salmon at this stage of their life. The parameters were derived from fish that were at the parr stage of their life.

Beyond the initial data points, we see that the parr undergo weight loss before settling down to fairly steady weight during the winter, which the model was unable to show with the temperature dependent biomass distribution. The data contained the total wet weights of fish, which would include the gut content. What we may see happening is that after emergence, the fry will consume as much food as it can and allocate resources to its digestive system in order to increase its uptake as quickly as possible. The result of this behaviour is that the faster growing fry will gain a size dependent advantage over its conspecifics.

After this period of rapid growth, it may reach a point where it stops feeding and has sufficient quantities of food in its stomach and remobilizable tissue for it to survive the winter on a very low diet. Thus the actual somatic growth of the fish will be different to the measurements that were taken. We must therefore estimate the gut contents in order to find out what proportion of weight that we are predicting is actually assimilated material.

Incorporating parameters that change as the condition of the parr varies may improve the model. Most of the parameters are held constant for all sizes and temperatures. Whilst this may seem unlikely to be true, it is the best that can be achieved with limited data. However when data does exist, these changes can be made. Examples of immediate changes to the model would be a variable to describe the carbon-wet weight ratio, which is much lower for smaller fish due to their higher water content. The water content will change during the winter, increasing as the fish metabolises material (Gardiner and Geddes 1980). Assimilation efficiency will also change depending on the amount of food that is consumed.

Salmon are territorial and once having established a territory they will not normally stray very far from it. Any parr that are unable to hold and defend a territory are likely to die as a result of this. The direct cause of death is likely to be predation but this would be due to a lack of fitness from having no territory. We have seen that as the salmon grow, so will the area in which they forage, as well as the range of food particle size. The number of food particles at their preferred food size is likely to decreases as the salmon grow, so competition for food will become more intense. Food density is a key factor in determining territory size, although the largest is the length of the parr (Keely and Grant 1995).

In the current model all the environmental parameters except for temperature are represented in a single parameter $\alpha_{CGM}, \alpha_{UFR}$ or $\alpha_S(t)$. This is a combination of water velocity, biomass size distribution function. It was held at various constant values during the simulations but will have to be examined in its component parts. Initial estimates of some of these are given in Appendix D.

Prey items in the wild, such as insect larvae have a different shape to the round food pellets used in this experiment, being long and thin. Hatchery reared fish have been observed to prefer food of this shape, (Stradmeyer et al. 1988) and

will also prefer wild prey to pelleted food (Stradmeyer and Thorpe 1987b) though maximum attack distances were not given. This implies that the attack distances derived from the Wankowski data may be under estimates. However these fish were starved prior to the Wankowski experiments, and the attack distances are similar to estimates in the wild.

The use of a step function in the model indicates that there is a behavioural change in the salmon at certain times of year. To examine this behaviour in the wild requires a more detailed account of the drift abundance and what are the triggers for such changes. The UFR model requires a wide range of environmental parameters that are likely to be highly dependent on the microhabitat of the parr. If they can be determined, then the UFR will be able to replace $\phi(t)$. This will allow within year variation in the consumption rates and be related to the size of the parr. The juvenile growth model will then be in a suitable state in order to predict the growth rates of the parr in the wild.

Chapter 9

General Discussion

9.1 Summary of the CGM_e Growth Model

9.1.1 Growth Modelling

The model attempts to determine growth rates of juvenile salmon using a number of functions and driving variables that describe a set of physiological processes within the parr that result in consumption being transferred into somatic weight. Elements of a bioenergetics and a semi-empirical growth model were combined into a hybrid model, which has been called the CGM_e, then further adaptations were introduced to account for the effects of size selective migration from the population. Because of these changes, other characteristics of the population dynamics of each cohort could be deduced.

Increased complexity of the model has lead to improvements in the fit of the model to the data and better descriptions of the overall dynamics of the population. In particular, the addition of an age-dependent variable threshold weight to determine the proportion of the population that would migrate has enabled the model to predict the mean lengths and its variation for the migrants. This is in addition to the mean weights and the variation for the resident parr from each age-class within each cohort. Such improvements can not carry on indefinitely, and further developments to the model have been halted due to the quantity and quality of the data that is available.

Greater resolution and scope of data and will indicate structural aspects of the

model that need to be addressed and whether they are functions describing the physiological or social behaviour of the parr. Developments can then be made to account for the inaccuracies that exist within the model and to derive further insights into the population. A description of the results from the CGM_e will be presented in this chapter along an interpretation of these results. Deductions made about the social structure and population dynamics of the juvenile salmon, with their implications, will also be presented.

9.1.2 Functions within the Model

The quantity of carbon consumed by an individual can be divided into a number of components, as described by equation (3.3) in a typical bioenergetics model. Broekhuizen et al (1994) used this basic format for the CGM with the two important additions of dividing the weight of the parr into structural and reserve tissue, and including the starvation response functions. This allowed to model to describe the observed behaviour of tank reared juvenile salmonids. Similar behaviour observed in wild salmon parr indicated that the model could be applied to salmon parr but required reparameterization.

The E&H model required a mechanism to prevent over winter weight loss although it fitted experimental data very well. This model provided the instantaneous growth rate given temperature and fish weight, and was parameterised using short term experimental data from fish that were fed to satiation and was collected over the summer and autumn.

The CGM and E&H model were combined to form the CGM_e, which was able to fit the data from Elliott and Hurley (1997), and additional parameters were found using data from the literature. It was assumed that the parr, which were fed to satiation, were growing at their maximum rate and that this rate would not be attained in the wild. The function $\phi(t)$ was used to indicate the difference between the growth rates of wild parr and those fed at satiation, and was assumed to be constant within years but variable between years.

The model had been fitted to the mean weights of the population whereas it was designed to predict the growth trajectories of individuals. The variation in the life history of the juveniles is too great to assume that they follow a single mean

trajectory so an age and size dependent smolting threshold was introduced. This considerably improved the fit of the model to the data as the whole cohort was now being modelled. Given that the growth trajectories for all the individuals were now being simulated, predictions of the behaviour of different groups within each cohort (e.g. the spring smolts) could be made.

The final important addition was the extension of $\phi(t)$ into the UFR foraging model, which allowed uptake to be dependent on foraging behaviour and environmental variables. It could not be fully implemented into the model as it was only partially parameterised but it does provide a mechanism to account for variable growth rates within years, that could not be accounted for by temperature alone.

9.1.3 Fitting the Model to the Data

The downhill simplex method of optimisation was used to fit the model to the data. This method is most effective when the error surface is sufficiently smooth to allow convergence to occur. If it is not then variation in the initial conditions and the size of the simplex may lead to the DSO being unable to find the global minimum. When the DSO was used to fit the CGM_e to the mean weights of the long term data set, we were unable to determine if the global minimum had been found. However, errors associated with the parameter estimates were calculated and the parameters from the different initial conditions did not vary considerably given the variation in and accuracy of the data.

Fitting to individual growth trajectories within years was straightforward with the DSO procedure appearing to converge to unique solutions each time. The DSO was wholly appropriate and the fit of the model was able to describe insufficiencies in the model.

Fitting the model to the different sections of the stream used many less fitted parameters and the variation in the derived $\phi(t)$ was smaller than previously. They were also able to show that there were differences between the sections and that there is sufficient accuracy in the model to distinguish between the quality of different habitat types.

However, as the complexity of the model increases, with more parameters being

used, there is a danger that the results that are being found will continue to become less reliable. A more sophisticate and accurate optimisation method will need to be devised in order to progress in to the development of the model.

9.1.4 Interpreting the Results from the Model

The most important feature of the model is the output which is in the form of $\phi(t)$. This gives a description of the state of the stream and the environment in which the parr is growing. A variety of methods of using $\phi(t)$ have been used throughout the thesis and are summarised below.

The model has shown that different individuals had their own unique value of ϕ_i. These values were significantly correlated with the size of the parr, although it was shown that this might have been an artefact of the sampling procedure. However, given an adjustment in the sampling procedure, the difference in the growth rates of different sized parr can be found and used to calculate proportions of the population that are migrating.

This variation in ϕ_i means that there is no single value which can be applied to all individuals at any site within the stream. It implies that the microhabitat of the parr is an important factor in their growth or that the individuals may be predisposed to have different growth rates. Increased resolution of data of all the fish in each cohort is required, rather than a size selective subset, to better understand the growth of individuals in the wild.

The annual values of ϕ_y were derived from fitting the model to the mean weights. These may be regarded as an average index of the growth of parr in that part of the stream once the effects of temperature have been removed. The values of ϕ_y were seen to increase with altitude. This is to be expected as the quality of habitat would be expected to improve in the higher parts of the burn.

In order for the model to predict within year growth, $\phi(t)$ must be variable within years. This has been seen when using data for parr, both individuals and means, to predict growth within years. The prediction of both the individuals and population mean weights within years was deficient in the spring, which indicates the necessity of varying $\phi(t)$ within years. This was further indicated as the values of $\phi(t)$ are between 0.95 and 1.3 in the final versions of the model.

If U_{max} is seasonal (as thought by Metcalfe et al (1990)) the E&H model may only be applicable for the parameterisation period. By using the parameterised UFR model, variation of U_{max} can be introduced into the CGM_e.

Variation of the input parameters was introduced in the sensitivity analysis and the values for $\phi(t)$ remained stable. A suite of models have been developed which can be applied to different data sets and make prediction relating to different aspects of the population dynamics. The next section will detail characteristics of the population that can be deduced using the model.

9.2 Population Structure

9.2.1 Social Structure

Adult salmon were prevented from spawning in the Girnock Burn in 1978, and consequently, no cohort was born in 1979. This represented a large change in the social structure of the stream, and was done in order to examine how these changes to the population would affect other cohorts.

In particular, the effect of the changes to the density of the parr on their growth rates needed to be examined. This information could then be used to estimate optimal stocking strategies. This could only be done once the effects of temperature had been removed from growth, which was one of the objectives of the model. An estimate of the growth potential, $\phi(t)$ of the resident parr could then be made for the year, and this would be examined to see how it changed when the 1979 cohort was absent.

Correlation between ϕ_y and density or biomass are weak and do not offer conclusive proof of any relationship. Comparisons over the period of low spawning do not show a strong relationship between ϕ_y and estimated ova deposition (EOD), which suggests that the social effects on the growth of the resident parr are small.

However, we have seen that ova deposition is negatively correlated with the lengths of the migrants, which suggests that density does depress growth. The density in the social environment does effect the growth of the parr but this is not apparent in the growth rates of the resident parr. It is apparent in the growth and behaviour of the fish that are migrating from the population.

9.2.2 Aspects of Migration

The model was adapted to predict several aspects of the population, in particular the lengths of the smolts. It was unable to make accurate predictions, with the greatest deviations from the mean error occurring during periods proceeding low EOD (see Figs. 1.1 and 6.15). During these periods the lengths were under predicted, which meant that ϕ_y was too low.

What may be happening is that an excess of good conditions is reflected by an increase in the mean lengths of the migrants rather than the residents. Larger parr will migrate whilst those that remain are in a relatively similar size to those who will remain during years when densities are higher. Therefore, the characteristics of the population that stays are more likely to be dictated by the characteristics of the stream rather than the social effects.

Alternatively, this homogeneity of the residents may be a reflection of the sampling procedure that may not have given an accurate description of the size composition of the stream. The larger parr may not have been sampled within the habitats on which the model is based (types T_1 and T_{1A}) or the larger parr may have a different habitat preference (see Table 2.4).

The smolting thresholds decrease as altitude increases for both the two and three year old smolts. This may be a result of the parr attaining a suitable state in which to smolt, but carrying on growing until the time is right i.e. parr will only smolt at certain times of the year, irrespective of size.

The fit of the model to the resident parr shows that the smolt threshold weights increase with age. This implies that there may be a trade-off between growth rate and age of smolting. This may be of the form of the increased chance of survival given a larger size against the risk of mortality when spending an extra year in freshwater.

9.2.3 Precocious Parr

The behaviour of the precocious parr (PP) provides an important component to the dynamics of the population. Little is known of their movement within the stream except that during autumn they will move in search of spawning females.

In the Girnock, when low numbers of adult females were spawning above the trap, the proportions of PP migrating compared to the whole population of migrants increases. This is often followed in the spring by relatively low mean lengths of the spring migrants.

The growth model groups the PP and the non-precocious parr (NPP) together during the autumn migration as their lengths are indistinguishable from each other. The same cannot be said of the weights, as it is likely that they will have a different weight-length relationship as they allocate resources towards reproduction.

The criterion that enables NPP to become PP is not known and the model has no specific mechanism to predict the dynamics of the PP and some PP may never migrate. To predict when they will become precocious and the effect that this will have on their growth and the timing of their migration requires more detailed data regarding the condition of the PP, both during and before early maturation.

9.3 Adaptation and Improvements to the Model

9.3.1 Spring Growth

The model is unable to produce acceptable predictions for the change in weight observed during spring, in the 1+ and 2+ parr. This indicated that although the parr may have been growing at their maximum rate when the model was parameterised, this was not necessarily the case throughout the year. The annual values of ϕ_y are not an indication of the difference between optimal and wild growth, but an index of average annual growth relative to the maximum growth rate attained over the period of the experiments.

These under predictions may be due to a behavioural or physiological mechanism that increases growth rates, such as a change in the appetite of the parr. The starvation response functions included in the model are insufficient to account the relatively large increase in the growth rate. In addition, the observed growth spurt occurs when the water temperature is low and the model predicts that the parr are actually losing weight. Accounting for these changes is likely to require a structural change in the main part of the CGM_e or the UFR model. This would

require additional data and knowledge of the physiological state of the parr, such as why the parr increases its growth so drastically, and the environmental and physical cues that trigger this response.

One variable that increases during spring will be the gut contents of the parr. After the winter during which feeding and digestion rates are low, the parr will have a lower gut content than at any other time of the year. As the water warms and their consumption rate increases, a larger proportion of observed weight will be due to gut contents. Accurate data regarding seasonal changes in the gut contents will greatly enhance the predictions and little data exist for wild salmon.

9.3.2 Greater Environment Dependence

Many environmental variables that have not been included in the model and the introduction of additional variables may unnecessarily complicate the model. There are some important changes that can be made which will improve the predictions of the CGM_e without a large addition to the complexity of the model.

Temperature is the most important driving variable in the model and is currently calculated using linear interpolation between the average monthly temperatures. This temperature resolution may be too low, particularly during the spring and autumn periods when the parr are their most sensitive to temperature changes. This may partially explain why spring growth is under predicted, as a few low temperatures may give an unrepresentative view of the actual changes in temperature, and hence predicted growth, as experienced by the parr.

Parr from different altitudes will have different growth rates, which is likely to be due to water temperature being dependent on altitude. As it is impractical to measure water temperature at all latitudes, local variations can be calculated with an altitude-temperature relationship. The model can then calculate the growth rates in different parts of the stream, and if the densities within the stream are known, then predictions of the weight-frequency distribution of the stream can be made.

The UFR model, which aims to replace $\phi(t)$, is a measure of the consumption rate of the parr. It requires a large amount of parameterisation, as sufficient data does not exist at present for it to be parameterised, and those that it lacks are

discussed below.

In order for the UFR model to be of any practical use, the main factor that is required is the annual size-frequency distribution of the invertebrate drift within the stream. Ideally, this would be specific to the microhabitat of the parr, and form of a separate model of invertebrate drift abundance. Although much literature does exist regarding the composition and size of benthic invertebrates, this will be different from the composition in the water column that is available to the salmon. However, if a relationship could be derived between the two, then the required predictions could be made. This would need new data measuring the drift available to the salmon in both the water column and the substrate.

The flow rates will determine how much food passes through the salmons territory, and we have so far assumed the food available is proportional to water velocity. The water velocity is not uniform with depth, with water current decreasing with distance from the surface. Its importance will depend upon the magnitude of the differences that exist.

Flow rates also affect the behaviour of the invertebrates in the stream, and increased flow rates will not necessarily result in increased food availability. Therefore, the quantity of invertebrate drift available to the salmon will be dependent on the flow rates and must be included in any predictions.

The UFR model estimates the consumption rate of the parr. In the simulations produced in chapter 8, a large number of unknown parameters were condensed into a single term which was then derived by fitting the model to the data. One of these terms was the assimilation efficiency. This term may be defined as the costs involved in the capture and digestion of the food, which has yet to be estimated. This may depend on the water temperature and the size of the food particle captured by the parr but would be best derived from experimentation.

More details of the environment of the parr will allow more detail into the model and allow it to be applied more widely. Parr have different preferences to different habitat types, and migrate between habitat types at different ages as immature juveniles. Water velocity and substrate are important in habitat selection and therefore the microhabitat available and its quantity may be an important factor, particularly in regards to the quantity and quality of food passing through these habitats.

9.3.3 Social vs. Physical Effects on Growth

The model has so far been based on driving variables based with the physical environment of the parr. There are large affects on growth, which are due to the social environment of the fish, which can be described as density dependent effects (Huntingford et al. (1998), Steingrimsson and Grant (1999)). Social effects may work on different scales, from density dependent mortality associated with dispersion from the redd and competition for territory to the movements of precocious parr and the autumn and spring migrations.

Ova deposition has been seen to affect the size of the smolts produced in the stream yet there are no mechanisms with the model to account for these affects. It is not known if size selective mortality occurs, although the larger and more dominant juveniles will secure the best territories, and force other parr to adopt an alternative growth strategy that may extend its time to migration. If size selective mortality is occurring, then fitting the model to the mean weights of each age-class is an inappropriate method of predicting the weight change of the resident parr.

A limiting factor on the capacity of a stream is the quantity and quality of available habitat, and its accessibility to the parr during different times of its juvenile life. A method of including limited territory into the model would be to produce a map of the stream based on the potential for growth in different sites and the probability of them being occupied. This would allow the dispersion from the redd to be estimated, and as the parr increased in size, this map would change as more of the stream became accessible and as the habitat requirements of the parr changes. Changes would also occur as a result of emigration from the resident population. The growth rates of the parr in different parts of the stream could then be calculated to determine the overall weight-frequency distribution of the parr in that part of the stream as well a estimating mortality rates.

In order to do this would require a detailed map of the habitat within the stream as well as knowledge of which were preferred by the parr. In order to parameterise it would require data regarding the densities of the parr in different habitat types.

When predicting the size of the migrants, it was assumed that on 1 April all the resident parr had a probability of smolting that increased with size. An additional

assumption was that those parr that migrated the previous autumn would have been part of the population that migrated in spring. It therefore assumed that the growth rates of the spring and autumn migrants were the same. It is not known if this is the case, however, when the autumn migrants are large, the following group of spring migrants are relatively small (see Figs. 2.9 and 2.10). The relationship between the autumn and spring migrants is likely to be a complex one and further electro-fishing data from individual marked parr is required to determine whether the spring and autumn migrants should be predicted separately.

9.3.4 Extrapolation to the Growth of Fry

The parameters for the model have been derived mainly from data regarding the parr and the growth trajectories produced by the model have attempted to predict growth from birth until smolting. This has meant that there has been a degree of extrapolation and the assumption the parameters will scale with the size of the parr. The salmon are isomorphic during the parr stage of their lives but this cannot be said of either the smolt stage or the fry stage.

Predictions regarding smolts have been made using the length rather than weight so any changes in shape (i.e. the condition of the fish) will not decrease the length. However the weights of the fry are predicted and the parameters may not be applicable at this stage of the juveniles life.

The model was used to predict the mean weights of populations in the Chapter 8 using the CGM. It was seen that even when the uptake rate was set at U_{max}, the model under predicted the growth rates when the salmon were approximately three to five months old. Two reason for these discrepancies are either the allometric relationships are invalid for the fry or there are high rates of size selective mortality within the population during this period.

Further data would be required to test if the same relationships will hold for the fry and the parr, and size selective mortality within the population will be discussed in the next subsection.

9.3.5 Modelling Mortality Rates

An important aspect of the population dynamics that has yet to be examined is the mortality rates within the cohorts. The model is capable of predicting the proportions of parr migrating at each age-class from the whole cohort, but mortality rates must be known if these predictions are to be of any use in predicting number of parr smolting.

It has been implicitly assumed that mortality rates are not size selective and that the mean weight of the 0+ parr will transform to the mean weight of the 1+ given the assumptions in the model. In the event of size selective mortality rates, this will not be the case. If the mortality rates are higher for the smaller fish, then the mean weights will be higher than expected. This has been observed to be the case when predicting the mean weights of the 0+ parr.

It is widely accepted that there is high density dependent mortality during and after dispersion from the redd. For the model to be able to attempt to predict numbers of fish migrating each year requires the addition of a mortality model. Whether this should be size selective will depend on whether data can be gathered to show this.

9.3.6 Modelling The Condition of the Parr

During the year, the condition of the juveniles change, such as during the winter when the consumption rate decreases and they experience weight loss. Also, in the spring, when they begin to feed, they will experience an apparent weight gain due to increased gut contents.

The majority of the data that has been used has been in the form of lengths converted into weights using a weight-length relationship. This relationship will change with time, and would be necessary to predict the fish lengths at any time during the year. This would enable the model to be fitted to the autumn migrants as well as the spring smolts.

Considering the condition of the parr at different times of the year may offer insights into whether the males will become PP (as this results in a change in condition as resources are diverted to the reproductive organs). This may also

indicate whether a parr will migrate, as condition changes during smolting.

9.4 Using the Model as a Management Tool

The ultimate aim of this thesis was too develop a model that could be developed into a tool to aid fisheries management and enhance salmon production. Below are a series of methods in which the model can be used to assess the suitability of streams and optimise production by examining the local populations and environment.

9.4.1 Habitat Assessment

The environment in which a salmon grows has a very large effect on the growth rate of the parr. The physical environment may be defined by the substrate type and the current or by the altitude. Either way, growth will be affected, and during the juvenile stage of the salmons life, different habitats may be preferable to others.

The model was fitted to data from different altitudes and it was found that $\phi(t)$ increased with altitude which was done by using different temperatures. The values of $\phi(t)$ can be used as a measure of the quality of the river, and therefore the likely changes in the sizes of the salmon given changes in temperature can be assessed. The implications for this is that in the event of global warming and changes in the long term mean monthly temperatures, as have been observed in the Girnock, changes in the expected sizes of the fish, which will determine migration patterns, can be estimated.

The model can be fitted to data from different rivers and the values of $\phi(t)$ used as a relative index of habitat quality. When fitted to different altitudes, it was found that $\phi(t)$ increased with altitude and the predictions became less accurate as altitude decreased. These values indicated that although the parr at higher altitudes grew slower and migrated at a smaller weight, this was due to temperature and the quality of habitat was better than down stream. Comparing $\phi(t)$ between rivers will indicate where that may be spare capacity (by the high values of $\phi(t)$) in the river and the more suitable environment in which to stock

fish.

The model can be applied to rivers where there are no fish to determine suitability. An assumed minimum smolt length will need to be determined, such that if the parr do not reach that weight in a certain time then the river is not viable. The model can then be fitted to these weights (given that temperature is known) and if $\phi(t)$ is too low, then turnover is likely to be low. High values will lead to fish migrating sooner and may mean that the river is more suitable to be stocked.

9.4.2 Optimising Production

The stocking of rivers with artificially reared stock is an important aspect of fisheries management and one that has received much attention (Verspoor and deLeaniz (1997), Largiader et al. (1996), Philippart et al. (1994)). There is much uncertainty as to knowing what the optimal stocking strategy should be to maximise the number of smolts given the costs that are involved. It is not accepted that stocking beyond the rivers estimated carrying capacity will maximise production as high densities may reduce growth rates so severely as to make the stocking procedure uneconomic.

The growth model has shown that variation in ova deposition will have little if no effect on the resident population, but will produce larger smolts. This means that although the population as a whole will grow faster, once the migrants have left, the remaining population will be of a similar size to those that would remain in years when ova deposition is higher.

The conclusions that can be drawn from this are that the average age of the migrants will be lower when ova deposition is lower. However, this relationship cannot be quantified, as accurate numbers of emigrants from the population in the Girnock is unknown. The proportion of the population migrating at each age-class cannot be estimated until the estimated mortality rates are derived. This would require reliable estimates of the numbers of autumn as well as spring migrants from the burn. Without this, the model can not determine how increasing ova deposition changes the number of smolts.

The model does make a considerable contribution to understanding the problem of optimal stocking densities. It has shown that once the effects of temperature

have been removed, the mean weights of the parr that stay in the burn remains steady in spite of large fluctuation in the ova deposition. The effect of density on the growth rates of the parr is only seen in the changes in the lengths of the smolts. During periods when ova deposition is low, followed by years when it is high, the extra capacity may be accounted for by the parr from other cohorts. This effectively means that because of the overlapping age-classes, cohort which are more populous are able to take advantage of the spaces left by the less populous cohorts. The result of which means that the benefits to the resident population born in a year of low ova deposition are small.

It is possible that the benefits of a year when ova deposition is low is gained during the period between the summer surveys (i.e. autumn and spring) which allow a proportion of the population to migrate earlier as relatively large smolts. This aspect of the growth has not been included in the model (and the model has been seen to predict smolt lengths badly) and is a period for which we have little data. However this analysis appear to indicate that the capacity of the river has yet to be exceeded, and for capacity to be exceeded may require several years of consistently high levels of ova deposition.

9.4.3 DeeCAMP GIS

One method in which the environment of the river Dee catchment is studied and managed is through the use of the Dee CAtchment Management Planning Geographical Information System (DeeCAMP GIS). This is funded by a consortium of interested parties, such as the Grampian Regional Council Water Services, Scottish Natural Heritage, the Scottish Environmental Protection Agency and the Dee Salmon Fishing Improvement Association and is based at the Institute of Terrestrial Ecology (ITE) Banchory. One of the aims of DeeCAMP was to identify areas of the river which were accessible to salmon and suitable for rearing viable salmon populations.

DeeCAMP GIS contains many environmental variables which can be used to assess the suitability of parts of the stream for salmon rearing. Gradients of rivers can be calculated to determine which parts of the streams are accessible to the salmon. The inaccessible areas could be made accessible through the introduction of fish ladders or the removal of impassable barriers. This would

only be done if it were thought that a viable population could exist above the barrier.

This requires a method of assessing whether the local environment was suitable. One such method could be by stocking the parts of the burn with trial populations and by conducting surveys of the stream. However, due to the large number of potential sites, these methods are prohibitively expensive, and a method is required to reduce the number of potential sites.

Given the data which are contained within the DeeCAMP GIS, the model can be adapted to be used as a tool to predict growth rates and estimate emigration times at the potential sites. This would enable further investigations to be conducted and allow stocking policies to be evaluated. This would then lead to the introduction, or reintroduction, of salmon to more parts of the river, and hence increase the overall production of the Dee.

9.5 Conclusions

This thesis has seen the development of an individual based model to predict the growth rates of salmon parr. The model has been applied to a wide range of data in a number of different forms and scenarios, each of which has lead to a greater understanding of the model and improvements to be made. It has then been extended to predict wider aspects of the population. Improvements to the model and applications have been given in the final chapter that lead us towards achieving the objective of enhancing salmon production in the river Dee.

The main deterrent to further progress with the thesis has been the lack of data on an individual level, both concerning the growth rates of individuals and measurements of the food that they consume. This situation has been realised, and with the beginning of the data set on individuals in Chapter 5 and plans to monitor invertebrates within the stream, promises to explain much of the life of the individuals.

The examination of the selection of, and competition for, microhabitat by the juveniles is also an area of great importance as it can have great implications for the parrs future life history. Prime locations will lead to increased growth rates

and earlier opportunities to smolt or become precocious parr. Therefore, events from dispersion of the redd will have a great bearing on the fate of the parr.

The future of salmon research will lie in the small scale examination of their life, as it is only by piecing together aspects from the individuals will the behaviour of the population be realised. The fascinating complexity and variety which the salmon exhibit, and the complexity of their population dynamics will ensure that they will remain the subject of much interest and research across different fields of science for many years to come.

Bibliography

Allen, K. (1940). Studies on the biology of the early stages of the salmon (*Salmo salar*). 1. Growth in the River Eden. *J. Anim. Ecol.* **9**, 1–23.

Allen, K. (1941a). Studies on the biology of the early stages of the salmon (*Salmo salar*). 2. Feeding Habits. *J. Anim. Ecol.* **10**, 47–76.

Allen, K. (1941b). Studies on the biology of the early stages of the salmon (*Salmo salar*). 3. Growth in the Thurso river system, Caithness. *J. Anim. Ecol.* **10**, 273–295.

Allen, K. (1969). *Salmon and trout in streams*, Chapter Limitations on the production in salmonid populations in streams., pp. 3–18. University of British Columbia, Vancouver, BC.

Anon. (1997). *Report of the Scottish salmon strategy task force*. The Scottish Office.

Armstrong, J. and C. West (1994). Relative ventricular weight of wild Atlantic salmon parr in relation to sex, gonad maturation and migratory activity. *J. Fish. Biol.* **44**(3), 453–457.

Ashley-Cooper, J. (1987). *The great salmon rivers of Scotland*. H.F. & G. Witherby Ltd.

Austreng, E., T. Storebakken, and T. Asgard (1987). Growth rate estimates for cultured Atlantic salmon and rainbow trout. *Aquaculture* **60**, 157–160.

Bagliniere, J. and G. Maisse (1985). precocious maturation and smoltification in wild Atlantic salmon, in the Armorican Massif, France. *Aquaculture* **45**, 249–263.

Baker, T., R. Lafferty, and T. Quinn (1991). A General Growth-Model from Mark-Recapture Data. *Fisheries Research* **11**(3-4), 257–281.

Berg, O. and G. Bremset (1998). Seasonal changes in the body composition of young Atlantic salmon and brown trout. *J. Fish Biol.* **52**, 1272–1288.

Berglund, I., M. Schmitz, and H. Lundqvist (1992). Seawater adaptability of Baltic salmon (*Salmon salar*): a bimodal smoltification pattern in previously mature males. *Can. J. Fish. Aquat. Sci.* **49**, 1097–106.

Bertalanffy, L. V. (1957). Quantitative Laws in Metabolism and Growth. *Q. Rev. Biol.* **32**, 217–31.

Blackwell, B., W. Krohn, N. Dube, and A. Godin (1997). Spring prey use by Double-crested Cormorants on the Penobscot River, Maine, USA. *Colonial Waterbirds* **20**(1), 77–86.

Brandt, S. and J. Kirsch (1993). Spatially Explicit Models of Striped Bass Growth Potential in Chesapeake Bay. *Trans. Am. Fish. Soc.* **122**(5), 845–869.

Brannas, E. (1986). Influence of photoperiod and temperature on hatching and emergence of Baltic salmon (*Salmo salar*L.). *Can. J. Zool.* **65**, 1503–1508.

Brannas, E. (1988). Emergence of Baltic salmon, *Salmo salar*L., in relation to temperature: a laboratory study. *J. Fish Biol.* **33**, 589–600.

Breck, J. (1993). Hurry up and wait - growth of young bluegills in pond and in simulations with an individual-based model. *Trans. Am. Fish. Soc.* **122**(3), 467–480.

Brodeur, R., R. Francis, and W. G. Pearcy (1992). Food-Consumption of Juvenile Coho (*Oncorhynchus-kisutch*) and Chinook Salmon (*O-tshawytscha*) on the continental-shelf off Washington and Oregon. *Can. J. Fish. Aquat. Sci.* **49**, 1670–1685.

Broekhuizen, N., W. Gurney, A. Jones, and A. Bryant (1994). Modelling Compensatory Growth. *Functional Ecology* **8**, 770–782.

Buck, R. and A. Youngson (1981). The downstream migration of precociously mature Atlantic salmon, *Salmo salar* L, parr in autumn - its relation to the spawning migration of mature adult fish. *J. Fish. Biol.* **20**, 279–288.

Buck, R. and A. Youngson (1982). The downstream migration of precociously mature Atlantic salmon, *Salmo salar* L., parr in autumn; its relation to the spawning migration of mature adult fish. *J. Fish Biol.* **20**, 279–288.

Buck, R. J. G. and D. W. Hay (1984). The relationship between stock size and progeny of Atlantic salmon, *Salmo salar* L., in a Scottish stream. *J. Fish Biol.* **23**, 1–11.

Buckfield, F. (1880). *Natural history of British Fishes*. Unwin Bros. S.P.C.K.

Bult, T., S. Riley, R. Haedrich, R. Gibson, and J. Heggenes (1999). Density-dependent habitat selection by juvenile Atlantic salmon (Salmo salar) in experimental riverine habitats. *Can. J. Fish. Aquat. Sci.* **56**(7), 1298–1306.

Calderwood, W. (1906). Autumn migration of salmon smolts in Scotland. *Rep. Fish. Bd. Scot., 1905* **II**, 70–74.

Carlin, B. (1969). The migration of salmon. *Swedish Salmon Research Institute* **4**, 14–21.

Carss, D., H. Kruuk, and J. Conroy (1990). Predation on Atlantic salmon, *Salmo salar*, by otters, *lutra lutra* (L), within the River Dee system, Aberdeenshire, Scotland. *J. Fish. Biol.* **37**(6), 935–944.

Carter, C. G., D. F. Houlihan, and I. D. McCarthy (1992). Feed Utilisation Efficiencies of Atlantic Salmon (*Salmo Salar* L.) Parr: Effect of a Single Supplementary Enzyme. *Comparative biochemistry and physiology A-Comparative Physiology.* **101**, 369–374.

Chen, Y., D. Jackson, and H. Harvey (1992). A Comparison of Von Bertalanffy and Polynomial Functions in Modelling Fish Growth Data. *Can. J. Fish. Aquat. Sci.* **49**(6), 1228–1235.

Crisp, D. (1981). A desk study of the relationship between temperature and hatching time for the eggs of five species of salmonid fishes. *Freshwater Biology* **11**, 361–368.

Crisp, D. (1988). Prediction, from temperature, of eyeing, hatching and 'swim-up' times for salmonid embryos. *Freshwater Biology* **19**, 41–48.

Crisp, D. and W. Beaumont (1995). The Trout (*Salmo-trutta*) Population of the Afon-Cwm, a small tributary of the Afon-Dyfi, Mid-Wales. *J. Fish Biol.* **46**, 703–716.

Crozier, W. and G. Kennedy (1995). The relationship between a summer fry (O+) abundance index, derived from semi-quantative electro-fishing, and egg deposition of Atlantic salmon, in the River Bush, Northern Ireland. *J. Fish Biol.* **47**(6), 1055–1062.

Cunjak, R. (1988). Physiological consequences of over wintering in streams - The cost of acclimatisation. *Can. J. Fish. Aquat. Sci* **45**, 443–452.

Davidson, K. and A. Bielak (1993). *Salmon in the sea and new enhancement strategies*, Chapter 16: New enhancement strategies in action, pp. 299–320. Fishing News Books.

Deangelis, D., B. Shuter, M. Ridgway, and M. Scheffer (1993). Modelling growth and survival in an age 0- fish cohort. *Trans. Am. Fish. Soc.* **122**(5), 927–941.

Dobson, S. and R. Holmes (1984). Compensatory growth on rainbow trout, *Salmo gairdneri* Richardson. *J. Fish Biol.* **25**, 649–656.

DSFIA (1994). *Final Report. Aberdeen: Grampian Enterprise*, Chapter Salmon rod fishing, River Dee, Grampian, pp. 75. Dee Salmon Fishing Improvement Association and Dee District Salmon Fishery Board.

Dulcic, J. and M. Kraljevic (1996). Weight-length relationships for 40 fish species in the eastern Adriatic (Croatian waters). *Fisheries Research* **28**(3), 243–251.

Dwyer, W. and R. Piper (1987). Atlantic salmon growth efficiency as affected by temperature. *Progressive Fish Culturist* **49**, 57–59.

Eby, L., L. Rudstam, and J. Kitchell (1995). Predator Responses to Prey Population-Dynamics - an Empirical-Analysis based on Lake Trout Growth-Rates. *Can. j. Fish. Aquat. Sci.* **52**, 1564–1571.

Egglishaw, H. (1967). The food, growth and population structure of salmon and trout in two streams in the Scottish Highlands. *Freshwat. Salm. Fish. Res., Scotland* **38**, 32pp.

Egglishaw, H. and P. Shackley (1977). Growth survival and production of juvenile salmon and trout in a Scottish stream, 1966-1975. *J. Fish. Biol.* **11**, 647–72.

Egglishaw, H. J. (1964). The distributional relationship between bottom fauna and plant detritus in streams. *J. Amin. Ecol.* **33**, 463–76.

Egglishaw, H. J. (1968). The quantitative relationship between bottom fauna and plant detritus in streams of different calcium concentrations. *J. Appl. Ecol.* **5.**, 731–740.

Egglishaw, H. J. and D. Mackay (1967). A Survey of the Bottom Fauna of Streams in the Scottish Highlands Part III Seasonal changes in the fauna of Three Streams. *Hydrobiologia* **30**, 305–334.

Egglishaw, H. J. and N. C. Morgan (1965). A Survey of the Bottom Fauna of Streams in the Scottish Highlands Part II the relationship of the fauna to the chemical and geological conditions. *Hydrobiologia* **26**, 173–183.

Elliott, J. (1975a). The growth rate of brown trout (*Salmo trutta*L.) fed on maximum rations. *Journal of Animal Ecology* **44**, 805–821.

Elliott, J. (1975b). The growth rate of brown trout (*Salmo trutta*L.) fed on reduced rations. *Journal of Animal Ecology* **44**, 823–824.

Elliott, J. (1991). Tolerance and resistance to thermal stress in juvenile Atlantic salmon *Salmo salar*. *Freshwater Biology* **25**, 61–70.

Elliott, J. and M. Hurley (1998). An individual-based model for predicting the emergence period of sea trout fry in a lake district stream. *J. Fish Biol.* **53**, 414–433.

Elliott, J. M. (1973). The Food of Brown and Rainbow Trout (Salmo trutta and S. gairdneri) in Relation to the Abundance of Drifting Invertebrates in a Mountain Stream. *Oecologia* **12**, 329–347.

Elliott, J. M. and M. A. Hurley (1995). The functional relationship between body size and growth rate in fish. *Functional Ecology.* **9**, 625–627.

Elliott, J. M. and M. A. Hurley (1997). A functional model for maximum growth of Atlantic Salmon parr, *Salmo salar*, from two populations in north-west England. *Functional Ecology.* **11**, 592–603.

Elliott, J. M., M. A. Hurley, and J. D. Allonby (1996). A functional model for maximum growth of immature stone-loach, *Barbatula barbabatula*, from three populations in north-west England. *Freshwater Biology* **36**, 547–554.

Elliott, J. M., M. A. Hurley, and R. J. Fryer (1995). A new, improved model for Brown Trout, it Salmo trutta. *Functional Ecology.* **9**, 290–298.

Elson, P. (1957). The importance of size in the change from parr to smolt in the Atlantic salmon. *Can. Fish. Cult.* **21**, 1–6.

Elson, P. (1962). Predator-prey relationships between fish-eating birds and Atlantic salmon. *Bull. Fish. Res. Bd. Can* **24**, 731–767.

Evans, G., J. Rice, and E. Chadwick (1985). Patterns of growth and smolting of Atlantic salmon (*Salmo salar*) parr in a south western Newfoundland river. *Can. J. Fish. Aquat. Sci.* **42**, 539–543.

Feltham, M. and J. MacLean (1996). Carlin tag recoveries as an indicator of predation on salmon smelts by goosanders and red-breasted mergansers. *J. Fish Biol.* **48**(2), 270–282.

Fleming, I. (1996). Reproductive strategies of Atlantic salmon: ecology and evolution. *Reviews in Fish Biology and Fisheries* **6**, 379–416.

Fleming, I. (1998). Pattern and variability in the breeding system of the Atlantic salmon, (*Salmo salar*), with comparisons to other salmonids. *Can. J. Fish. Aquat. Sci.* **55**(S1), 59–76.

Fleming, I., B. Jonsson, M. Gross, and A. Lamberg (1997). An experimental study of the reproductive behaviour and success of farmed and wild Atlantic salmon. *J. App. Ecol.* **33**, 893–905.

Folt, C., K. Nislow, and M. Power (1998). Implications of temporal and spatial scale for Atlantic salmon, (*Salmo salar*) research. *Can. J. Fish. Aquat. Sci.* **55**(S1), 9–21.

Fontoura, N. and A. Agostinho (1996). Growth with seasonally varying temperatures: An expansion of the Von Bertalanffy growth model. *J. Fish. Biol.* **48**(4), 569–584.

From, J. and G. Rasmussen (1984). A growth model, gastric evacuation and body composition in rainbow trout, *Salmo gairdneri*, Richardson, 1836. *Dana* **3**, 61–139.

Garcia de Leaniz, C., E. Verspoor, and A. Hawkins (1989). Genetic determination of the contribution of stocked and wild Atlantic salmon, Salmo salaer L., to the angling fisheries in two Spanish rivers. *J. Fish. Biol.* **35**(Suppl.A.), 261–270.

Gardiner, W. and P. Geddes (1980). The influence of body composition on the survival of juvenile salmon. *Hydrobiologia* **69**, 67–72.

Gee, A., J. Milner, and R. Hemsworth (1978). The effect of density on mortality in juvenile Atlantic salmon (*Salmon salar*). *Journal of Animal Ecology* **47**, 497–505.

Gibson, R. (1983). Large Atlantic salmon (*Salmon salar*) of a boreal river in Quebec. *Naturaliste can. (Rev. Ecol. Syst.)* **110**, 135–141.

Gibson, R. and R. Cunjak (1986). An investigation of the competitive interactions between brown trout, (*Salvelinus fontinalis*) and juvenile Atlantic salmon (*Salmo salar* L.) in the rivers of the Avalon Peninsula, Newfoundland. *Can. Tech. Rep. Fish. Aquat. Sci.* **1472**, 82pp.

Gibson, R. and T. Dickson (1984). The effects of competition on the growth of juvenile Atlantic salmon. *Naturaliste Can.* **111**, 175–91.

Gibson, R. J. (1978). Recent changes in the population of juvenile Atlantic salmon in the Matamek River, Quebec, Canada. *J. Cons. Perm. Int. Explor. Mer.* **38**, 201–7.

Gorodilov, Y. (1996). Description of the early ontogeny of the Atlantic salmon, *Salmo salar*, with a novel system of interval (state) identification. *Envir. Biol. Fish.* **47**, 109–127.

Gotceitas, V. and J. Godin (1992). Effects of location of food delivery and social status on the foraging-site selection by juvenile Atlantic salmon. *Envir. Biol. Fish.* **35**, 291–300.

Gowans, A., J. Armstrong, and I. Priede (1999). Movements of adult Atlantic salmon in relation to a hydroelectric dam and fish ladder. *J. Fish Biol.* **54**(4), 713–726.

Goyke, A. and S. Brandt (1993). Spatial Models of Samonine Growth Rates in Lake Ontario. *Trans. Am. Fish. Soc.* **122**(5), 870–883.

Grant, J. and D. Kramer (1990). Territory as a predictor of the upper limit to population density of juvenile salmonid in streams. *Can. J. Fish. Aquat. Sci.* **47**, 1724–1737.

Gross, M. (1998). One species with two biologies: Atlantic salmon, (*Salmo salar*) in the wild and in aquaculture. *Can. J. Fish. Aquat. Sci.* **55**(S1), 131–144.

Gunnes, K. (1979). Survival and development of Atlantic salmon eggs and fry at three different temperatures. *Aquaculture* **16**, 211–218.

Harris, G. (1978). Salmon propagation in England and Wales. A report by the association of river authorities/National water council working party. National water council, London.

Hay, D. (1987). The relationship between redd counts and the numbers of spawning salmon in the Girnock burn. *Journal Du Conseil* **43**(2), 146–148.

Heggberget, T. (1988). Timing and spawning of Norwegian Atlantic salmon (*Salmo salar*). *Can. J. Fish. Aquat. Sci.* **45**, 845–849.

Heggenes, J., J. Bagliniere, and R. Cunjak (1999). Spatial niche variability for young Atlantic salmon (Salmo salar) and brown trout (S-trutta) in heterogeneous streams. *Ecology of Freshwater Fish* **8**(1), 1–21.

Hewson, R. (1995). The use of salmon carcasses by vertebrate scavengers. *Journal of Zoology* **235**, 53–65.

Holling, C. (1959). Some Characteristics of Simple Types of Predation and Parasitism. *The Canadian Entomologist* **91**, 385–398.

Huntingford, F., V. Braithwaite, J. Armstrong, D. Aird, K. Thorpe, and P. Joiner (1998). Social status and growth rates as determinants of site attachment in juvenile Atlantic salmon. *J. Fish Biol.* **53**(2), 314–321.

Hutchings, J. and M. Jones (1998). Life history variation and growth rate thresholds for maturity in Atlantic salmon, *Salmo salar*. *Can. J. Fish. Aquat. Sci.* **55**(S1), 22–47.

Ismen, A. (1995). Growth, mortality and yield per recruit model of Picarel (*Spicara smaris*L) on the eastern Turkish black sea coast. *Fisheries Research* **22**(3-4), 299–308.

Jensen, A., B. Johnsen, and T. Heggberget (1991). Initial feeding time of Atlantic salmon, *Salmon salar*, alevins compared to river flow and water temperature in Norwegian streams. *Envir. Biol. Fish.* **30**, 379–385.

Jensen, A., B. Johnsen, and L. Saksgard (1989). Temperature requirements in Atlantic salmon (*Salmo salar*), and Arctic char (*Salvelinus alpinus*) from hatching to initial feeding compared with geographic distribution. *Can. J. Fish. Aquat. Sci.* **46**, 786–789.

Jones, J. W. (1959). *The Salmon.* Collins.

Jonsson, N., B. Jonsson, and L. Hansen (1998). The relative role of density-dependent and density-independent survival in the life cycle of Atlantic salmon *Salmo salar*. *J. Amin. Ecol.* **67**(5), 751–762.

Jordan, W., E. Verspoor, and A. Youngson (1997). The effect of natural selection on estimates of genetic divergence among populations of Atlantic salmon. *J. Fish. Biol.* **51**, 546–560.

Jordan, W. and A. Youngson (1992). The use of genetic marking to assess the reproductive success of mature male Atlantic salmon (*Salmo salar*L.) under natural spawning conditions. *J. Fish. Biol.* **41**, 613–8.

Kalleberg, H. (1958). Observations in a tank of territoriality and competition in juvenile salmon and trout (*Salmo salar* L. and *S. trutta*) in the rivers of the Avalon Peninsula, Newfoundland. *Report of the Institute of Freshwater Research, Drottningholm* **39**, 55–98.

Keely, E. and W. Grant (1995). Allometric and environmental correlates of the territory size of juvenile Atlantic salmon (*Salmo salar*). *Can. J. Fish. Aquat. Sci.* **52**, 186–196.

Keenleyside, M. and F. Yamamoto (1962). Territorial behaviour of juvenile Atlantic salmon (*Salmo salar* L.). *Behaviour* **19**, 139–169.

Kennedy, G. (1988). *Atlantic salmon: Planning for the future*, Chapter Stock enhancement of Atlantic salmon (Salmo salar L.), pp. 345–72. Croom Helm, London.

Kennedy, G. and J. Greer (1988). Predation by cormorants (*Phalacrorax carbo* (L.)) on the salmonid populations of the river Bush. *Aquau. Fish. Manag.* **19**(2), 159–70.

Kitchell, J., D. Stewart, and D. Weininger (1977). Application of a bioenergetics model to yellow perch (*perca flavescens*) and walleyes (*Stizostedion vitreum vitreum*). *J. Fish. Res. Bd. Can,* **34**, 1922–1935.

Kristiansen, H. (1998). Effects of handling, discrete meals and body weight on the individual variation of gastric emptying parameters. *Aquaculture research* **29**, 717–729.

Lantry, B. and D. Stewart (1993). Ecological Energetics of Rainbow Smelt in Laurentian Great Lakes: An Interlake Comparison. *Trans. Am. Fish. Soc.* **122**(5), 951–976.

Largiader, C., R. Guyomard, and P. Roche (1996). Evidence for natural reproduction of Atlantic salmon (Salmo salar L) in a French tributary of

the Rhine based on genetic analysis of eggs collected from redds. *Bullitin Francais de la Peche et de la Pisciculture* **343**, 183–188.

Lee, R. and G. Power (1976). Atlantic salmon (*Salmo salar*) in the Leaf River, Ungava Bay. *Can. J. Fish. Aquat. Sci.* **33**, 2616–2621.

Limburg, K. (1996). Modelling the ecological constraints on growth and movement of juvenile American shad (*Alosa sapidissima*) in the Hudson River Estuary. *Estuaries* **19**(4), 794–813.

Lorenzen, K. (1996). A simple Von Bertalanffy model for density-dependent growth in extensive aquaculture, with an application to common carp (*Cyprinus carpio*). *Aquaculture* **142**(3-4), 191–205.

MacCrimmon, D., T. Dickson, and R. Gibson (1983). Implications of differences in the emergent times on growth and behaviour of juvenile Atlantic salmon (*Salmo salar*) and brook charr (*Salvelinus fontinalis* in a sympatric stream population. *Naturaliste Can* **110**, 379–84.

Madenjian, C. and S. Carpenter (1991). Individual Based Model for Growth of Young-of-the-Year Walleye - A Piece of the Recruitment Puzzle. *Ecological Applications* **1**, 268–279.

Maizels, J. (1985). *The biology and management of the River Dee*, Chapter The physical background of the river Dee, pp. 7–22. Institute of Terrestrial Ecology, Huntingdon, UK.

Mangel, M. (1994). Climate-change and salmonid life-history variation. *Deep-Sea Research Part II-Topical Studies in Oceanography* **41**(1), 75–106.

Manooch, C. and J. Potts (1997). Age, growth and mortality of greater amberjack from the south eastern United States. *Fisheries Research* **30**(3), 229–240.

May, A. (1993). *Salmon in the sea and new enhancement strategies*, Chapter 12: A review of management and allocation of the Atlantic salmon resource in Atlantic Canada, pp. 220–232. Fishing News Books.

Mckeon, J. and L. Stolte (1993). *Salmon in the sea and new enhancement strategies*, Chapter 22: Uses for the domestic Atlantic salmon brood stock in the Merrimack River anadromous fish programme, pp. 390–401. Fishing News Books.

Metcalfe, N., F. Huntingford, and J. Thorpe (1986). Seasonal changes in feeding motivation of juvenile Atlantic salmon (*Salmon salar*). *J. Anim. Ecol.* **57**, 463–474.

Metcalfe, N., F. Huntingford, and J. Thorpe (1987). The Influence of Predation on the Feeding Motivation and Foraging Strategy of Juvenile Atlantic Salmon. *Anim. Bahav.* **35**, 901–911.

Metcalfe, N., F. Huntingford, and J. Thorpe (1988). Feeding intensity, growth rates, and the establishment of life-history patterns in juvenile Atlantic salmon *Salmon salar*. *J. Anim. Ecol.* **57**, 463–474.

Metcalfe, N., F. Huntingford, J. Thorpe, and C. Adams (1990). The effects of social status on life-history variation in juvenile salmon. *Can. J. Zool.* **68**, 2630–6.

Metcalfe, N. and J. Thorpe (1992). Anorexia and Defended energy levels in over-wintering juvenile salmon. *J. Anim. Ecol.* **61**, 175–181.

Miglavs, I. and M. Jobling (1989a). Effects of feeding regime on food consumption, growth rates and tissue nucleic acids in juvenile arctic charr, *salvelinus alpinus*, with particular reference to compensatory growth. *J. Fish Biol.* **34**, 947–957.

Miglavs, I. and M. Jobling (1989b). The effects of feeding regime on proximate body composition and patterns of energy deposition in juvenile arctic charr, *salvelinus alpinus*. *J. Fish Biol.* **35**, 1–11.

Mills, D. (1962). The goosander and the red-breasted merganser as predators of salmon in Scottish water. *Freshwat. Salm. Res., Scotland* **29**, 10pp.

Mills, D. (1964). The ecology of the young stages of the Atlantic salmon in the River Bran, Ross-shire. *Freshwat. Salm. Res., Scotland* **32**, 58pp.

Mills, D. (1965). The distribution and food of the cormorant in Scottish inland waters. *Freshwat. Salm. Res., Scotland* **35**, 16pp.

Mills, D. (1993). *Salmon in the sea and new enhancement strategies*, Chapter 13: Control and marine exploitation, pp. 233–248. Fishing News Books.

Mills, D. H. (1989). *Ecology and management of Atlantic salmon.* Chapman and Hall.

Moir, H., C. Soulsby, and A. Youngson (1998). Hydraulic and sedimentary characteristics of habitat utilised by Atlantic salmon for spawning in the Girnock Burn, Scotland. *Fish. Manage. Ecol.* **5**, 241–254.

Mortense, A. and B. Damsgard (1993). Compensatory growth and weight segregation following light and temperature manipulation of juvenile salmon (*Salmo salar L*) and arctic charr (*Salvelinus alpinus L*). *Aquaculture* **114**, 261–272.

Mundie, J. H. (1969). Ecological Implications of the diet of Juvenile Coho in Streams. *Symposium on Salmon and Trout in Streams, Vancover.*, 135–152.

Myers, R. (1984). Demographic consequences of precocious maturation of Atlantic salmon (*Salmon salar*). *Can. J. Fish. Aquat. Sci.* **41**, 1349–53.

Myers, R., J. Hutching, and R. Gibson (1986). Variation in male parr maturation within and among populations of Atlantic salmon *Salmon salar*. *Can. J. Fish. Aquat. Sci.* **43**, 1242–8.

Nelder, J. and R. Mead (1965). A simplex method for function minimisation. *Computer Journal* **7**, 308–313.

Nicieza, A. and F. Brana (1993). Compensatory growth and optimal size in one-year-old smolts of Atlantic salmon (*Salmo salar*). *Can. Spec. Publ. Fish. Aquat. Sci.* **118**, 225–237.

Nicieza, A. and N. Metcalfe (1997). Growth compensation in juvenile Atlantic salmon: Responses to depressed temperature and food availability. *Ecology* **78**, 2385–2400.

Økland, F., B. Jonsson, A. J. Jensen, and L. Hansen (1993). Is there a threshold size regulating seaward migration of brown trout and Atlantic salmon? *J. Fish. Biol.* **42**, 541–550.

Osterdalh, L. (1969). *Salmon and trout in streams*, Chapter The smolt run of a small Swedish river, pp. 205–15. University of British Columbia, Vancouver, BC.

Parrish, D., R. Behnke, S. Gephard, and G. Reeves (1998). Why aren't there more Atlantic salmon (Salmo salar)? *Can. J. Fish. Aquat. Sci.* **55**(S1), 281–287.

Peterson, J. H. and D. L. Deangelis (1992). Functional-Response and Capture Timing in an Individual-Based Model - Predation by Northern Squawfish

(*Ptychocheilus-Oregonensis*) on Juvenile Salmonids in the Columbia River. *Can. j. Fish. Aquat. Sci.* **49**, 2551–2565.

Peterson, R. and D. Martin-Robichaud (1989). First feeding of Atlantic salmon (*Salmo salar*L.) fry as influenced by temperature regime. *Aquaculture* **78**, 35–53.

Petrakis, G. and K. Stergiou (1995). Weight-length relationships for 33 fish species in Greek waters. *Fisheries Research* **21**(3-4), 465–469.

Philippart, J., J. Micha, E. Baras, C. Prignon, A. Gillet, and S. Joris (1994). The Belgium Project Meuse Salmon 2000 - 1st results, problems and future prospects. *Water Science and Technology* **29**(3), 315–317.

Planes, S., O. Hertel, and J. Jouvenel (1997). Analysis of condition and swimming performance in juveniles of white sea bream, *Diplodus vulgaris*. *J. Mar. Biol. Assoc. of the UK* **77**(3), 913–916.

Pope, J., D. Mills, and W. Shearer (1961). The fecundity of Atlantic salmon (*Salmo salar* L.). *Sci. Invest. Freshwat. Fish. Res. Scotl.* **26**, 12.

Potts, J., C. Manooch, and D. Vaughan (1998). Age and growth of vermilion snapper from the south eastern United States. *Trans. Am. Fish. Soc.* **127**(5), 787–795.

Power, M. and G. Power (1994). Modelling the dynamics of smolt production in Atlantic salmon. *Trans. Am. Fish. Soc.* **123**(4), 535–548.

Powers, G. (1969). The salmon of Ungava Bay. *Arctic Inst. N. Am. Tech. Pap.* **22**, 72.

Press, W., B. Flannery, and W. Vetterling (1989). *Numerical Recipes in Pascal: The Art of Scientific Computing.* Cambridge University Press.

Prouzet, P. (1978). Relationship between density and growth of Atlantic salmon reared in nursery streams in natural condition. *International Council for the Exploration of the Sea* **C.M**(1978/M), 13.

Pyefinch, K. and D. Mills (1963). Observations on the movements of Atlantic salmon (*Salmo salar* L.) in the river Conan and the river Meig, Ross-shire. *Freshwat. Salm. Fish. Res., Scotland* **31**, 24pp.

Rand, P., D. Stewart, P. Seelbach, M. Jones, and L. Wedge (1993). Modelling Steelhead Populations Energetics in Lakes Michigan and Ontario. *Trans.*

Am. Fish. Soc. **122**(5), 977–1001.

Randall, R. (1982). Emergence, population densities, and growth of salmon and trout fry in two New Brunswick streams. *Can. J. Zool.* **60**, 2239–44.

Randall, R. and U. Paim (1982). Growth, Biomass and Production of juvenile Atlantic salmon (*Salmo salar* L.) in two Miramichi River, New Brunswick, tributary streams. *Can. J. Zool.* **60**, 1647–59.

Rea, B. (1960). Seals and Scottish fisheries. *Marine Res. Ser., Scotland* **2**, 39pp.

Rea, B. and W. Shearer (1965). Seal damage to salmon fisheries. *Marine Res. Ser., Scotland* **2**, 39.

Ricker, W. (1954). Stock and Recruitment. *J. Fish. Res. Bd. Canada* **11**(5), 559–623.

Rimmer, D., U. Paim, and R. L. Suanders (1983). Autumnal habitat shift of juvenile Atlantic salmon (*Salmon salar*) in a small river. *Can. J. Fish. Aquat. Sci.* **40**, 671–680.

Robitaille, J., Y. Cote, G. Shooner, and G. Hayeur (1986). *Salmonid age at Maturation*, Chapter Growth and maturation patterns of Atlantic salmon, *Salmo salar*, in the Koksoak River, Ungava, Quebec., pp. 62–69. Can. Spec, Publ. Fish. Aquat. Sci.

Schnute, J. (1981). A Versatile Growth Model with Statistically Stable Parameters. *Can. J. Fish. Aquat. Sci.* **38**, 1128–1140.

Seiwarth, G. and R. Summerfelt (1993). Performance Comparisons and growth models for Walleyes and Walleye X sauger hybrids reared for two years in intensive culture. *Progressive Fish-Culturist* **55**(4), 229–235.

Shackley, P. and M. Donaghy (1992). *The Distribution and growth of juvenile salmon and trout in the major tributaries of the River Dee catchment (Grampian Region)*. The Scottish Office Agriculture and Fisheries Department, Scottish Fisheries report Number 51.

Shackley, P., C. Talbot, A. Cowan, and A. Watt (1994). The use of body water, sodium, potassium and calcium content to investigate the nutritional status of first year Atlantic salmon parr in two Scottish Highland streams. *J. Fish. Biol.* **44**, 693–706.

Shearer, W. (1985). *The biology and management of the River Dee*, Chapter Salmon catch statistics for the River Dee, 1952-83, pp. 127–141. (ITE Symposium Series, 14). Huntingdon: Institute of Terrestrial Ecology.

Shearer, W. (1993). *Salmon in the sea and new enhancement strategies*, Chapter 21: River enhancement strategies on a time-shared river, pp. 367–389. Fishing News Books.

Skalski, J., G. Johnson, C. Sullivan, E. Kudera, and M. Erho (1996). Statistical evaluation of turbine bypass efficiency at Wells Dam on the Columbia River, Washington. *Can. J. Fish. Aquat. Sci.* **53**(10), 2188–2198.

Skilbrei, O. (1988.). Growth Pattern of Pre-Smolt Atlantic Salmon (Salmon Salar L.): the Percentile Increment Method (PIM) as a New Method to Estimate Length-Dependant Growth. *Aquaculture* **69**, 129–143.

Soderburg, R. (1992). Linear fish growth Models for intensive aquaculture. *Progressive Fish-Culturist* **54**(4), 255–258.

Steingrimsson, S. and J. Grant (1999). Allometry of territory size and metabolic rate as predictors of self-thinning in young-of-the-year Atlantic salmon. *J. Anim. Ecol.* **68**(1), 17–26.

Stewart, D., D. Weininger, D. Rottiers, and T. Edsall (1983). Energetics Model for Lake Trout, *salvelinus namaycush*: Application to Lake Michigan Population. *Can j. fish aquat. sci.* **40**, 681–98.

Stockwell, J. and B. Johnson (1997). Refinement and Calibration of a Bioenegetics-Based Foraging Model for Kokanee (*Oncorhynchus nerka*). *Can. J. Fish. Aquat. Sci.* **54**, 2659–2676.

Stradmeyer, L., N. B. Metcalfe, and J. E. Thorpe (1988). The effect of food pellet shape on the feeding response of juvenile Atlantic salmon. *Aquaculture* **73**, 217–228.

Stradmeyer, L. and J. Thorpe (1987a). Feeding behaviour of wild Atlantic salmon, *Salmo salar*L., parr in mid to late summer in a Scottish river. *Aquaculture and Fisheries Management* **18**, 33–49.

Stradmeyer, L. and J. E. Thorpe (1987b). The response of hatchery reared Atlantic salmon, Salmo salar L., parr to pelleted and wild prey. *Aquaculture and Fisheries Management* **18**, 51–61.

Symons, P. (1971). Behavioural adjustment of population density to available food by juvenile Atlantic salmon. *J. Anim. Ecol.* **40**, 569–587.

Symons, P. (1979). Estimated escapement of Atlantic salmon (*Salmo salar*) for maximum smolt production in rivers of different productivity. *J. Fish, Res. Bd. Can.* **36**, 132–140.

Talbot, C., P. Higgins, and A. Shanks (1984). The effects of pre- and post-prandial starvation on meal size and evacuation rate of juvenile Atlantic salmon, *Salmo salar.* . *J. Fish. Biol.* **25**, 551–560.

Thornton, K. and A. Lessem (1978). A temperature algorithm for modifying biological rates. *Trans. Am. Fish. Soc.* **107**(2), 284–287.

Trebitz, A. and N. Nibbelink (1996). Effect of pattern of vegetation removal on growth of bluegill: A simple model. *Can. J. Fish. Aquat. Sci.* **53**(8), 1844–1851.

Van Winkle, W., H. Jager, S. Railsback, B. Holcomb, T. Studley, and J. Baldrige (1998). Individual based model of sympatric populations of brown and rainbow trout for instream flow assessment: model description and calibration. *Ecological Modelling* **110**, 175–207.

Verspoor, E. and C. deLeaniz (1997). Stocking success of Scottish Atlantic salmon in two Spanish rivers. *J. Fish. Biol.* **51**(6), 359–366.

Vigfusson, O. and A. Ingolfsson (1993). *Salmon in the sea and new enhancement strategies*, Chapter 14: Quota purchase, pp. 249–263. Fishing News Books.

Wainwood, B., K. Haya, and L. Van Eeckhaute (1992). Energy metabolism of hatchery reared juvenile salmon (*salmo salar*) exposed to low pH. *Comp. Biochem. Physiol.* **101**, 49–56.

Walker, A. and A. Walker (1991). *The little Gruinard salmon catch and release experiment.* Scottish Fisheries Research Services Report, Number 2/91.

Wankowski, J. (1979). Morphological limitations, prey size selectivity, and growth response of juvenile Atlantic salmon, *Salmo salar. J. Fish Biol.* **14**, 89–100.

Wankowski, J. (1981). Behavioural aspects of predation by juvenile Atlantic salmon (*salmo salar*) on particulate drifting prey. *J. Fish Biol.* **29**, 557–571.

Wankowski, J. and J. Thorpe (1979a). The role of food particle size in the growth of juvenile Atlantic salmon (*Salmo salar*L.). *J. Fish Biol.* **14**, 351–370.

Wankowski, J. and J. Thorpe (1979b). Spatial distribution and feeding in juvenile Atlantic Salmon. *J. Fish Biol.* **14**, 239–247.

Warren, J. (1985). *The biology and management of the River Dee*, Chapter Hydrology of the river Dee and its tributaries, pp. 23–28. Institute of Terrestrial Ecology, Huntingdon, UK.

Waters, T. F. (1969). Invertebrate Drift-Ecology and Significance to Stream Fishes. *Symposium on Salmon and Trout in Streams, Vancover.*, 121–134.

Webb, A. and P. Bacon (1999). Using GIS for catchment management and freshwater salmon fisheries in Scotland: the DeeCAMP project. *J. Environ. Managmnt.* **55**(2), 127–143.

Webb, J. (1998). *Catch and release: the survival and behaviour of Atlantic salmon angled and returned to the Aberdeenshire Dee, in spring and early summer*. Scottish Fisheries Research Report, Number 62.

Webb, J. and H. Mclay (1996). Variation in the time of spawning of Atlantic salmon (*Salmon salar*) and its relationship to temperature in the Aberdeenshire Dee, Scotland. *Can. J. Fish. Aquat. Sci.* **53**, 2739–2744.

Wheeler, A. and D. Gardner (1974). Survey of the literature of marine predators on salmon in the north-east Atlantic. *Fish. Mgmt.* **5**(3), 63–6.

Wolf, P. (1950). A trap for the capture of fish and other organisms moving downstream. *Trans. Am. Fish. Soc.* **80**, 41–45.

Wootton, R. J. (1990). *Ecology of teleost Fishes.*, Chapter 6, pp. 148–157. Chapman and Hall.

Wright, R., L. Crowder, and T. Martin (1993). The Effects of Predation on the Survival and Size-Distribution of Estuarine Fishes - an Experimental Approach. *Environ. Biol. Fish.* **36**, 291–300.

Xiao, Y. (1994). Growth Model with Corrections for Retardative Effects of Tagging. *Can. J. Fish. Aquat. Sci.* **51**(2), 263–267.

Yang, Y. (1998). A bioenergetics growth model for Nile tilapia (*Oreochromis niloticus*) based on limiting nutrients and fish standing crop in fertilised

ponds. *Aquacultural Engineering* **18**(3), 157–173.

Youngson, A. (1994). *Spring Salmon.* Atlantic salmon trust publications.

Youngson, A., R. Buck, T. Simpson, and D. Hay (1983). The autumn and spring emigrations of juvenile Atlantic salmon, *Salmo salar* L., from the Girnock Burn, Aberdeenshire, Scotland: environmental release of migration. *J. Fish Biol.* **23**, 625–639.

Youngson, A., W. Jordan, and D. Hay (1994). Homing of Atlantic salmon (*Salmo salar* L.) to a tributary spawning stream in a major river catchment. *Aquaculture* **121**(1-3), 259–267.

Youngson, A. F. and D. Hay (1996). *The Lives of Salmon.* Swan Hill Press.

Appendix A

The Downhill Method of Optimisation

The downhill methods of optimisation (DSO) is a procedure whereby the error between a function and the data is minimised by altering parameters of the function, and was developed by Nelder and Mead (1965). The DSO algorithm that will be used is from Press et al (1989) and is able to parameterise models in the following way.

Estimates of each parameter, along with a step size are specified. The procedure will then create a shape, the simplex, whose size and the corners are defined by the parameters and the step size. The simplex will have $N+1$ dimensions, where N is the number of parameters to be found. The error value is then derived at each of the corners, which is based on the output from the model and the data. Once the corner with the lowest error value has been determined, the simplex undergoes a transformation about a corner, such as a reflection, expansion or contraction, and a new set of errors are derived from the new set of corners. This process is repeated until the change in the error is less than a specified convergence criterion.

In effect, what the simplex is doing is moving down the error surface, and then moving across it to its lowest point. Ideally, the lowest point would be the global minimum, which would require a fairly smooth error surface.

Appendix B

Derivation of the Type II Functional Response

A population of N individuals can be divided into two groups during bouts of foraging. Those that are searching for prey, N_S, or handling prey, N_H. The average time to handle one biomass of food shall be defined as τ_h. If we let the rate at which food is found whilst foraging be Φ, then we can use the expression

$$\frac{dN_S}{dt} = \frac{N_H}{\tau_h} - \Phi N_S. \tag{B.1}$$

This is constant when $N_H = \tau_h \Phi N_S$ and because N_H=N-N_S we can derive N in terms of N_S,

$$N = N_S(1 + \tau_h \Phi) \tag{B.2}$$

The uptake for the population is $U_N = \Phi N_S$ therefore for an individual it is $U = \Phi N_S/N$ and by substitution gives the uptake per individual as

$$U = \frac{\Phi}{1 + \tau_h \Phi} \tag{B.3}$$

U_{max} will occur when all the time spent is handling so the most food that can be handled per unit time is $1/\tau_h$. We shall define $U_{max} \equiv 1/\tau_h$. Therefore if we divide through by U_{max}/Φ we get our desired form,

$$U = U_{max} \left(\frac{1}{1 + \frac{U_{max}}{\Phi}} \right). \tag{B.4}$$

Appendix C

Proof that $A_T(L)$ will scale with L^3

As the length of the salmon increases, both the maximum attack distance and the ranges of particle sizes that are available will increase in absolute terms. If we convert our definition of $A_T(L)$ into absolute units of length (x cm) this can shown. First we note that $r = x/L$ and $\gamma = p/L$, then from our definition of $D(p, L)$ in section 8.2.2. we covert it into absolute units of p and L.

$$D(\gamma) = a_1 + a_2\gamma + a_3\gamma^2 \tag{C.1}$$

$$D(p, L) = a_1 + a_2\frac{p}{L} + a_3\left(\frac{p}{L}\right)^2 \tag{C.2}$$

for $D(p, L)$.). To find the probability of attack over all r we must integrate

$$A_s(p, L) = \int_{rL=0}^{LD(p,L)} \sqrt{1 - \left(\frac{r^2}{D^2(p, L)}\right)}\pi rLd(rL). \tag{C.3}$$

This can be rewritten as

$$A_s(p, L) = \int_{x=0}^{LD(p,L)} \sqrt{1 - \left(\frac{x^2}{L^2D^2(p, L)}\right)}\pi x dx, \tag{C.4}$$

which integrates to

$$A_s(p, L) = \frac{\pi L^2 D^2(p, L)}{3} \tag{C.5}$$

$$= \frac{\pi L^2}{3}(a_1 + a_2\frac{p}{L} + a_3\left(\frac{p}{L}\right)^2)^2. \tag{C.6}$$

To determine A_T we must integrate across γ.

$$\begin{aligned} A_T(L) &= \int_{p=\gamma_{min}L}^{\gamma_{max}L} A_s(p,L)dp, && \text{(C.7)} \\ &= L^2 \int_{p=\gamma_{min}L}^{\gamma_{max}L} \frac{\pi D^2(p,L)}{3} dp, && \text{(C.8)} \\ &= L^2 \int_{p=\gamma_{min}L}^{\gamma_{max}L} \frac{\pi}{3}\left(a_1 + a_2\frac{p}{L} + a_3\left(\frac{p}{L}\right)^2\right)^2 dp, && \text{(C.9)} \\ &= \frac{\pi L^2}{3}\int_{p=\gamma_{min}L}^{\gamma_{max}L}\left(a_1^2 + 2a_1a_2\frac{p}{L} + 2a_1a_3\left(\frac{p}{L}\right)^2 + a_2^2\left(\frac{p}{L}\right)^2\right. \\ &+ \left. 2a_2a_3\left(\frac{p}{L}\right)^3 + a_3^2\left(\frac{p}{L}\right)^4\right)dp. && \text{(C.10)} \end{aligned}$$

For simplicity we shall redefine

$$\begin{aligned} a &\equiv \frac{\pi}{3}a_1^2 && \text{(C.11)} \\ b &\equiv \frac{\pi}{3}2a_1a_2 && \text{(C.12)} \\ c &\equiv \frac{\pi}{3}(2a_1a_3 + a_2^2) && \text{(C.13)} \\ d &\equiv \frac{\pi}{3}2a_2a_3 && \text{(C.14)} \\ e &\equiv \frac{\pi}{3}a_3^2 && \text{(C.15)} \end{aligned}$$

Thus

$$\begin{aligned} A_T(L) &= L^2\int_{p=\gamma_{min}L}^{\gamma_{max}L} a + b\frac{p}{L} + c\left(\frac{p}{L}\right)^2 + d\left(\frac{p}{L}\right)^3 + e\left(\frac{p}{L}\right)^4 && \text{(C.16)} \\ &= L^2\left[ap + b\frac{p^2}{2L} + c\frac{p^3}{3L^2} + d\frac{p^4}{4L^3} + e\frac{p^5}{5L^4}\right]_{p=\gamma_{min}L}^{\gamma_{max}L}. && \text{(C.17)} \\ &= L^3(a(\gamma_{max} - \gamma_{min}) + \frac{b}{2}(\gamma_{max}^2 - \gamma_{min}^2) + \frac{c}{3}(\gamma_{max}^3 - \gamma_{min}^3) \\ &+ \frac{d}{4}(\gamma_{max}^4 - \gamma_{min}^4) + \frac{e}{5}(\gamma_{max}^5 - \gamma_{min}^5)) && \text{(C.18)} \end{aligned}$$

Thus, we shall redefine

$$\begin{aligned} \alpha &\equiv a(\gamma_{max} - \gamma_{min}) + \frac{b}{2}(\gamma_{max}^2 - \gamma_{min}^2) + \frac{c}{3}(\gamma_{max}^3 - \gamma_{min}^3) \\ &+ \frac{d}{4}(\gamma_{max}^4 - \gamma_{min}^4) + \frac{e}{5}(\gamma_{max}^5 - \gamma_{min}^5) && \text{(C.19)} \end{aligned}$$

Therefore $A_T(L) = \alpha L^3$, where $\alpha = 5.479$.

Appendix D

Parameters for the UFR Model

There are a number of parameters that are necessary in order to implement the URF model. These are outlined and estimated below.

The handling time, $\tau(\mathbf{L})$

A lower estimate for $\tau(L)$ can be derived from a study by Stradmeyer and Thorpe (1987a) who observed 25 captures in a 15 minute foraging bout for a wild salmon in a stream with high food density (this is the higher of two estimates given, the other from a stream having lower food density). Thus $\tau(L) = 36$ second per attempts. The mean length of the observed fish is known but due to only having one point we are unable to deduce the relationship between $\tau(L)$ and L. However, this will include the ingestion of non-nutritional foods such as exuviae. This has been observed in the stomach contents of coho salmon to be up to 35% of the items (Mundie 1969).

The water velocity, v

The surface current velocities are given in Egglishaw and Shackley (1977) of the different sections of the Shelligan Burn studied, which can be used to simulate the data set from Gardiner and Geddes (1980).

Total time spent foraging per day

Salmon may have more than one feeding period, dependent on temperature or photoperiod, at dusk or/and dawn, which correspond to the daylight peak activity levels of the invertebrates in the drift. Between these periods, the salmon are able to digest their food. They are thought to spend between 10-20% of their time foraging (Keely and Grant 1995).

Salmon Length-Weight relationship

We are examining two methods of finding the uptake. One is in the CGM, which has units of salmon weight the other is the functional response uptake model, which is in terms of salmon length. To make these models interchangeable we require a weight-length relationship. As the structural weight is being used as a surrogate for length, it will be more convenient to have a structural weight-length relationship. To derive this, corresponding measurements of total wet-weight and length were used. These points were taken when the fish were in their most rapid periods of growth and assumed to healthy. Using the ideal reserve to structural weight ratio, we were able to deduce the structural wet-weight at these points. This was then fitted with the model

$$S = a_s L^{b_s}. \tag{D.1}$$

The parameters derived from fitting equation (D.1) to the data from Gardiner and Geddes (1980) are:

For Structural Wet Weight (g), the residual sum of squares is 0.00272 and the parameters are $a_s = 0.0170$ and $b_s = 2.425$ from five observations.

For Structural Carbon Weight (mgC), the residual sum of squares is 61.429 and the parameters are $a_s = 2.547$ and $b_s = 2.425$ from five observations.